Republic of Iraq

Ministry of Higher Education and

Scientific Research

University of Babylon

College of Engineering

Environmental Engineering Department

Environmental Modelling of Surface Water Quality Using GIS and Remote Sensing Techniques: A Case Study of Hilla River, Iraq

A Thesis

Submitted to the Council of the College of Engineering, University of Babylon

in Partial Fulfillment of the Requirements for the Degree of

Master in Engineering / Environmental Engineering

By

Fatima Dhaiban Hadi

Supervised By

Asst. Prof. Dr. Hussein A. M. Al-Zubaidi

Prof. Dr. Nisren J. Al-Mansori

2023 A.D. 1444 A.H.

بسم الله الرحمن الرحيم

أَنْزَلْنَا مِنَ السَّمَاءِ مَاءً بِقَدَرٍ فَأَسْكَنَّاهُ فِي الْأَرْضِ وَإِنَّا عَلَى ذَهَابٍ بِهِ لَقَادِرُونَ

صدق الله العلي العظيم

سورة المؤمنون

الآية 18

DEDICATIONS

To

First and foremost, I have to thank my parents for their love and support throughout my life. Thank you both for giving me strength to reach for the stars and chase my dreams. I ask god to protect and save them for us.

To

Who have the widest hearts which always give

My brothers , My Sister .

To

My husband, Mustafa , who has been a constant source of support and encouragement during the challenges of life. I am truly thankful for having you in my life. This work is also dedicated to my kids, Malak and Ali, You are the source of joy and happiness in my life , and I always hope to be a source of pride and a good example to imitate in.

Fatima

2023

ACKNOWLEDGEMENTS

"In the Name of Allah, the Most Gracious, the Most Merciful"

Praise to Allah his Majesty before anything and after anything and to the prophet "Mohammed and Ahl-Al-Bait" for the strength, courage, and wisdom that Allah gave me to complete this humble work and lengthy journey this degree.

I would like to express my deepest gratitude and respect to my thesis supervisor Asst. Prof. Dr. Hussein Ali Al-Zubaidi, and Prof. Dr. Nisren J. Al-Mansori. I am very grateful for his precious time spent and useful suggestions which provided valuable guidance and important role in the completion of thesis as well as the moral support continued for the duration of the search, calling God richly rewarded him.

Fatima

2023

Abstract

Since industrial and human activities have been developed in different ways in Iraq, water quality has been declining along Hilla River, the only water resource in Hilla City for drinking water. In this research, the Weighted Arithmetic Water Quality Index (WQI) was simulated along the river based on GIS (Geographic Information Systems) technique and IDW (Inverse Distance Weighted) method. Water quality parameters including Turbidity (Turb), Electric Conductivity (EC), pH, Total Suspended Solid (TSS), Chloride ions (Cl), Sulfate ions (SO_4), Alkaline (ALK), Total Hardness (TH), Calcium ions (Ca^{+2}), Potassium ions (k^{+}), Sodium (Na^{+}), Magnesium ions (Mg^{+2}), and Total Dissolved Solid (TDS) were utilized to determine WQI from January 2016 to June 2021 depending on datasets from five sampling stations located along the river at the main city, Hilla City.

The results of this study showed that Hilla River is seriously polluted since WQI values are high. Linear regression models were developed statistically to find a significant relationship between the WQI and the water quality parameters. It was noticed that WQI in Hilla River has a significant relationship with Turbidity only (positive proportion). This relationship between WQI and Turbidity in the river is limited by WQI value, which is (220), Thus, two linear regression models were developed and validated: One for WQI values greater than 220 and another for the values less than 220.

Using remote sensing technology provides data for assessing and monitoring water quality in surface water bodies. Thus, in this study, Landsat 8 satellite images (2016 to 2021) were statistically tested for

developing linear models capable of estimating the water quality parameters in the river based on field data, Results showed that seven parameters have a significant relationship with the spectral bands ratio (p-value less than 0.05). Some of them (TDS, SO_4, and ALK) are positively correlated with bands ratio (Band10/Band3, Band10/Band3 and Band10/Band4, and Band3/Band7), respectively. Others (Mg^{+2}, Ca^{+2}, TH, and pH) are inversely correlated with (Band4/Band7, Band1/Band4, Band1/Band4, and Band1/Band2), respectively. However, K^{+}, Na^{+}, TDS, Cl^{-}, EC, and Turb have insignificant correlation with any bands ratio.

In addition, the correlation matrix between the WQI and spectral bands showed that WQI have Pearson Correlation more than 50% and p value less than 0.05 with band 3 and band 10. The significant relationship between WQI and spectral bands in the river is limited by WQI values, which are (WQI less than 50, WQI between 50 and 250, and WQI more than 250). WQI value less than 50 showed a significant relationship with band 3, WQI value between 50 and 250 showed a significant relationship with band 3, and WQI value more than 250 showed a significant relationship with band 10. As a result, three linear regression models were developed and validated depending on the WQI limit values.

Furthermore, the GIS maps were utilizing to predict maps for WQI and turbidity as a distribution map to cover the entire study region. The GIS maps for Hilla River reach along Hilla City showed that the worst WQI value was in 2019 due to the high turbidity. On the other hand, the best WQI and turbidity value was in 2018. However, in 2020 and 2021, there were some improvement in WQI and turbidity compared to 2019.

List of Contents

List of Figure

List of Tables

List of Abbreviations and Symbols

Abbreviations	Description
GIS	**Geographic Information Systems**
RS	**Remote Sensing**
IDW	**Inverse Distance Weighted**
WQI	**Water Quality Index**
Turb	**Turbidity**
EC	**Electric conductivity**
pH	**Hydrogen ions**

TSS	**Total suspended solids**
Cl^-	**Chloride ions**
Na^+	**Sodium ions**
SO_4^{-2}	**Sulfate ions**
ALK	**Alkalinity**
TH	**Total hardness**
Mg^{+2}	**Magnesium ions**
Ca^{+2}	**Calcium ions**
TDS	**Total dissolved solids**
K	**Potassium ions**
RMSE	**Root Mean Squared Error**
MSE	**Mean Square Error**
R^2	**Coefficient of determination**
WHO	**World Health Organization**
NTU	**Nephelometric Turbidity Unit**
^oC	**Degrees Celsius**
mg/l	**Milligram per Liter**
%	**Percent**
µS/cm	**Micro Siemens per centimeter**

Chapter One

Introduction

1.1 Introduction

The most valuable resource that nature offers to humans is water. It is crucial to our survival and necessary for all human endeavors, including agriculture, trade, industry, the production of power, daily hydration, and other activities (Abbas, 2013; Kannan & Ramasubramanian, 2011). However, over the past two or three decades, as human activity has expanded, the quality of water in numerous large rivers has decreased internationally (Avid Hirst & ob Morris, 2001; Ochir & Davaa, 2011). River water quality declines as a result of numerous factors including unidentified causes (Carpenter et al., 1998; Kotti et al., 2005). Several physical, chemical, and biological indicators can describe the type and extent of water pollution (Chitmanat & Traichaiyaporn, 2010). Surface runoff is a seasonal phenomenon that is seriously influenced by various meteorological circumstances, in contrast to human discharges, which represent a nonstop polluting source (Divya Raj & Kani, 2018).

In Iraq, water bodies cover more than 5% of the country's surface (Abbas et al., 2018), including lakes, marshes, rivers (Tigris, Euphrates, and Shatt al-Arab), as well as regions with stagnant water such as lakes and marshes. Since the last few decades, there has been a decline in the quality of surface water. As a result of urbanization, agricultural development, population growth, and increased water demand from growing industries and metropolitan areas, inland water bodies are facing difficulties. A water quality evaluation, organization, and management effort is necessary to address this issue, and a key component of this effort is water quality monitoring (Abbas et al., 2018). In order to conduct research and make policy decisions, it may be useful to monitor and evaluate polluted water. In actuality, in-situ measurements and the

collection of water samples for later laboratory research are used to evaluate water quality. These measures are precise at a particular moment and location, but they do not provide a spatial or temporal assessment of the water quality over a substantial area. As a result, technologies such as remote sensing and GIS applications are excellent tools for assessing and tracking water quality (Dekker et al., 1996). For more than 25 years, satellite remote sensing technology has made it possible to evaluate water quality in a synoptic and multi-temporal manner (Malthus & Dekker, 1995; Cracknell et al., 2001; Mishra et al., 2019; Wu et al., 2009).

The term "water quality" refers to the chemical, physical, and biological factors. It indicates the likelihood that it will be used by humans for a specific purpose, such as drinking, farming, recreation, or industry (Ewaid et al., 2018). One of the most important techniques for categorizing and distributing water quality data to the general public and the appropriate decision-makers in the water quality index (WQI) (Mohammed & Shakir, 2012; Oko et al., 2014). As a result, it has become an essential factor in the management and evaluation of water. WQI is a rating method that considers the combined impact of various water quality parameters. It is determined based on the suitability of various water sources for human consumption (Al-Shujairi, 2013). Finding a WQI linkage with satellite sensors is very important for water quality monitoring.

Hence, the amount of solar radiation reflected by surface water at different wavelengths can be measured by satellite sensors and linked to various water quality metrics (Hossain et al., 2010; Hossain et al., 2014). With three important advantages over ground sampling, this is an alternate method of determining the quality of the water. F, synoptic estimates across vast areas

are possible due to the nearly constant geographic coverage of satellite data. Second, because satellites have global coverage, it is possible to estimate the water quality in isolated and inaccessible locations. Third, historical water quality can be estimated when no ground measurements can be made due to the comparatively long record of archived imagery (such as Landsat images that have been launched since the early) (Hossain et al., 2021). The current study included using remote sensing technology, statistical analysis, and computer software to find a relationship between the water quality index and water quality parameters and remote sensing.

1.2 The study problems and significances

Due to Iraq's expanding population, anthropogenic use, poor management, and low environmental awareness, it will be challenging to regulate, monitor, and assess water resources quality over time, which are frequently exposed to different pollutants as a result of the diffusion from point and non-point sources like sewage, agricultural and industrial effluents. Additionally, global warming seriously contributes to Iraq's acute freshwater scarcity, as recent studies showed a marked decline in precipitation (Al-Zubaidi et al., 2020). Recently, the Hilla River basin has faced drought conditions due to the low amount of water reaching the basin. Therefore, surface water quality information is needed to manage the river and monitor global environmental changes (Al-Mansori, 2017).

It is significant to understand the problem by using currently available satellite data as input information along with the measured data to analyze the relationship between the selected data precision and the accuracy of this

water quality information. However, for monitoring and evaluating the quality of water bodies, Iraqi currently uses in-situ measurements (traditional) and/or the collection of water samples for laboratory testing to determine the chemical, physical, and biological features. This research will use historical senses from several satellite sources, such as NASA and USGS data, to generate practical models. To relate the components of water quality to the satellite data visually and statistically, data processing and characterization will be done based on the GIS and statistical tools that are now accessible.

1.3 Research objectives

The main objectives of this study are:

1. To qualify the Hilla River water based on its physical and chemical properties.
2. To develop a linear model capable of estimating the water quality of Hilla River, Iraq based on in-situ water quality data or Landsat 8 images.
3. To clearly display Hilla River water quality spatially and temporally using remote sensing and GIS techniques.

1.4 Thesis structure

Five separate chapters contain the complete presentation of the thesis. Below is a short description of each chapter.

Chapter one introduces the study, the significance of the research, the study issue statement, and the study goals.

Chapter two gives a revision to the concepts related to the research. It begins with water quality parameters, water quality index, remote sensing and Landsat 8, and geographic information systems.

Chapter three shows the techniques utilized in the research. It describes the research area and datasets.

Chapter four represents the results and discussion of this study.

Chapter five presents the main findings in addition to giving basic recommendations for further research.

Chapter Two

Theoretical Concepts and Literature Review

2.1 Introduction

This chapter indicates the concepts adopted in this research. It gives a description of water quality parameter and water quality index, explain remote sensing and Landsat sensing 8, and presented An overview of Geographic Information Systems (GIS). Finally, the Literature review discussed the concept of previous related studies.

2.2 Water quality parameters

Parameters of water quality can be classified into physical and chemical (Gray, 1994). In the current investigation, the authors deal with physical, and chemical parameters only.

2.2.1 Some of the water quality physical parameters

2.2.1.1 Turbidity

Turbidity could be defined as water cloudiness (Miner, 2006). It is a measure for traveling light through a water well. It results from suspended particles in water, including clay, silt, organic matter, plankton, and other particulate elements. The turbidity of drinking water is considered unaesthetic because of the unappetizing appearance of water. A device known as a nephelometric turbid meter is utilized to measure turbidity. Turbidity is expressed in units of NTU, equaling 1 mg/l of suspended silica (Alley, 2007). Turbidity can be seen visually over 5 NTU, but turbidity in muddy water approaches 100 NTU (Alley, 2007).

2.2.1.2 Solids

Solids could be dissolved in water or remain suspended. A sample of water could be filtered to separate these two solids types (Tchobanoglus et al., 2003). The suspended particles are retained at the filter head while the others seep out of the filter with water (Alley, 2007).

Total solid (TS) = Total dissolved solids (TDS) + Total suspended solid (TSS)

Drying the residual TSS and TDS for a specific period and heating degree results type of solids known as fixed. Solids lost on ignition are referred to as volatile solids (heating to 550°C) (Alley, 2007).

2.2.1.3 Electrical conductivity (EC)

It is a term that describes the solution's ability for transferring or conducting electricity. Water is usually used for measuring (Tchobanoglus et al., 2003). The conductivity rises as ion concentration rises because ions in solution carry the electrical current (Alley, 2007). As a result, it is significant for assessing parameters for water suitability to be used in irrigation and firefighting. A poor conductor of electricity is pure water (Alley, 2007; Federation & Association, 2005).

2.2.2 Some of water quality chemical parameters

2.2.2.1 pH

The pH of water is one of its significant characteristics. It is the (- log) of the concentration of H^+. It is an arbitrary value without dimensions that indicates the effectiveness of the solution in terms of acidity or basicity (Cheremisinoff, 2019). Actually, the pH of water indicates how acidic or basic

the water is (Cheremisinoff, 2019; Omer, 2019). The percentage of (H^+) and (OH^-) ions are high in acidic and basic solutions, respectively (Federation & Association, 2005). The range of pH is between 0 and 14 and has a balanced value of 7. The basic solution has a pH value greater than 7 while that of the acidic solution is less than 7. The pH of normal water is 7 at 25 °C (6.5 - 8.5) is the pH range for drinking water that is suitable for residential use and what is needed by living things (WHO, 2004).

2.2.2.2 Acidity

Acidity is a term used to indicate that a solution contains acids. The quantitative ability of water to neutralize a strong base to a chosen pH level is referred to as its acidity. The main factors that raise the acidity of water are mineral acids, CO_2, and hydrolyzed salts like Fe and $Al_2(SO_4)_3$. The principal processes that are influenced by acids are chemical, biological, and corrosion. Sources of CO_2 are the ambiance or breathing of aqueous creatures which is dissolved in water-producing (H_2CO_3) (Tomar, 1999; Alley, 2007).

2.2.2.3 Alkalinity

The total of all titratable bases serves as a gauge for how water can neutralize acids (Tomar, 1999). Measurement of the water alkalinity is fundamental in order to determine how much lime and soda are needed for softening of water (for instance, to protect the boiler from corrosion by feed water). The ions hydroxide (OH^-), bicarbonate (HCO_3), and carbonate (CO_3^{-2}), or a mix of them, are the main sources of alkalinity in water (Tchobanoglus et al., 2003).

2.2.2.4 Sulfate

Sulfate ions (SO_4^{2-}) are present in both raw water and wastewater. The high concentration of sulfate in natural water is regularly caused by the leaching of natural deposits of sodium sulfate (Glauber's salt) or magnesium sulfate (Epson salt). If high concentrations are consumed in drinking water, there may be objectionable tastes or unwanted laxative effects, but there is no significant danger to public health (Davis & Cornwell, 2008; Davis, 2010).

2.2.2.5 Iron and manganese

The impact of Iron (Fe) and (Mg) ions in consumable water is a bitter taste even in very low quantities (Alley, 2007; Davis, 2010). In groundwater solutions, these metals are frequently present as ions of ferrous (Fe^{2+}) and magnesium (Mg^{2+}). Air exposure to these ions leads to forming of the insoluble ferric (Fe^{3+}) and manganic (Mg^{3+}), transferring water to be murky and generally unsuitable to human beings (Alley, 2007). Brown or black stains could be seen on clothing and plumbing equipment as a result of these ions. These ions could be quantitatively measured using different techniques, including inductively coupled plasma, flame atomic absorption spectrometry, and cold vapor atomic absorption spectrometry (Alley, 2007).

2.2.2.6 Hardness

The term "hardness" is utilized to describe the characteristics of highly mineralized waters (Alley, 2007). Different water issues could be noticed when dissolved minerals are present in water including reducing the lather of soap and raising the scale in tubes of hot water (Davis, 2010).

Hardness in natural water occurs due to ions of calcium (Ca^{2+}) and magnesium (Mg^{2+}) (Spellman, 2017). When water flows through soil and

rock, it could carry these ions. They could be present in various forms including bicarbonates, sulfates, and occasionally chlorides and nitrates (Alley, 2007; Davis & Cornwell, 2008). The hardness of groundwater is more than that of surface water, and it could be sorted into two types:

- Temporary hardness: it is caused by carbonates and bicarbonates that could be dissolved by heating water up to 100 ^{o}C.
- Permanent hardness: the remaining permanent hardness after the process of boiling water could be attributed to the sulfates and chlorides.

2.3 Water Quality Index (WQI)

Water quality refers to the features of water that are determined by its composition. The term Water quality (WQ) refers to the chemical, physical and biological characteristics of water usually with respect to its suitability for designated use (Johnson et al., 1997). Assessing the quality of water helps in establishing if water is suitable to be consumed or safe for the environment. It is commonly done by comparing the water's physicochemical and biological qualities or variables with a list of regulations (Chapman, 2021). The parameters of the WQ are utilized as a guide to a group of regulations depending on the required water utilization, which is widely categorized into industrial/domestic usage, consumption of human beings, and recuperation (in the climate /ecosystem, to maintain the health of human being as well as aqueous life). Standards for WQ are mainly utilized to safeguard various water uses. Each of these approved uses has substantially different standards from the others. For instance, drinkable water has stricter requirements than water utilized for industrial and agricultural purposes (home water should be free of hazardous materials and organisms to prevent waterborne infections)

(Ouyang, 2005). Both public health and aquatic life have a lot to do with water quality assessment. Water quality greatly affects water supply and regularly affects supply alternatives (Lodder et al., 2010). Minimizing possible threats to public health requires determining the source(s) of contamination and creating effective control plans (Carroll et al., 2006). Furthermore, data gathered from evaluating and monitoring water quality provide empirical support for environmental and health decision-making. Managing water resources requires a good knowledge of water quality because it could indicate alerts in the physicochemical composition of the water status (Cambers & Ghina, 2005). The (WQI), first established by Horton (Tyagi et al., 2013), is a mathematical formula that combines various water quality parameters to provide a single value that may be utilized to describe WQ. The index describes the quality of a body of water, such as a lake, river, or ocean, utilizing a few of the often-used water metrics. The WQI is based on the measurement of various WQ characteristics, offering a system for delivering a numerical expression for defining water quality that is a cumulatively derived stream (Kankal et al., 2012). Data of WQ is decreasing due to the quality of water to a known scale and they are combined together to a number according to a specified calculation model or method. WQI is calculated from the standpoint of whether surface and groundwater are appropriate for their intended uses, and it exhibits the combined influence of various water quality factors. The usage of the water quality index has a number of advantages and benefits (Akter et al., 2016) involving:

1. Reducing the required comparison factors of the water quality for a particular use.
2. Giving one value that clarifies the total WQ at a particular place and time.

3. Characterization of the dynamics of place and time in water quality.
4. Giving assurances regarding the safety of a water body to those who use it, such as those who use it as a homeland for aquatic life, irrigation water for farming and raising cattle, for enjoyment and aesthetic purposes, or as a supply of drinking water.
5. It is particularly effective in monitoring water quality.
6. It offers a way to compare various rivers and sampling locations.
7. The use of indices is one of the clearest ways to explain the classification of water quality to members of the public or those in positions of power.
8. It turns a complicated dataset into information that is simple to grasp and use.
9. The specific index value, which is produced from a number of characteristics, offers crucial information regarding water quality that is simple for non-technical people to understand.
10. The index is a helpful instrument for informing the general public and legislative decision-makers on water quality.

The Weighted Arithmetic Water Quality Index Method offers data on how well a body of water is regarded. This technique makes advantage of the most widely used indicators of water quality. This method makes it possible to take into account a variety of physicochemical factors, an aspect that supports getting more precise results aimed to give useful information about the river's true quality. There are numerous benefits to this approach; that will go through a few of them, and there are also some of its drawbacks (Iticescu et al., 2013; Boah et al., 2015; Oni & Fasakin, 2016).

2.4 Remote Sensing Technology (RS)

The challenges of traditional water quality monitoring can be clearly addressed with remote sensing. In this research, it starts with a description of how light interacts with matter since remote sensing for water quality relies on sunlight reflected by water and its components. In a medium like air or water, light can be absorbed, reflected, and scattered (Lehmann et al., 2017). The amount of incoming solar radiation that is scattered back and reflected into a light-sensing device is the remotely perceived signal in Figure (2.1).

Light can enter the sensor through a wide range of channels. First, the atmosphere absorbs and scatters light from the sun. Some of this light enters the sensor's field of view but does not interact with the water. Direct sunlight and diffuse light, or light that has been spread by the atmosphere, are both types of light that reach the water's surface (Olmanson et al., 2015). Some light bounces back at the water's surface and can come to the sensor as the sun glint. When the light finally penetrates below the air-water boundary, water molecules and other elements present in the water absorb and disperse the light. Again, a satellite sensor can only measure the portion of this light that travels through the atmosphere and is dispersed back into the sensor's line of sight. It is necessary to account for air absorption and scattering with the purpose of assessing the optical characteristics of the water. An estimate of surface reflectance is obtained after accounting for the atmosphere and solar glint, a process known as atmospheric correction (Olmanson et al., 2015).

The ratio of light leaving the water's surface and coming from the sun is known as surface reflectance. By comparing the light coming up from the ocean to the sunlight falling down, variations in the strength and spectrum of

the incoming solar radiation are taken into consideration (Gholizadeh et al., 2016).

It is important to keep in mind that each light-related quantity is computed over a set of wavelengths within the spectral band, which are specific to the sensor's construction. After remote sensing has determined the spectrum of light reflected and scattered from the water column, calculated the amounts of constituent matter inside the water column and evaluate the water quality by applying retrieval techniques (i.e., spectral reflectance). Retrieval algorithms can be created in a variety of ways, from simple empirical relationships between in-situ samples and radiant reflectance at certain wavelengths to spectral additive models based on radiative transfer theory (Lehmann et al., 2017).

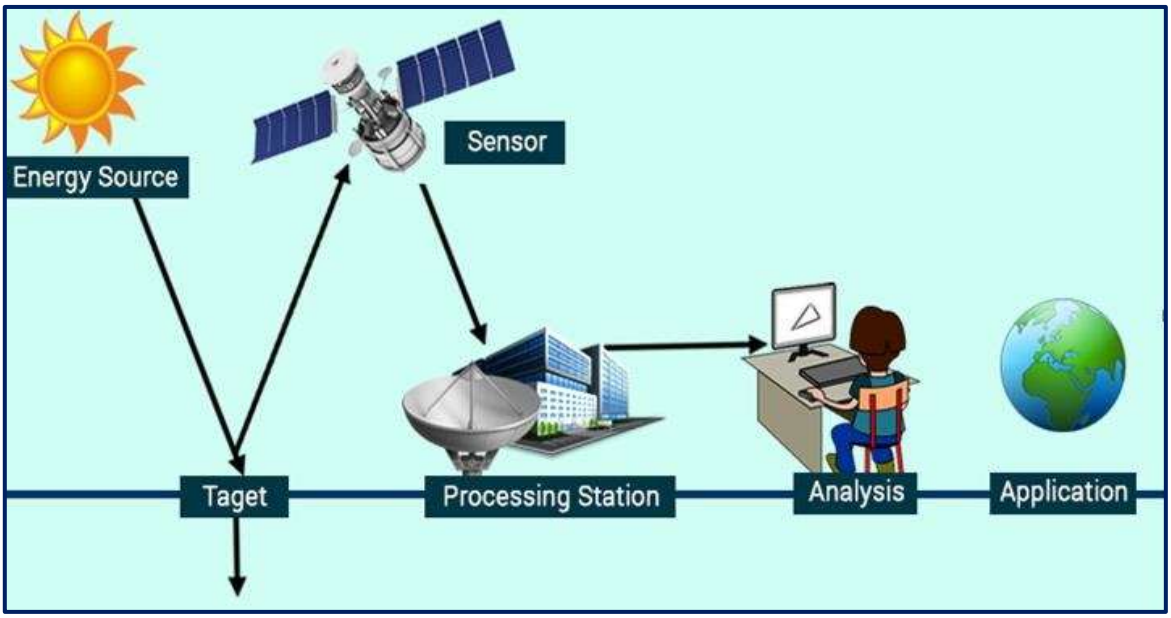

Figure (2.1): A step-by-step representation of the Remote Sensing Process for obtaining outputs (Source:https://www.google. remotesensing).

2.4.1 Landsat Collection 2 Level-2

The significant improvement in the absolute geolocation accuracy of the global ground reference dataset in Collection 2 improves the interoperability of the Landsat archive over time. Collection 2 also includes new worldwide digital elevation modeling sources, as well as revisions to calibration and validation. Landsat Level-1 data for all sensors since 1972 is included in Collection 2. Global Level-2 surface reflectance and surface temperature scene-based products for Landsat data from 1982 to the present are available (Nelson, 2011). Figure (2.2) depicts the differences between each level and collection, collection 2 from Landsat 8 Image of the top of atmospheric reflectance at level one, an atmospherically corrected surface reflectance picture from Landsat 8 Collection 2 level-2 and a picture of the surface temperature from Landsat 8 Collection 2. The fraction of incoming solar radiation reflected from the Earth's surface to the Landsat sensor is measured as surface reflectance (unit less). Surface reflectance algorithms such as LEDAPS (Landsat Ecosystem Disturbance Adaptive Processing System) and LaSRC (Land Surface Reflectance Code) account for the temporally, geographically, and spectrally variable scattering and absorbing effects of atmospheric gases, aerosols, and water vapor, which is required to accurately characterize the Earth's land surface.

All Landsat Level-1 data are processed and calibrated consistently based on Landsat Collections, and the origin of the data's quality can be traced. Landsat Collection 2 includes enhancements that make use of current advances in data processing, algorithm development, data access, and distribution capabilities. Landsat Level-1 data for all sensors since 1972 are

included in Collection 2, as are global Level-2 surface reflectance and surface temperature scene-based outputs for data obtained from 1982, beginning with the Landsat Thematic Mapper sensor era. Table (2.1) depicts the link between bands, wavelengths, and color reflection in the solar spectrum (Nelson, 2011).

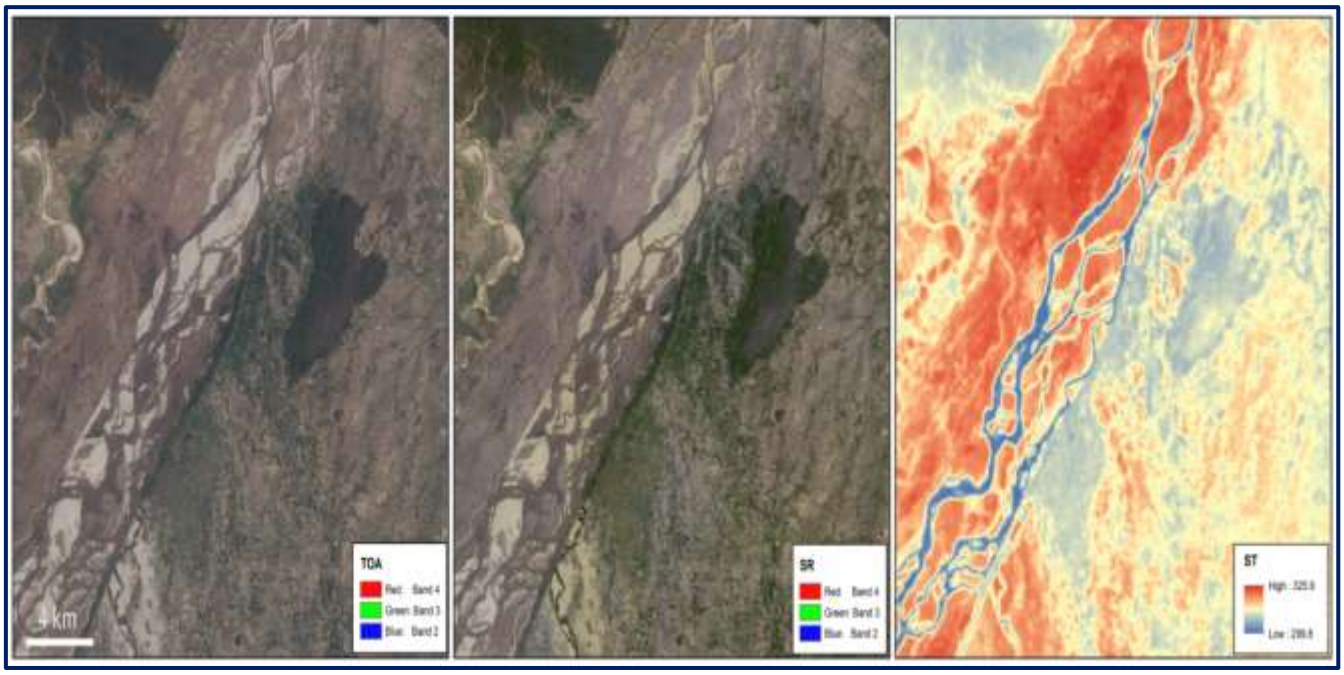

Figure (2.2): depicts the differences between each level and collection (Sources/Usage: Public Domain).

Table (2.1): Bands of Landsat-8 imagery (level-2) examined for this study (Danbara, 2014).

Band	Wavelength (µm)	Band center (nm)	Resolution (meters)
Band 1 - Coastal aerosol	0.43-0.45	443	30
Band 2 - Blue	0.45-0.51	482	30
Band 3 - Green	0.53-0.59	562	30
Band 4 - Red	0.64-0.67	655	30
Band 5 - Near Infrared (NIR)	0.85-0.88	865	30
Band 6 - SWIR 1	1.57-1.65	1610	30
Band 7 - SWIR 2	2.11-2.29	2200	30

Band 8 - Panchromatic	0.50-0.68	590	15
Band 9 - Cirrus	1.36-1.38	1372	30
Band 10 - Thermal Infrared (TIRS) 1	10.60-11.19	10800	100
Band 11 - Thermal Infrared (TIRS) 2	11.50-12.51	12000	100

2.5 Geographic Information Systems (GIS)

A technology called a Geographical Information System (GIS) enables the gathering and use of geographic data to enhance improvement in the water quality field. A digital map is frequently more beneficial than a paper one since it contains data origins for analyzing information and presenting them in graphical form (Huisman & de By, 2009).

GIS software allows users to synthesize vast volumes of heterogeneous data by merging distinct information layers to better organize and restore the data. Geographical information systems are used for scientific research, resource and asset management, EIA, city planning, earth science, criminology, history, economics, marketing, and logistics. By combining information on soil, terrain, and rainfall to determine the suitable biological regions in terms of size and location, agricultural planners, for instance, could use geographic data to identify the best locations for location-specific crop planning. Overlays with property ownership, transportation, infrastructure, labor availability, and distance to market centers could all be included in the final output (Huisman & de By, 2009).

2.5.1 Data representation

Digital representations of real-world elements like roadways, land use, and elevation are found in GIS data. In reality, abstractions could be divided into two types: continuous fields (like the quantity of rain or height) and

discrete objects (such as a house). For both abstractions, there are two major approaches for storing data in a GIS: Vector and Raster.

Raster: In essence, a raster data type is any sort of digital image. Anyone familiar with digital photography will recognize the pixel as the image's smallest individual unit. A combination of these pixels will produce an image that is distinct from the vector model's regularly used scalable vector graphics. While a digital picture is concerned with the output as a representation of reality, the raster data type in a photograph or art transmitted to the computer will reflect an abstraction of reality (Huisman & de By, 2009; Longley et al., 2005).

Other raster data sets will include height, a DEM (Digital Elevation Model), or Spectral reflectance. Data of raster could be an image (raster images) having a color value in each pixel. Additional variables may be discrete, like land uses, continuous, like temperature, or none, if no data are obtainable, for each cell. A raster cell can be expanded even if it only stores one value by using raster bands to represent the RGB (red, green, and blue) colors, color mappings (which convert theme codes into RGB values), or a table featured with one row for each variable value. The width of each cell represents units of ground to indicate the raster data resolution.

Vector: As seen in Figure (2.3), in a straightforward vector map, wells are represented by points, rivers by lines, and the lake by a polygon that makes use of each vector element. Geometric forms are commonly used to represent geographic features as vectors in a GIS. Shapefiles are specifically referred to in the popular ESRI Arc line of tools. Distinct styles of geometry better express different geographical features (Longley et al., 2005; Huisman & de By, 2009).

Points of geographical qualities that can best be stated by a single grid reference; in other words, simple location, and zero-dimensional points are used. For example, well locations, peak heights, points of interest, or trailheads. Of these file types, points communicate the least amount of information (Longley et al., 2005).

Polylines or lines, rivers, highways, railroads, trails, and topographic lines are all examples of one-dimensional lines or polylines. Polygons two-dimensional polygons are used to represent geographical features that cover a specific area of the earth's surface. Lakes, park boundaries, structures, city boundaries, and land usage are examples of such features (Longley et al., 2005). The most file data amount is involved in Polygons as shown in Figure (2.4).

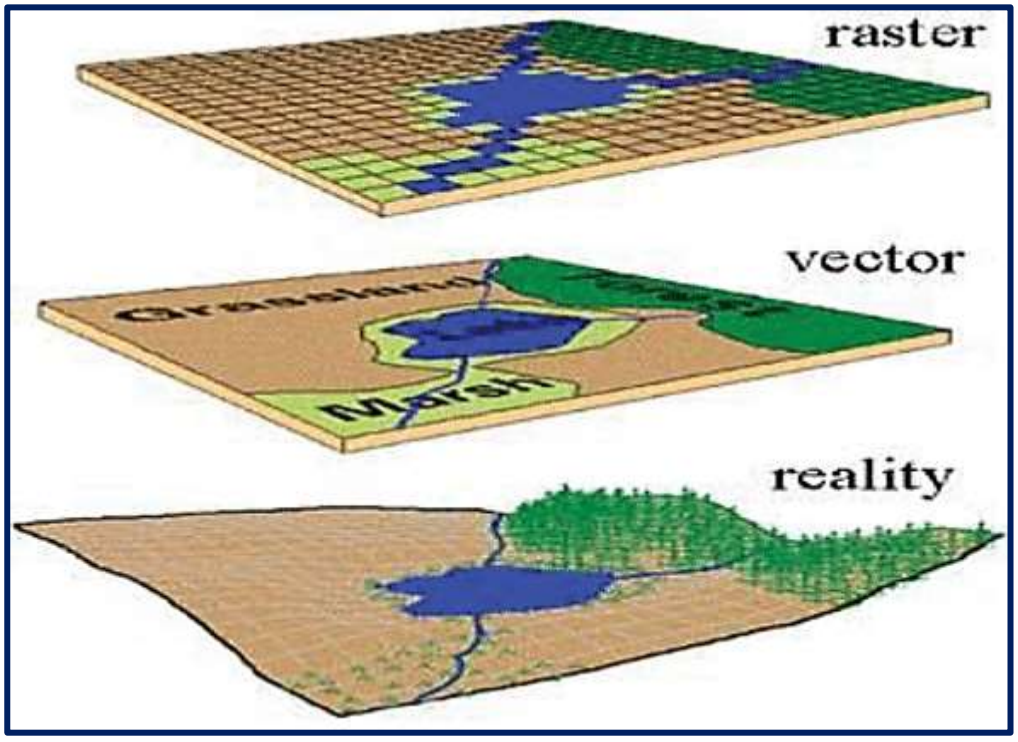

Figure (2.3): Example of vector data vs. raster data (source:http://2.bp.blogspot.com).

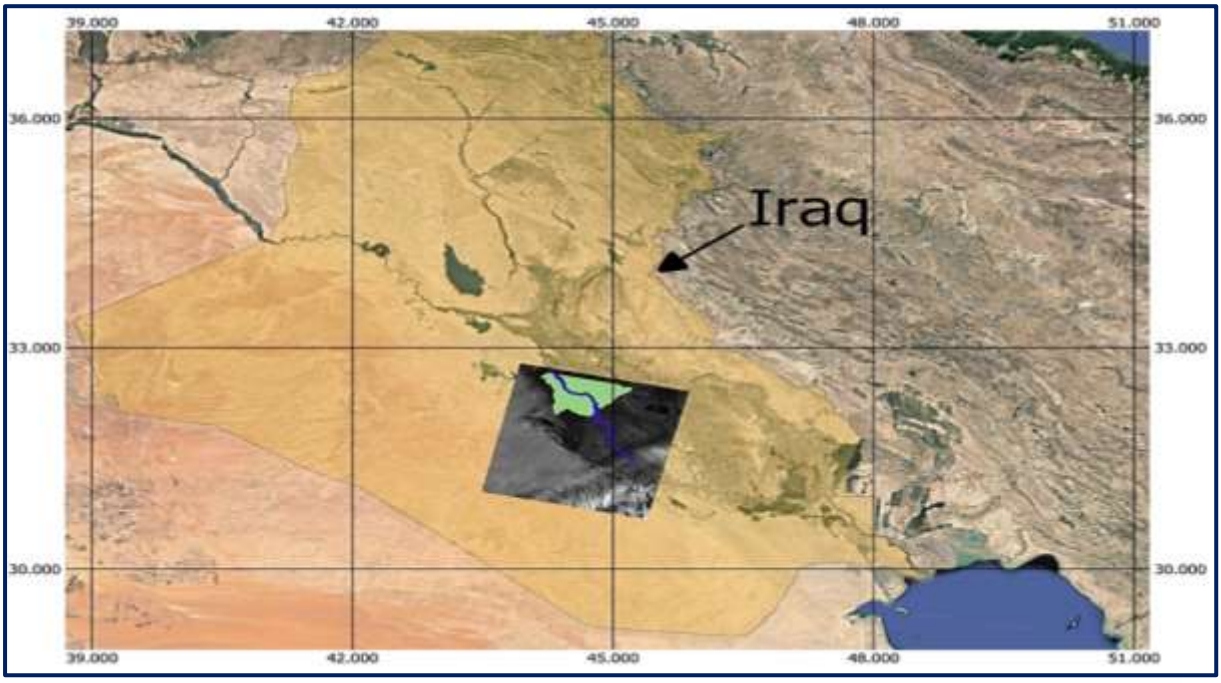

Figure (2.4): An example of Babylon Governorate is polygon data.

2.6 GIS-based Inverse Distance Weighted (IDW) interpolation

Managing sources of water is beneficial in divesting, safeguarding, functional use, and quality control. Areas with important concerns are usually assessed in terms of water quality, even though operations linked to assessing and managing quantity regarding river flow and water resource organization are prioritized at the watershed level of contamination. Depending on a water quality information system and spatial analysis utilizing Inverse Distance Weighted (IDW) interpolation, water quality indicators were mapped using a Geographical Information System (GIS) (Khouni et al., 2021).

Spatial interpolation algorithms are used in GIS to anticipate attribute values at unsampled sites in order to provide spatially continuous data, which are separated into two groups: deterministic interpolation methods and geo-statistical interpolation methods (Qu et al., 2017). The most often used interpolation techniques include IDW, kriging, Spline, and Trend

interpolations (Nas, 2009; Alaguraja et al., 2010). The selection of interpolation models must be based on the individual research objectives and characteristics of the study objects (Qiao et al., 2018). It has, however, proved inconsistent in terms of the potential superiority of one interpolation approach over another (Gong et al., 2014). Thus, interpolation methods for example IDW and kriging have been widely utilized in water assessment and contamination mapping (Mirzaei & Sakizadeh, 2016). Actually, Inverse Distance Weighted (IDW) interpolation and kriging have been utilized for different backgrounds.

This methodology is an exact method with a linear combination set of data, and the name "inverse" signifies that when compared to distant sample points, nearby points have higher weights and have a greater influence on the calculation of missing or unknown points (Nusret & Dug, 2012). Based on this premise, IDW could improve river basin management systems' monitoring and evaluation capabilities, resulting in better pollution monitoring and control (Arslan, 2001).

2.7 Literature review: Previous related studies

The use of water quality index, in situ- measurement, remote sensing, and GIS modeling in water monitoring with management, had been long recognized. Here are the several main recent previous studies which have considered the issue of this study.

Abayazid & El-Gamal (2017) discovered the utility of using satellite-based methodologies to determine water purity trends. In the study area (coastal section of the Nile delta), the Geographical Information System (GIS) and Landsat 7 satellite are used. Turbidity and Total Suspended Solids

(TSS) are two indicators of water purity in the Nile delta's coastal region. The retrieval technique featured visible and near-infrared bands, as well as a sample station. For calibration, turbidity and suspended solids data from distributed sampling stations from 2008 to 2011 were used (R^2 values of 0.92 and 0.70, respectively). Validation of the developed algorithm, using data from the years 2012 and 2013, proved successful estimations (R^2 were 0.78 and 0.65 for turbidity and suspended solids, respectively). The study establishes a predictive relationship with acceptable accuracy results to follow changes in clarity indications along the delta coastline, allowing the development of a wide spatial and temporal database.

Noori et al. (2017) investigate the quality of water and the concentration of various parameters using Water Quality Index (WQI) and Geographic Information System (GIS) techniques, which can provide an accurate and adequate evaluation while also indicating pollution, saving required time, water quality management, and decision-making. As a result, WQI methodologies were used in this study to examine, compare, and judge the appropriateness of the Euphrates River in various areas within Iraqi territory for drinking purposes. The analysis includes several WQ parameters: pH, Temperature, Dissolved Oxygen, Biochemical Oxygen Demand, Orthophosphate, Nitrate, Calcium, Magnesium, Total Hardness, Potassium, Sodium, Sulfate, Chloride, Total Dissolved Solids, Electrical Conductivity and Alkalinity were utilized to WQI determination. These factors were taken at the intakes of five water treatment plants (Al-Kifl, Al-Kufa, Al- Shamiya, Al-Manathera, and Al-Shannafiya) for the years 2015 and 2016. According to the Weighted Arithmetic WQI, the river quality in the research area ranges from good to extremely poor. According to the findings of this study, the

influence of human activity, sewage disposal, and industrial wastes in the river were severe on the majority of the criteria. The WQI categorization findings were integrated with "ArcGIS" software to create layers and spatial distribution maps of these indices, as well as to depict the pollution zones in the river. The data were interpreted using the spatial analyst tool and the Inverse Distance Weighted (IDW) interpolation method.

Al-Bayati et al. (2018) discovered through investigated field Spector-radiometers by developing relationships between water quality parameters and spectral data. The study included 20 stations for sampling on Hilla River, Babylon Province, Iraq to measure the physical and chemical parameters (pH, TSS, EC, TDS, and Cl). Landsat 8 satellite images were employed to be linked with field data statistically for only one day of investigation. It has been found that apposite spectral ranges and bands for water quality parameters, EC and Cl associated with a spectra range of (0.851–0.87) μm and (2.107–2.294) μm, respectively. Also, (TSS and Turb), and TDS at a spectral range of (0.533–0.590) μm and (1.566–1.561) μm, respectively.

González-Márquez et al. (2018) created empirical models to estimate water quality parameters to demonstrate the benefits of satellite remote sensing applications in the characterization of coastal waterways. The study site was Playa Colorada Bay in northwest Mexico. On-site and laboratory characterizations of phosphates (PO_4^{-3}), electrical conductivity (EC), total suspended solids (TSS), turbidity, and pH of water were performed during two seasons of the year. Samplings were chosen to correspond with Landsat 8 satellite overpasses in the study area. The models were created using a step-by-step linear regression technique, with water quality metrics and their

logarithms serving as dependent variables and corrected reflectance values from Landsat images serving as independent variables. The water quality models developed showed coefficients of determination (R^2) ranging from 0.637 to 0.955, demonstrating the practicality of using Landsat 8 photos to characterize water quality parameters in Playa Colorada Bay.

Al-Ridah et al. (2020) used the water quality index of the Canadian Council of Ministers of the Environment (CCME WQI) and the Weighted Arithmetic models to assess the water quality for drinking. The outcomes of these two models were compared as well. Four water treatment facilities on the Hilla River, a tributary of the Euphrates River in central Iraq, were included in the study area. From January to December 2018, water samples were taken on a monthly basis, and nine parameters of raw water were examined, such as turbidity (Tur), pH, electric conductivity (EC), alkalinity (Alk), total hardness (TH), calcium (Ca^{-2}), magnesium (Mg^{+2}), chloride (Cl^{-1}), and total dissolved solids (TDS). For all stations, the Weighted Arithmetic model showed that the raw water quality was categorized from "severely polluted" to "unfit for human consumption". However, the CCME WQI method categorized the river water as "fair" and treated water as "good" for drinking. The comparison results of the two models showed that CCME WQI gave a greater water quality value than the value from the other method, or the CCME WQI was possibly considered more flexible.

Chabuk et al. (2020) assessed the water quality of the Tigris River using the water quality index method and GIS software. Twelve parameters (Ca^{+2}, Mg^{+2}, Na^{+1}, K^{+1}, Cl^{-1}, SO^{-2}_4, HCO_3, TH, TDS, BOD_5, NO_3, and EC) were taken from 14 stations along the river. The weighted arithmetic method was applied to compute the water quality index (WQI). The interpolation

method (IDW) was applied in ArcGIS 10.5 to produce the prediction maps for 12 parameters along the Tigris River during the wet and dry seasons in 2016. The regression prediction was applied on three stations in the Tigris River between observed values and predicted values, from the prediction maps, in both seasons. The results showed that the regression prediction for all parameters was given the acceptable values of the determination coefficient (R^2). Additionally, the state of water quality for the Tigris River was degraded downstream of the Tigris River, especially at the station (8) in Aziziyah in the wet and dry seasons, and increased degradation clearly at Qurnah (Basrah province) in the south of Iraq. This paper considers the whole length of the Tigris River for the study. This is important to give comprehensive knowledge about the contamination reality of the river. Such that it becomes easier to understand the problem of contamination, analyze it, and then find suitable treatments and solutions.

Abbas et al. (2021) utilized Landsat 8 satellite images to estimate TDS, EC, NO3, and pH. These models offer the capability of evaluating the water quality parameters dispersal lengthways of the Shatt Al-Arab River in the south of Iraq. Results built on R-squared, RMSE, SE, and p-value highlighted the feasibility of these models for the study area. The four bands (band 2, band 3, band 4, and band 5) of Landsat 8 were used to develop the water quality models. EC models were estimated for the winter, summer, and autumn seasons based on band 5 for winter and band 4 for the summer and autumn seasons. For NO_3 models, it was linked with band 4, band 3, and band 2 for winter, spring, and summer, respectively. pH models were developed depending on a single band for all seasons (band 4, band 5, band 4, and band 5 for winter, spring, summer, and autumn, respectively). For the remaining

parameter (TDS), it was a too more complex model in this study. One of them was estimated by combining band 3, band 4, and band 5 in terms of band ratios.

Al-Zubaidi et al. (2021) utilized R-studio software and data from Sawa Lake in Iraq, and an integrated linear regression strategy for simulating dissolved oxygen in salt lakes was developed and verified. In the face of WQ data limitations, the technique aids in understanding and assessing salty aquatic environments. Selecting essential WQ parameters with a significant statistical relationship to dissolved oxygen was part of the strategy. The validation approach was linked with the model in order to make the regression construction simpler. Linearity, homogeneity, normality, outliers, and significant data points were all investigated. The simulation approach might also show the link between the selected WQ metrics and other minor variables. The results of the statistical study revealed that total dissolved solids affect dissolved oxygen in salt lakes. With an R-squared of 90.73 percent and a p-value of 1.08E-06, the model represented dissolved oxygen. The established dissolved oxygen model was shown to be significantly influenced by temperature. Furthermore, the model simulation revealed that salt melting surrounding the lake increased total dissolved solids in the lake water as a result of temperature fluctuations during the year cycle.

Hossain et al. (2021) observed the water quality in the Tennessee River might benefit greatly from the use of satellite remote sensing technology, which has been utilized successfully for many years to investigate indicators of surface WQ. This work developed a numerical model to estimate turbidity for the Tennessee River and its tributaries in Southeast Tennessee using Landsat 8 satellite data and nearly real-time on-site observations. The

findings show that turbidity in these water bodies may be accurately estimated using a nonlinear regression-based numerical model based on Landsat 8 spectral Band 4 (red) surface reflectance observations. The root means square error (RMSE) and coefficient of determination (R^2) values for the accurate evaluation of the estimated turbidity were as high as 1.41 NTU and 0.97, respectively.

Khouni et al. (2021) found that the mapping of water quality indicators in the watershed of Wadi El Bey, Tunisia, was made possible by the use of a Geographical Information System (GIS) based on a water quality information system and spatial analysis with Inverse Distance Weighted (IDW) interpolation. WQ indicators were tracked from 2012 to 2016 using 13 sampling stations, spanning the entire hydrological season. Maps of spatiotemporal fluctuations in various parameters, including temperature, pH, chemical oxygen demand, biochemical oxygen demand, and total suspended solids, were used to assess water quality across monitoring stations and identify causes of water pollution along river courses. The creation of water quality maps will increase monitoring, as well as the enforcement of norms and laws aimed at improved pollution management and control. Patterns were clearly described; procedures were statistically valid; and IDW predictions were made with good accuracy. Thus, the geographical distribution maps demonstrate that agricultural activities, household, and industrial discharges are major sources of water pollution in the research area, particularly in the Grombalia industrial zone.

Chabuk et al. (2022) applied the groundwater quality index model (GWQI) to calculate groundwater quality and its suitability for consumption before usage. An evaluation of the groundwater in the research

area was done in comparison to both regional and global criteria. Utilizing the GWQI and GIS techniques, groundwater distribution maps have been created for drinking purposes. Researchers will be able to identify the GWQI and learn more about its ranges and distribution in the study region thanks to the maps that have been developed. Twelve water quality indicators taken in 56 stations in Hilla City, Iraq was coupled with the IDW technique and GIS to develop interpolation maps for groundwater quality for consumption uses. The parameters utilized in the weighted arithmetic method to calculate the GWQI for drinking uses are Ca^{+2}, Mg^{+2}, Na^{+1}, k^{+2}, Cl^{-1}, SO_4, HCO_3, TH, TDS, NO_3, and EC. Based on the WQI values, six classifications on the producer map of groundwater quality ranged from excellent to extremely contaminated. For each variable, Utilizing the prediction method IDW, the prediction map was created as a distribution map to cover the entire study area.

CHAPTER THREE

Data & Methodology

3.1 Study area description and field data

Hilla City is located in the center of Iraq on the Hilla River. The river is a branch of the Euphrates River, 100 km south of Baghdad, as shown in Figure (3.1). Hilla City is the capital of Babylon Province where the ancient city of Babylon is located. It is located in a predominantly agricultural region that is heavily irrigated with water supplied by the Hilla River, producing a wide range of crops, fruit, and textiles. Figure (3.1) shows the present study area. It is situated between, Longitude (44º26º55" & 44º31º10") E and Latitude (32º26º30" & 32º31º33") N. **Five stations** were selected along the Hilla River as follows:

Station 1 (S1): The new Hilla Water Treatment Plant situates in the center of Hilla City in the Zuweir area. It was built in 1991 and produces about 6000 m^3/hr for Hilla City consumption. **Station 2 (S2):** The old Al-Tayarah Water Treatment Plant locates in the center of Al-Hilla City in the Al-Tayarah area. It was built in 1972 and produces about 1200 (m^3/hr.) for the Hilla City consumption too. **Station 3 (S3):** Al-Hashmiya Water Project with a capacity of 6000 (m^3) to serve the districts of Al-Hashmiya, Al-Shuwaili, Al-Qasim and Al-Tali`ah in the province of Babylon. **Station 4 (S4):** Al-Atayej Project locates in the city center (in the tourist area), and it produces 900 (m^3/hr.). **Station 5 (S5):** The Annanah Water Project is located on the right bank of the Hilla River near the village of Annanah as shown in Table (4.1).

Table (3.1): Sample station along the Hilla River

Station	Sample
The new Hilla Water Treatment Plant	**S1**
The old Al-Tayarah Water Treatment Plant	**S2**
Al-Hashmiya Water Project	**S3**
Al-Atayej Water Project	**S4**
The Annanah Water Project	**S5**

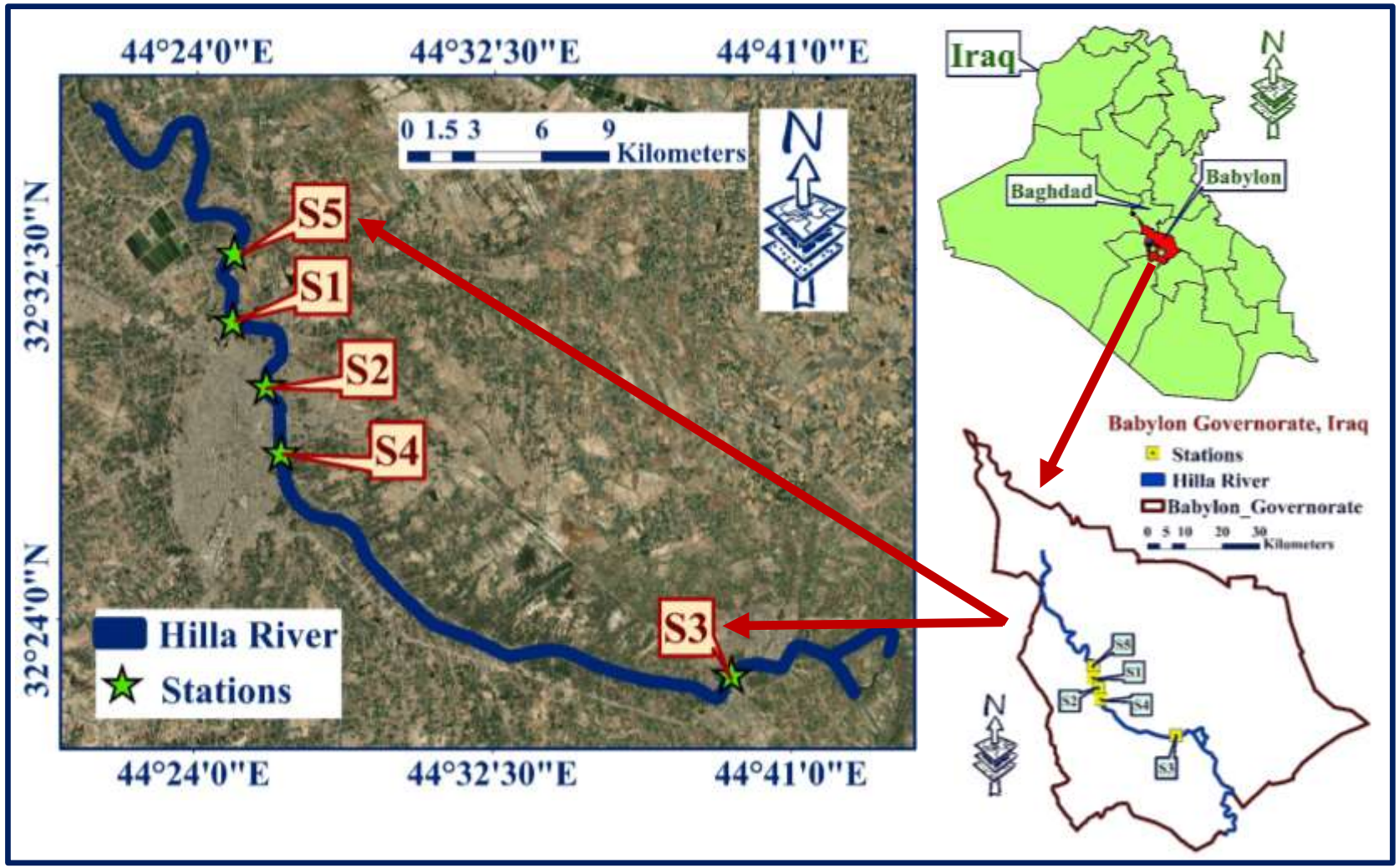

Figure (3.1): Study area and sampling location.

Samples were collected sparsely by the Ministry of Water Resources Department of Water Resources in Babylon Governorate, Iraq at each sampling station from January 2016 to June 2021. The collection process has included taking one or two samples monthly during this period. Many water quality parameters were measured from 2016 to 2021 including turbidity (Turb), electric conductivity (EC), hydrogen ions (pH), total suspended solids (TSS), chloride (Cl^-), Sodium (Na^+), sulfate (SO_4^{-2}), Alkalinity (ALK), total hardness (TH), magnesium (Mg^{+2}), calcium (Ca^{+2}), total dissolved solids (TDS) and potassium (K).

3.2 Remote sensing data

The satellite images were taken from Landsat 8. The images were obtained over the study site by the Landsat 8 (collection 2 level 2) satellite from January 2016 to June 2021. To explore the relationships between WQ indicators and spectral data from the satellite, Landsat 8 senses were acquired and downloaded from the United States Geological Survey (USGS) website at the same sampling time and for the entire study period, covering the sampling process spatially and temporally, as shown in Figure (3.1). Hilla City lies around path 168 and row 38 of Landsat 8 satellite orbit. The GIS analysis was carried out utilizing QGIS software to display the spatial distribution of the spectral bands to be correlated with field data. The boundary of the river was digitized to make the polygon shape of the river extract the river water. The features of Landsat 8 images are provided in Table (3.2) from January 2016 to December 2016 and the features of Landsat 8 imagery for the rest of the study years are in Appendix A.

Table (3.2): Landsat-8 sense details used in this study for 2016.

Date	Landsat-8 sense identifier	Date Acquired	Sensor identifier
2016	LC81680382016024LGN01	1/24/2016	**OLI_TIRS**
	LC81680382016056LGN01	2/25/2016	
	LC81680382016072LGN01	3/12/2016	
	LC81680382016104LGN01	4/13/2016	
	LC81680382016136LGN01	5/15/2016	
	LC81680382016168LGN01	6/16/2016	
	LC81680382016184LGN01	7/2/2016	
	LC81680382016232LGN01	8/19/2016	
	LC81680382016264LGN01	9/20/2016	
	LC81680382016296LGN01	10/22/2016	
	LC81680382016328LGN01	11/23/2016	
	LC81680382016360LGN01	12/25/2016	

3.3 Methodology

The general framework of this study was summarized in Figure (3.2) which is the conceptual model of the study. WQI was calculated from in-situ water quality data for the five sampling stations on the Hilla River, then a linear regression model was found between the WQI and the water quality parameters. WQI from the five sampling stations and the related images from the Landsat 8 satellites were linked by linear models statistically, and WQI was split into two sets train dataset and the test dataset. The Landsat 8 images were collected 2 level 2 (surface reflectance) that contains 8 spectral bands (1 to 7 and 10) (Hereher et al., 2010; Al-Masaodi & Al-Zubaidi, 2021).

In addition, in-situ water quality data from the five sampling stations and the related images from the Landsat 8 satellites were linked by linear models statistically, and in-situ data were split into two sets train dataset and test dataset. After extracting the surface reflectance of each band from Landsat senses, R-Studio software was utilized to develop linear models between the train water quality parameters and WQI with the spectral bands. The GIS analysis was

carried out utilizing QGIS software in order to display the spatial and temporal distribution of the WQI. Finally, the test dataset was utilized to validate the developed model's robustness.

3.4 Data exploration methods

3.4.1 Water Quality Index (WQI)

Horton (1965) introduced and defined WQI as a calculated form of WQI choosing, ranking, and mixing the important physical, chemical, and biological factors of water in a simple way in the mid-twentieth century (Chabuk et al., 2022). Water quality is an important criterion in matching the demand and supply of water and gives expression simpler and easier to interpret data observer. Several Water Quality Indicators (WQI) were utilized to evaluate the quality of surface water. However, the well-known one is the Arithmetic Weighted Water Quality Index (WQI).

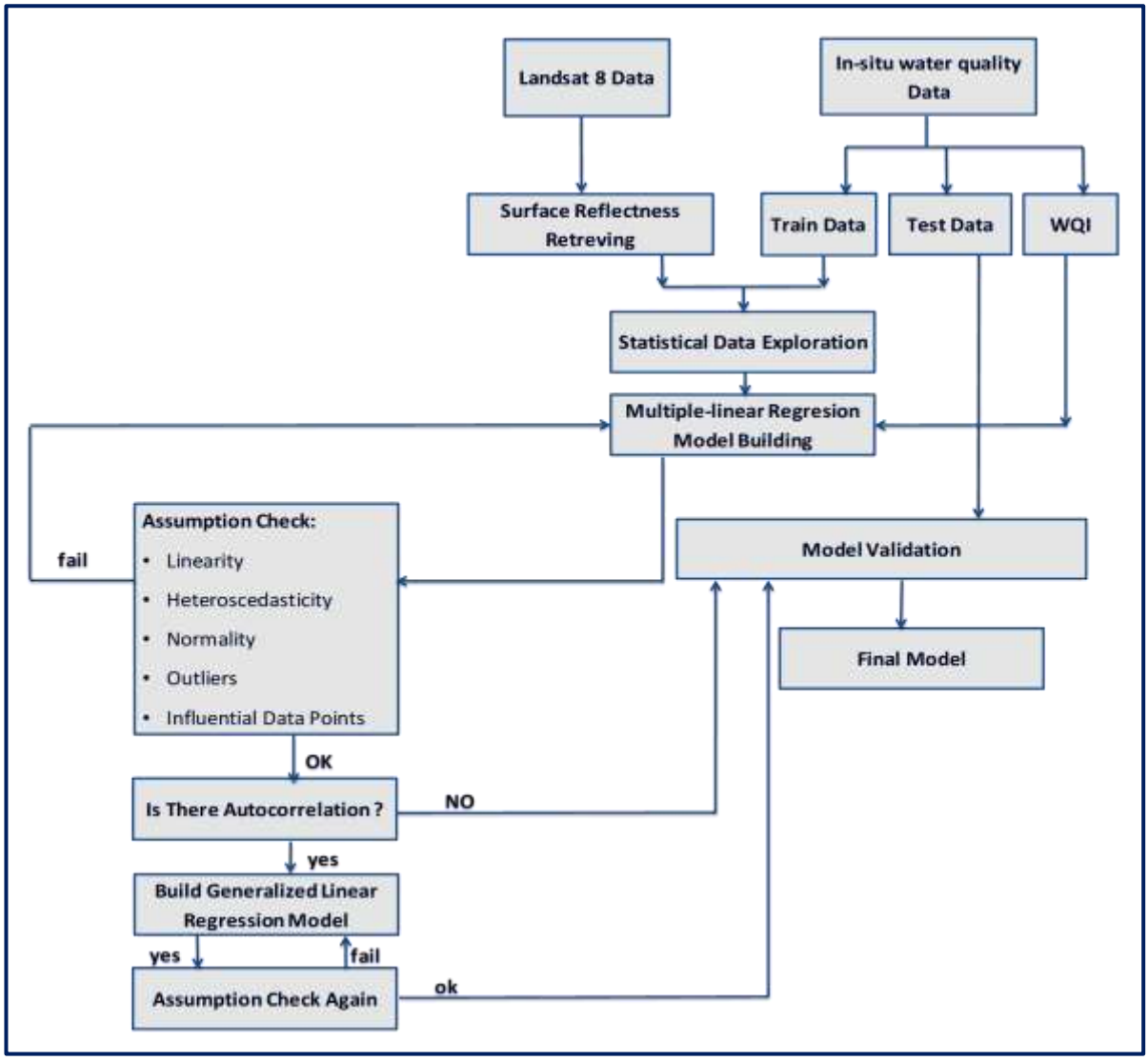

Figure (3.2): Data processing flowchart.

3.4.1.1 Arithmetic Weighted Water Quality Index (WQI)

This method categorized the water quality according to the degree of purity, by using the most normally measured water quality. The method had been widely used by various scientists (Pathak et al., 2015), and the calculation of the water quality index (WQI) was made by using the following equation (Alobaidy et al., 2010; Kankal et al., 2012).

$$\mathbf{WQI} = \frac{\sum_{i=1}^{n} \mathbf{W_i q_i}}{\sum_{i=1}^{n} \mathbf{W_i}} \qquad \mathbf{(3.1)}$$

Where: n is the number of variables or parameters, W_i is the relative weight of the i^{th} parameter, q_i is the water quality rating of the i^{th} parameter and *Wi* is the unit weight of the water quality parameter where:

$$\mathbf{Wi = k/si} \qquad \mathbf{(3.2)}$$

Where: s_i is the standard parameter value, and k is the constant of proportionality, and it is assumed as:

$$\mathbf{K} = \frac{\mathbf{1}}{\frac{\mathbf{1}}{\mathbf{vs_1}} + \frac{\mathbf{1}}{\mathbf{vs_2}} + \cdots + \frac{\mathbf{1}}{\mathbf{vs_n}}} \qquad \mathbf{(3.3)}$$

Where: vsn: Standard permissible value of i^{th} factor according to the Iraqi standard as shown in Table (3.3). The value of q_i is estimated by utilizing the following equation:

$$\mathbf{q_i = 100\ [(Va - Vi)\ /(Si - Vi)]} \qquad \mathbf{(3.4)}$$

Va: average water sample values at one station for twelve months

Vi: ideal value for pure water (0 for all parameters, except pH and DO).

S: Standard parameter value. Therefore, Equation (4) becomes as follows:

$$\mathbf{q_i = 100\ [Va\ /\ Si]} \qquad \mathbf{(3.5)}$$

After repeating the previous mathematical steps for all WQ parameters, WQI is calculated for each sampling station from Equation (1). Based on the estimated WQI (Tyagi et al., 2013), the water quality levels classification is shown in Table (3.4).

Table (3.3): Iraqi drinking water standards (Al-Mayah, 2021).

Parameter	Unit	Iraqi Standard
pH	-	8.5
Electrical Conductivity (EC)	µs/cm	2000
Alkalinity (ALK)	mg/l	200
Total Hardness as $CaCO_3$ (TH)	mg/l	500
Calcium (Ca^{+2})	mg/l	150
Magnesium (Mg^{+2})	mg/l	100
Chloride (Cl^{-1})	mg/l	350
Total Dissolved Solids (TDS)	mg/l	1000
Turbidity (TUR)	NTU	5

Table (3.4): Water Quality Index (WQI) and water quality status (Reza & Singh, 2010).

Water Quality Status	Water Quality Index Level
Excellent	0 - 25
Good	26 - 50
Moderately polluted	51 - 75
Severely polluted	76 - 100
Unfit and unsuitable for drinking	> 100

3.4.2 Inverse Distance Weighting (IDW)

All interpolation methods have been developed based on the theory that points closer to each other have more correlations and similarities than those farther (Khouni et al., 2021). The degree of correlations and similarities between adjacent points is expected to be proportional to the space between the point, which could be defined as a space invert function of every point from adjacent points in the IDW method (Setianto & Triandini, 2013). It is important to remember that in this method, the definition of adjacent points radius and the related power to the space invert function are regarded as critical problems. In this method, it will be utilized by a state that has a sufficient number of sample points with a suitable dispersion in local scale levels. The value of the power

parameter is the most important factor influencing the accuracy of inverse distance interpolations (Burrough & McDonnell, 1998). Furthermore, the size and the number of adjacent points is also relevant to the accuracy of the results.

$$\mathbf{Z_O = \frac{\sum_{i=1}^{N} Z_i * d_i^{-n}}{\sum_{i=1}^{N} d_i^{-n}}} \qquad \mathbf{(3.6)}$$

Z_O: The estimated value of variable z in point I.

Z_i: The sample value in point I.

d_i: The distance of the sample point to the estimated point.

N: The coefficient that determines weight based on distance.

n: The total number of predictions for each validation case.

3.4.3 Statistical analysis

This section covers the nature of the statistical relation between water quality and a spectral band of a satellite image (Landsat-8) for forecasting the parameters. This relation is an essential preliminary step prior to undertaking a formal statistical analysis. Two main statistical methods are used in data analysis: (1) descriptive statistics, which summarizes data using indexes such as mean and median and another is (2) inferential statistics, which draws conclusions from data using statistical tests. The selection of an appropriate statistical method depends on the following three points: the aim and objective of the study, the type and distribution of the data used, and the nature of the observations (paired/unpaired) (Mandel, 2012). There are some statistical processes used in this study as follows:

Correlation: The correlation analysis is utilized to determine how closely related the variables under consideration are. The Pearson correlation coefficient

(Zhang, 2017), which ranges from (-1 to +1), is the linear relationship's index and it has been taken into account in this study and can be measured by the following equation:

$$\mathbf{r} = \frac{\mathbf{n}(\sum(\mathbf{x}.\mathbf{y}) - (\sum \mathbf{x}.\sum \mathbf{y}))}{\sqrt{(\mathbf{n}\sum \mathbf{x^2} - (\sum \mathbf{x})^2)\,(\mathbf{n}\sum \mathbf{y^2} - (\sum \mathbf{y})^2)}} \qquad \textbf{(3.7)}$$

Where:

n: is the number of observations.

$\sum x$: is the summation symbol 1 (x_1, x_2, x_3, …...).

$\sum y$: is the summation symbol 2 (y_1, y_2, y_3, ……).

Regression models: A statistical method for determining the relationship between two or more variables is regression. It is among the most frequently utilized statistical tools because it offers straightforward procedures for determining a functional relationship between variables. Simple, multiple, and nonlinear regressions are the three different types of regression (Zare Abyaneh, 2014), Simple and multiple regressions, as described below, were utilized in this study.

a. **Simple regression:** is thought to investigate the connection between two variables that appear in a data set. The true relationship between Y and x is approximated by equation (8) in the formula below (Zare Abyaneh, 2014).

$$\mathbf{Y} = \boldsymbol{\beta_0} + \boldsymbol{\beta_1}\mathbf{X} \qquad \textbf{(3.8)}$$

Where:

β_1 and $\beta_{0:}$ are regression coefficients.

x: independent variable in the model.

Y: dependent variable.

b. Multiple regressions : The relationship between one (dependent) parameter and several (independent) parameters is thought to be studied using multiple regressions. It is crucial to recognize the fundamental differences between regression analysis and finding the correlations between various variables. While regression aims to provide a more detailed explanation of the relationship between these parameters, correlation assesses the strength of the association between parameters. The following are the multiple linear regression model's basic structures (Zare Abyaneh, 2014).

$$\mathbf{Y = \beta_0 + \beta_1 . x_1 + \beta_2 . x_2 + \ldots + \beta_n . x_n} \qquad \mathbf{(3.9)}$$

Where:

Y: is a dependent variable.

β_2, β_1, β_0, …, β_n: are regression coefficients.

x_1, x_2, …, x_n: are independent variables in the model.

The term "root mean squared error" refers to the square root of the mean of the square of all errors (RMSE). For numerical forecasts, RMSE is commonly used and is regarded as a superior all-purpose error metric (Chai et al., 2009).

$$\mathbf{RMSE} = \sqrt{\frac{1}{n}\sum_{i=1}^{n}(Pi - Oi)^2} \qquad \mathbf{(3.10)}$$

Where:

Oi: are the observations.

Pi: predicted values of a variable.

n: the number of observations available for analysis.

Since RMSE is scale-dependent, it would utilize to contrast prediction errors of numerous models or model configurations for one variable, not between variables (Chai et al., 2009).

The prediction error per square is represented by the Mean Square Error (MSE):

$$\mathbf{MSE} = \frac{\mathbf{1}}{\mathbf{m}} \sum_{\mathbf{i=1}}^{\mathbf{n}} (\mathbf{Yi} - \mathbf{yi})^{\mathbf{2}} \qquad \mathbf{(3.11)}$$

Where:

n: characterizes the number of elements of data from the whole test process.

y: is a calculation of the average response.

The mean square error made in the test data is measured using this criterion. In general, a low MSE value indicates that the projected values are reasonably close to the actual values (Zare Abyaneh, 2014).

Coefficient of determination: Commonly known as R^2 range from (0-1) that is utilized as a guide to measuring the precision of the linear model. In addition, the coefficient of determination is a measure of statistical analysis that evaluates a model (the level of variability in the data set) and predicts future outcomes (Johnson & Bhattacharyya, 2019).

P-Value: A statistical measurement known as a p-value is employed to check a hypothesis' validity against actual data. A p-value calculates the likelihood of getting the outcomes that were observed, presuming that the null hypothesis is correct. The statistical significance of the difference that was found increases with decreasing p-value. The p-value serves as an alternative to rejection points by indicating the least level of significance at which the null hypothesis would be ruled out. The alternative hypothesis is more likely to be supported if the p-value is lower. Spreadsheets, statistical software, or p-value tables are frequently utilized to find P-values. These calculations are performed using the presumed or known likelihood distribution of the specific statistic

under test (Ioannidis, 2018). The alteration between the observed value and a chosen reference value is utilized to calculate p-values given the likelihood distribution of the statistic, with a lower p-value signifying a greater difference between the two values. The zone below the likelihood distribution curve for all statistical values that are at least as far from the reference value as the observed value is divided by the total zone below the likelihood distribution curve to arrive at the p-value. The approach is taken to determine a p-value relies on the type of test that was conducted. In a nutshell, a lower p-value indicates that the difference between two observed values is less likely to be the result of simple random chance the larger the difference between the two observed values (Edwards, 2005).

CHAPTER FOUR

Results &

Discussions

4.1 Introduction

Geographical Information System (GIS) with remote sensing, distribution mapping with IDW, and in-situ measurement have essential parts to participate in all geographic and spatial parts of the improvement and management of water resources. These methods offer strong analytical and visualization tools that can be used to describe, examine, and model the processes and functions of natural systems. Additionally, experimenting with satellite image analysis and cross-referencing with field data can produce a different and precise parameter detection method (Bishop et al., 2001; Carré & Girard, 2002; Bouaziz et al., 2011).

Spatial analysis modeling and interpolate approaches have undergone extensive research. These methods for calculating and generating quantitative or qualitative water maps range from analytical to semi-empirical methods (Dekker, 1993). Though more hydraulics and hydrodynamics data are needed for mathematical modeling of river water quality, as well as widespread validation, the water quality index (WQI) jointly with geographic information systems (GIS) can be utilized to get over most of the issues raised up and can assign the status of the water (Huda & Al-Ansari, 2018).

It is possible to combine QGIS and Rstudio programs with additional mathematical models to obtain useful results pertaining to a variety of topics. The GIS includes instruments for spatial analysis to handle unique, enormous data. The quality of the water, whether it be an index or a concentration, is estimated by using statistical correlation and developing a model from the processed and transformed satellite image data. The processes are dependent on the Landsat 8 spectral band's spectral reflectance properties.

4.2 In-situ measurements and correlation analysis

Many water quality parameters were measured from January 2016 to June 2021, See Appendix B for water quality parameters monthly averaged values for all stations during the study period. A graphical summary (boxplots) of the water quality parameters is shown in Figures (4.1 & 4.2). Raw data statistical analysis reveals the presence of outliers, but these outliers will be retained because no evidence refers to errors or mistakes made when samples were collected, such as errors in parameter measurements, calculations, or from any other source that could change the measured values (Al-Zubaidi et al., 2021).

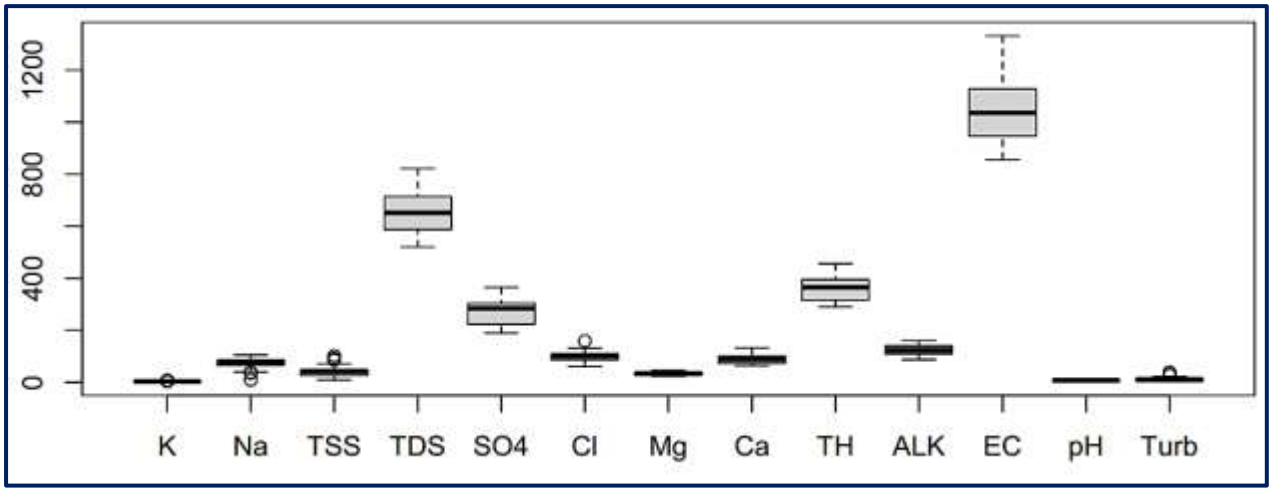

Figure (4.1): Boxplots of all water quality parameters used in this study.

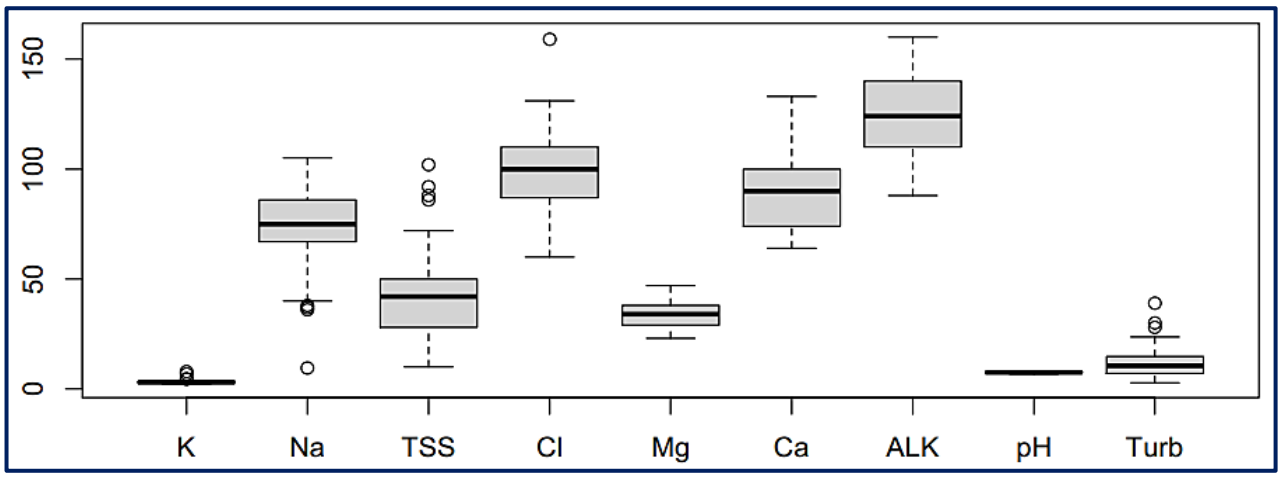

Figure (4.2): Boxplots of the water quality parameters used in this study after excluding EC, TH, SO_4, and TDS.

The variation of water quality parameters in Hilla River for each station during the study period is shown in Appendix C, and the parameters average value was summarized in Tables (4.1 - 4.5).

For station S1, during the study period, the maximum average yearly values of Turb concentration were in 2019, and the Turbidity value variation in the same year was varying from (5.9 to 52.6) NTU, as shown in Appendix B. The high value of EC was recorded in 2018; however, EC value variation through the study period is very small. The values of pH, TH, Mg, Ca, SO_4, TDS, Na, K, TSS, and ALK approximately remain constant or with small changes during the years of study. The maximum value of Cl^- was in 2016 and 2018 as shown in Table (4.1).

For station S2, during the study period, the maximum average yearly values of Turb concentration were in 2019, and the Turb value variation in the same year ranged from 7.2 to 36.05 NTU. The high value of EC was recorded in 2018, but EC value variation through the study period was very small. The values of pH, TH, Mg, Ca, SO_4, TDS, Na, K, and ALK were approximately constant or have a small change during the years of study. The maximum concentration value of TSS was in 2020, and Cl has the same maximum value in 2016 and 2018.

For station S3, during the study period, the lowest average annual Turb concentration was recorded in 2018. Also, the EC value reached a high point in 2018, there was relatively little change throughout the study period. During the years of investigation, the values of the following parameters remained steady or barely changed: pH, TH, Mg, Ca, SO_4, TDS, Na, K, and ALK. TSS has the same maximum concentration value in 2016 and 2020 while Cl has the same maximum concentration value in 2016 and 2018.

For station S4, during the study period, the maximum annual value of Turb concentration was in 2019 and 2020. Although the EC value reached a high point

in 2018, there was relatively little change during the study period. The values of pH, TH, Mg, Ca, SO4, TDS, Na, K, and ALK have remained rather consistent over the years of investigation or have very slightly changed. Cl also has the same maximum value in 2016 and 2018, and TSS had the highest concentration possible in 2016.

During the study period, the highest average annual Turb readings for station S5 were in 2019. The highest EC value was reported in 2018, although there was relatively little EC value change throughout the study period. During the years of investigation, the values of the following parameters remained steady or barely changed: pH, TH, Mg, Ca, SO4, TDS, Na, K, and ALK. TSS had the highest possible concentration in 2016, while Cl had the same maximum value in both 2016 and 2018.

Table (4.1): The parameters' yearly average value for **S1** during the study period.

	Parameters												
Year	**Cl**	**ALK**	**TSS**	**K**	**Na**	**TDS**	**SO_4**	**Mg**	**Ca**	**TH**	**EC**	**Turb.**	**pH**
2016	124.6	119.4	49.1	3.6	81.5	685.1	291.7	39.8	86.8	379.6	1063.7	13.8	**7.8**
2017	104.7	126.6	32.4	3.0	79.3	653.4	249.5	31.5	79.2	331.6	1015.5	7.4	**7.7**
2018	124.6	133.3	36.9	3.3	89.7	691.7	265.2	35.6	85.6	360.1	1142.7	5.9	**7.1**
2019	91.6	136.4	49.8	3.2	68.4	643.4	267.9	30.3	99.5	372.9	1020.8	28.9	**7.3**
2020	83.1	120.4	46.4	3.3	66.2	593.0	251.4	34.4	95.4	372.4	950.4	13.1	**7.6**
2021	88.8	104.8	26.9	3.4	72.2	611.0	259.4	35.1	85.3	356.6	997.9	7.4	**7.9**

Table (4.2): The parameters' yearly average value for **S2** during the study period.

	Parameters												
Year	**Cl**	**ALK**	**TSS**	**K**	**Na**	**TDS**	**SO_4**	**Mg**	**Ca**	**TH**	**EC**	**Turb.**	**pH**
2016	122.8	119.5	50.0	3.2	80.7	675.5	288.1	40.0	86.5	377.7	1061.1	16.2	**7.8**
2017	104.8	129.3	33.1	3.0	79.8	634.1	245.7	31.4	77.8	328.5	1013.0	12	**7.7**
2018	122.8	133.7	44.9	3.3	90.0	682.3	266.2	35.5	84.7	356.8	1131.3	8	**7.2**
2019	94.7	133.5	48.6	3.2	70.0	647.9	271.6	30.8	99.5	375.0	1030.0	20.3	**7.3**
2020	85.1	119.2	61.2	3.3	69.7	607.5	261.0	33.1	96.4	377.0	967.1	13.7	**7.4**
2021	88.9	104.4	51.4	3.4	73.2	622.1	269.1	35.3	86.0	359.5	1004.1	15.3	**7.9**

Table (4.3): The parameters' yearly average value for **S3** during the study period.

	Parameters												
Year	**Cl**	**ALK**	**TSS**	**K**	**Na**	**TDS**	**SO_4**	**Mg**	**Ca**	**TH**	**EC**	**Turb.**	**pH**
2016	125.6	118.1	61.0	3.4	83.7	675.0	294.9	38.4	88.2	376.1	1069.2	18.1	**8.0**
2017	104.3	126.8	37.7	2.9	77.8	636.3	244.8	32.9	77.2	332.8	997.0	10.8	**7.6**
2018	125.6	130.9	36.6	3.4	87.3	695.0	269.8	36.4	88.1	367.7	1154.6	5.6	**6.9**
2019	89.1	134.5	41.8	3.1	66.2	631.0	274.2	31.1	101.3	378.9	1017.8	15.8	**7.3**
2020	85.1	119.2	61.2	3.3	69.7	607.5	261.0	33.1	96.4	377.0	967.1	13.5	**7.4**
2021	87.8	104.8	28.8	3.4	70.3	608.0	258.0	33.3	84.6	347.6	991.0	8.5	**7.9**

Table (4.4): The parameters' yearly average value for **S4** during the study period.

	Parameters												
Year	**Cl**	**ALK**	**TSS**	**K**	**Na**	**TDS**	**SO4**	**Mg**	**Ca**	**TH**	**EC**	**Turb.**	**pH**
2016	128.3	118.9	53.7	3.7	85.9	691.2	306.4	40.3	90.7	392.4	1103.8	15.6	**7.8**
2017	107.1	128.1	36.8	3.0	81.5	646.3	254.3	32.8	78.9	335.7	1024.9	7.3	**7.7**
2018	128.3	135.5	43.7	3.6	88.3	701.3	259.5	35.3	85.7	360.0	1149.9	5	**7.1**
2019	100.8	133.5	40.9	3.8	73.7	625.5	246.5	31.6	99.6	373.6	1041.4	16.7	**7.3**
2020	88.3	126.7	43.3	3.7	72.3	586.7	223.3	37.7	83.0	362.3	931.0	16.3	**7.7**
2021	93.8	112.8	23.7	3.5	78.0	626.2	253.0	37.0	81.3	361.2	1013.0	8.78	**7.6**

Table (4.5): The parameters' yearly average value for **S5** during the study period.

	Parameters												
Year	**Cl**	**ALK**	**TSS**	**K**	**Na**	**TDS**	**SO_4**	**Mg**	**Ca**	**TH**	**EC**	**Turb.**	**pH**
2016	128.2	120.6	51.4	3.3	83.5	668.8	290.1	38.8	86.3	372.9	1051.1	13.1	**8.0**
2017	108.4	128.1	35.4	3.0	82.4	628.8	249.1	32.2	79.9	336.3	1017.4	7.6	**7.8**
2018	128.2	132.0	40.2	3.3	90.7	698.7	269.5	36.7	87.0	366.6	1157.5	5	**7.1**
2019	93.9	134.5	34.0	3.1	71.7	654.5	268.2	31.7	98.1	374.6	1031.5	16.4	**7.4**
2020	83.3	135.5	32.0	3.6	67.3	554.0	218.3	36.0	82.8	353.8	910.3	13.3	**7.8**
2021	89.1	104.8	35.7	3.3	73.8	637.5	271.4	33.5	89.9	362.0	1018.1	10.4	**7.9**

Statistical correlation analysis has been found to be a highly useful tool for relating different parameters. Correlation analysis measures the closeness of the relationship between chosen independent and dependent variables (Jain & Sharma, 2002; Sharma & Jain, 2005). The analysis that attempts to base on the best subset procedure (R and p-value) is used in water quality parameters for predicting the

river water quality management. Figure (4.3) shows the water quality data correlation matrix for the five stations. In the correlation matrix of water quality parameters, there is a significant relationship between some parameters and each other. The higher Pearson correlation coefficient and p-value prove this relationship.

In Figure (4.3) some of the water quality parameters show a significant correlation with each other. Electrical conductivity (EC) has a significant correlation with three water quality parameters (chloride ions (Cl), sulfate ions (SO4), and total dissolved solids (TDS) (with a value of r more than 70% and a p-value less than 0.05. Total hardness (TH) shows a significant correlation with three water quality parameters (calcium ions (Ca), total dissolved solids (TDS), and sulfate ions (SO4)(with avalue of r more than 70% and a p-value less than 0.05. Total dissolved solids (TDS) is linked with a significant correlation with four water quality parameters (chloride ions (Cl), sulfate ions (SO_4), total hardness (TH), and electric conductivity (EC) (with a value of r more than 70% and p-value less than 0.05. Since other parameters and their functions can be explained by using these matrices, utilization of such a methodology will thus greatly facilitate the task of rapid monitoring of the status of pollution of water economically.

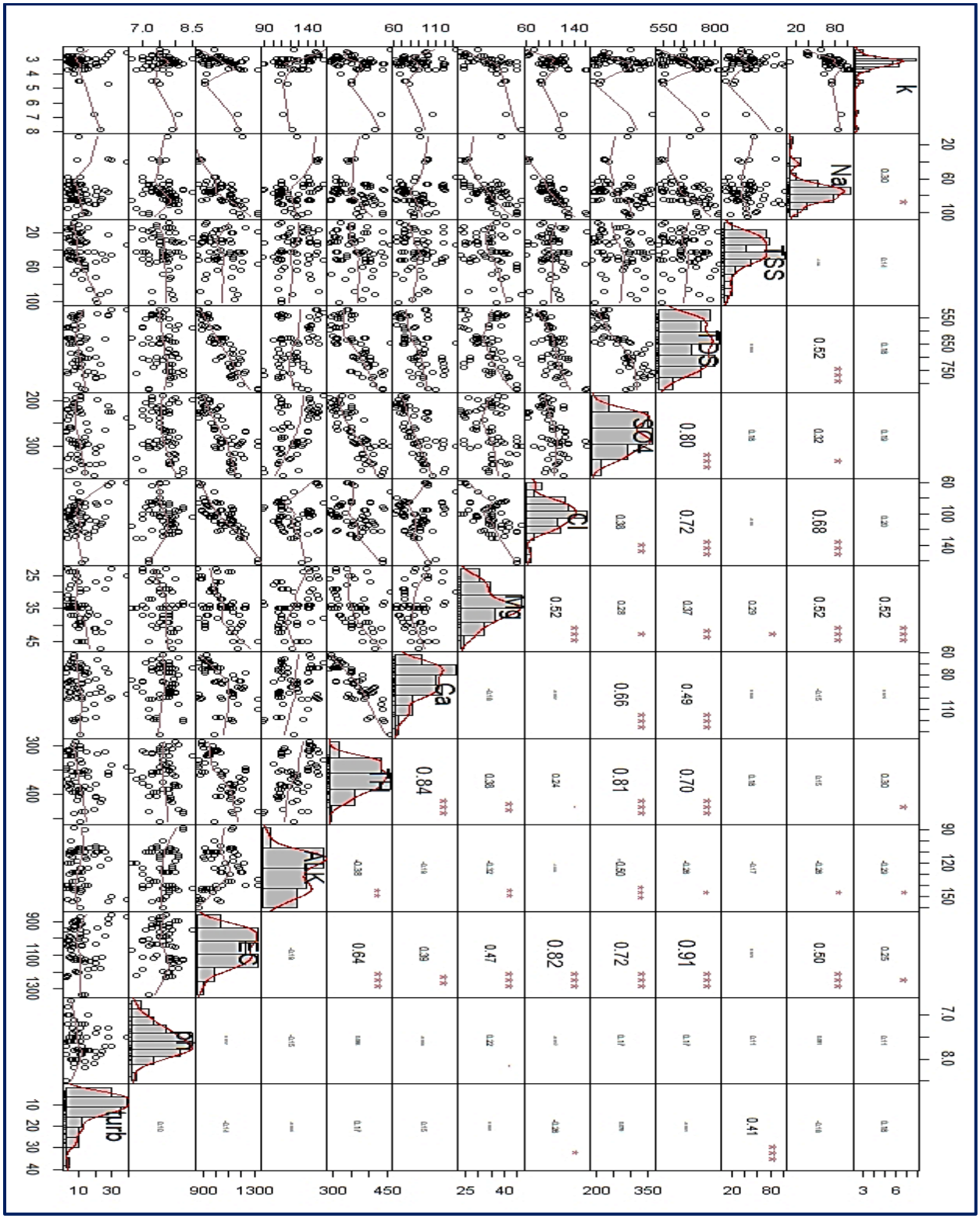

Figure (4.3): Correlation matrix for the five stations of water quality data using Rstudio software (the red stars mean there is a significant relationship).

4.3 Hilla River Water Quality Index (WQI)

Monitoring water quality can assist investigators in predicting natural environmental processes, learning from them, and assessing the effects of humans on ecosystems. Additionally, it aids in restoration efforts or upholds environmental standards. Among the initial methods of water quality indices was the weighted arithmetic method. Using the most frequently measured water quality variables, this index categorized the purity of the water according to its level (Tyagi et al., 2013; Chandra et al., 2017).

The results of the average monthly WQI for all sampling stations are shown in Figures (4.4 - 4.9). WQI values ranged between (2.38) at station S3 in April 2018 and (462.49) at station S1 in August 2019. Similar results were revealed by other research related to the same study area. Al-Ridah et al. (2020) found the results for all sampling stations in Hilla River, WQI values the lowest value at Al-Hashimyah station in April 2018 and the highest value at Al-Hesain station in August 2018.

Based on Table (3.3), Hilla River water in all stations in 2016 was considered “severely polluted” to “Unfit and unsuitable for humming use”. In 2017 and for all study stations there was an improvement in WQI in the river compared to 2016, but still, WQI is considered “severely polluted”. In 2018, the lowest WQI values for all stations were considered the best during the study period, and WQI can be categorized as “Good to Moderately polluted”. The WQI value in 2019 was the worst in all stations during the study period “Unfit and unsuitable for drinking”. Also, in 2020 and 2021 the WQI value can be characterized as “severely polluted”.

The high WQI value of the River was due to the untreated domestic pollution disposal site, which was directly dumped by the lateral outfalls (Reza &

Singh, 2010). The water cycle and water quality are significantly impacted by increasing pollution levels, rising water demand, and related increases in pollutant discharges (Whitehead et al., 2006; Whitehead et al., 2009). Increased temperatures and altered rainfall patterns are two additional signs that climate change is beginning to have an impact. Natural low flows are frequently a barrier to intensive water usage, and rivers with low flows are more vulnerable to the impact of wastewater discharges from cities, businesses, and agriculture. In the warmer months, diminishing river flows and rising air temperatures are the main issues (Al-Mansori, 2017). Because of the combined effect of the decline in rainfall and the rise in potential evaporation as a result of warming air, the water of the river has tended to decrease in recent years. This circumstance shows that drought might happen more frequently as a result of the effects of global warming (Abdulkareem, 2020).

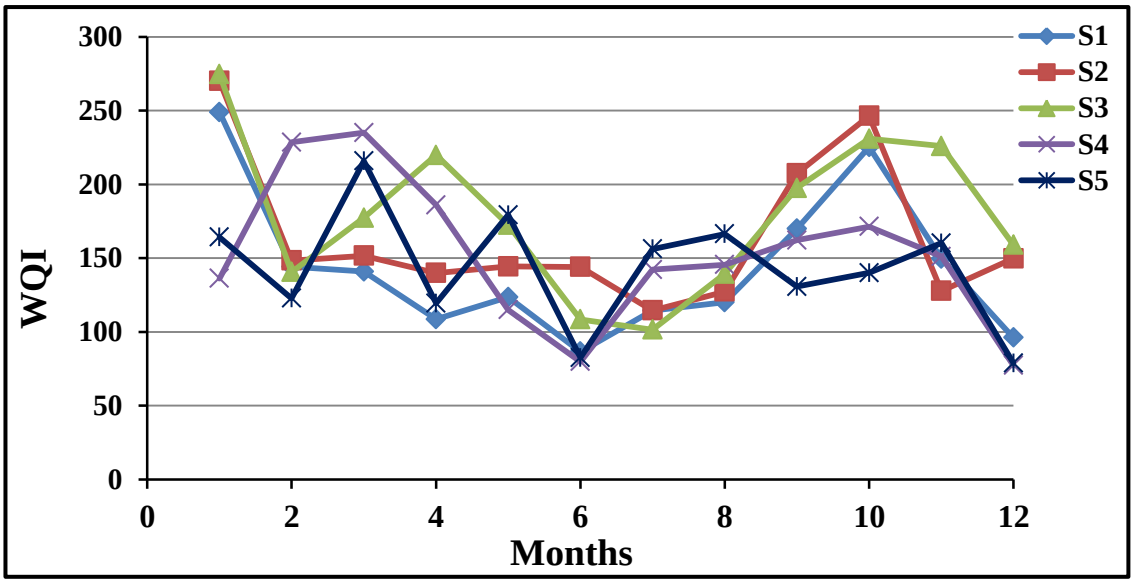

Figure (4.4): Water quality index for the five stations in 2016.

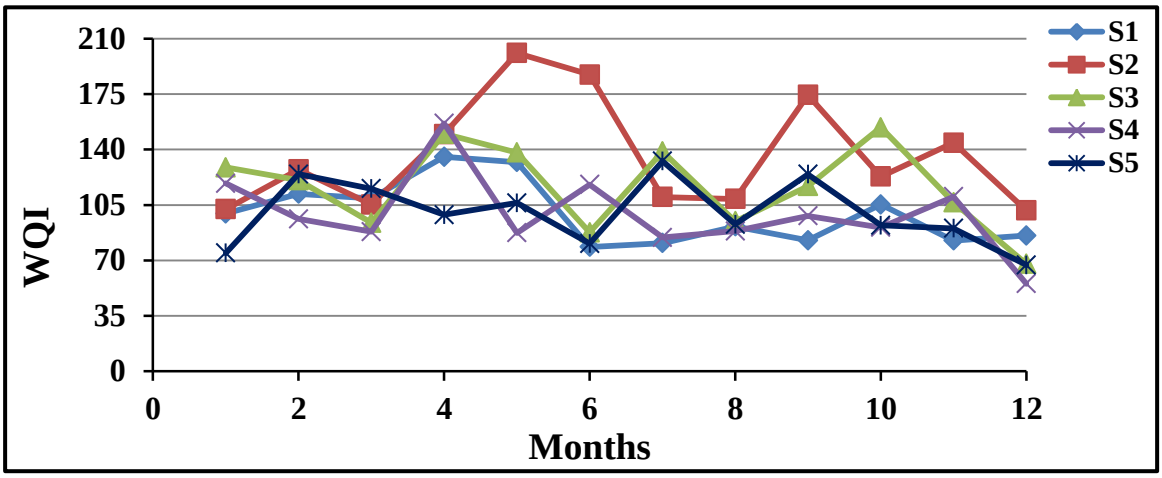

Figure (4.5): Water quality index for the five stations in 2017.

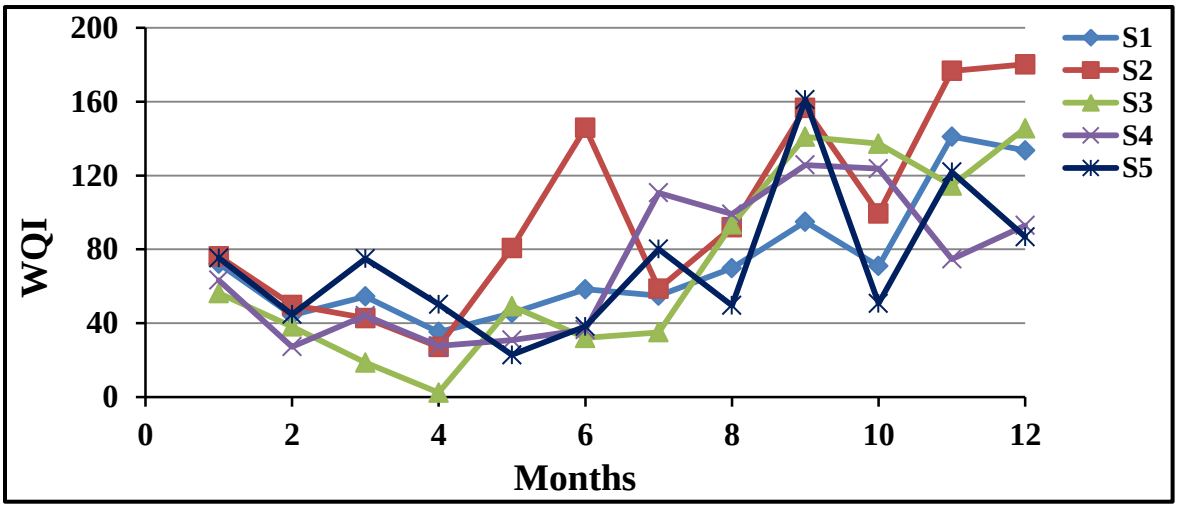

Figure (4.6): Water quality index for the five stations in 2018.

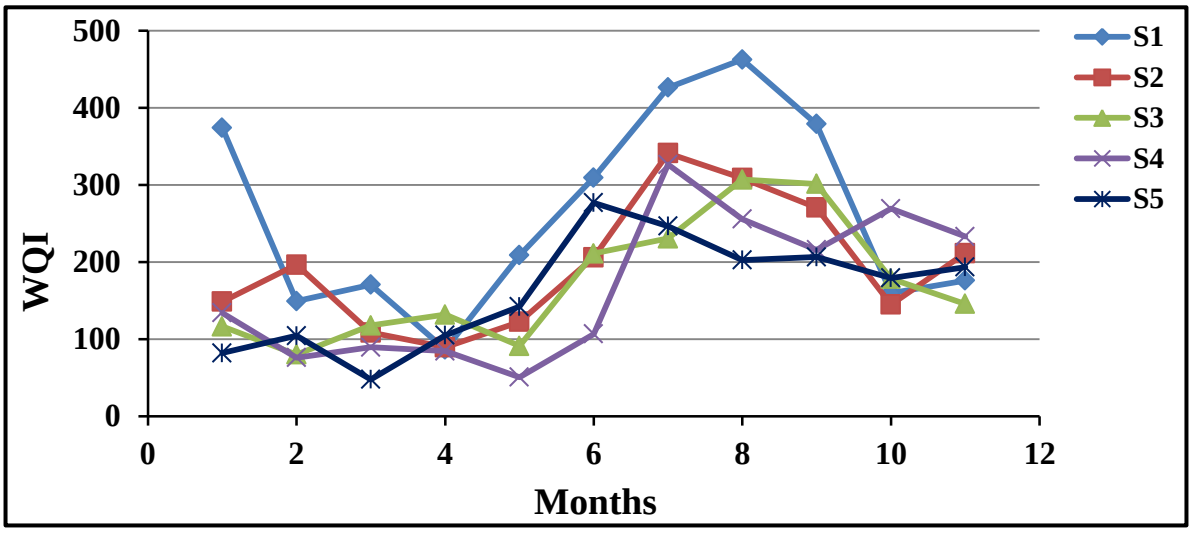

Figure (4.7): Water quality index for the five stations in 2019.

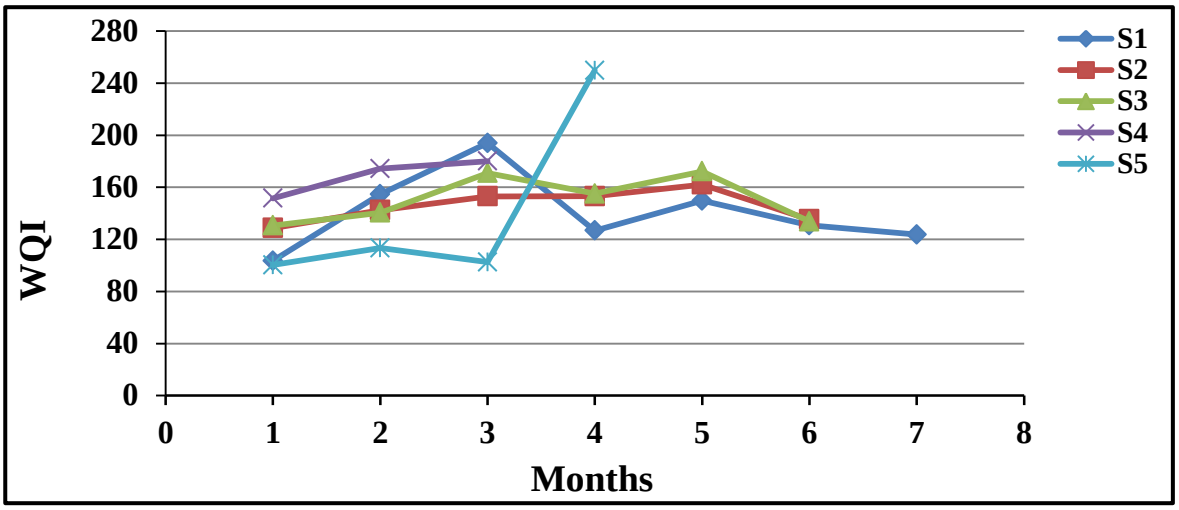

Figure (4.8): Water quality index for the five stations in 2020.

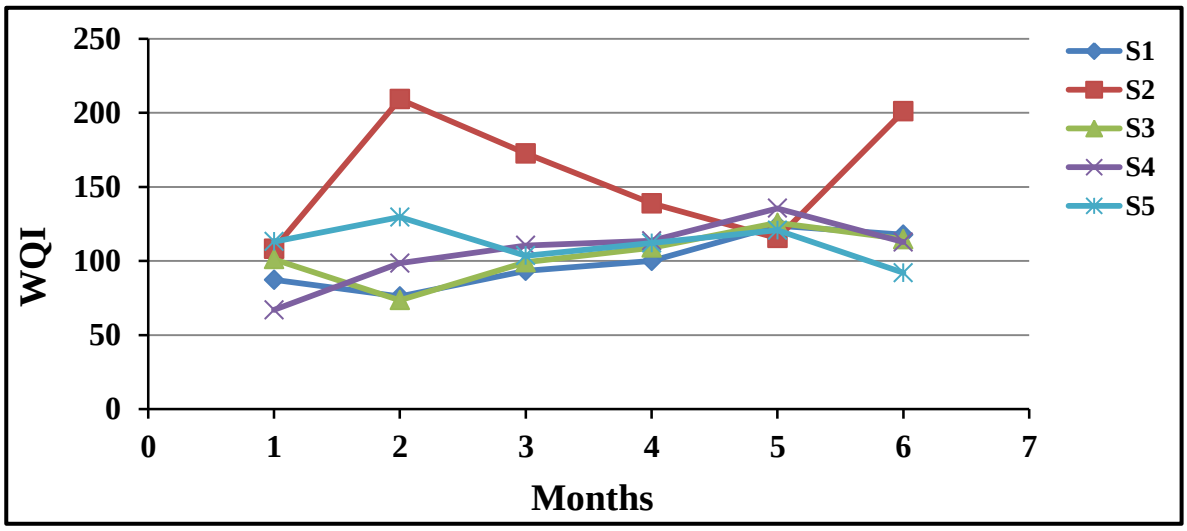

Figure (4.9): Water quality index for the five stations in 2021.

4.4 Linear models development and statistical analysis

4.4.1 Models based on WQI and WQ parameters

The correlation matrix between the water quality index and water quality parameters is shown in Figure (4.10). The 13 water quality parameters' relationships with WQI showed that turbidity has a significant relation with WQI (p-value less than 0.05 and R^2 more than 0.85), as shown in Figure (4.10).

Firstly, the data must be tested with the Shapiro-Wilk normality test for WQI as shown in Table 4.6. In order to make the data normal distribution, WQI values were divided into less than 220 and more than 220 to get the best validated linear regression model. As a result, the normality test results showed good agreement, as shown in Table (4.7).

To build the required linear regression model, the data were divided into two sets: Train Dataset and Test Dataset. 291 data points from the in-situ measurements were used for the WQI calculation. It was noticed that 264 data points have WQI values of less than 220, and WQI values of more than 220 were 27 data points. Train data points of WQI < 220 are 183 data points, and to validate the result the test data points are 81 points. The correlation matrix for WQI < 220 showed there is a significant relationship with turbidity, Figure (4.11). Train data for WQI > 220 are 18 date points and test data points were 9 points. The correlation matrix for WQI > 220 showed also there is a significant relationship with turbidity, Figure (4.12). Tables (4.8 and 4.9) show the full linear regression model summary statistics for these relationships. Table (4.8) shows the statistics result of WQI values of less than 220. The linear regression model has a p-value equal to 2.2e-16 and R^2 of more than 70%. Table (4.9) shows the statistics result of WQI values of more than 220 and the linear regression model that has a p-value of 6.507e-6 and R^2 of more than 86%. Table (4.10) shows the final linear regression models to estimate WQI based on turbidity. The MSE and RMSE were used to validate the difference between the measured values (Test Data) and the model predictions. Results showed that there is good agreement with field data.

Table (4.6): Shapiro-Wilk normality test for WQI.

W	p-value	Normality case
0.90614	1.724e-12	**Not normal**

Table (4.7): Shapiro-Wilk normality test for the divided WQI.

WQI	W	p-value	Normality case
WQI <220	0.99238	0.2159	**normal**
WQI >220	0.902	0.0529	**normal**

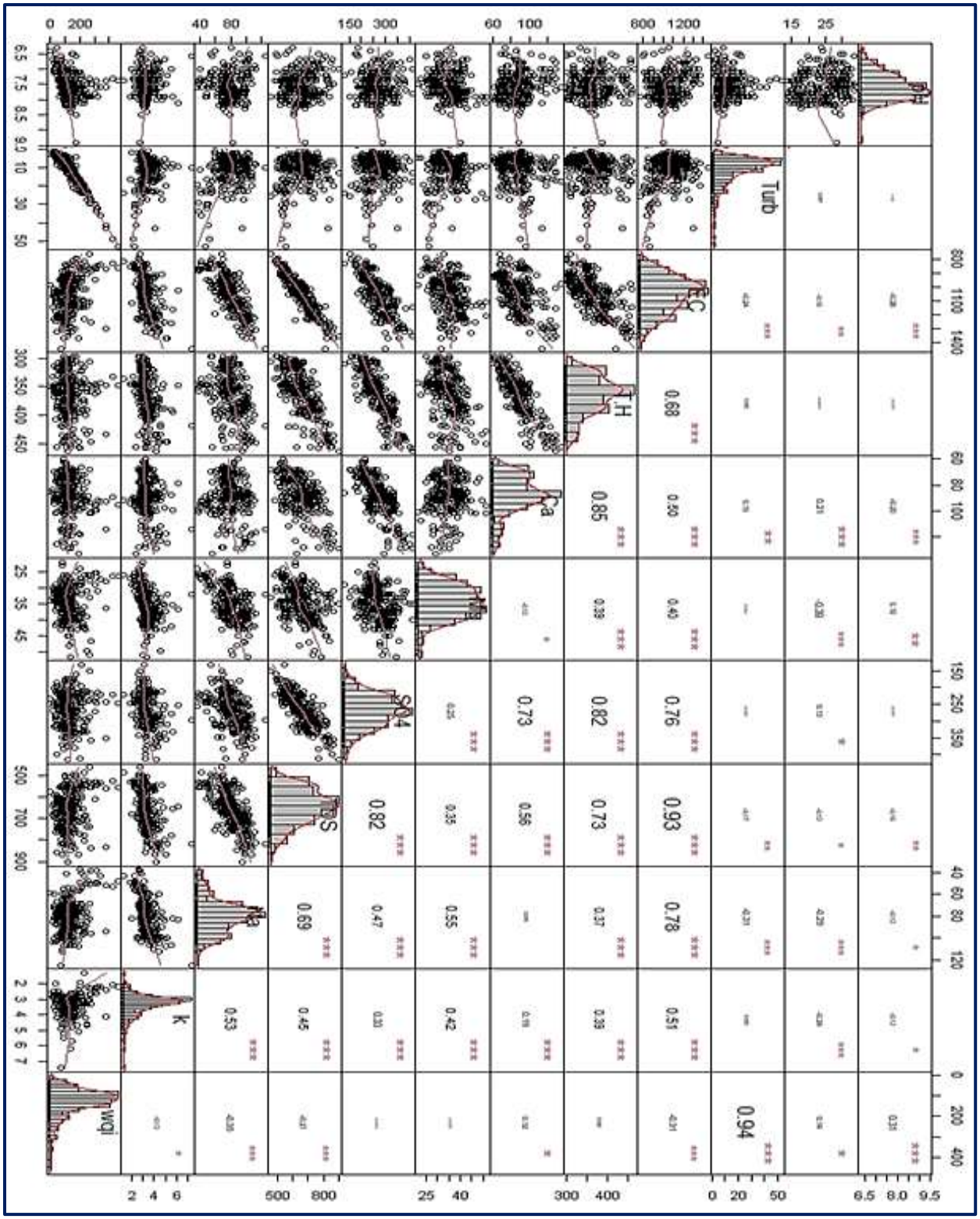

Figure (4.10): Correlation matrix for the five stations of water quality index data with water quality parameters.

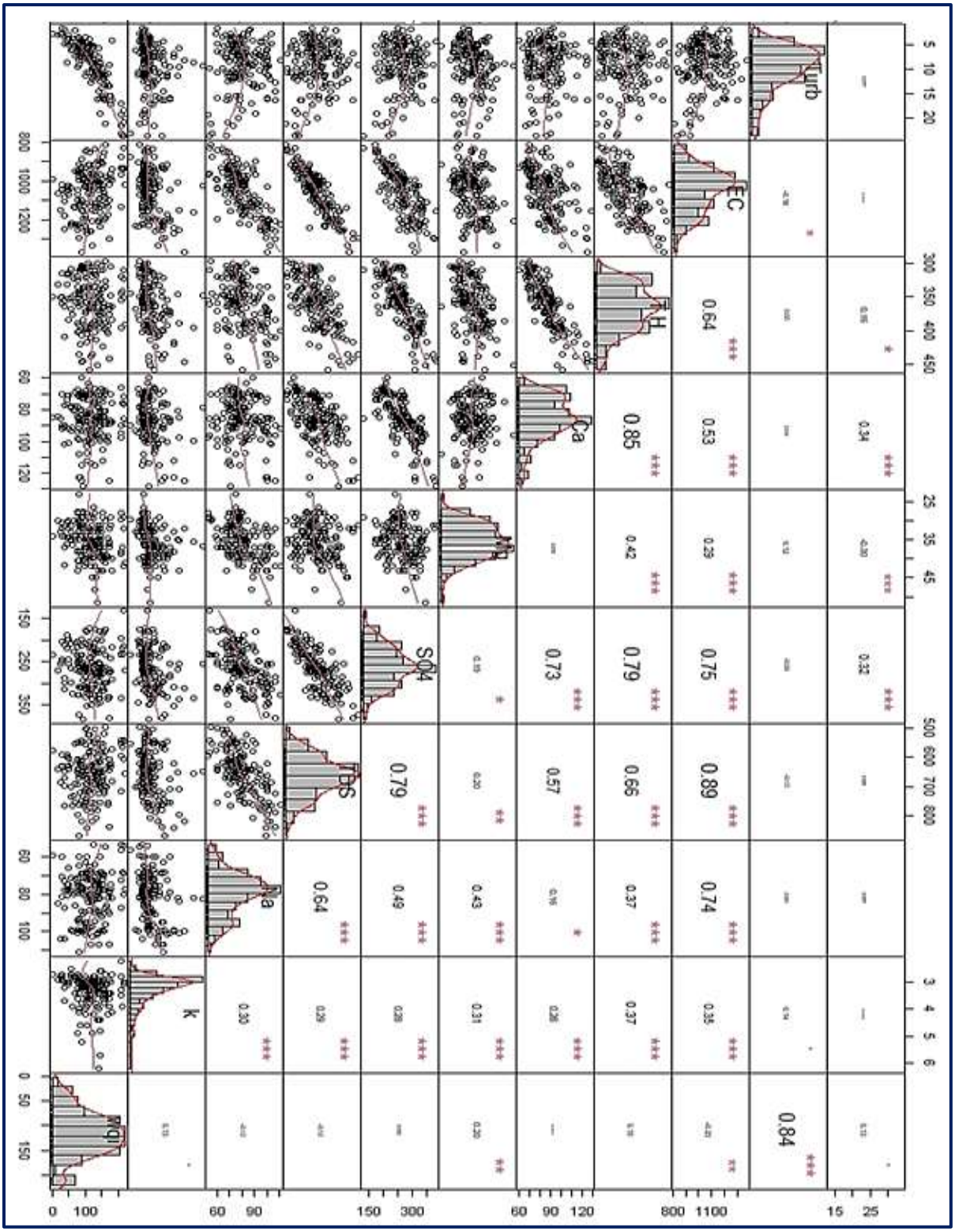

Figure (4.11): Correlation matrix for train data of WQI < 220.

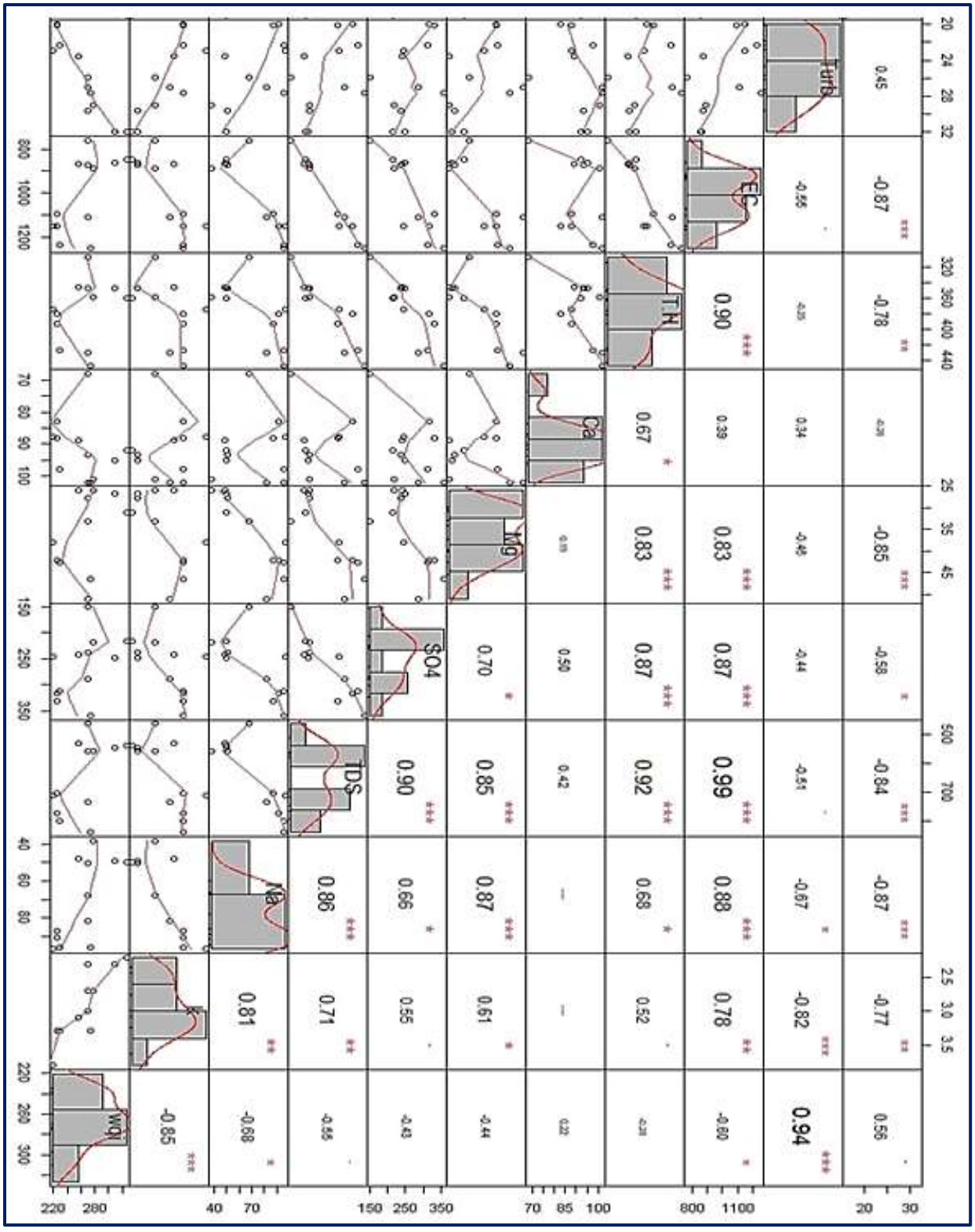

Figure (4.12): Correlation matrix for train data of WQI > 220.

Table (4.8): The full linear regression model summary statistics for the data WQI values of less than 220 with water quality parameters

Residuals:

Min	1Q	Median	3Q	Max
-68.966	-17.195	4.057	13.348	101.682

Coefficients:

	Estimate	Std. Error	t value	Pr (>|t|)	
(Intercept)	46.7579	3.8477	12.15	<2e-16	***
dataf$Turb	7.7177	0.3807	20.27	<2e-16	***

Residual standard error: 23.89 on 169 degrees of freedom

Multiple R-squared: 0.7086, Adjusted R-squared: 0.7069

F-statistic: 411 on 1 and 169 DF, p-value: < 2.2e-16

Table (4.9): The full linear regression model summary statistics for the data WQI values of more than 220 with water quality parameters

Residuals:

Min	1Q	Median	3Q	Max
-19.426	-6.982	0.556	7.435	19.059

Coefficients:

	Estimate	Std. Error	t value	Pr (>|t|)	
(Intercept)	69.3391	22.8720	3.032	0.0126	*
dataf$Turb	7.4363	0.8691	8.556	6.51e-06	***

Residual standard error: 12.23 on 10 degrees of freedom

Multiple R-squared: 0.8798, Adjusted R-squared: 0.8678

F-statistic: 73.2 on 1 and 10 DF, p-value: 6.507e-06

Table (4.10): The final valid linear regression models for WQI and turbidity.

Model Limitation	Model	MSE	RMSE	R^2
WQI < 220	WQI = ((46.7579) + (7.7177) × (Turb))	17.469	21.384	70
WQI > 220	WQI= ((69.3391) + (7.4363) × (Turb))	8.9890	12.138	86

4.5 Models based on Landsat 8 spectral bands and WQ parameters

There is no boundary to gaining and utilizing Landsat 8 satellite imagery (González-Márquez et al., 2018). Landsat 8 satellite series are commonly utilized to find relationships between WQ parameters of surface waters and spectral bands (Kulkarni, 2011; El Saadi et al., 2014; El-Zeiny & El-Kafrawy, 2017; Japitana & Burce, 2019). For more than 25 years, remote sensing technology has made it possible to view water quality in a synoptic and multi-temporal manner (Cracknell et al., 2001; Hossain et al., 2010; Abdelmalik, 2018). Satellite sensors can monitor the amount of solar radiation reflected by surface water at various wavelengths, which can be connected to various water quality indices (Alsaqqar et al., 2015; Olmanson et al., 2015).

In-situ measurements of water quality parameters from January 2016 to June 2021 and Landsat 8 images data obtained from the USGS website were utilized to build the required linear regression model.

First, the WQ parameters should be tested for normality as shown in Table (4.11). The correlation matrix between the water quality parameters and the spectral bands' ratio values of the satellite images is shown in Table (4.12). Statistical results for the 13 water quality parameters showed that 7 parameters have a significant relationship with band ratio (p-value less than 0.05). These parameters were lineally regressed with the related band ratio values by a linear model. The resulting models of the 7 parameters with bands ratio have a p-value less than 0.05. TDS is positively correlated with B10/B3 (P = 0.034), SO_4 is

positively correlated with B10/B3 and B10/B4 (P = 0.001), Mg is inversely correlated with B4/B7 (P = 0.003), Ca is inversely correlated with B1/B4 (P = 0.038), TH is inversely correlated with B1/B4 (P = 0.024), ALK is positively correlated with B3/B7 (P = 0.016), and pH is inversely correlated with B1/B2 (P=0.003). The remaining parameters (K, Na, TDS, Cl, EC, and Turb) have an insignificant correlation with band ratio (p-value greater than 0.05) as shown in Table (4.13). The MSE and RMSE show the difference between the measured data and the model predictions. The best result was for pH with very low errors.

These models will be useful for forecasting and calculating WQ parameters. This work showed encouraging outcomes in calculating WQ parameters, which, if further confirmed with multi-temporal datasets, can be taken into consideration for the creation of an operational RS-based monitoring and assessment system that can be scaled at a regional and national level. According to the findings of the model comparison, this study can conclude that it is not essential to purchase high-resolution satellite photos because a free satellite image, like the Landsat series, can be a trustworthy input image provided the proper pre-processing approach is used.

Table (4.11): Shapiro–Wilk test for water quality parameters.

WQ parameter	W-value	p-value	Normality case
pH	0.9736	0.3879	Normal
TDS	0.9562	0.0873	Normal
TSS	0.9221	0.005	Not normal
K^{+1}	0.62398	1.68E-09	Not normal
Na^{+}	0.9126	0.0024	Not normal
SO_4^{-2}	0.9337	0.0127	Not normal
Cl^{-1}	0.9742	0.4078	Normal
Mg^{+2}	0.96445	0.1803	Normal
Ca^{+2}	0.9555	0.0825	Normal
TH	0.95907	0.1125	Normal
ALK	0.95459	0.07588	Normal
EC	0.9624	0.1513	Normal
Turb	0.88487	0.000331	Not normal

Table (4.12): The correlation matrix of water quality parameters and bands' ratio.

NO.	WQ parameter	Band Ratio	r	P-Value	NO.	WQ parameter	Band Ratio	r	P-Value
1	**ALK**	B4/B7	0.4	0.00607	**27**	**Mg^{+2}**	B7/B4	0.4	0.00594
2	**ALK**	B7/B4	-0.39	0.00828	**28**	**Mg^{+2}**	B4/B6	-0.4	0.0061
3	**ALK**	B4/B6	0.39	0.00846	**29**	**Mg^{+2}**	B6/B4	0.38	0.00987
4	**ALK**	B6/B4	-0.37	0.01335	**30**	**Mg^{+2}**	B4/B7	-0.28	0.06742
5	**ALK**	B3/B7	0.35	0.01675	**31**	**Na**	B7/B4	0.26	0.08499
6	**ALK**	B3/B6	0.34	0.02132	**32**	**pH**	B1/B2	-0.43	0.00352
7	**Ca^{+2}**	B1/B4	-0.31	0.0382	**33**	**pH**	B2/B1	0.42	0.00375
8	**Ca^{+2}**	B2/B4	-0.3	0.04724	**34**	**pH**	B1/B10	-0.35	0.01894
9	**Ca^{+2}**	B4/B1	0.29	0.05102	**35**	**pH**	B5/B2	-0.01	0.94711
10	**Ca^{+2}**	B4/B2	0.28	0.059	**36**	**SO_4^{-2}**	B10/B1	0.39	0.00789
11	**Cl^{-1}**	B2/B3	0.26	0.08636	**37**	**SO_4^{-2}**	B10/B2	0.39	0.00848
12	**Cl^{-1}**	B3/B1	-0.26	0.08758	**38**	**SO_4^{-2}**	B10/B3	0.38	0.00934
13	**Cl^{-1}**	B1/B3	0.26	0.08788	**39**	**SO_4^{-2}**	B10/B4	0.31	0.0382
14	**Cl^{-1}**	B1/B4	0.26	0.0904	**40**	**SO_4^{-2}**	B3/B10	-0.27	0.07218
15	**Cl^{-1}**	B3/B2	-0.26	0.09091	**41**	**TDS**	B10/B3	0.32	0.034
16	**Cl^{-1}**	B4/B1	-0.24	0.11258	**42**	**TDS**	B10/B2	0.3	0.04339
17	**Cl^{-1}**	B2/B4	0.23	0.13073	**43**	**TDS**	B10/B1	0.3	0.04544
18	**Cl^{-1}**	B4/B2	-0.22	0.14884	**44**	**TH**	B1/B4	-0.33	0.02451
19	**Cl^{-1}**	B2/B1	-0.21	0.15854	**45**	**TH**	B1/B3	-0.33	0.02609
20	**Cl^{-1}**	B1/B2	0.21	0.15963	**46**	**TH**	B3/B1	0.33	0.02642
21	**EC**	B1/B2	0.08	0.58264	**47**	**TSS**	B7/B6	-0.03	0.37276
22	**EC**	B7/B5	0.01	0.97074	**48**	**TSS**	B6/B7	0.17	0.26971
23	**K**	B6/B1	0.24	0.10946	**49**	**TSS**	B6/B5	-0.01	0.96854
24	**K**	B6/B7	0.24	0.11317	**50**	**Turb**	B7/B10	-0.25	0.09302
25	**K**	B6/B3	0.24	0.11657	**51**	**Turb**	B1/B10	-0.25	0.10011
26	**Mg^{+2}**	B4/B7	-0.42	0.00385	**52**	**Turb**	B6/B10	-0.25	0.10078

Table (4.13): The final linear regression model for water quality parameters and bands' ratio.

WQ parameters	Model	r	p-value	Bands ratio	MSE	RMSE
K	-	0.24	0.10946	B6/B1	-	-
Na	-	-0.28	0.06742	B4/B7	-	-
TSS	-	-0.03	0.37276	B7/B6	-	-
TDS	TDS=276+86.16*B10/B3	0.32	0.034	B10/B3	76.1	89.7
SO_4	SO_4=156.99+134.19*B10/B3-99.2*B10/B4	0.39	0.00160	B10/B3 +B10/B4	44.9	47.0
Cl	-	0.21	0.08636	B1/B2	-	-
Mg	Mg=65.215 - 28.599*B4/B7	-0.42	0.00385	B4/B7	4.6	6.1
Ca	Ca =158.18-77* B1/B4	-0.31	0.0382	B1/B4	11.4	13.5
TH	TH =547.91-210.5* B1/B4	-0.33	0.02451	B1/B4	36.0	40.7
ALK	ALK =55.95+ 57.95* B3/B7	0.4	0.01675	B3/B7	12.4	14.5
EC	-	0.08	0.58264	B1/B2	-	-
pH	pH =13.886-6.841*B1/B2	-0.43	0.00352	B1/B2	0.35	0.46
Turb	-	-0.25	0.09302	B7/B10	-	-

r: Pearson Correlation coefficient, MSE: Mean Squared Error, and RMSE: Root Mean Squared Error.

4.6 Models based on WQI and Landsat 8 spectral bands

Simple linear regression models between WQI and surface reflectance data obtained from Landsat 8 satellite images were developed by using Rstudio in addition to the related statistical analysis. QGIS software was used for processing the geographic images and analysis.

Data were explored by the Shapiro-Wilk normality test for WQI to extract the best normal distribution as shown in Table (4.14). Also, WQI values were divided as shown in Table (4.14) for better linear regression model selection. The natural logarithm of WQI was taken for the values between 50 and 250 to transform data and make it normally distributed to reduce the skewness of the data. 240 data points were gathered from Landsat 8 spectral bands for the related WQI

calculated values. WQI values of less than 50 were 20 data points, WQI values between 50 and 250 were data 205 data points, and WQI values of more than 250 were 15 data points. In addition, to build the required linear regression model, the data points were divided into Train Dataset and Test Dataset. 70% of the WQI values were taken as a Train Dataset, and the remaining 30% values were used to validate the final model.

The correlation matrix between the divided WQI and spectral bands showed that WQI values have a Pearson correlation coefficient of more than 50% and p-value less than 0.05 with band 3 and band 10 as shown in Figures (4.13, 4.14, and 4.15). The full linear regression model summary statistics for WQI data and specter bands are in Tables (4.15, 4.16, and 4.17) WQI values of less than 50 show a significant relationship with band 3 (R 64% and p-value 0.00047), log WQI values between 50 and 250 have a significant relationship with band 3 (R 78% and p-value $2.2*10^{-16}$), and logWQI values of more than 250 show a significant relationship with band 10 (R 57% and p-value 0.015). Table (4.18) shows the final required linear regression model for WQI with Landsat 8 spectral bands. The MSE and RMSE show the difference between the measured data and the model predictions, revealing the models' robustness.

Table (4.14): Shapiro-Wilk normality test of WQI.

WQI Limitation	w-value	p-value	Normality case
50 < logWQI < 250	0.99113	0.2438	Normal
WQI < 50	0.91265	0.07161	Normal
WQI > log250	0.88331	0.05317	Normal

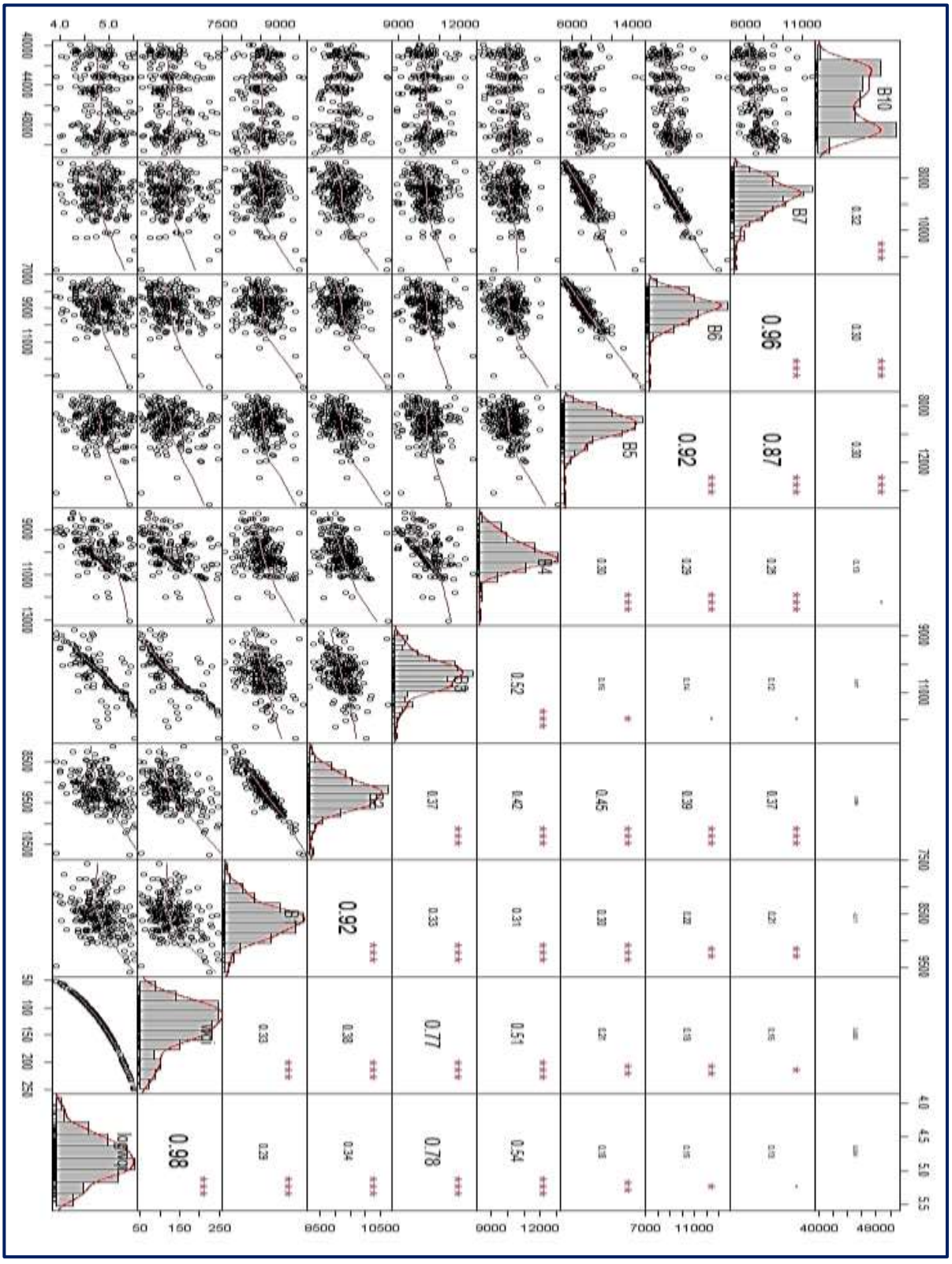

Figure (4.13): Correlation matrix for the five stations' water quality data between spectral bands and WQI (50 < WQI < 250).

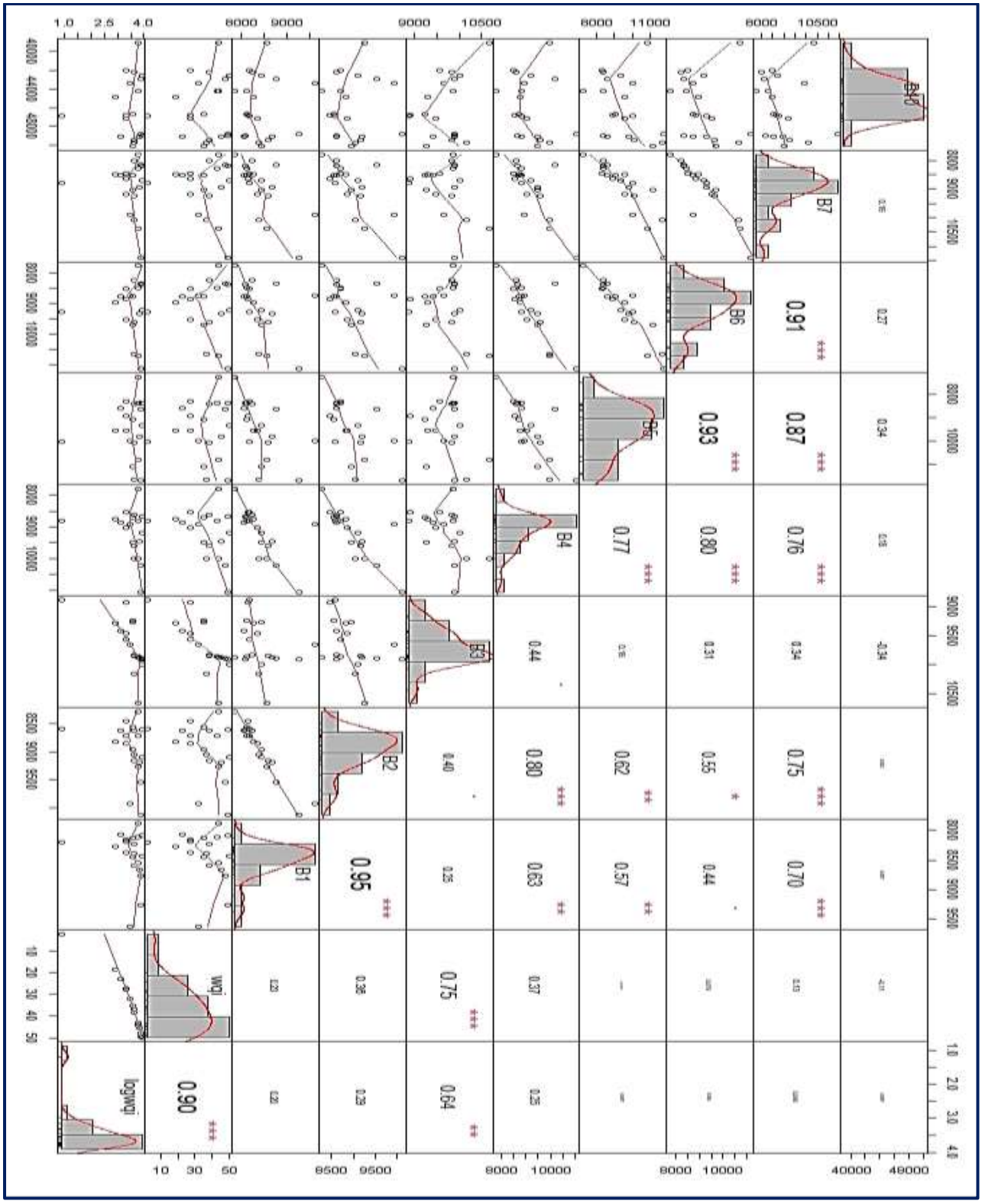

Figure (4.14): Correlation matrix for the five stations' water quality data between spectral bands and WQI (WQI < 50).

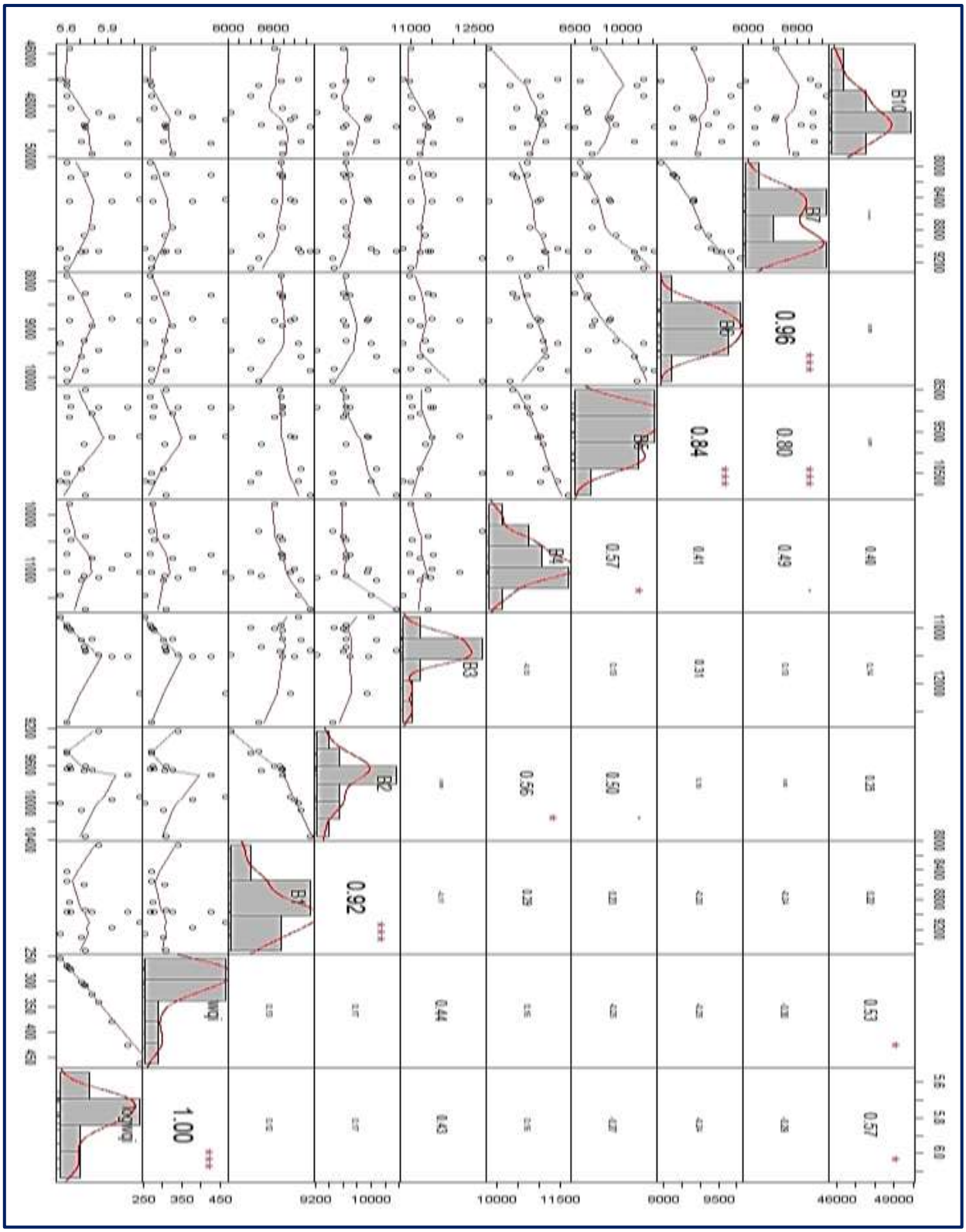

Figure (4.15): Correlation matrix for the five stations' water quality data between spectral bands and WQI (WQI > 250).

Table (4.15): The full linear regression model summary statistics for the WQI data and specter bands (WQI < 50).

Residuals:

Min	1Q	Median	3Q	Max
-16.0157	-5.4375	0.6377	6.9500	11.6306

Coefficients:

	Estimate	Std. Error	t value	Pr (>|t|)
(Intercept)	-208.70453	51.36913	-4.063	0.001574 **
dataf$B3	0.02521	0.00531	4.747	0.000474 ***

Residual standard error: 8.904 on 12 degrees of freedom

Multiple R-squared: 0.6525, Adjusted R-squared: 0.6236

F-statistic: 22.54 on 1 and 12 DF, p-value: 0.0004743

Table (4.16): The full linear regression model summary statistics for the WQI data and specter bands (WQI > 250).

Residuals:

Min	1Q	Median	3Q	Max
-16.0157	-5.4375	0.6377	6.9500	11.6306

Coefficients:

	Estimate	Std. Error	t value	Pr (>|t|)
(Intercept)	1.915e+00	1.271e+00	1.507	0.1660
dataf$B10	7.845e-05	2.632e-05	2.981	0.0154 *

Residual standard error: 0.1042 on 9 degrees of freedom

Multiple R-squared: 0.4969, Adjusted R-squared: 0.441

F-statistic: 8.888 on 1 and 9 DF, p-value: 0.01542

Table (4.17): The full linear regression model summary statistics for WQI data and specter bands (50 < WQI < 250).

Residuals:

Min	1Q	Median	3Q	Max
-0.75106	-0.01405	0.03352	0.06564	0.44253

Coefficients:

	Estimate	Std. Error	t value	Pr (>|t|)	
(Intercept)	-6.744e-01	3.080e-01	-2.19	0.0304	*
dataf$B3	5.287e-04	3.002e-05	17.61	<2e-16	***

Residual standard error: 0.17 on 125 degrees of freedom

Multiple R-squared: 0.7128, Adjusted R-squared: 0.7105

F-statistic: 310.2 on 1 and 125 DF, p-value: < 2.2e-16

Table (4.18): The final linear regression models for WQI with spectral bands.

MODEL	Model limitation	MSE	RMSE	R^2
WQI = exp [(-0.6744) + (0.0005287) × (B3)]	50 < WQI < 250	12.422	26.690	71
WQI = (-208.70453) + (0.02521) × (B3)	WQI < 50	6.1325	7.6639	62
WQI = exp [(1.915) + (0.00007845) × (B10)]	WQI > 250	69.065	89.206	44

4.7 GIS-Based spatial and temporal variation of WQI and turbidity

Water resource issues can be better solved by utilizing GIS technology to display and analysis water quality, determine water availability, and comprehend the natural environment on a local or regional scale. GIS can be utilized to map the spatial distribution of various contaminants, and the data gathered is invaluable for helping decision-makers execute corrective measures (Latha & Rao, 2010).

GIS is a powerful tool for storing, managing, creating solutions, and displaying geographical data that is frequently encountered in local or regional management of sanitary and water resources (Alanbari et al., 2015). Spatial, statistical, and geostatistical analyses are only a few of the many techniques available in GIS. The outcome will be shown in a raster format with a colorful gradient that shows the values at the various stations' different locations. In contrast, several techniques, including Inverse Distance Weighted (IDW), Spline, Kriging, and Natural Neighbor can be applied to interpolation procedures (Matejicek, 2005).

The study results have been merged using the QGIS 3.20.2 program to produce layers that show the geographical distribution of WQI in colored maps that show change zones in the water quality of the Hilla River at the study region. Analysis has been used to diagnose damaged areas and assist in locating the appropriate water quality zones.

Utilizing a tool from the GIS, the prediction technique IDW, the prediction map for WQI was created as a distribution map to cover the entire study region. The GIS maps shown in Figures (4.16, 4.18, 4.20, 4.22, 4.24, and 4.26) represent WQI variation in Hilla River during the study period (for the years of 2016 to 2021) especially and temporally.

As shown earlier, WQI has a significant relationship with turbidity. Therefore, the special and temporal changes in turbidity value will affect WQI values as shown in Figures (4.17, 4.19, 4.21, 4.23, 4.25, and 4.27).

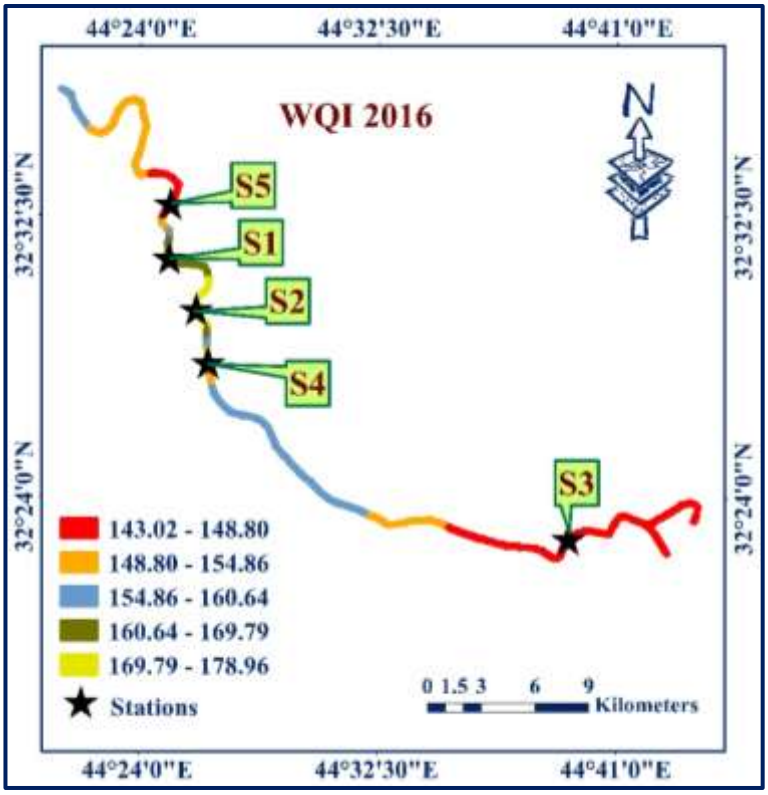

Figure (4.16): WQI distribution in Hilla River in 2016.

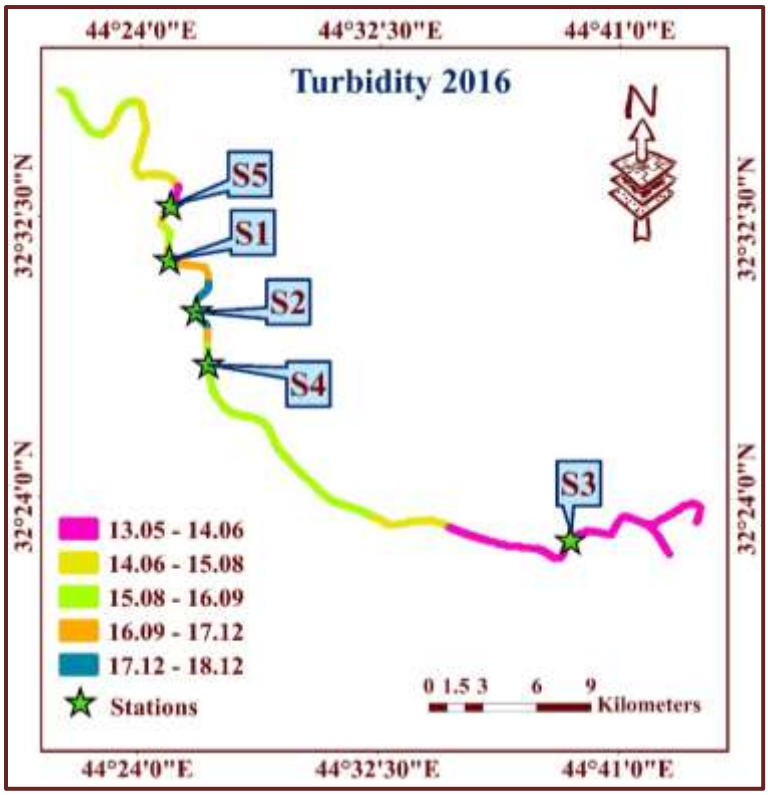

Figure (4.17): Turbidity distribution in Hilla River in 2016.

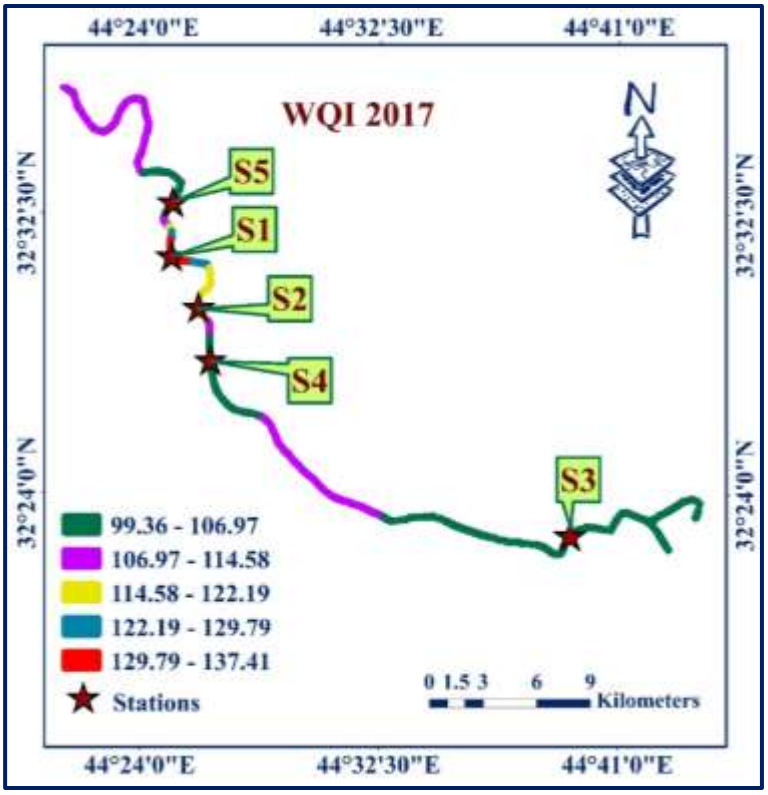

Figure (4.18): WQI distribution in Hilla River in 2017.

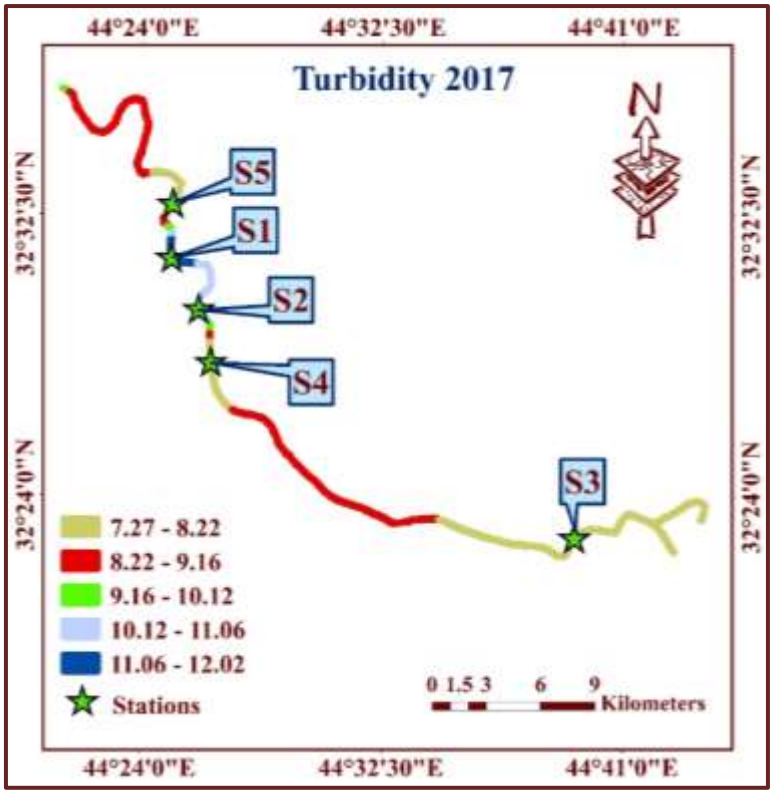

Figure (4.19): Turbidity distribution in Hilla River in 2017.

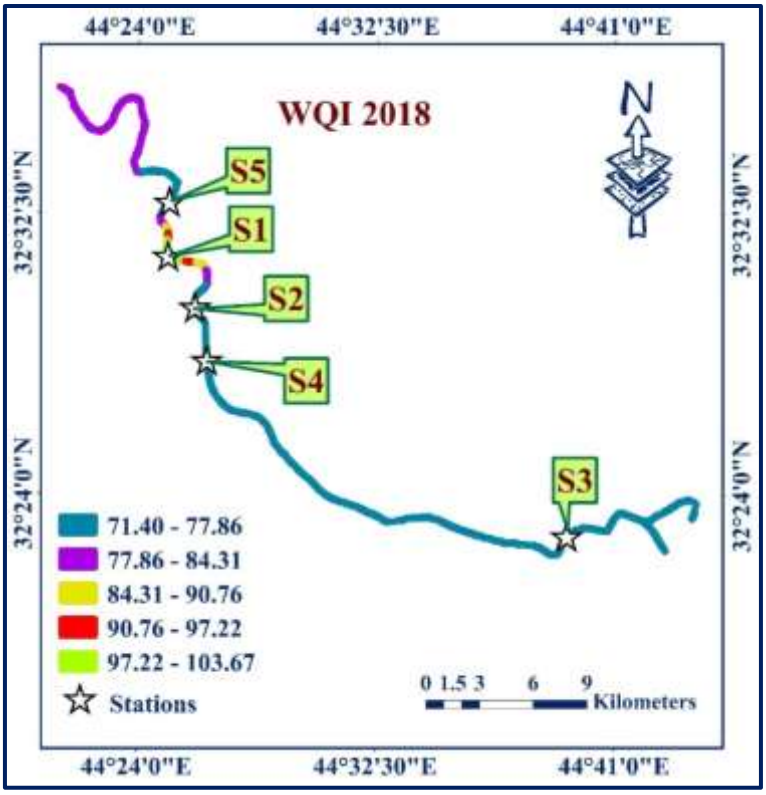

Figure (4.20): WQI distribution in Hilla River in 2018.

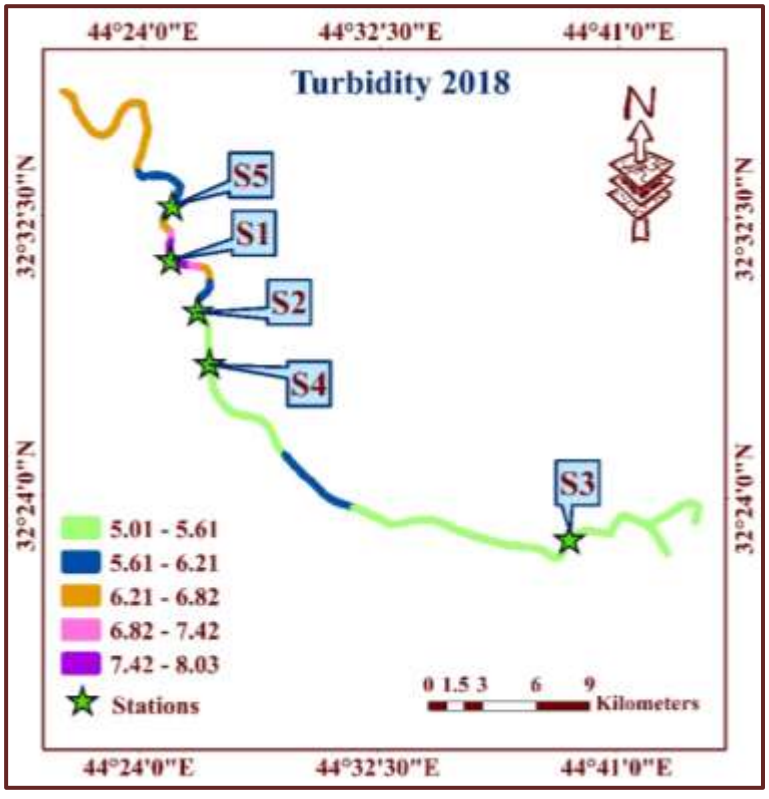

Figure (4.21): Turbidity distribution in Hilla River in 2018.

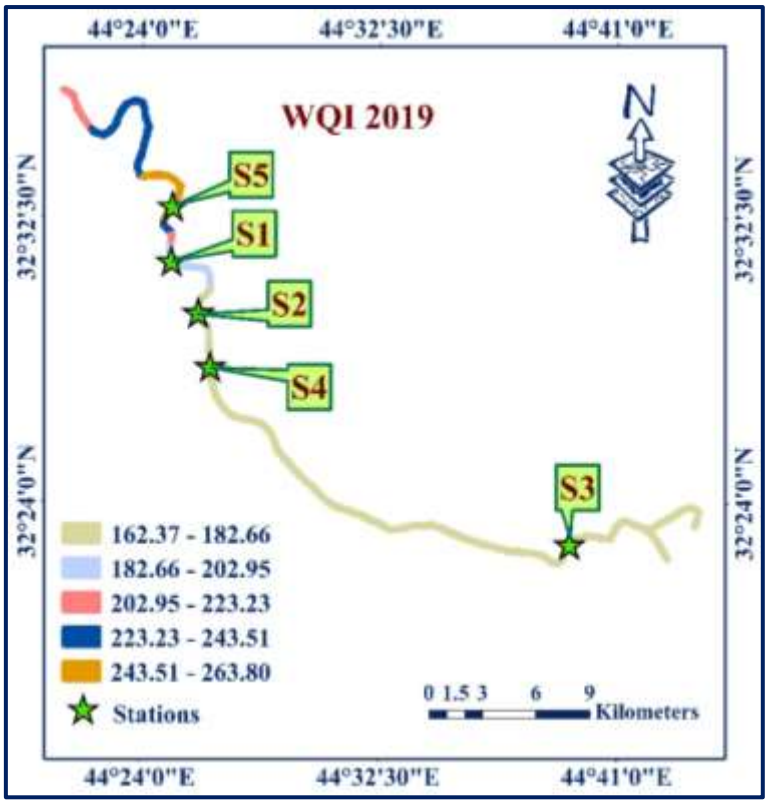

Figure (4.22): WQI distribution in Hilla River in 2019.

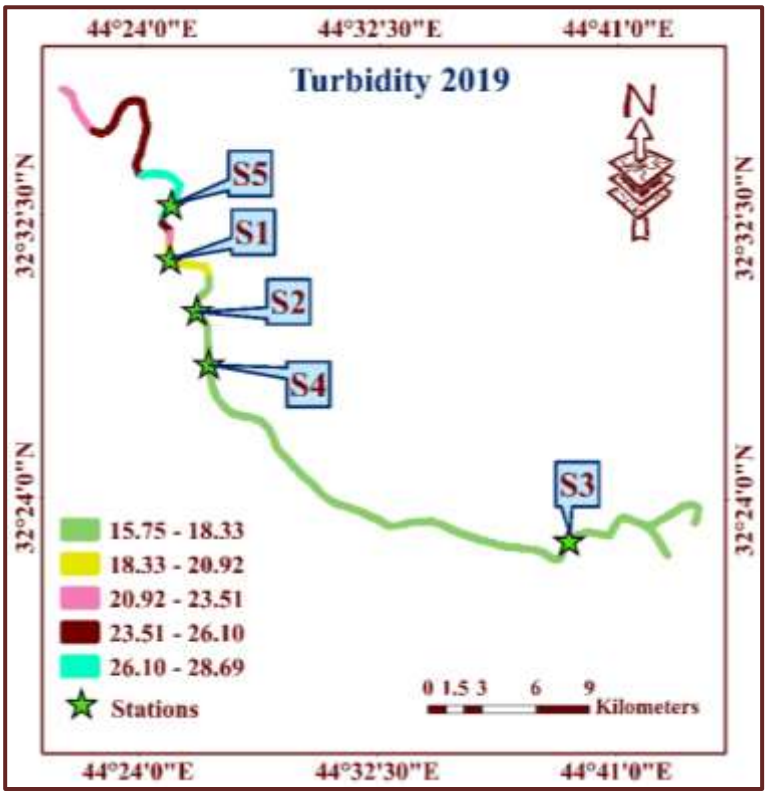

Figure (4.23): Turbidity distribution in Hilla River in 2019.

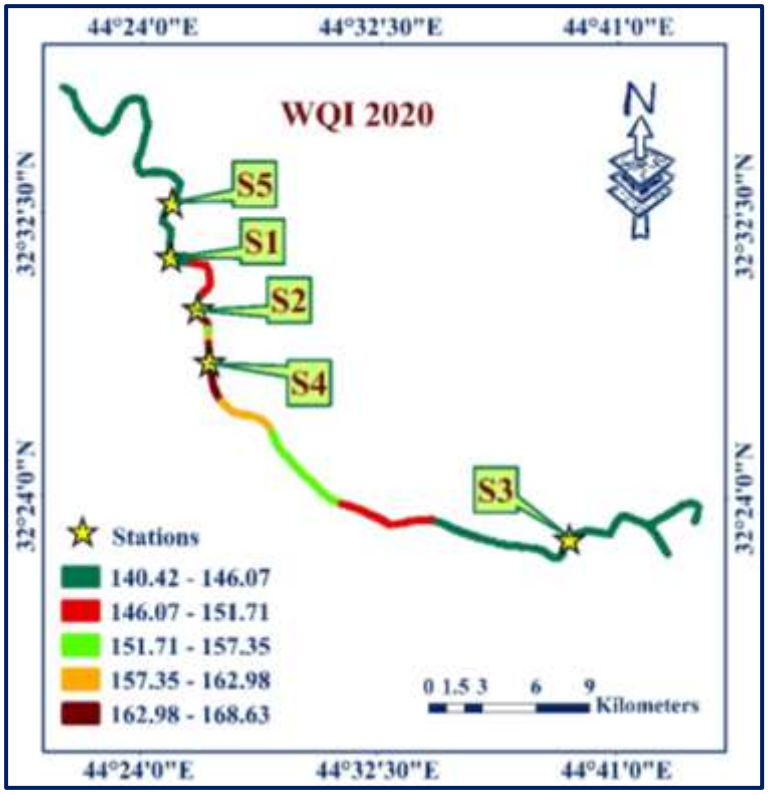

Figure (4.24): WQI distribution in Hilla River in 2020.

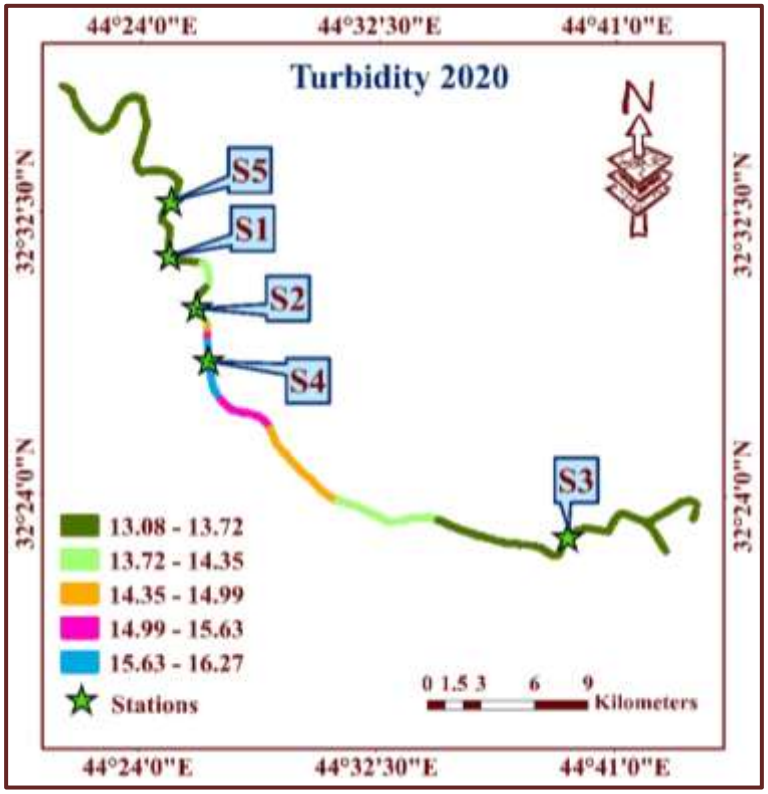

Figure (4.25): Turbidity distribution in Hilla River in 2020.

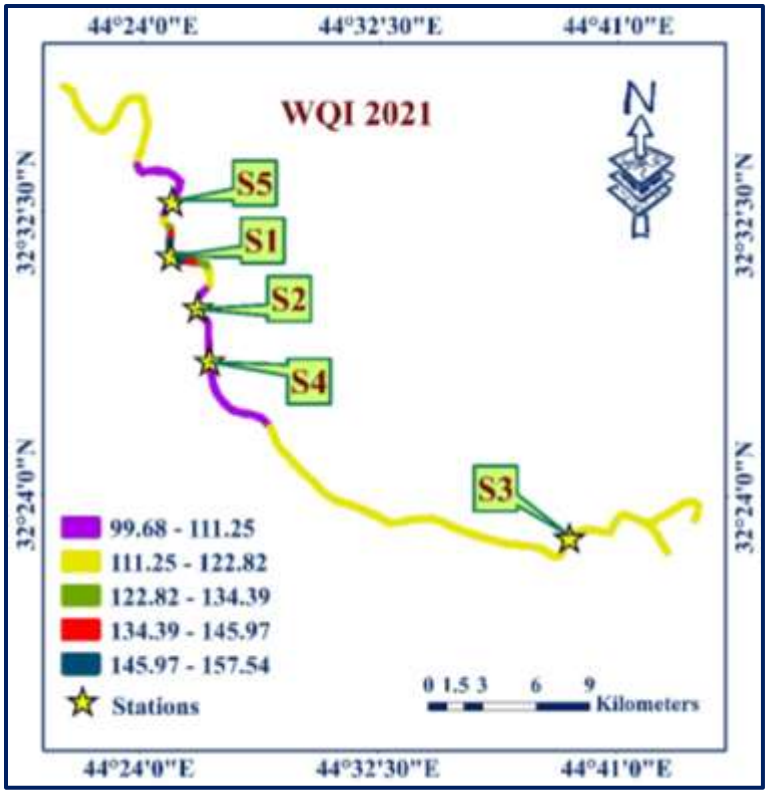

Figure (4.26): WQI distribution in Hilla River in 2021.

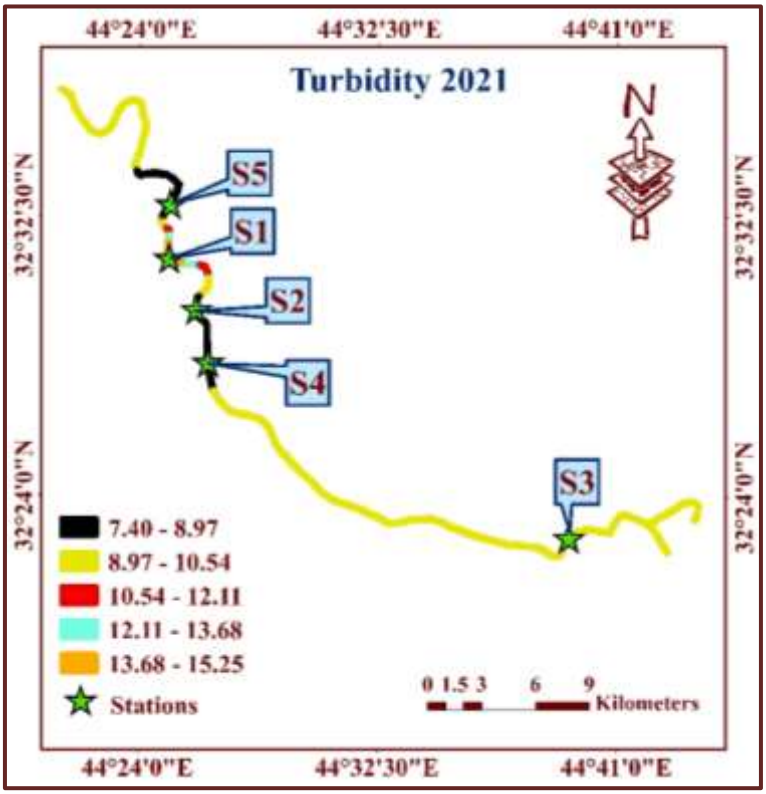

Figure (4.27): Turbidity distribution in Hilla River in 2021.

Visually, temporal variation in WQI and turbidity can be highlighted as shown in Figures (4.28 and 4.29). In station S1, the WQI and turbidity have the highest value in 2019. Station S2 also has the highest value of WQI and turbidity in 2019. In station S3, the highest WQI value is in 2016 and 2019 (roughly the same WQI value), but turbidity has the highest value in 2016. In station S4, the WQI value has the highest in 2016, 2019, and 2020, and also turbidity has the highest value in the same year. In station S5, the WQI and turbidity have the highest value in 2019.

Monitoring the origins of the contaminants and attempting to minimize or reduce their effects are strategies that can be used to preserve the surface water in Iraq. Identifying the sources of the contaminants, analyzing the results, explaining the causes of the contamination, and identifying techniques that can be used to decrease their impact or, in the worst cases, identify appropriate techniques that can be used to treat the contaminated water are all part of the most formal method. Thus, applying all of the above-developed models to predict Hilla River water quality is useful to monitor and assess the river status (Chabuk et al., 2020).

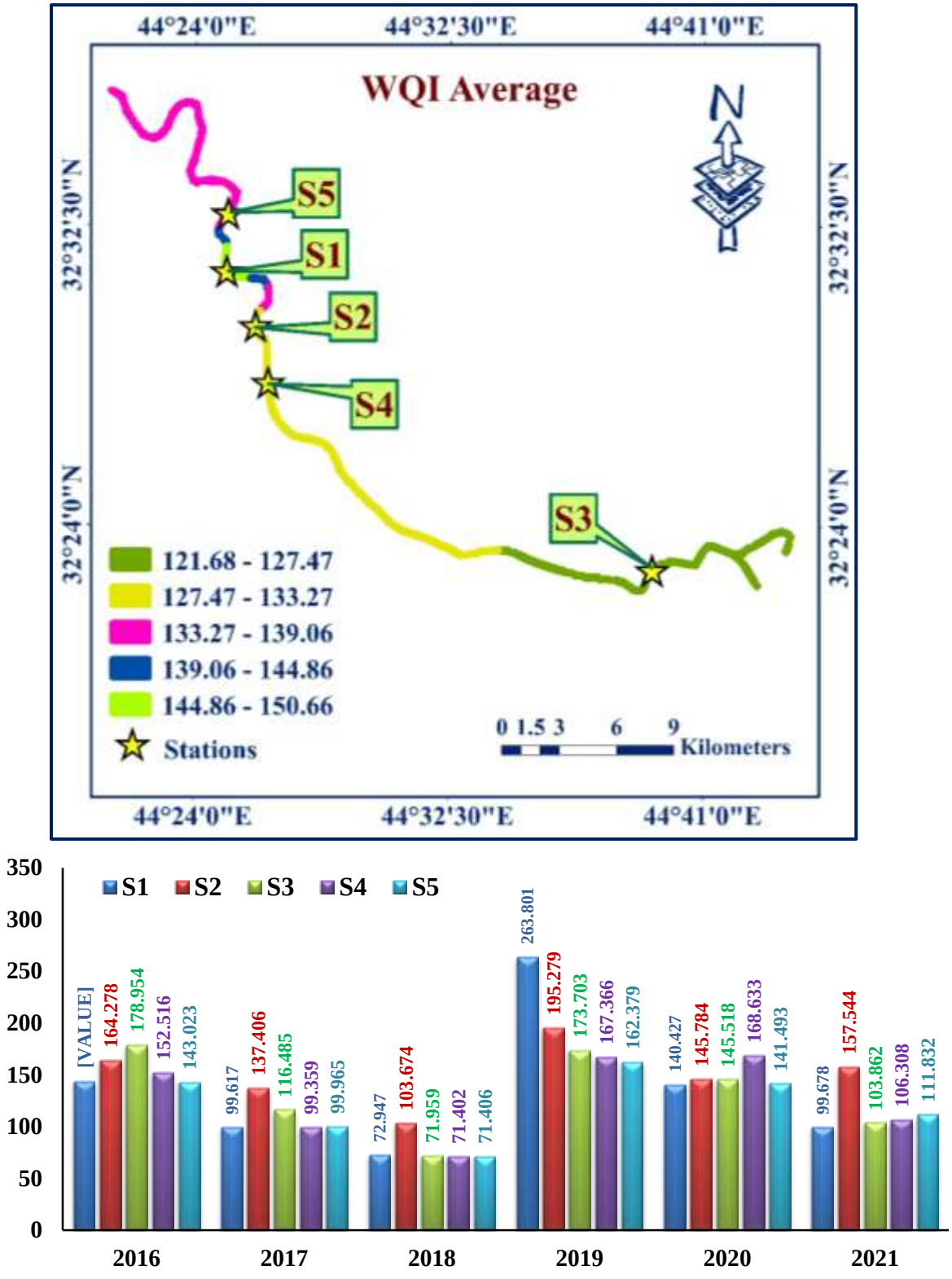

Figure (4.28): WQI variation in Hilla River during the study period.

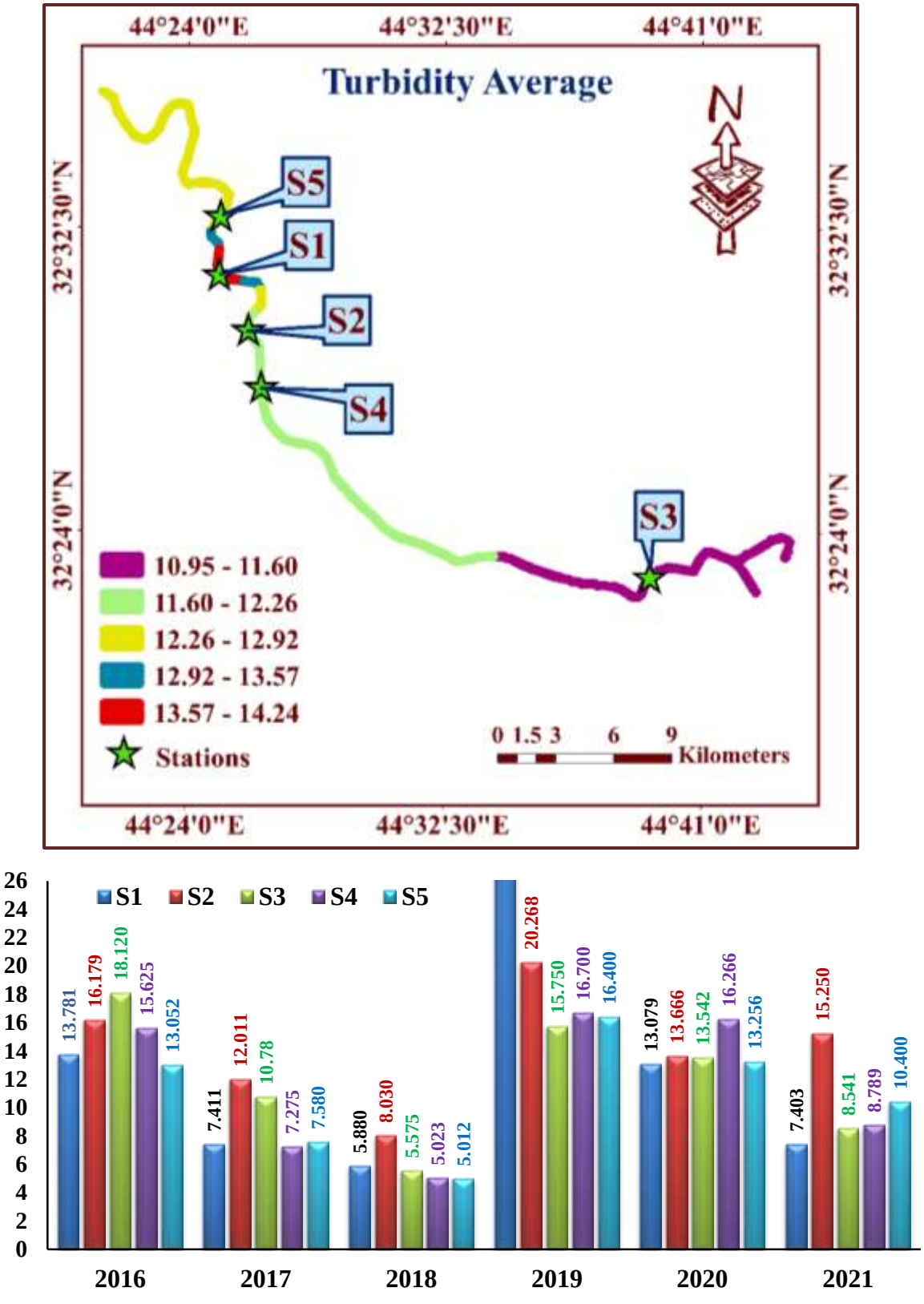

Figure (4.29): Turbidity (NTU) variation in Hilla River during the study period.

CHAPTER FIVE

Conclusions & Recommendations

5.1 Conclusions

Based on the results obtained, the most efficient, affordable, and trustworthy instruments for monitoring water quality parameters in various water bodies are remote sensing and GIS approaches combined with conventional in-situ sampling. The key conclusions of the present study are:

1. The main result of calculating WQI by weighted arithmetic method for Hilla River to the five sampling stations showed that the river can be categorized as "severely polluted".
2. Statically analysis for WQI and water quality parameters showed there is a significant relationship between WQI and turbidity in the river.
3. Two linear regression models were developed and validated for WQI and turbidity:
   - **A.** WQI values of less than 220 are positively correlated with turbidity, andthe statistical analysis result showed the linear regression model has a p-value of $2.2e^{-16}$ and R^2 of more than 70%.
   - **B.** WQI values of more than 220 are positively correlated withturbidity, and the statistical result showed the linear regression model has a p-value of $6.507e^{-6}$ and R^2 of more than 86% .
4. Some water quality parameters showed a significant relationship with the spectral bands' ratio such as (Band10/Band3, Band10/Band4, Band4/Band7, Band1/Band4, Band1/Band4, Band3/Band7, and Band1/Band2) of the Landsat 8 satellite.
5. A linear regression model between WQI and the surface reflectance images of Landsat 8 spectral bands showed a significant relationship between WQI and bands such as (Band 3 and Band 10).
6. Three linear regression models were developed and validated for WQI and the spectral bands:

A. WQI values of less than 50 have a considerable relationship with band 3, and the statistical analysis result showed the linear regression model has a p-value of 0.0004743 and R^2 of more than 60%.

B. WQI values of more than 50 and less than 250 have a considerable relationship with band 3, and the statistical analysis result showed the linear regression model has a p-value of $2.2e^{-16}$ and R^2 of more than 70%.

C. 250 WQI values of more than have a considerable relationship with band 3 and the statistics result in the statistics result show the linear regression model that has a p-value equal to 0.01542 and R^2 of more than 44%.

7. The GIS maps for Hilla River reach along Hilla City showed that the worst WQI value was in 2019 due to the high turbidity. On the other hand, the best WQI and turbidity values were in 2018. However,i n 2020 and 2021, there were some improvements in WQI and turbidity compared to 2019.

5.2 Recommendations

The following recommendations can be helpful for future studies:

1. More research is required to monitor and manage pollution sources in Iraq in order to safeguard and improve the quality of water, particularly in the upcoming years since the nation may be facing a water crisis.
2. The dates of the Landsat satellite images related to the relevant locations will be coordinated with the government's efforts to monitor water quality. More water characterization information and corresponding satellite images can be used in this way to create more accurate empirical WQ models and validate such models.
3. Correlating the water quality index with spectral bands utilizing nonlinear multiple regression, various spectral band ratios, and combinations, and various satellite image data are advised for further investigations.
4. Expand the investigation from the headwaters to the downstream at all times, taking into account additional factors like microbiological research and heavy metals to provide a complete picture of how the river is behaving.

REFERENCES

Abayazid, H., & El-Gamal, A. (2017). Employing remote sensing for water clarity monitoring in the Nile Delta Coast. International Water Technology Journal IWTJ, 7(4), 265-277.

Abbas, J. (2013). Assessment of water quality in Tigris River-Iraq by using GIS mapping. Natural Resources, 2013.

Abbas, M. R., Ahmad, B. B., & Abbas, T. R. (2021). Statistical Remote Sensing for Prediction of Inland Water Quality Parameters for Shatt Al-Arab River in Iraq. IOP Conference Series: Earth and Environmental Science,

Abbas, N., Wasimi, S., Al-Ansari, N., & Sultana, N. (2018). Water resources problems of Iraq: Climate change adaptation and mitigation. Journal of Environmental Hydrology, 26.

Abdelmalik, K. (2018). Role of statistical remote sensing for Inland water quality parameters prediction. The Egyptian Journal of Remote Sensing and Space Science, 21(2), 193-200.

Abdulkareem, I. H. (2020). Temperature and precipitations trends for hilla city using noaa/esrl gridded high-resolution data. Journal of Engineering Science and Technology, 15(3), 1883-1894.

Akter, T., Jhohura, F. T., Akter, F., Chowdhury, T. R., Mistry, S. K., Dey, D., Rahman, M. (2016). Water Quality Index for measuring drinking water quality in rural Bangladesh: a cross-sectional study. Journal of Health, Population and Nutrition, 35(1), 1-12.

Al-Bayati, Z. M. K., Nayle, I. H., & Jasim, B. S. (2018). Study of the Relationship Between Spectral Reflectivity and Water Quality Index in Hilla River. International Journal of Engineering & Technology, 7(3.36), 196-200.

Al-Mansori, N. J. (2017). Develop and Apply Water Quality Index to Evaluate Water Quality of Shatt-Al-Hilla River. Journal of University of Babylon, 25(2), 368-374.

Al-Masaodi, H. J., & Al-Zubaidi, H. A. (2021). Spatial-temporal changes of land surface temperature and land cover over Babylon Governorate, Iraq. Materials Today: Proceedings.

Al-Mayah, W. T. (2021). Chemical and microbial health risk assessment of drinking water treatment plants in Kut City, Iraq. Materials Today: Proceedings, 42, 3062-3067.

Al-Ridah, Z. A., Al-Zubaidi, H., Naje, A., & Ali, I. (2020). Drinking water quality assessment by using water quality index (WQI) for Hillah River, Iraq. Ecology, Environmental & Conservation, 26, 390-399.

Al-Shujairi, S. O. H. (2013). Develop and apply water quality index to evaluate water quality of Tigris and Euphrates Rivers in Iraq. International Journal of Modern Engineering Research, 3(4), 2119-2126.

Al-Zubaidi, H. A., Naje, A. S., Abed Al-Ridah, Z., Chabuck, A., & Ali, I. M. (2021). A statistical technique for modelling dissolved oxygen in salt lakes. Cogent Engineering, 8(1), 1875533.

Alaguraja, P., Yuvaraj, D., Sekar, M., Muthuveerran, P., & Manivel, M. (2010). Remote sensing and GIS approach for the water pollution and management in Tiruchirappli Taluk, Tamil Nadu, India. International Journal of Environmental Sciences, 1(1), 66.

Alanbari, M. A., Alquzweeni, S. S., & Aldaher, R. A. (2015). Spatial distribution mapping for various pollutants of al-kufa river using geographical information system (GIS). International Journal of Civil Engineering and Technology (IJCIET), 6(10), 1-14.

Allawai, M. F., & Ahmed, B. A. (2019). Using GIS and Remote Sensing Techniques to Study Water Quality Changes and Spectral Analysis of Tigris River within Mosul City, North of Iraq. Iraqi Journal of Science, 2300-2307.

Alley, E. R. (2007). Water quality control handbook. McGraw-Hill Education.

Alobaidy, A. H. M. J., Maulood, B. K., & Kadhem, A. J. (2010). Evaluating raw and treated water quality of Tigris River within Baghdad by index analysis. journal of water resource and protection, 2(7), 629.

Alsaqqar, A. S., Hashim, A., & Mahdi, A. (2015). Water quality index assessment using GIS case study: Tigris River in Baghdad City. International Journal of Current Engineering and Technology, 5(4), 2515-2520.

Arslan, I. (2001). Treatability of a simulated disperse dye-bath by ferrous iron coagulation, ozonation, and ferrous iron-catalyzed ozonation. Journal of Hazardous Materials, 85(3), 229-241.

Avid Hirst, D., & ob Morris, R. (2001). Water quality of Scottish rivers: spatial and temporal trends. Science of the Total Environment, 265(1-3), 327-342.

Bishop, T., McBratney, A., & Whelan, B. (2001). Measuring the quality of digital soil maps using information criteria. Geoderma, 103(1-2), 95-111.

Boah, D. K., Twum, S. B., & Pelig-Ba, K. B. (2015). Mathematical computation of water quality index of Vea dam in upper east region of Ghana. Environ Sci, 3(1), 11-16.

Bouaziz, M., Leidig, M., & Gloaguen, R. (2011). Optimal parameter selection for qualitative regional erosion risk monitoring: A remote sensing study of SE Ethiopia. Geoscience Frontiers, 2(2), 237-245.

Burrough, P. A., & McDonnell, R. A. (1998). Creating continuous surfaces from point data. Principles of Geographic Information Systems. Oxford University Press, Oxford, UK.

Cambers, G., & Ghina, F.(2005). An educational tool for sustainable development.

Carpenter, S. R., Caraco, N. F., Correll, D. L., Howarth, R. W., Sharpley, A. N., & Smith, V. H. (1998). Nonpoint pollution of surface waters with phosphorus and nitrogen. Ecological applications, 8(3), 559-568.

Carré, F., & Girard, M. (2002). Quantitative mapping of soil types based on regression kriging of taxonomic distances with landform and land cover attributes. Geoderma, 110(3-4), 241-263.

Carroll, S. P., Dawes, L. A., Goonetilleke, A., & Hargreaves, M. (2006). Water quality profile of an urbanising catchment–Ningi Creek Catchment.

Chabuk, A., Al-Madhlom, Q., Al-Maliki, A., Al-Ansari, N., Hussain, H. M., & Laue, J. (2020). Water quality assessment along Tigris River (Iraq) using water quality index (WQI) and GIS software. Arabian Journal of Geosciences, 13(14), 1-23.

Chabuk, A., AM Al-Zubaidi, H., Abdalkadhum, A. J., Al-Ansari, N., Ali Abed, S., Al-Maliki, A., . . . Ewaid, S. (2022). Application ArcGIS on Modified-WQI Method to Evaluate Water Quality of the Euphrates River, Iraq, Using Physicochemical Parameters. Proceedings of Sixth International Congress on Information and Communication Technology,

Chabuk, A., Jahad, U. A., Majdi, A., Isam, M., Al-Ansari, N., SH Majdi, H., . . . Abed, S. A. (2022). Creating the Distribution Map of Groundwater for Drinking Uses Using Physio-Chemical Variables; Case Study: Al-Hilla City, Iraq. Water, Air, & Soil Pollution, 233(6), 1-14.

Chai, T., Carmichael, G. R., Tang, Y., Sandu, A., Heckel, A., Richter, A., & Burrows, J. P. (2009). Regional NOx emission inversion through a four-dimensional variational approach using SCIAMACHY tropospheric NO2 column observations. Atmospheric Environment, 43(32), 5046-5055.

Chandra, D. S., Asadi, S., & Raju, M. (2017). Estimation of water quality index by weighted arithmetic water quality index method: A model study. International Journal of Civil Engineering and Technology, 8(4), 1215-1222.

Chapman, D. (2021). Water quality assessments: a guide to the use of biota, sediments and water in environmental monitoring. CRC Press.

Cheremisinoff, P. N. (2019). Handbook of water and wastewater treatment technology. Routledge.

Chitmanat, C., & Traichaiyaporn, S. (2010). Spatial and temporal variations of physical-chemical water quality and some heavy metals in water,

sediments and fish of the Mae Kuang River, Northern Thailand. International Journal of Agriculture and Biology, 12(6), 816-820.
Cracknell, A., Newcombe, S., Black, A., & Kirby, N. (2001). The ABDMAP (algal bloom detection, monitoring and prediction) concerted action. International Journal of Remote Sensing, 22(2-3), 205-247.
Danbara, T. T. (2014). Deriving water quality indicators of lake tana, ethiopia, from landsat-8 University of Twente].
Davis, M. L. (2010). Water and wastewater engineering: design principles and practice. McGraw-Hill Education.
Davis, M. L., & Cornwell, D. A. (2008). Introduction to environmental engineering. McGraw-Hill.
Dekker, A. (1993). Detection of optical water parameters for eutrophic lakes by high resolution remote sensing. Free University, Amsterdam.
Dekker, A., Zamurović-Nenad, Ž., Hoogenboom, H., & Peters, S. (1996). Remote sensing, ecological water quality modelling and in situ measurements: a case study in shallow lakes. Hydrological Sciences Journal, 41(4), 531-547.
DeZuane, J. (1997). Handbook of drinking water quality. John Wiley & Sons.
Divya Raj, S., & Kani, K. M. (2018). Water quality assessment of sasthamcotta lake, Kollam, Kerala. International Journal of Engineering and Advanced Technology (IJEAT), 7(3), 119-129.
Edwards, A. W. (2005). RA Fischer, statistical methods for research workers, (1925). In Landmark Writings in Western Mathematics 1640-1940 (pp. 856-870). Elsevier.
El-Zeiny, A., & El-Kafrawy, S. (2017). Assessment of water pollution induced by human activities in Burullus Lake using Landsat 8 operational land imager and GIS. The Egyptian Journal of Remote Sensing and Space Science, 20, S49-S56.
El Saadi, A. M., Yousry, M. M., & Jahin, H. S. (2014). Statistical estimation of Rosetta branch water quality using multi-spectral data. Water Science, 28(1), 18-30.
Ewaid, S. H., Abed, S. A., & Kadhum, S. A. (2018). Predicting the Tigris River water quality within Baghdad, Iraq by using water quality index and regression analysis. Environmental Technology & Innovation, 11, 390-398.
Federation, W. E., & Association, A. (2005). Standard methods for the examination of water and wastewater. American Public Health Association (APHA): Washington, DC, USA, 21.

Gholizadeh, M. H., Melesse, A. M., & Reddi, L. (2016). A comprehensive review on water quality parameters estimation using remote sensing techniques. Sensors, 16(8), 1298.

Gong, G., Mattevada, S., & O'Bryant, S. E. (2014). Comparison of the accuracy of kriging and IDW interpolations in estimating groundwater arsenic concentrations in Texas. Environmental research, 130, 59-69.

González-Márquez, L. C., Torres-Bejarano, F. M., Rodríguez-Cuevas, C., Torregroza-Espinosa, A. C., & Sandoval-Romero, J. A. (2018). Estimation of water quality parameters using Landsat 8 images: application to Playa Colorada Bay, Sinaloa, Mexico. Applied Geomatics, 10(2), 147-158.

González-Márquez, L. C., Torres-Bejarano, F. M., Torregroza-Espinosa, A. C., Hansen-Rodríguez, I. R., & Rodríguez-Gallegos, H. B. (2018). Use of LANDSAT 8 images for depth and water quality assessment of El Guájaro reservoir, Colombia. Journal of South American Earth Sciences, 82, 231-238.

Gray, N. F. (1994). Drinking water quality: problems and solutions. John Wiley & Sons.

Hereher, M., Salem, M., & Darwish, D. (2010). Mapping water quality of Burullus Lagoon using remote sensing and geographic information system. Journal of American science, 7(1), 138-143.

Hossain, A., Jia, Y., & Chao, X. (2010). Development of remote sensing based index for estimating/mapping suspended sediment concentration in river and lake environments. Proceedings of 8th international symposium on ECOHYDRAULICS (ISE 2010),

Hossain, A., Jia, Y., Chao, X., & Altinakar, M. (2014). Application of advanced remote sensing techniques to improve modeling estuary water quality. In Remote sensing and modeling (pp. 295-313). Springer.

Hossain, A., Mathias, C., & Blanton, R. (2021). Remote Sensing of Turbidity in the Tennessee River Using Landsat 8 Satellite. Remote Sensing, 13(18), 3785.

Huda M, M., & Al-Ansari, N. (2018). Geographical Information System and Remote Sensing for WaterResources Management Case Study: The Diyala River, Iraq. International J. of Civil Engineering and Technology, 9(12), 971-984.

Huisman, O., & de By, R. A. (2009). Principles of geographic information systems. ITC Educational Textbook Series, 1, 17.

Ioannidis, J. P. (2018). The proposal to lower P value thresholds to. 005. Jama, 319(14), 1429-1430.

Iticescu, C., Georgescu, L. P., & Topa, C. M. (2013). Assessing the Danube water quality index in the city of Galati, Romania. Carpathian Journal of Earth and Environmental Sciences, 8(4), 155-164.

Jain, C., & Sharma, M. (2002). Regression analysis of ground water quality data of Malprabha river basin, Karnataka. J. Indian Water Resources Society, 22(1).

Japitana, M. V., & Burce, M. E. C. (2019). A satellite-based remote sensing technique for surface water quality estimation. Engineering, Technology & Applied Science Research, 9(2), 3965-3970.

Johnson, D. L., Ambrose, S. H., Bassett, T. J., Bowen, M. L., Crummey, D. E., Isaacson, J. S., . . . Winter-Nelson, A. E. (1997). Meanings of environmental terms. Journal of environmental quality, 26(3), 581-589.

Johnson, R. A., & Bhattacharyya, G. K. (2019). Statistics: principles and methods. John Wiley & Sons.

Kankal, N., Indurkar, M., Gudadhe, S., & Wate, S. (2012). Water quality index of surface water bodies of Gujarat, India. Asian J. Exp. Sci, 26(1), 39-48.

Kannan, K. S., & Ramasubramanian, V. (2011). Assessment of fluoride contamination in groundwater using GIS, Dharmapuri district, Tamilnadu, India. International Journal of Engineering Science and Technology, 3(2).

Khouni, I., Louhichi, G., & Ghrabi, A. (2021). Use of GIS based Inverse Distance Weighted interpolation to assess surface water quality: Case of Wadi El Bey, Tunisia. Environmental Technology & Innovation, 24, 101892.

Kotti, M. E., Vlessidis, A. G., Thanasoulias, N. C., & Evmiridis, N. P. (2005). Assessment of river water quality in Northwestern Greece. Water Resources Management, 19(1), 77-94.

Kulkarni, A. (2011). Water quality retrieval from Landsat TM imagery. Procedia Computer Science, 6, 475-480.

Lehmann, M. K., Schallenberg, L. A., & Allan, M. G. (2017). Feasibility of water quality monitoring by remote sensing in the Waikato Region.

Li, J., & Heap, A. D. (2011). A review of comparative studies of spatial interpolation methods in environmental sciences: Performance and impact factors. Ecological Informatics, 6(3-4), 228-241.

Lodder, W., Van Den Berg, H., Rutjes, S., & de Roda Husman, A. (2010). Presence of enteric viruses in source waters for drinking water production in The Netherlands. Applied and environmental microbiology, 76(17), 5965-5971.

Longley, P. A., Goodchild, M. F., Maguire, D. J., & Rhind, D. W. (2005). Geographic information systems and science. John Wiley & Sons.

Malthus, T., & Dekker, A. (1995). First derivative indices for the remote sensing of inland water quality using high spectral resolution reflectance. Environment international, 21(2), 221-232.

Mandel, J. (2012). The statistical analysis of experimental data. Courier Corporation.

Matejicek, L. (2005). Spatial modelling of air pollution in urban areas with GIS: a case study on integrated database development. Advances in geosciences, 4, 63-68.

Miner, G. (2006). Standard methods for the examination of water and wastewater. American Water Works Association. Journal, 98(1), 130.

Mirzaei, R., & Sakizadeh, M. (2016). Comparison of interpolation methods for the estimation of groundwater contamination in Andimeshk-Shush Plain, Southwest of Iran. Environmental Science and Pollution Research, 23(3), 2758-2769.

Mishra, S., Stumpf, R. P., & Meredith, A. (2019). Evaluation of RapidEye data for mapping algal blooms in inland waters. International journal of remote sensing, 40(7), 2811-2829.

Mohammed, A. A., & Shakir, A. A. (2012). Evaluation the performance of Al-wahdaa project drinking water treatment plant: A case study in Iraq. International Journal of advances in applied sciences, 1(3), 130-138.

Nas, B. (2009). Geostatistical Approach to Assessment of Spatial Distribution of Groundwater Quality. Polish Journal of Environmental Studies, 18(6).

Nelson, J. S. (2011). US Geological Survey (USGS) Earth Resources Observation and Science (EROS) Center-fiscal year 2010 annual report (2331-1258).

Noori, M. M., Abdulrazzaq, K., Mohammed, A., & Abbas, A. (2017). Assessment of water quality and suitability of Euphrates river in Iraq for drinking purpose by applying water quality indices (WQIs) and geographical information system (GIS) techniques. International Journal of Science and Nature, 8(4), 741-756.

Nusret, D., & Dug, S. (2012). Applying the inverse distance weighting and kriging methods of the spatial interpolation on the mapping the annual precipitation in Bosnia and Herzegovina.

Ochir, A., & Davaa, G. (2011). Application of index analysis to evaluate the water quality of the Tuul River in Mongolia. Journal of Water Resource and Protection, 2011.

Oko, O. J., Aremu, M. O., Odoh, R., Yebpella, G., & Shenge, G. A. (2014). Assessment of water quality index of borehole and well water in Wukari Town, Taraba State, Nigeria. Assessment, 4(5), 1-9.

Olmanson, L. G., Brezonik, P. L., & Bauer, M. E. (2015). Remote sensing for regional lake water quality assessment: capabilities and limitations of current and upcoming satellite systems. In Advances in watershed science and assessment (pp. 111-140). Springer.

Omer, N. H. (2019). Water quality parameters. Water quality-science, assessments and policy, 18, 1-34.

Oni, O., & Fasakin, O. (2016). The use of water quality index method to determine the potability of surface water and groundwater in the vicinity of a municipal solid waste dumpsite in Nigeria. American Journal of Engineering Research, 5(10), 96-101.

Organization, W. H., & WHO. (2004). Guidelines for drinking-water quality (Vol. 1). world health organization.

Ouyang, Y. (2005). Evaluation of river water quality monitoring stations by principal component analysis. Water research, 39(12), 2621-2635.

Pathak, S., Prasad, S., & Pathak, T. (2015). Determination of water quality index river Bhagirathi in Uttarkashi, Uttarakhand, India. International Journal of research granthaalayah, 3(9), 1-7.

Qiao, P., Lei, M., Yang, S., Yang, J., Guo, G., & Zhou, X. (2018). Comparing ordinary kriging and inverse distance weighting for soil as pollution in Beijing. Environmental Science and Pollution Research, 25(16), 15597-15608.

Qu, L., Xiao, H., Zheng, N., Zhang, Z., & Xu, Y. (2017). Comparison of four methods for spatial interpolation of estimated atmospheric nitrogen deposition in South China. Environmental Science and Pollution Research, 24(3), 2578-2588.

Reza, R., & Singh, G. (2010). Assessment of ground water quality status by using Water Quality Index method in Orissa, India. World Appl Sci J, 9(12), 1392-1397.

Setianto, A., & Triandini, T. (2013). Comparison of kriging and inverse distance weighted (IDW) interpolation methods in lineament extraction and analysis. Journal of Applied Geology, 5(1).

Sharma, M., & Jain, C. (2005). Fluoride modeling using best subset procedure. J Appl Hydrol, 18, 12-22.

Spellman, F. R. (2017). The drinking water handbook. CRC Press.

Swarna Latha, P., & Nageswara Rao, K. (2010). Assessment and spatial distribution of quality of groundwater in zone II and III, Greater Visakhapatnam, India using water quality index (WQI) and GIS. International Journal of environmental sciences, 1(2), 198-212.

Tchobanoglus, G., Burton, F., & Stensel, H. D. (2003). Wastewater engineering: treatment and reuse. American Water Works Association. Journal, 95(5), 201.

Tomar, M. (1999). Quality assessment of water and wastewater. CRC press.

Tyagi, S., Sharma, B., Singh, P., & Dobhal, R. (2013). Water quality assessment in terms of water quality index. American Journal of water resources, 1(3), 34-38.

Whitehead, P., Wilby, R., Butterfield, D., & Wade, A. (2006). Impacts of climate change on in-stream nitrogen in a lowland chalk stream: an appraisal of adaptation strategies. Science of the total environment, 365(1-3), 260-273.

Whitehead, P. G., Wilby, R. L., Battarbee, R. W., Kernan, M., & Wade, A. J. (2009). A review of the potential impacts of climate change on surface water quality. Hydrological sciences journal, 54(1), 101-123.

Wu, M., Zhang, W., Wang, X., & Luo, D. (2009). Application of MODIS satellite data in monitoring water quality parameters of Chaohu Lake in China. Environmental monitoring and assessment, 148(1), 255-264.

Zare Abyaneh, H. (2014). Evaluation of multivariate linear regression and artificial neural networks in prediction of water quality parameters. Journal of Environmental Health Science and Engineering, 12(1), 1-8.

Zhang, D. (2017). A coefficient of determination for generalized linear models. The American Statistician, 71(4), 310-316.

Zubaidi, S. L., Al-Bugharbee, H., Muhsin, Y. R., Hashim, K., & Alkhaddar, R. (2020). Forecasting of monthly stochastic signal of urban water demand: Baghdad as a case study. IOP Conference Series: Materials Science and Engineering,

Zubaidi, S. L., Hashim, K., Ethaib, S., Al-Bdairi, N. S. S., Al-Bugharbee, H., & Gharghan, S. K. (2020). A novel methodology to predict monthly municipal water demand based on weather variables scenario. Journal of King Saud University-Engineering Sciences.

Appendix

A

Appendix A

Table (A.1): Landsat-8 sense details used in this study in 2017.

Date	Landsat-8 Sense Identifier	Date Acquired	Sensor Identifier
2017	LC81680382017010LGN01	10/01/2017	OLI_TIRS
	LC81680382017042LGN00	11/02/2017	
	LC81680382017074LGN00	15/03/2017	
	LC81680382017106LGN00	16/04/2017	
	LC81680382017138LGN00	18/05/2017	
	LC81680382017170LGN00	19/06/2017	
	LC81680382017202LGN00	21/07/2017	
	LC81680382017234LGN00	22/08/2017	
	LC81680382017250LGN00	07/09/2017	
	LC81680382017282LGN00	09/10/2017	
	LC81680382017330LGN00	26/11/2017	
	LC81680382017362LGN00	28/12/2017	

Table (A.2): Landsat-8 sense details used in this study in 2018.

Date	Landsat-8 Sense Identifier	Date Acquired	Sensor Identifier
2018	LC81680382018013LGN00	13/01/2018	OLI_TIRS
	LC81680382018045LGN00	14/02/2018	
	LC81680382018077LGN00	18/03/2018	
	LC81680382018109LGN00	19/04/2018	
	LC81680382018141LGN00	21/05/2018	
	LC81680382018157LGN00	06/06/2018	
	LC81680382018205LGN00	24/07/2018	
	LC81680382018237LGN00	25/08/2018	
	LC81680382018269LGN00	26/09/2018	
	LC81680382018301LGN00	28/10/2018	
	LC81680382018317LGN00	13/11/2018	
	LC81680382018349LGN00	15/12/2018	

Table (A.3): Landsat-8 sense details used in this study in 2019.

Date	Landsat-8 Sense Identifier	Date Acquired	Sensor Identifier
2019	LC81680382019016LGN00	16/01/2019	OLI_TIRS
	LC81680382019048LGN00	17/02/2019	
	LC81680382019064LGN00	05/03/2019	
	LC81680382019096LGN00	06/04/2019	
	LC81680382019144LGN00	24/05/2019	
	LC81680382019176LGN00	25/06/2019	
	LC81680382019208LGN00	27/07/2019	
	LC81680382019224LGN01	12/08/2019	
	LC81680382019272LGN00	29/09/2019	
	LC81680382019288LGN00	15/10/2019	
	LC81680382019320LGN00	16/11/2019	
	LC81680382019352LGN01	18/12/2019	

Table (A.4): Landsat-8 sense details used in this study in 2020.

Date	Landsat-8 Sense Identifier	Date Acquired	Sensor Identifier
2020	LC81680382020003LGN00	03/01/2020	OLI_TIRS
	LC81680382020035LGN00	04/02/2020	
	LC81680382020083LGN00	23/03/2020	
	LC81680382020115LGN00	24/04/2020	
	LC81680382020131LGN00	10/05/2020	
	LC81680382020163LGN00	11/06/2020	
	LC81680382020211LGN00	29/07/2020	
	LC81680382020227LGN00	14/08/2020	
	LC81680382020259LGN00	15/09/2020	
	LC81680382020291LGN00	17/10/2020	
	LC81680382020323LGN00	18/11/2020	
	LC81680382020355LGN00	20/12/2020	

Table (A.5): Landsat-8 sense details used in this study in 2021.

Date	Landsat-8 Sense Identifier	Date Acquired	Sensor Identifier
2021	LC81680382021021LGN00	21/01/2021	OLI_TIRS
	LC81680382021053LGN00	22/02/2021	
	LC81680382021069LGN00	10/03/2021	
	LC81680382021101LGN00	11/04/2021	
	LC81680382021133LGN00	13/05/2021	
	LC81680382021165LGN00	14/06/2021	

Appendix

B

Table (B.1): Monthly average of water quality parameters for S1 2016.

month	1	2	3	4	5	6	7	8	9	10	11	12
pH	7.9	7.9	7.8	7.8	8.1	7.4	7.6	7.9	7.8	7.9	8.2	7.7
Turb	27	15.2	15.2	8.1	7.2	7.8	13.6	8.6	13.3	22.1	13.9	13.3
EC	1137.7	1009	913.3	1056.5	1013	976.3	1023	1151	1134.5	1096	1128.5	1125
TH	433.3	346.7	338	393.5	365	359.7	397.7	389	403	392.5	386.5	350.7
Ca	92	81	71	89	86.5	91	99	97.7	96.5	88	78	71.3
Mg	49.7	35	39.3	41.5	37.5	32	37	35.3	39.5	42	47	42
SO4	299.7	266.7	227.7	290.5	264.5	269.7	324	337	336	331	279.5	273.7
TDS	738	651	576.7	717	673	614.7	655.3	709.3	763	703	702	718.7
Na	81.3	82	75	79.5	77.5	66.3	67.7	83.7	89	87	99	89.7
k	4.6	4.8	2.9	3.1	3.3	3.2	3.1	4.9	3.4	3.3	3.3	3.1
TSS	79.7	29.7	52.7	46	16	40	34.7	46	38	79	61	66
ALK	120	128	140	128	117	119.3	112.7	106	106	109	116	131.3
Cl	116	109	97	118.5	109.5	96.3	95	99.3	110	113	118.5	116.7

Table (B.2): Monthly average of water quality parameters for S2 2016.

month	**1**	**2**	**3**	**4**	**5**	**6**	**7**	**8**	**9**	**10**	**11**	**12**
pH	7.9	7.9	8	7.9	8	7.5	7.6	7.9	7.9	7.8	8	7.7
Turb	29.75	16.7	13.8	12.1	10.9	16	9.9	12.8	19.1	26.9	10.7	15.9
EC	1110.5	1013	912	1048.7	1005	967	1067.7	1132	1134	1107	1116	1120.7
TH	429	348.7	337.5	376.3	372.5	354	395.7	391	395.7	390.5	386	355.3
Ca	102	81.3	68.5	86.7	84	90.7	97	94.7	95	92.5	75	71
Mg	51	35.7	40.5	38.7	39.5	31	37	37.7	38.7	39	48	43
SO4	287.5	264.3	220	279.7	282	270.3	316.3	326.3	334	331	277	269
TDS	737	665.3	570	676	656	618	670	758.7	718	710	644	682.7
Na	82	82	77.5	79	77.5	68.3	67	82.7	87.3	85.5	88	92
k	3	3.1	3	4.4	2.9	2.9	3.5	3.2	3.3	3.3	3.1	3.1
TSS	68	54	36	30	41	59.3	34	30	53.3	68	56	70
ALK	114	127.3	138	128	118	117.3	113	105.3	110.7	107	120	135.3
Cl	117.5	109.7	93.5	112.3	108.5	100	94.7	98.3	104.3	116	113	116

Table (B.3): Monthly average of water quality parameters for S3 2016.

month	1	2	3	4	5	6	7	8	9	10	11	12
pH	7.9	8.1	8	7.8	8.5	7.5	7.6	8	7.7	8.1	8	8.2
Turb	29.9	12.9	18.7	23.9	12.9	10.6	10.8	11.4	21.5	23.5	25	16.1
EC	1254.5	1021.7	911	1017	991	1001	1021.5	1139.5	1135	1100	1150	1088
TH	446	347.7	337.5	390	368	355.8	398.5	386.5	394	374	380	335
Ca	102	78.7	71.5	89	88	97.4	100.5	98.5	92	90	83	68
Mg	46.5	36.7	38.5	41	36	34	36	34.5	40	36	42	40
SO4	358	253	225.5	270	276	272.6	314.5	335	322	333	316	263
TDS	839	646.7	586	656	606	616.8	633	697	716	688	776	640
Na	96	82.7	73	77	79	80.7	68.5	82	93	94	91	87
k	3.3	6.2	3.1	3	2.9	3.3	3	3.3	3.2	3.3	3.3	3.1
TSS	41	63.3	66	94	50	55	31	30	88	72	98	44
ALK	108	129.3	140	122	120	115	112	107	110	112	110	132
Cl	148.5	110.7	98.5	105	104	96	94	101.5	113	111	117	114

Table (B.4): Monthly average of water quality parameters for S4 2016.

month	1	2	3	4	5	6	7	8	9	10	11	12
pH	8.1	7.8	7.7	8	8	7.4	7.7	7.9	7.8	7.9	8.3	7.3
Turb	12.8	24.9	26.8	17.8	9.7	10.7	13.9	12.6	14.9	17.4	13.6	11.9
EC	1208	1234.5	1017	1104	988	997	1076	1164	1137	1097.5	1126	1096
TH	451	426	401	389	378	393	389	395	410	376	366	335
Ca	96	98	92	89.5	85	99	96.9	99.5	98	89	75	71
Mg	51.5	42.5	42.9	40.5	40	35	37.1	35.5	40	37	43	38
SO4	346	312	295	288	281	308	315	333	340	332	278	249
TDS	783	802	685	710	656	640	666	656	750	626	680	640
Na	101.5	96	89.4	90.5	76	60	68.3	82	84	90	99	94
k	3.3	3.3	4.2	4.7	2.9	3.4	4.1	5.7	3.3	3.4	3.1	3.2
TSS	86	56	66	32	46	40	31	37	72	74	80	24
ALK	116	128	142	126	114	118	111	107	108	111	120	126
Cl	131.5	109	99	126	99	105	100	102	102	113	109	114

Table (B.5): Monthly average of water quality parameters for S5 2016.

month	1	2	3	4	5	6	7	8	9	10	11	12
Ph	8.1	8	8.1	8.1	9.4	7.7	7.6	8	7.7	7.9	7.8	7.8
Turb	15	11.2	21.4	7.9	9	8.8	15	15.8	10.9	13.2	15.8	12.8
EC	1115	1044.7	932	975	994	953	1058	1171	1141	1091	1009.3	1129.5
TH	401	366	352	358	384	346	397	392.3	413	387.5	333	345
Ca	99.2	86.7	72	83	88	86	97	100	92	86	73.7	71.5
Mg	38.9	36.7	42	36.5	40	32.5	38	34.7	45	43	38	40.5
SO4	298.5	281.3	232	252.5	290	262	316	331	316	327.5	300.5	273.5
TDS	700.6	666	544	624	684	618	600	756	808	689	675	661
Na	86	83	80	81.5	82	64.5	78	81.7	89	89	92	95
k	3.1	3	3	3	2.7	2.9	3.3	4.2	3.3	3.3	4.1	3.1
TSS	71	42	78	45	20	34	38	51.3	24	64	88	62
ALK	124	126.7	140	138	120	117	110	108	110	110	111	132
Cl	107	110.3	102	109	111	98	99	99.3	111	116.5	103	118

Table (B.6): Monthly average of water quality parameters for S1 2017.

month	1	2	3	4	5	6	7	8	9	10	11	12
pH	7.7	8	8	7.8	7.6	7.3	7.6	7.4	7.6	7.7	7.8	7.85
Turb	8.5	7.9	6.5	11.3	11.2	6.5	4.4	7.4	5	7.6	5	6.9
EC	1196	945.5	915	1001.5	972	944.3	980.5	973.5	960	1005	1113	1180
TH	391.5	310.5	301	328.5	343	359	341.5	307.5	309	309	341.5	337.5
Ca	89.5	71	63	78	84	98.3	89	73	70	73.5	80.5	81
Mg	41	32.5	35	32.5	32	28	29.5	27.5	30	28	31.5	30.5
SO4	305.5	219	210	224	229	251	261	257	234	267	269	267
TDS	768	578	524	669	664	609.3	641	648	630	672	720	718
Na	96.5	88.5	84	80.5	73	71	77.5	76.5	71	72.5	76.5	83.5
k	3.2	3.1	3.1	3.2	3.3	2.9	3	3	2.8	2.9	2.8	2.8
TSS	70	27	50	43	36	32.7	26	32	40	8	11	13
ALK	129	142	148	138	130	130	123	111	108	104	123	133
Cl	116.5	102	101	108.5	93	92	99.5	103.5	102	108	114	116

Table (B.7): Monthly average of water quality parameters for S2 2017.

month	1	2	3	4	5	6	7	8	9	10	11	12
pH	7.7	8	8	7.8	7.6	7.5	7.5	7.5	7.6	7.8	7.8	7.8
Turb	8.7	9.6	6.6	12.8	21.9	18.8	8.8	8.6	16.4	9.2	12.6	7.95
EC	1229	964.5	918	957	939.5	954.5	1001	969	959.5	995.5	1088.5	1179.5
TH	395	312	301	300	323	350	338.5	324	304.5	306	347	341.5
Ca	94	69.5	62	71.5	76.5	87.5	88	74.5	70	75	82	83
Mg	39	34	34	29.5	32	31.5	29	30.5	29	26.5	32	30
SO4	283	226.5	202	212	212	253	262.5	247.5	241.5	260.5	278	269.5
TDS	692	650	534	580	607	604	647	608	621	667	691.5	708
Na	98	90.5	85	77	69	74	78	77	74.5	75.5	78	80.5
k	3.2	3.2	3.2	3	3	3	3.1	3	3	2.9	2.9	2.8
TSS	69	35	50	30	30	39	27	30	41	13	15	18
ALK	130	139	140	146	134	132	124	116	112	117	128	133
Cl	119	103	102	100	93.5	94.5	98.5	103	103.5	107.5	116.5	117

Table (B.8): Monthly average of water quality parameters for S3 2017.

month	1	2	3	4	5	6	7	8	9	10	11	12
pH	7.8	7.8	7.6	8	7.6	7.4	7.5	7.2	7.7	7.8	7.7	7.4
Turb	11.6	21.1	7.9	11.7	13.4	6.9	12.1	8.9	8.4	12.8	8.8	6.4
EC	1153	972.5	923	903	899	928	1000	1028	962	991	1064	1141
TH	392	320	297	304	300	361	358	342	306	311	345	357
Ca	87.5	69.5	62	67	69	93	85	91	70	72.5	80	80
Mg	42	35.5	35	33	31	31	36	26	29	29	32.5	35
SO4	303.5	218	217	201	198	235	251	262	239.5	264.5	280.5	268
TDS	774	643	548	578	534	612	640	660	629	650	677	690
Na	94.5	84.5	85	68	73	69	75	79	77	74.5	74.5	79
k	3.1	3	3	2.6	3	2.9	3	3.1	3	3	2.8	2.8
TSS	66	44	68	28	44	48	30	22	38	30	10.5	24
ALK	128	140	142	136	132	132	122	122	111	113	123	120
Cl	120	102.5	101	100	94	98	99	105	104.5	106.5	113.5	108

Table (B.9): Monthly average of water quality parameters for S4 2017.

month	1	2	3	4	5	6	7	8	9	10	11	12
pH	7.845	8.04	7.95	7.8	7.5	7.9	7.5	7.5	7.6	7.7	7.8	7.3
Turb	9.8	6	5	13.9	6.8	7.5	6	5.9	7.1	5.8	8	5.5
EC	1205.5	1031	933	1076	885	989	987	960	962	985	1065	1220
TH	393	335	310	360	304	366	343	306	313	309	337	352
Ca	92.5	73	60	84	69	89	101	71	75	71	83	78
Mg	39.5	37	39	37	34	35	22	29	28	29	29	35
SO4	311	259	214	268	198	250	256	256	250	252	274	264
TDS	754	662	540	726	550	560	622	616	632	644	716	734
Na	97.5	100	89	90	76	83	75	76	67	69	78	78
k	3.15	3.2	3.2	3.4	3	3	3	3	2.8	2.9	2.9	2.8
TSS	55	46	46	52	30	40	18	34	44	46	10	20
ALK	127	128	142	134	140	128	126	122	114	112	124	140
Cl	119.5	108	103	115	94	98	98	102	103	104	112	129

Table (B.10): Monthly average of water quality parameters for S5 2017.

month	1	2	3	4	5	6	7	8	9	10	11	12
pH	7.8	8.1	7.9	8.2	7.6	7.3	7.6	7.6	7.7	7.8	7.9	7.9
Turb	5.5	9.7	8.9	4.9	9.2	7	10.9	8.1	9.2	7.5	6	3.9
EC	1228.5	995	911	993.5	890	916	997	989	967	995	1100	1227
TH	401.5	323	301	338	317	365	343	338	303	306	354	346
Ca	94	68	64	78	71	108	91	86	68	73	80	78
Mg	40.5	37	34	35	34	23	28.5	28	30	28	34	34
SO4	325	228	210	224	184	241	260	263	247	266	274	267
TDS	693	560	520	633	570	618	620	636	614	666	660	756
Na	99	94	85	81	73	75	78.5	77	83	80	77	86
k	3.2	3	3.1	3.1	3	2.9	3.1	3.1	3.3	2.9	2.9	2.9
TSS	74	34	56	33	22	46	29	48	54	4	11	14
ALK	134.5	142	150	138	142	112	123	100	108	114	134	140
Cl	118	107	101	109.5	95	102	96	110	105	110	121	126

Table (B.11): Monthly average of water quality parameters for S1 2018.

month	1	2	3	4	5	6	7	8	9	10	11	12
pH	7.5	7.2	6.9	6.9	7.2	6.8	6.8	7.1	7.1	6.8	7.1	7.3
Turb	5.1	2.9	4.8	3.2	2.2	5	4.5	4.2	7.2	6	13.6	12
EC	1072.8	1025	1038	1080	1119	1228	1208	1220	1205.3	1191.5	1171	1154
TH	323.2	317	315	356.3	352	368	370.7	391	381.3	385	385.7	375.7
Ca	77.4	71	75.7	91	87	93	92.3	89	86.5	85	91.7	88
Mg	31	34.3	30.7	31.3	33	33	34.3	41.5	40	39.5	40	38.3
SO4	221	197.3	215.3	288.7	246	299	322	312.5	296.5	284	253.7	246
TDS	651.6	627.5	600	648	676	700	750.7	726	738	747	718.7	717.3
Na	73.2	77.8	76.7	72.7	88	99	102	89	100.5	98.5	101	98
k	2.7	3	3	3	2.8	2.5	3.5	3.7	3.9	4.3	3.6	3.9
TSS	23.6	34.8	8.7	21.3	34	114	42.7	46	24.5	14	40.7	38
ALK	152.4	134.5	140	131.3	144	120	122	118	125	130	142.7	140
Cl	119.6	124.8	115.7	107	122	130	131	127.5	130.8	127.5	130	129.7

Table (B.12): Monthly average of water quality parameters for S2 2018.

month	1	2	3	4	5	6	7	8	9	10	11	12
pH	7.4	7.1	6.9	6.8	7.3	7.7	6.8	7.3	7.1	6.8	7.1	7.6
Turb	4.5	3.8	4	2.7	4.6	8	4.5	5.1	12	9.6	18.2	19.3
EC	1070	1025	1034	1047	1116	1237	1220.5	1197	1200	1196	1084	1148.7
TH	320	317	315	349.8	352	378	376	384	382.4	371.5	361.5	374.3
Ca	78	70.8	76.3	90	87	95	91	87	88	85	80	87.7
Mg	30.2	34.3	30.3	30.5	33	34	36.5	40.5	39.8	39	39.5	38
SO4	217	196.5	219.3	243.5	246	343	323.5	294	300.8	331.5	234	245.7
TDS	653.2	604	592	627.5	672	702	765	733	717.6	756	654	710.7
Na	73.4	77	75	70.8	93	100	100	91	100	101.5	102	96.7
k	2.7	3	3	2.9	2.8	2.6	3.9	3.6	3.8	4.2	3.5	3.8
TSS	14	28	16	29.5	48	102	58	67	34.8	20	61	60.7
ALK	150.4	134.5	136	137	146	120	121	118	126	135	142	138.7
Cl	118	125	116.7	105.3	122	124	130	128	130.4	131	113.5	130

Table (B.13): Monthly average of water quality parameters for S3 2018.

month	1	2	3	4	5	6	7	8	9	10	11	12
pH	7.4	7.1	6.7	6.4	6.8	7	6.5	7.2	7	6.8	7	7.2
Turb	2.9	2.7	2.4	2.1	4	1.8	2.9	5.8	10.5	12	8.9	11.3
EC	1038	1103.5	1063	987	1114	1234	1245	1201	1208	1209	1260	1193
TH	308.5	363.5	332	350	361	368	408	384	383.3	372	411	371
Ca	78.5	77.5	84	85	89.3	94	102	86.5	90	86	96	88
Mg	31.5	41.5	30	34	33.7	32	37	41	38.7	38	42	37
SO4	208.5	211	269	235	257	315	314	311.5	296	284	284	253
TDS	623	671	642	576	671.3	694	766	715	726	710	790	756
Na	71	77.5	85	59	87	101	104	88.5	106.7	101	107	60
k	2.7	3.2	2.9	2.7	3	2.5	3.7	3.7	4	4.4	3.6	4.4
TSS	12	6	16	14	16.7	60	50	82	66	70	20	26
ALK	150	138	130	136	124	120	122	121	122	130	138	140
Cl	113.5	139.5	110	96	122	123	125	127.5	131	134	154	132

Table (B.14): Monthly average of water quality parameters for S4 2018.

month	1	2	3	4	5	6	7	8	9	10	11	12
pH	7.6	7	6.3	7	7.1	7	7	7.7	7.3	7.2	6.7	7
Turb	3.5	2.3	6.2	1.5	1	1.6	8.1	3.9	8.8	7.8	7.5	8.2
EC	1131	1019.5	1051	1043	1068	1114	1257	1234	1135	1233	1252	1261
TH	324	314.5	331	360	359	346	365	374	388	379	389	391
Ca	81	70	74	92	92	91	93	84	89	89	85	88
Mg	30	34	36	32	31	29	32	40	37	38	43	42
SO4	227	202	187	250	244	283	325	286	290	288	254	278
TDS	732	590	600	632	676	680	772	744	685	730	796	778
Na	80	81.5	81	60	72	82	98	95	101	101	101	107
k	2.8	2.7	3	2.8	3.5	2	3.6	4	3.8	4.2	4.9	5.5
TSS	8	9	40	12	18	82	40	26	85	86	20	98
ALK	156	132	156	134	124	126	120	124	134	134	140	146
Cl	123	120	128	105	117	111	127	125	138	136	152	157

Table (B.15): Monthly average of water quality parameters for S5 2018.

month	1	2	3	4	5	6	7	8	9	10	11	12
pH	7.8	7.2	7.2	7.1	6.7	7.1	6.9	6.9	7.5	6.7	7.2	7.4
Turb	3.4	3.1	5.3	3.2	2.7	1.7	6	2.9	11.1	5	10.1	5.8
EC	1078	1024	1049	1069.8	1149	1178	1222	1221	1192	1201	1331	1175
TH	322	316	325	352.3	352	356	401	388	389	386	435	377
Ca	77.7	70.5	84.5	91.8	86	90	92	88	89	87	101	86
Mg	31.3	34	27.5	30	33	34	42	41	41	41	45	40
SO4	225.7	197.5	236	253.3	255	297	327	312	298	287	300	245
TDS	663.3	614.8	606	639.5	686	699	764	744	698	726	818	726
Na	74.3	80	79.5	75	104	87	111	83	96	103	103	92
k	2.7	3	3	3	2.8	3	4	3.1	3.4	4.2	3.7	3.9
TSS	26	21.8	52	32	68	70	46	42	34	26	18	46
ALK	150.7	135	135	134.5	134	129	124	120	120	136	134	132
Cl	122.3	123.8	118	105	125	128	128	130	128	131	162	137

Table (B.16): Monthly average of water quality parameters for S1 2019.

month	1	2	3	4	5	6	7	8	9	10	11
pH	7.4	7.3	7.5	7.4	7.6	7.4	7.3	7.4	7.6	6.5	7.3
Turb	43.4	16.2	16.3	5.9	19.2	33.7	48.9	52.6	41.5	21.3	18.5
EC	1300	1326.3	1299	1146	965.7	874	832.5	864.7	870.7	813	937
TH	434.5	445	442	407.7	353.7	352	333	347	347	297.5	342
Ca	114.3	119.3	125	115.3	97.3	99	89.5	95.3	92.7	70	77
Mg	36.3	35.7	32	29	28	25.5	26.5	26.3	28	30	36
SO4	352.5	342	379	306.3	231	232	222.5	247.3	244.3	173.5	217
TDS	832	828.7	840	746.7	595.3	532	526	554	562.7	498	562
Na	94.3	104.7	107	81.3	53	38	52.5	48.3	51.3	54.5	68
k	4.1	4.5	3.9	3.6	2.8	2.6	2.1	2.2	2.4	2.7	3.9
TSS	130	45.3	28	16.7	20	61	65	56	34	44	48
ALK	136.5	140	120	138.7	162	153	136	118	114	142	140
Cl	128	135	125	112	83	62.5	60	58	65.3	78.5	100

Table (B.17): Monthly average of water quality parameters for S2 2019.

month	1	2	3	4	5	6	7	8	9	10	11
pH	7.2	7.5	7.3	7.3	7.5	7.6	7.6	7.6	7.3	6.5	7.2
Turb	16.3	19.9	10.3	7.2	9.7	19.3	36.05	32	29.6	19	23.6
EC	1296.8	1366	1278	1149.3	959.7	871.5	841	861.3	871	900	935
TH	434.3	447.3	437	407.7	360.3	346.5	344.5	347.3	347	311	342
Ca	114.5	117.3	121	115.3	96	99.5	92.5	95	93.3	74	76
Mg	36.3	37.3	33	29	29.3	24	27.5	26.7	27.7	31	37
SO4	356.8	355.3	373	309.3	233.3	257	220.5	247	237.7	179	219
TDS	815.3	868	817	747.3	582.7	539	536	546.7	555.3	554	566
Na	94.3	107.3	97.5	78.7	53.3	37.5	43	49.3	50.3	91	68
k	4.2	5.1	3.3	3.8	2.8	2.6	2.2	2.3	2.3	3	3.9
TSS	80	32.7	41	25.3	23.3	38	75	88	59.3	24	48
ALK	130.5	132.7	121	136.3	154	151	134	118.7	118	132	140
Cl	128	152.3	123	111.3	83.7	61	57.5	58.3	67	100	100

Table (B.18): Monthly average of water quality parameters for S3 2019.

month	1	2	3	4	5	6	7	8	9	10	11
pH	7.4	7	7	7.7	7.1	7.3	7.4	7.8	7.8	6.6	7.1
Turb	9	7	11.8	8.7	7.3	20	22	28.1	27.9	18.3	13.5
EC	1325.5	1311	1352	1059	1012.5	876.5	818	860	945	796	840
TH	438.5	449	464	420	375.5	345.5	337	345	362	298	333
Ca	119	117	129	112	102.5	94	92	96	99	78	76
Mg	34.5	38	35	34	29	27	26	25.5	29	25	39
SO4	377.5	348	415	279	246	224.5	220	239.5	272	185	210
TDS	817	814	904	574	615	548	488	529	608	504	540
Na	91.5	113	94	70	55	40	43	49.5	50	57	65
k	4.3	4.5	4.2	3.2	3.1	2.6	1.3	2.3	2.5	2.6	3.1
TSS	25	12	48	56	33	54	26	72	42	54	38
ALK	128	136	124	140	148	154	140	117	112	140	140
Cl	126.5	129	131	99	90.5	63.5	60	57.5	73	71	79

Table (B.19): Monthly average of water quality parameters for S4 2019.

month	1	2	3	4	5	6	7	8	9	10	11
pH	6.8	6.6	7.2	7.1	7.2	7	7.9	7.9	7.2	7.9	7.8
Turb	16.8	10.1	8	7.5	2.9	11	32	23.5	23.7	25.9	22.3
EC	1284	1445	1370	1240	1048	873	848	865	830	762	890
TH	456	418	446	420	384	349	359	345	310	307	316
Ca	129	114	125	123	101	97	92	89	86	68	72
Mg	33	32	32	38	32	26	31	26	29	33	36
SO4	364	297	310	309	244	236	216	241	132	151	212
TDS	846	816	820	621	630	554	538	530	543	462	520
Na	87	125	100	100	66	41	50	48	54	68	72
k	4.2	7.4	5.2	4.6	3.1	2.8	2.2	3.1	3.1	2.7	3
TSS	40	36	32	40	45	30	62	76	20	30	39
ALK	128	136	122	129	140	154	140	117	126	136	141
Cl	119	209	148	140	95	59	61	57	71	70	80

Table (B.20): Monthly average of water quality parameters for S5 2019.

month	1	2	3	4	5	6	7	8	9	10	11
pH	7	7.8	6.7	7.6	7.5	7.5	7.9	7.9	7.1	7.1	7.8
Turb	10	8.8	7.5	7.2	12.3	30	23.4	17.7	24.1	21.2	18.3
EC	1295	1250	1324	1272	1000	889	848	859	874	804	932
TH	435	399	456	416	368	358	359	345	345	298	342
Ca	123	99	125.5	112	98.5	101	92	94	90	69	75
Mg	31	37	35	33	30	26	31	27	29.5	31	38
SO4	372	298	399.5	351	239	219	216	248	232.5	160	215
TDS	868	782	859	842	611	556	538	532	554	498	560
Na	99	95	98	99	58	38	50	49	56	71	76
k	4.1	3.9	3.2	4.6	2.9	2.7	2.2	1.9	2.2	2.6	4
TSS	10	20	20	10	46	46	62	50	60	26	24
ALK	126	140	121	130	158	152	140	112	118	142	140
Cl	121	132	125.5	138	87.5	64	61	58	71.5	74	100

Table (B.21): Monthly average of water quality parameters for S1 2020.

month	2	3	7	9	10	11	12
pH	7.4	8.2	7.6	7.3	7.6	7.6	7.5
Turb	11.2	11.9	18.8	12.2	13.4	11.7	12.4
EC	839	852.5	981	1038	1032	995.5	914.5
TH	320	365	456	402	390	319	355
Ca	70	81	133.5	115	103.5	88	76.5
Mg	35	39.5	29.5	28	32	36.5	40
SO4	180	179.5	295	301	312.5	275	216.5
TDS	500	520	629	691	650	617	544
Na	60	69.5	56.5	70.5	59	75.5	72.5
k	3	3.2	2.4	2.8	3.5	3.8	4.2
TSS	54	25	74	54	69	9	40
ALK	138	158	116	110	98	110	113
Cl	84	82.5	73.5	84.5	85	87.5	85

Table (B.22): Monthly average of water quality parameters for S2 2020.

month	2	7	9	10	11	12
pH	7.9	7.3	7	7.2	7.3	7.7
Turb	10.1	12.8	16	15.4	16.4	11.2
EC	832.5	1006	1024	1040	979	921
TH	334	435	393	424	327	349
Ca	74	128.5	112	105	81	78
Mg	36	27.5	28	39	30	38
SO4	173.5	309.5	316	309	235	223
TDS	504	675	668	668	578	552
Na	64	68	70	69	78	69
k	3.4	2.6	2.9	3.6	3.6	3.9
TSS	29	18	88	42	76	114
ALK	165	122	104	100	114	110
Cl	82	76.5	85	89	89	89

Table (B.23): Monthly average of water quality parameters for S3 2020.

month	2	7	9	10	11	12
pH	7.9	7.3	7	7.2	7.3	7.7
Turb	9.6	12.6	16	15.4	16.4	11
EC	832.5	1006	1024	1040	979	921
TH	334	435	393	424	327	349
Ca	74	128.5	112	105	81	78
Mg	36	27.5	28	39	30	38
SO4	173.5	309.5	316	309	235	223
TDS	504	675	668	668	578	552
Na	64	68	70	69	78	69
k	3.4	2.6	2.9	3.6	3.6	3.9
TSS	29	18	88	42	76	114
ALK	165	122	104	100	114	110
Cl	82	76.5	85	89	89	89

Table (B.24): Monthly average of water quality parameters for S4 2020.

month	2	11	12
pH	8	7.4	7.76
Turb	12.9	18.3	17.8
EC	875	982	936
TH	374	348	365
Ca	85	88	76
Mg	39	31	43
SO4	184	271	215
TDS	554	634	572
Na	72	77	68
k	3.5	3.4	4.1
TSS	24	80	26
ALK	148	110	122
Cl	87	89	89

Table (B.25): Monthly average of water quality parameters for S5 2020.

month	2	3	10	12
pH	7.9	8.2	7.6	7.5
Turb	8.4	7.2	8.1	29.4
EC	844	851	1034	912
TH	315	348	399	353
Ca	68	82	103	78
Mg	35	35	35	39
SO4	177	173	311	212
TDS	504	522	646	544
Na	68	65	60	76
k	3.1	3	3.6	4.7
TSS	64	6	36	22
ALK	160	160	106	116
Cl	84	79	85	85

Table (B.26): Monthly average of water quality parameters for S1 2021.

month	1	2	3	4	5	6
pH	7.4	7.6	7.7	8.1	8.2	8.1
Turb	9.4	6.8	7.4	5.3	7.2	8
EC	923	956.7	1014	1005.5	979.5	1108.5
TH	317.3	324.3	359	357	344.5	437.5
Ca	67.7	67.7	87.5	87.5	88	113.5
Mg	36.3	37.7	34.5	34	30.5	37.5
SO4	214	204	267	263	259.5	349
TDS	550	550.7	618	598	619	730
Na	70	75.3	77	71	71	69
k	3.5	3.6	3.6	3.3	3	3.2
TSS	22.7	36.7	36	26	22	18
ALK	109.3	112.7	103	113	104	87
Cl	84.7	89.7	88.5	94	87	89

Table (B.27): Monthly average of water quality parameters for S2 2021.

month	1	2	3	4	5	6
pH	7.6	7.6	7.7	8.4	8.2	7.8
Turb	13	24.6	17.3	7.6	9.3	20
EC	923.3	934	1017.5	1019.5	981	1149
TH	312.7	320.5	362.5	357	346.5	458
Ca	69	66	86.5	89.5	87	118
Mg	34	38	35.5	32.5	31.5	40
SO4	215	194.5	268	264	262.5	410.7
TDS	546	543	643	613	616	771.3
Na	70	72.5	78.5	74	71	73.3
k	3.5	3.5	3.6	3.4	3.1	3.2
TSS	35.3	71	76	29	37	60
ALK	108	111	104	111	105	87.3
Cl	84.7	88	88.5	94	87	91.3

Table (B.28): Monthly average of water quality parameters for S3 2021.

month	1	2	3	4	5	6
pH	7.8	7.6	7.5	8.15	8.3	7.8
Turb	8.5	8.8	10.3	6.1	6.4	10.8
EC	931	943	917	1065	999	1091
TH	321	321	304	378.5	353	408
Ca	68	68	66	95.5	92	118
Mg	37	37	34	34	30	28
SO4	208	227	215	284	265	349
TDS	556	548	536	654	618	736
Na	63	75	75	75	70	64
k	4	3.3	3.4	3.35	3.1	3.2
TSS	8	52	36	33	18	26
ALK	110	110	108	111	100	90
Cl	89	90	82	97	85	84

Table (B.29): Monthly average of water quality parameters for S4 2021.

month	1	2	3	4	5	6
pH	7.1	7.6	7.6	8.1	7.6	7.7
Turb	8.9	8.2	8.88	6.7	11.5	8.5
EC	947	1038	1027	1040	1008	1018
TH	314	338	333	368	357	457
Ca	69	72	70	92	84	101
Mg	35	39	38	34	36	40
SO4	206	230	240	270	261	311
TDS	554	628	635	628	600	712
Na	72	84	81	72	79	80
k	3.4	4	3.8	3.3	3.2	3.5
TSS	24	14	29	30	18	27
ALK	110	120	123	110	114	100
Cl	91	102	95	95	90	90

Table (B.30): Monthly average of water quality parameters for S5 2021.

month	1	2	3	4	5	6
pH	7.8	7.9	7.6	8.2	8.2	7.7
Turb	12	13.9	9.6	8.4	8.1	10.6
EC	915	941.5	1117	976	1003	1156
TH	312.5	317.5	404	336	357	445
Ca	65.5	67	107	80	92	128
Mg	36.5	36.5	33	33	31	31
SO4	202.5	205	323	242	274	382
TDS	547	552	694	582	684	766
Na	70	75.5	82	71	73	71
k	3.3	3.5	3.5	3.3	3.1	3.2
TSS	38	26	42	40	4	64
ALK	113	112	106	110	100	88
Cl	82.5	88	93	93	88	90

Appendix

C

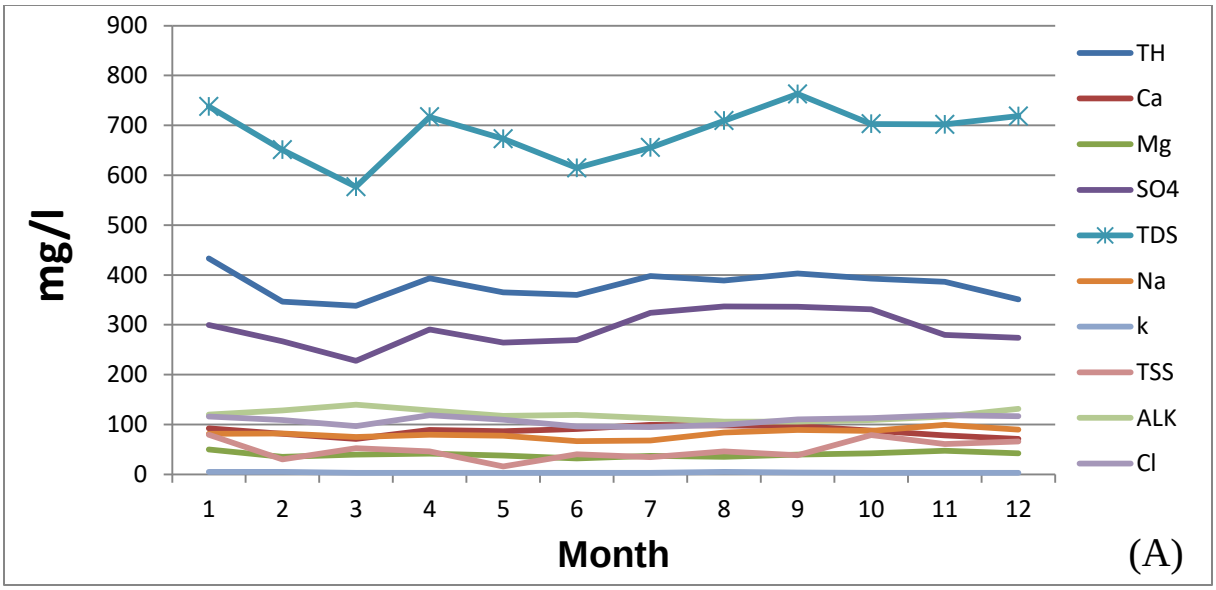
900
800
700
600
500
400
300
200
100
0
mg/l
1 2 3 4 5 6 7 8 9 10 11 12
Month
TH
Ca
Mg
SO4
TDS
Na
k
TSS
ALK
Cl
(A)

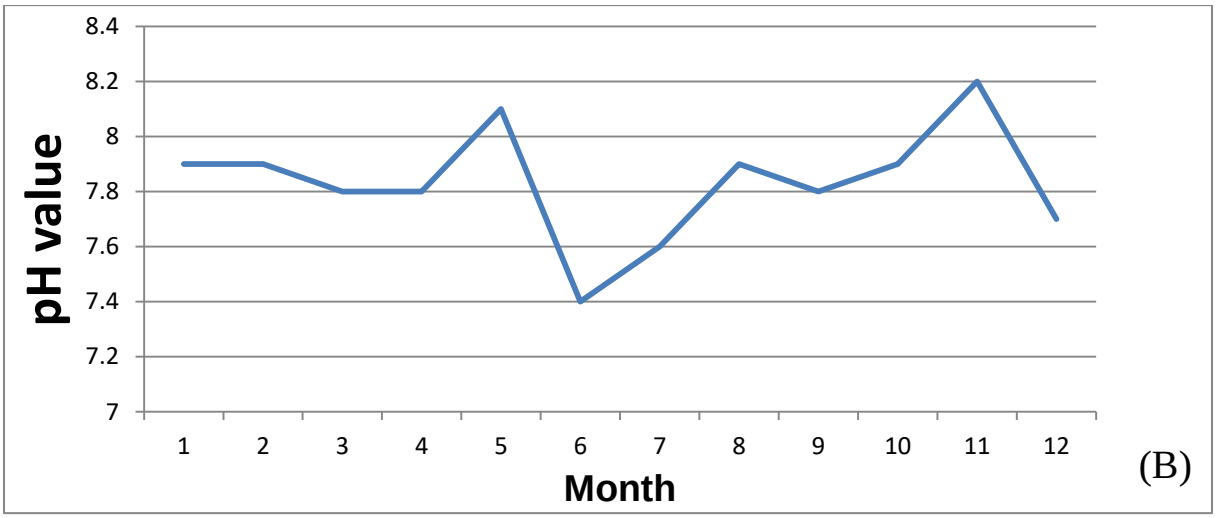
8.4
8.2
8
7.8
7.6
7.4
7.2
7
pH value
1 2 3 4 5 6 7 8 9 10 11 12
Month
(B)

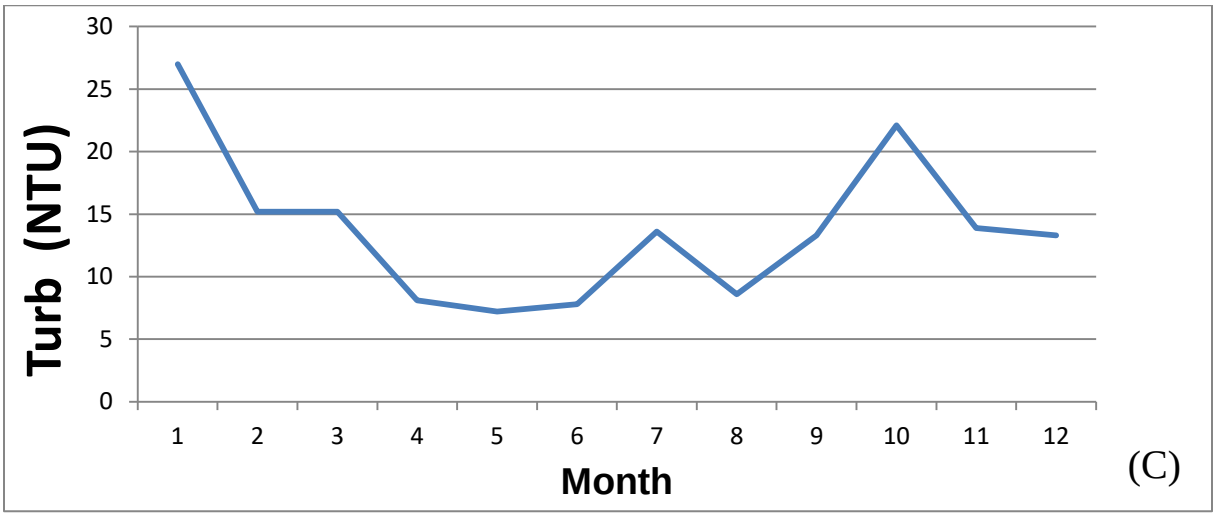
30
25
20
15
10
5
0
Turb (NTU)
1 2 3 4 5 6 7 8 9 10 11 12
Month
(C)

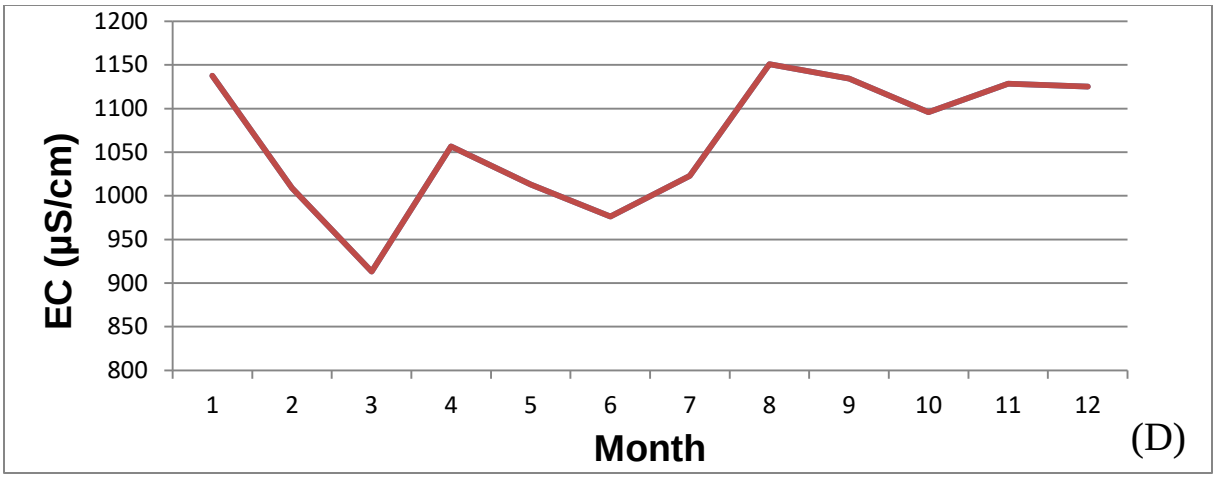

Figure (C.1): (A , B , C , D) water quality parameters variation in station (S1) for year 2016.

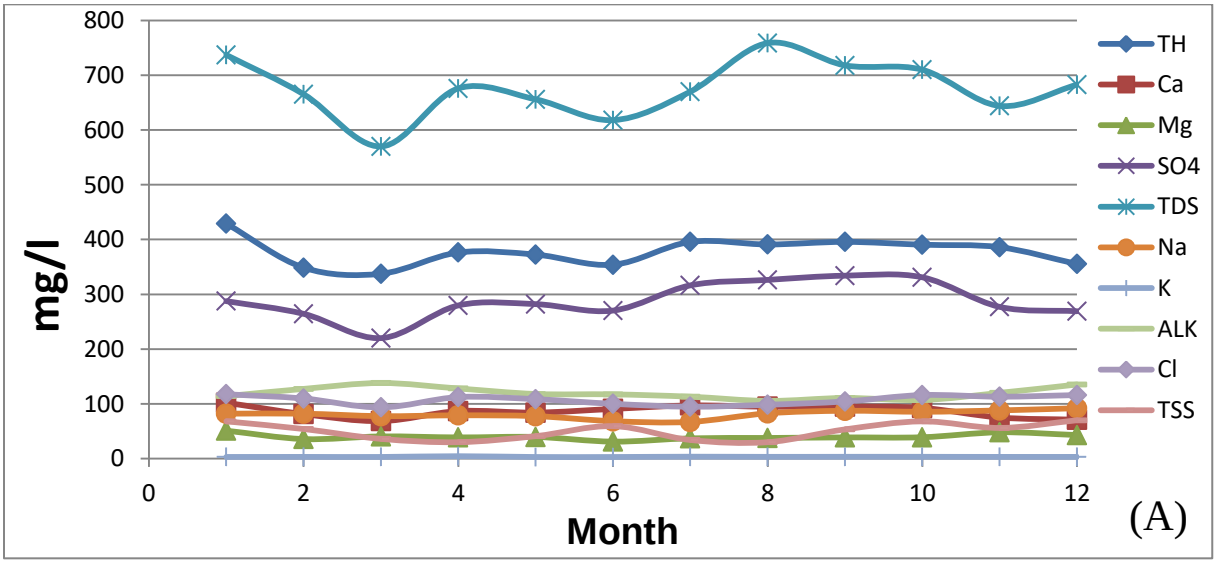

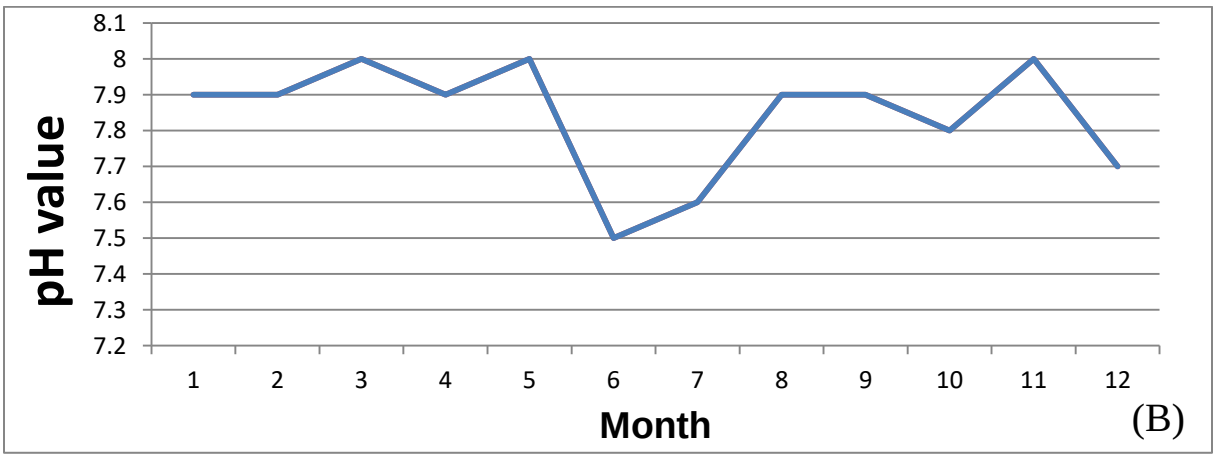

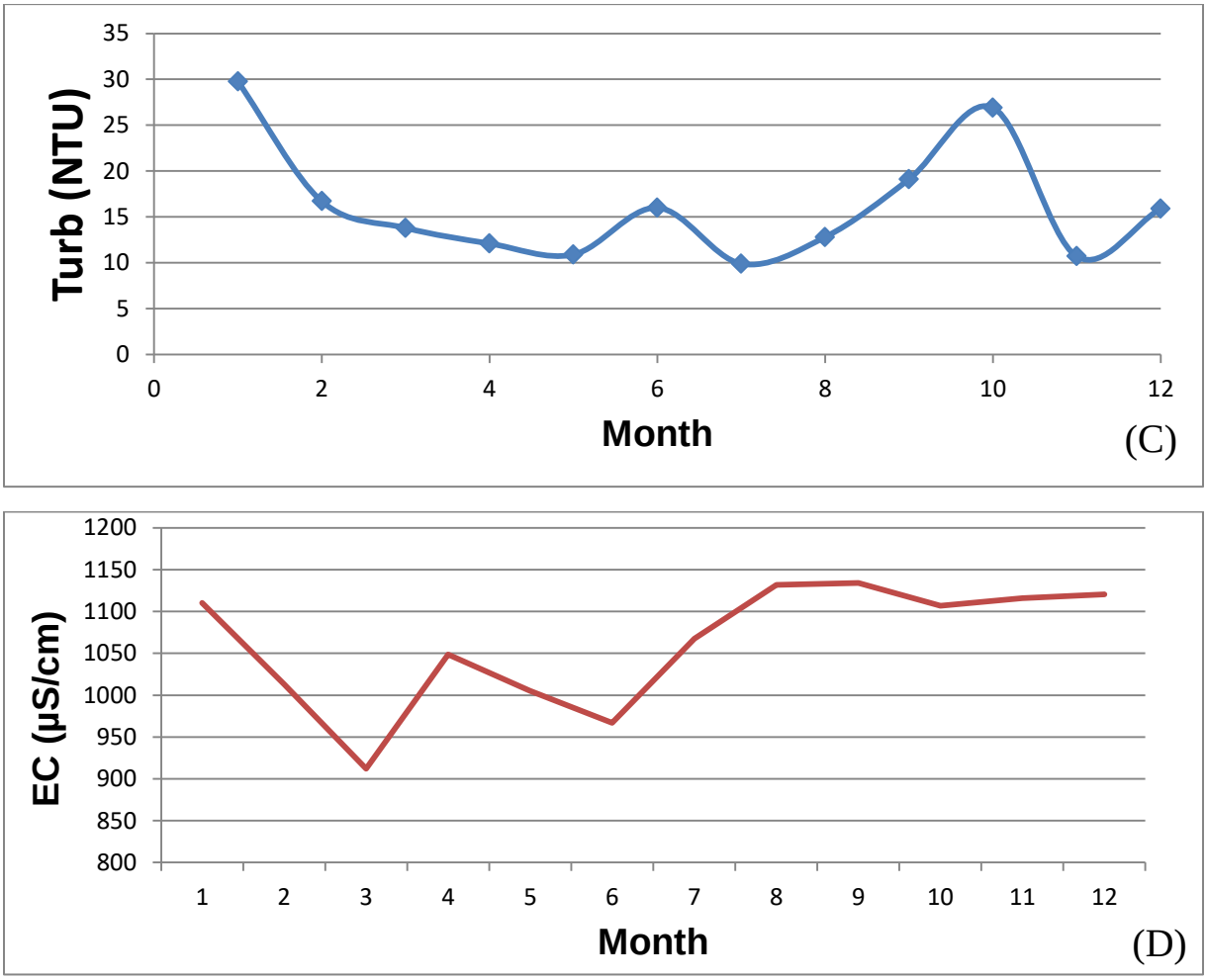

Figure (C.2): (A , B , C , D) water quality parameters variation in station (S2) for year 2016.

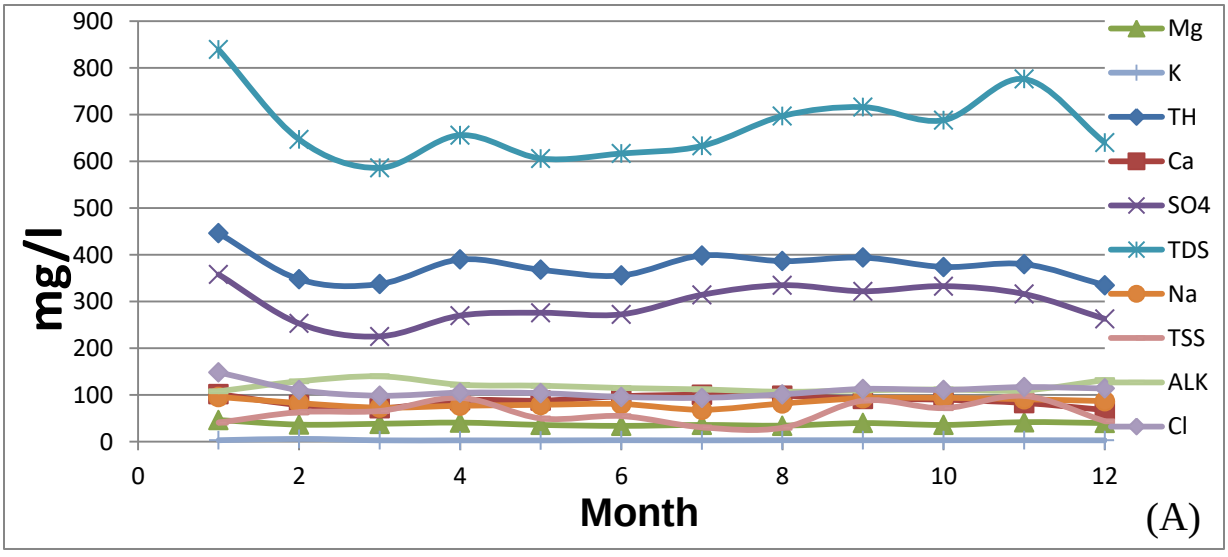

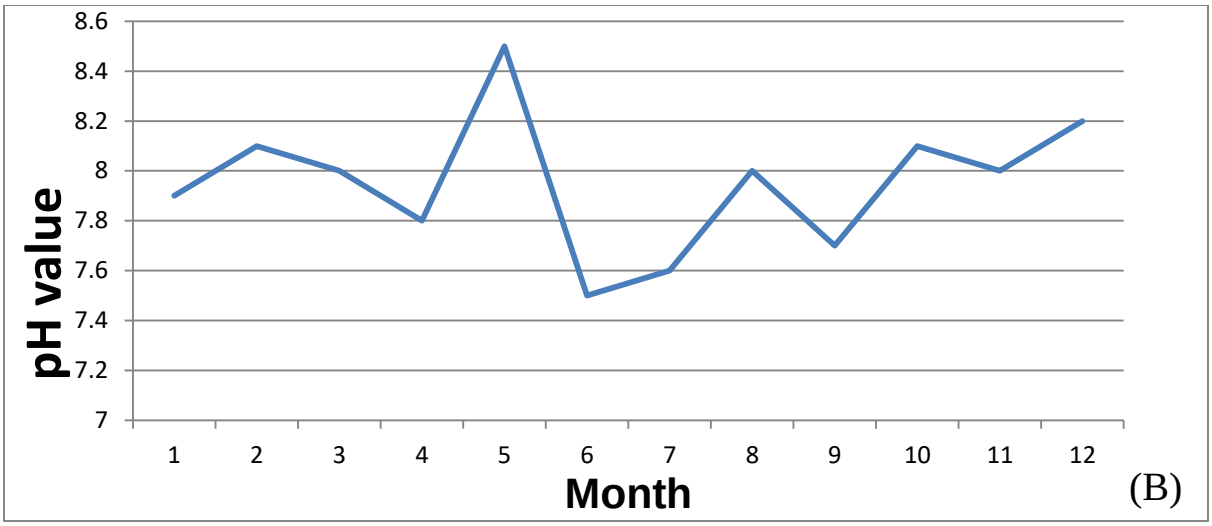

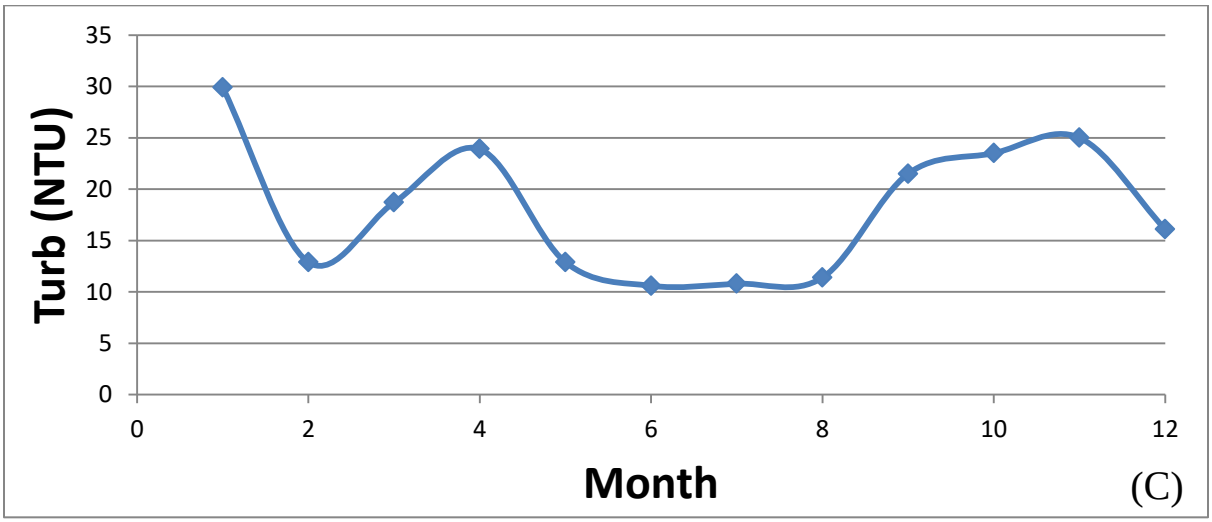

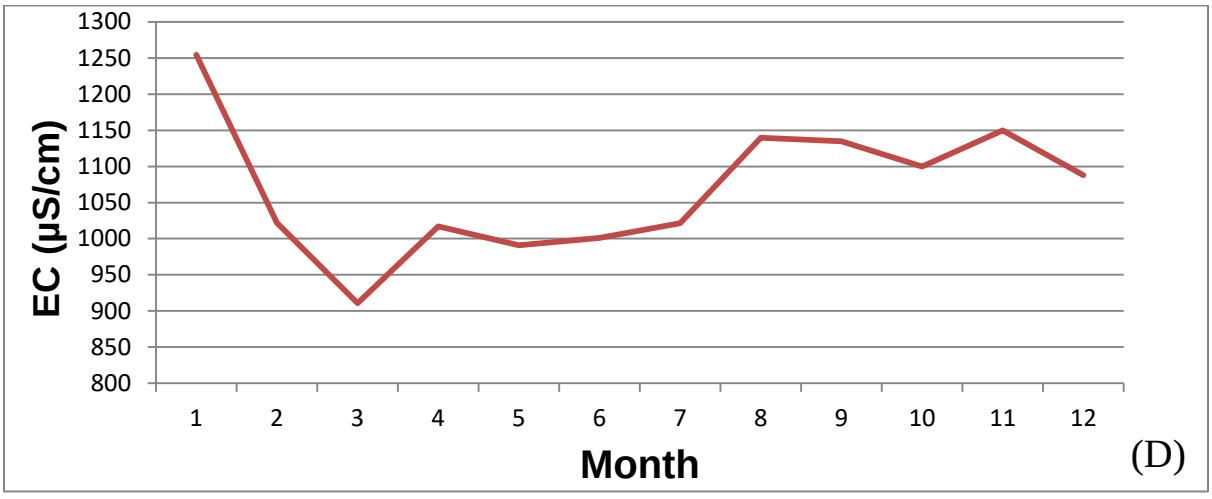

Figure (C.3): (A , B , C , D) water quality parameters variation in station (S3) for year 2016.

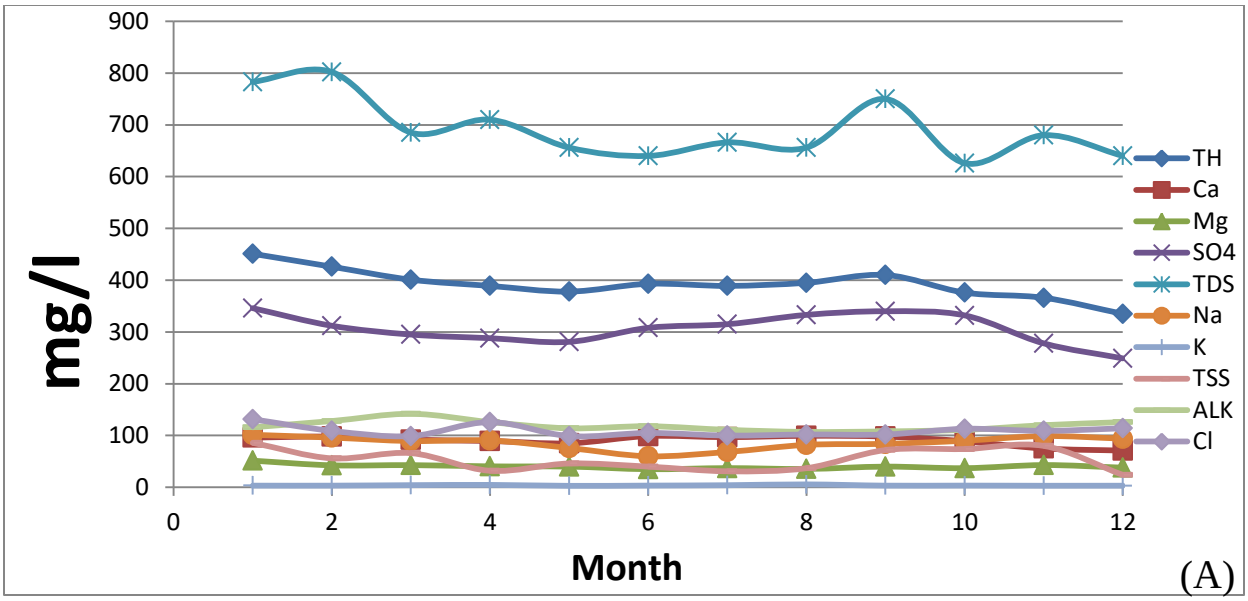
900
800
700
600
500
400
300
200
100
0
mg/l
0
2
4
6
8
10
12
Month
TH
Ca
Mg
SO4
TDS
Na
K
TSS
ALK
Cl

(A)

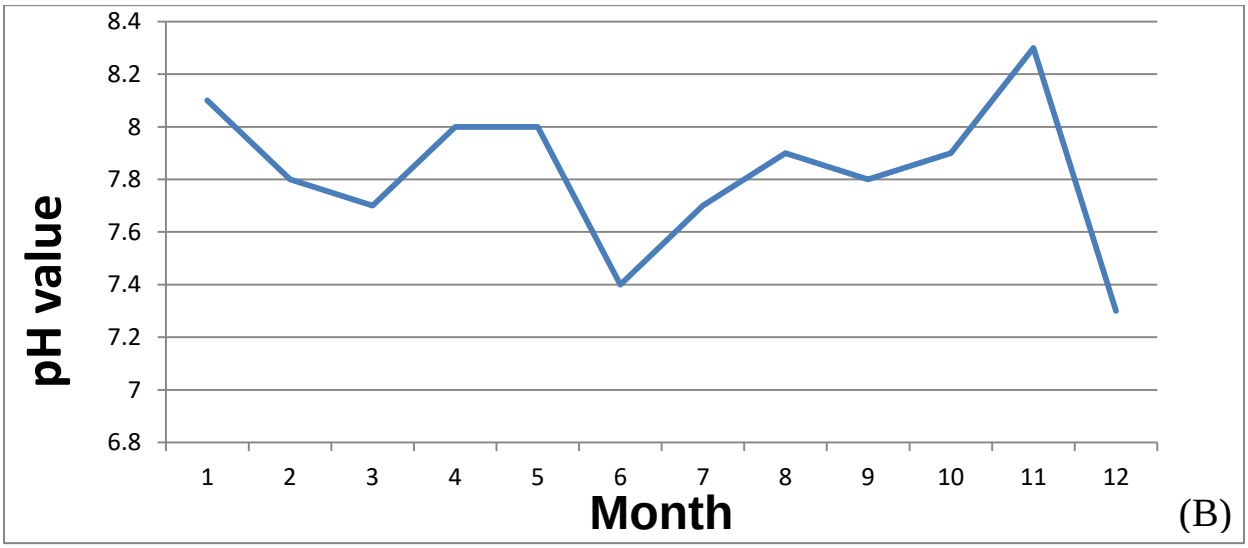
8.4
8.2
8
7.8
7.6
7.4
7.2
7
6.8
pH value
1
2
3
4
5
6
7
8
9
10
11
12
Month

(B)

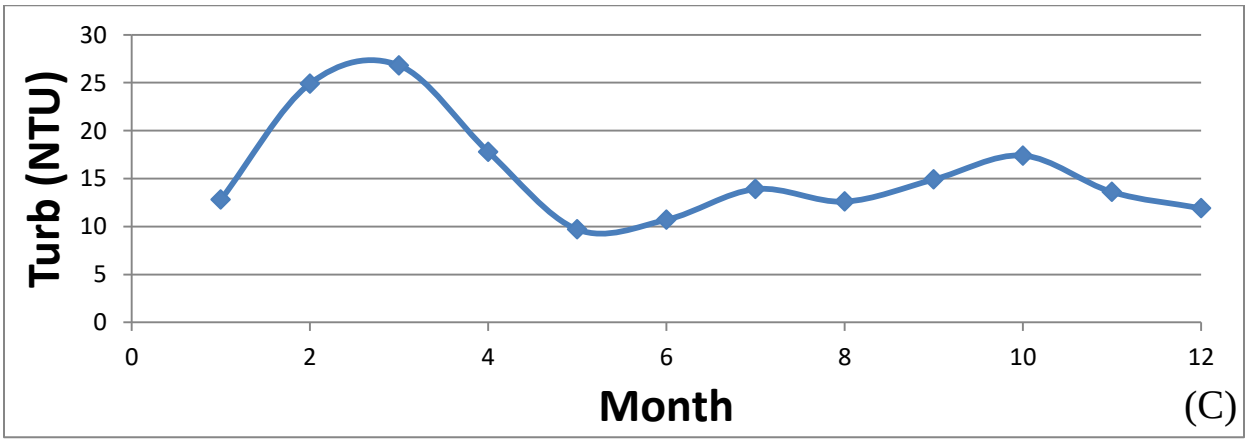
30
25
20
15
10
5
0
Turb (NTU)
0
2
4
6
8
10
12
Month

(C)

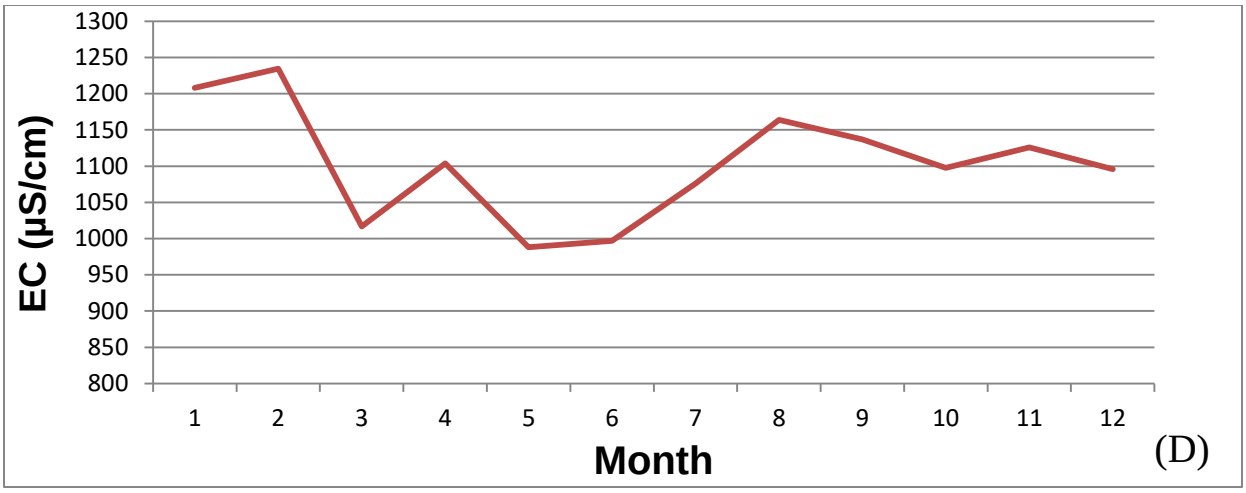

Figure (C.4): (A , B , C , D) water quality parameters variation in station (S4) for year 2016.

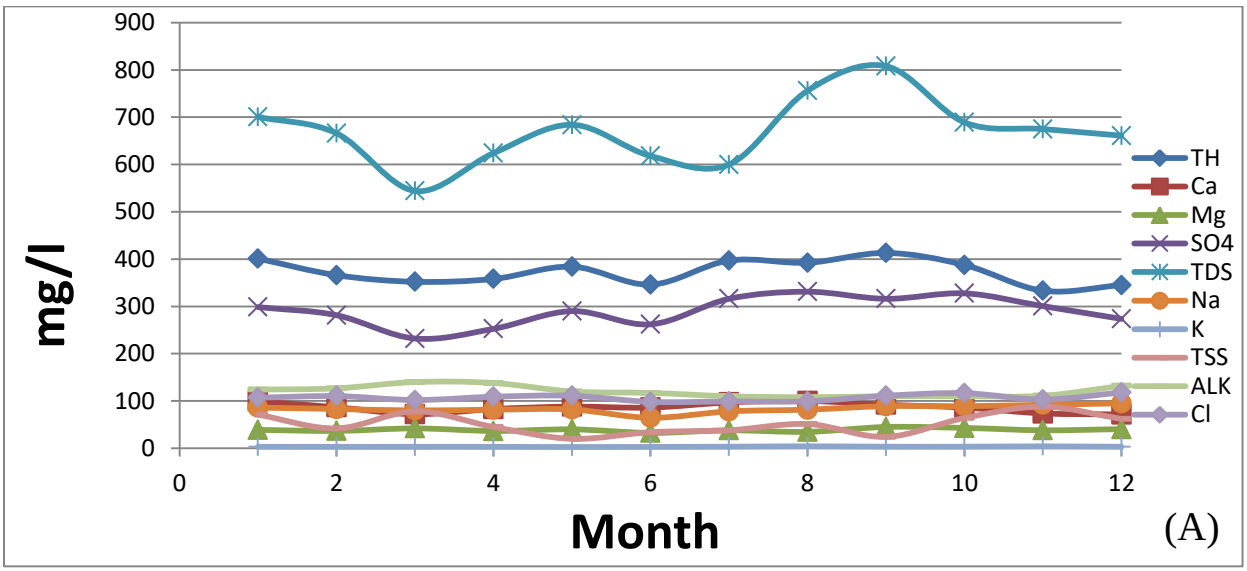

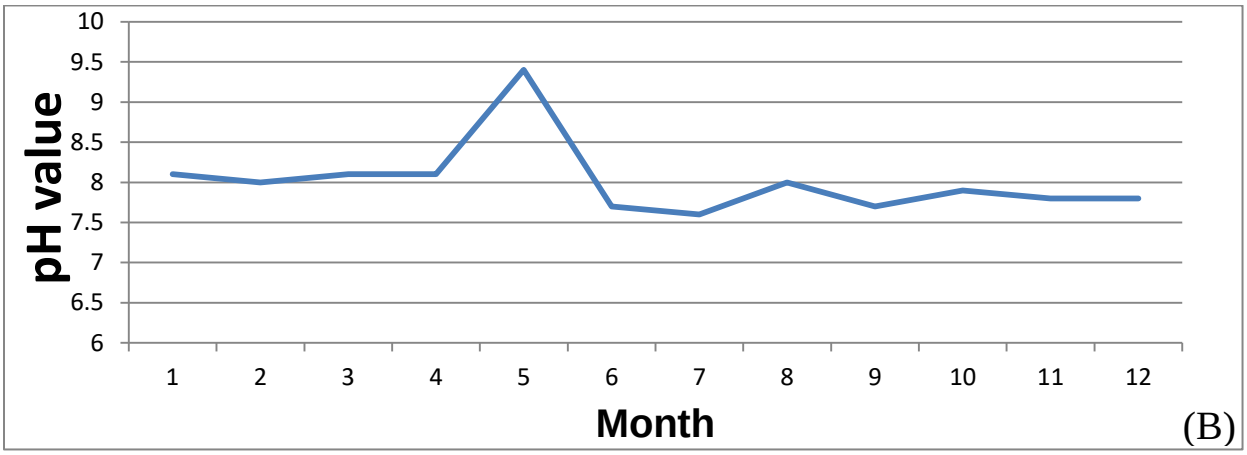

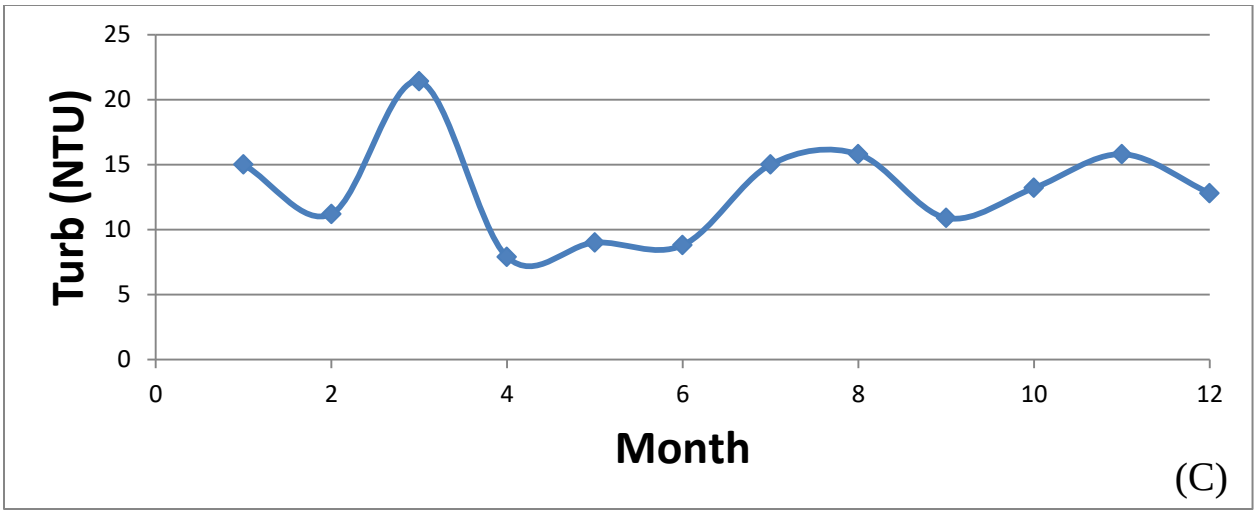

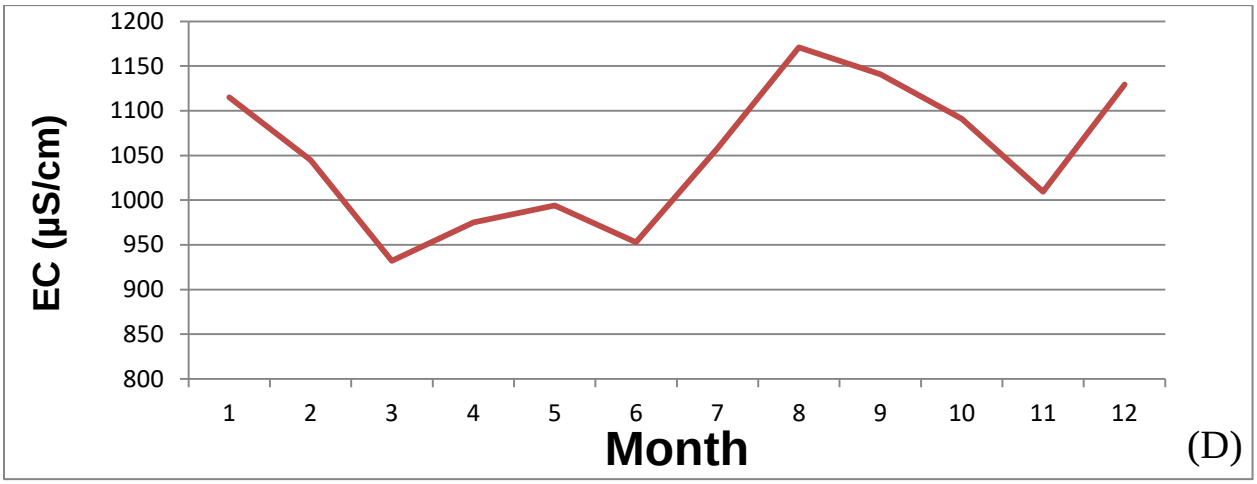

Figure (C.5): (A , B , C , D) water quality parameters variation in station (S5) for year 2016.

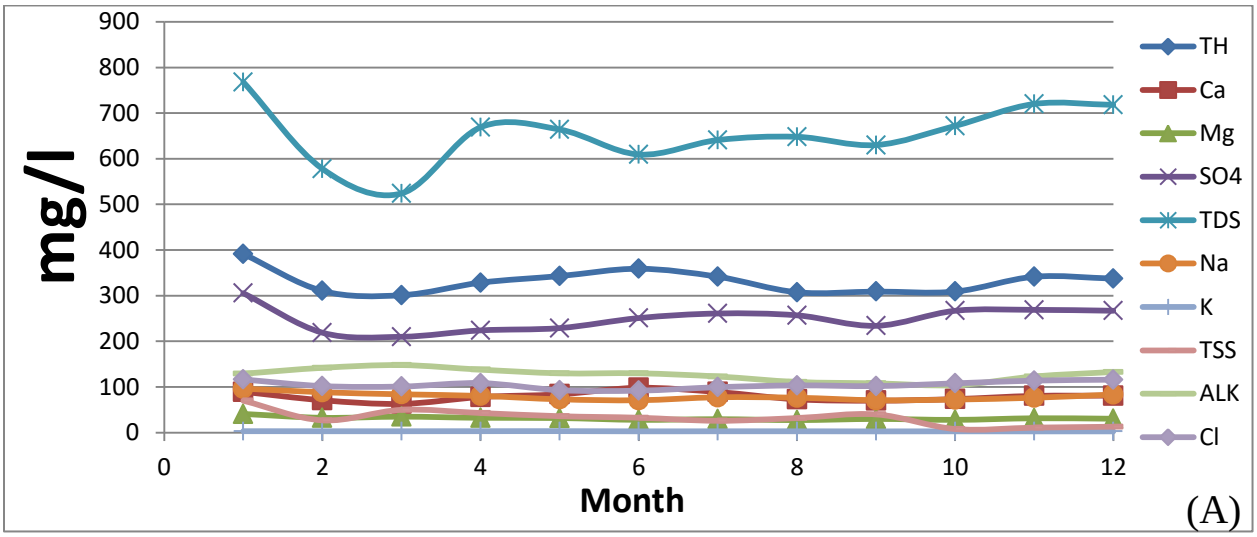

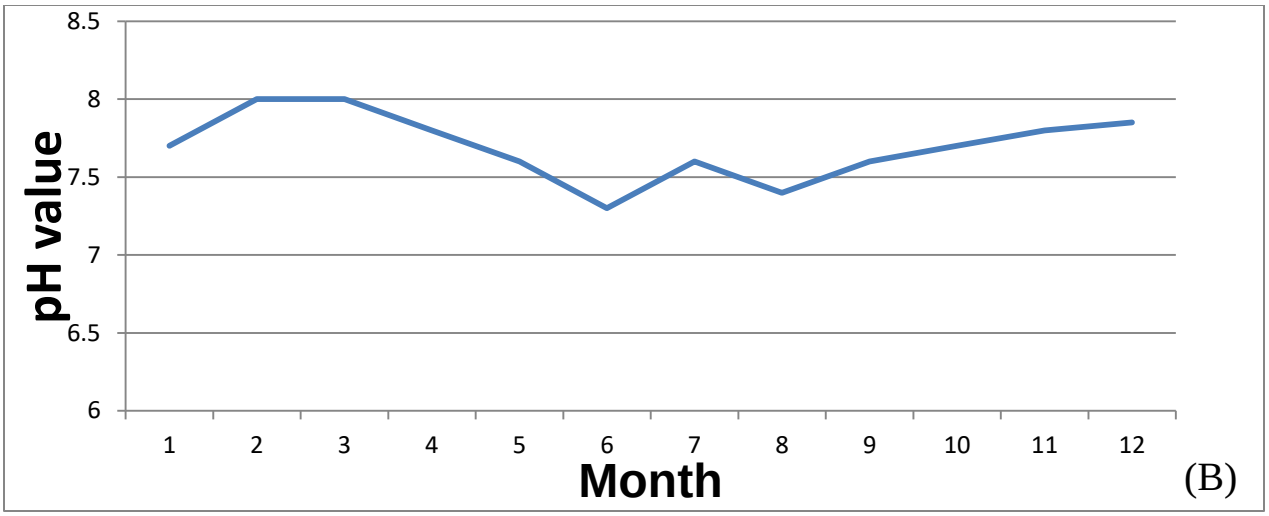

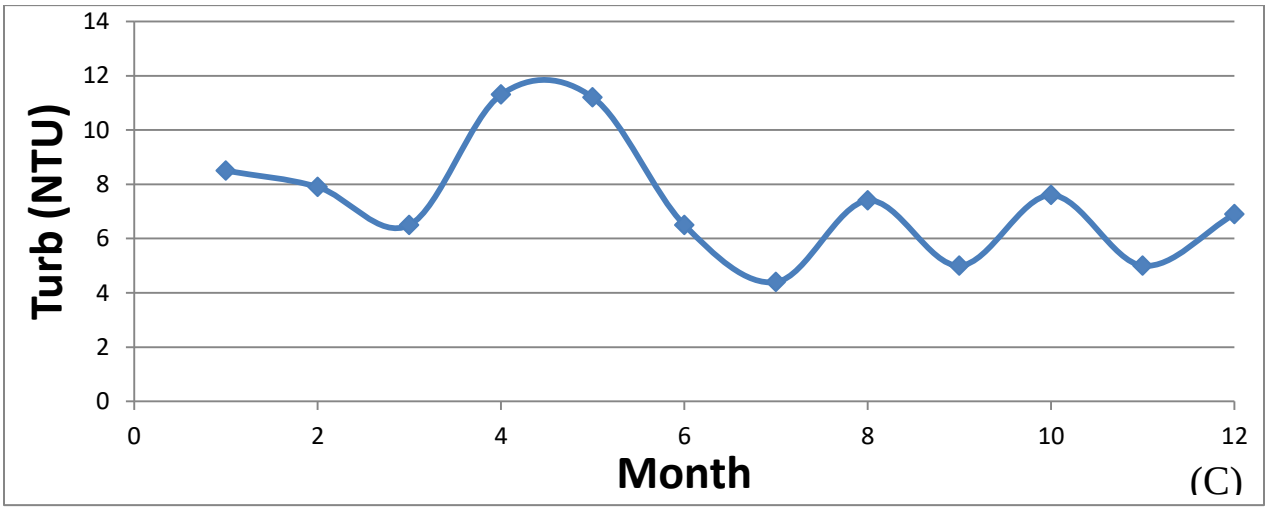

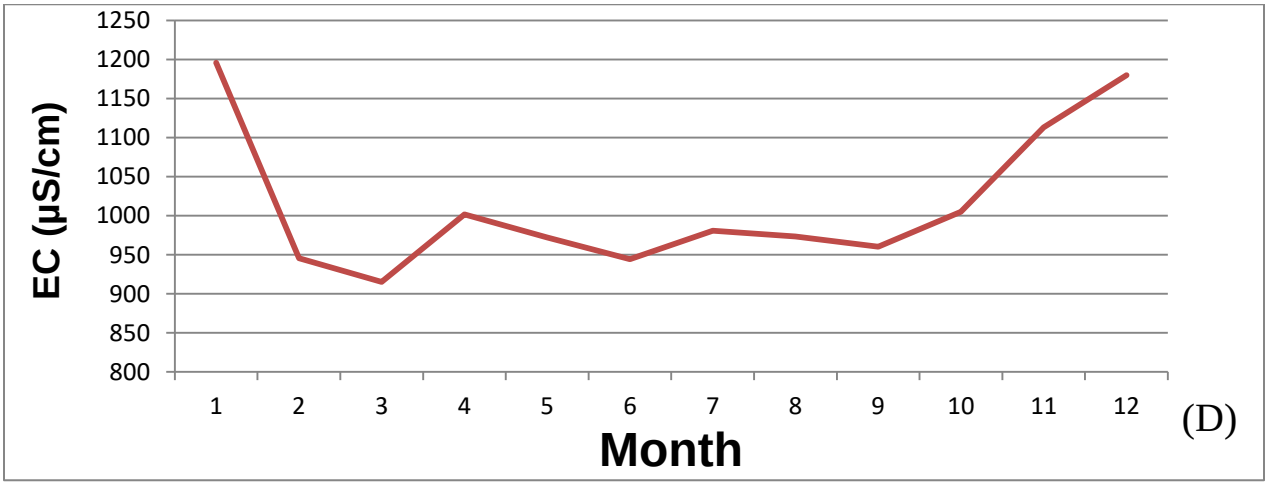

Figure (C.6): (A , B , C , D) water quality parameters variation in station (S1) for year 2017.

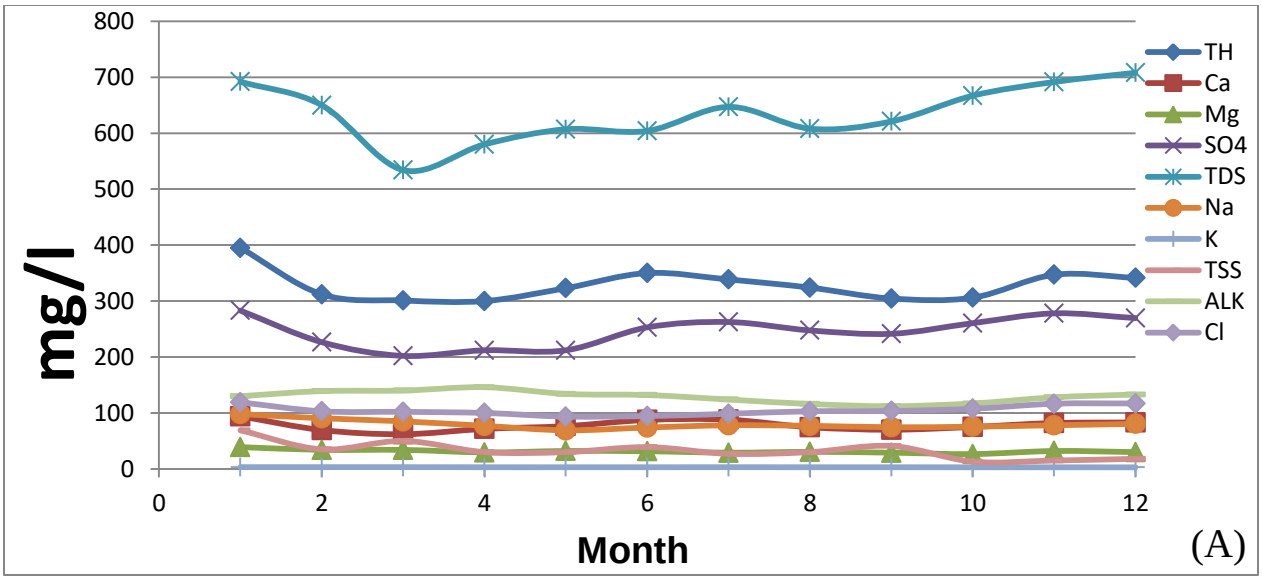
800
700
600
500
400
300
200
100
0
mg/l
0
2
4
6
8
10
12
Month
TH
Ca
Mg
SO4
TDS
Na
K
TSS
ALK
Cl
(A)

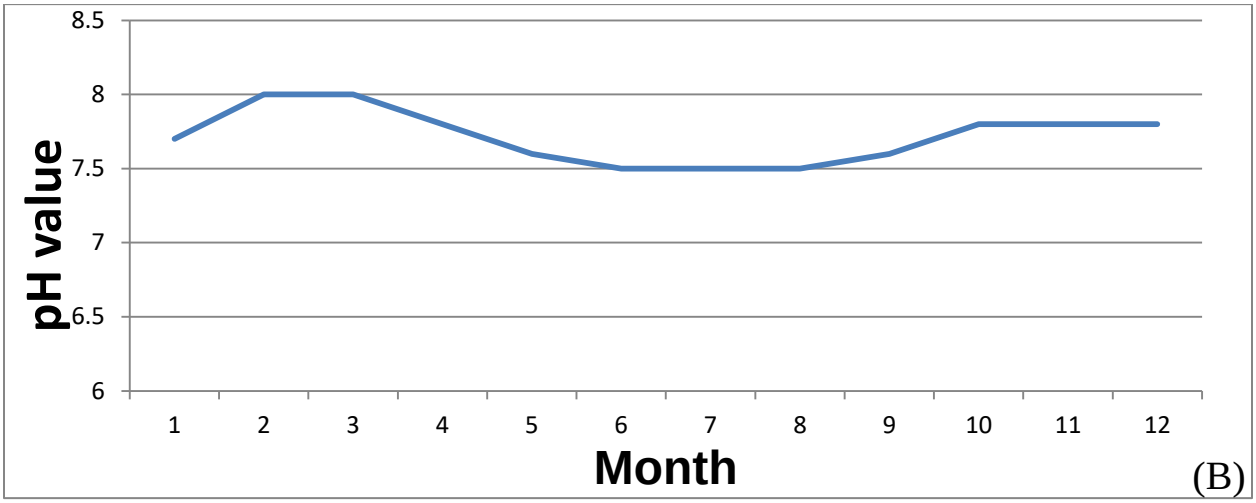
8.5
8
7.5
7
6.5
6
pH value
1
2
3
4
5
6
7
8
9
10
11
12
Month
(B)

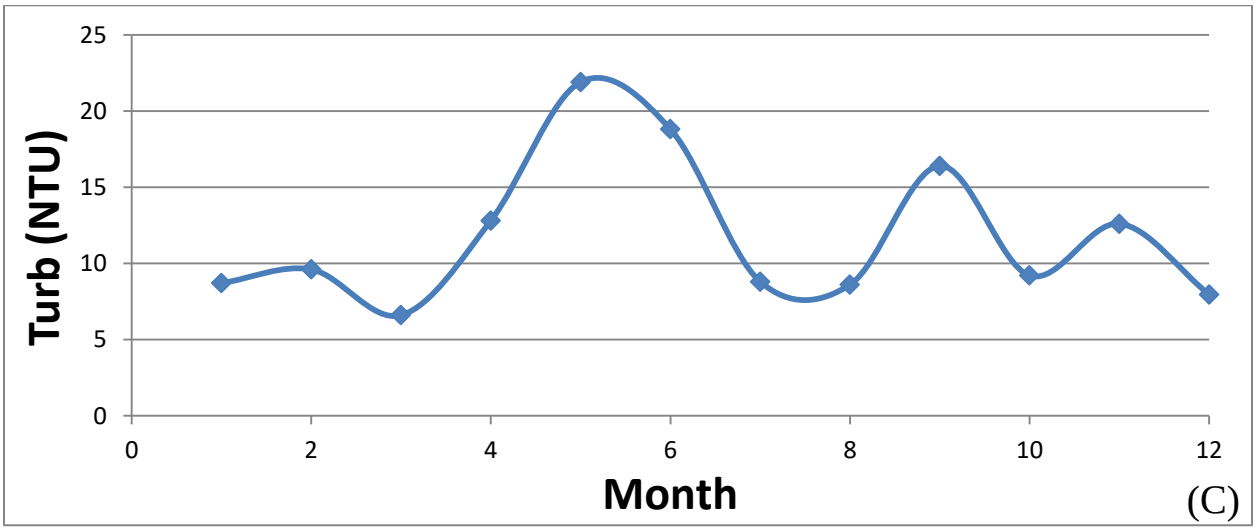
25
20
15
10
5
0
Turb (NTU)
0
2
4
6
8
10
12
Month
(C)

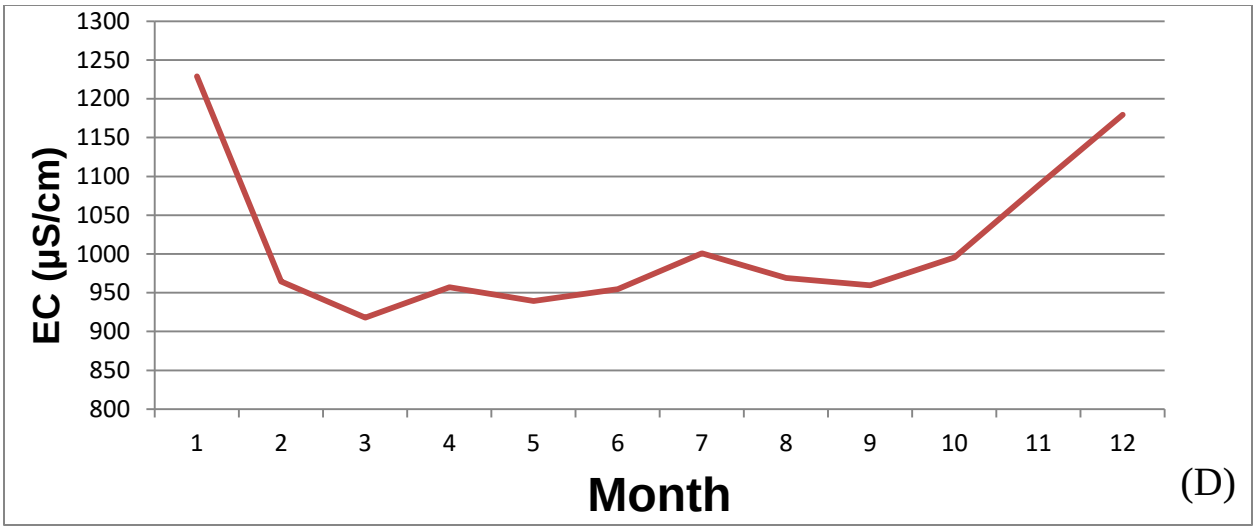

Figure (C.7): (A , B , C , D) water quality parameters variation in station (S2) for year 2017.

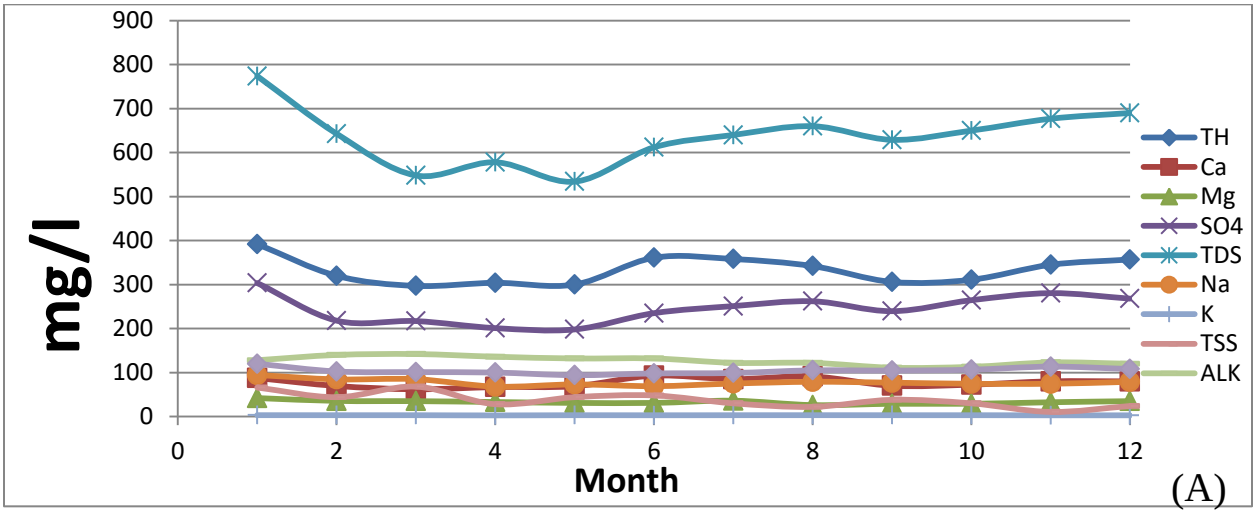

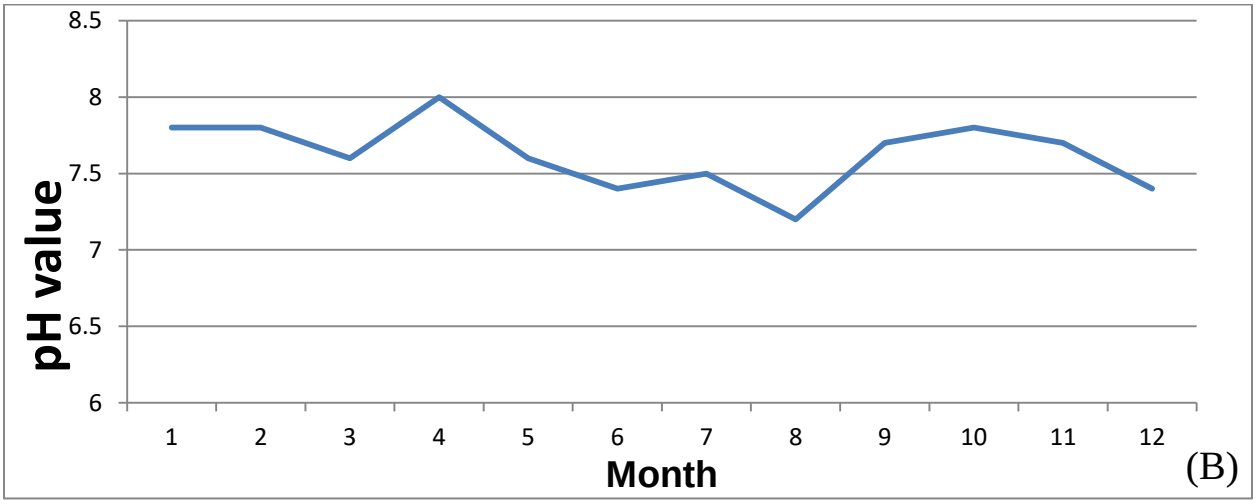

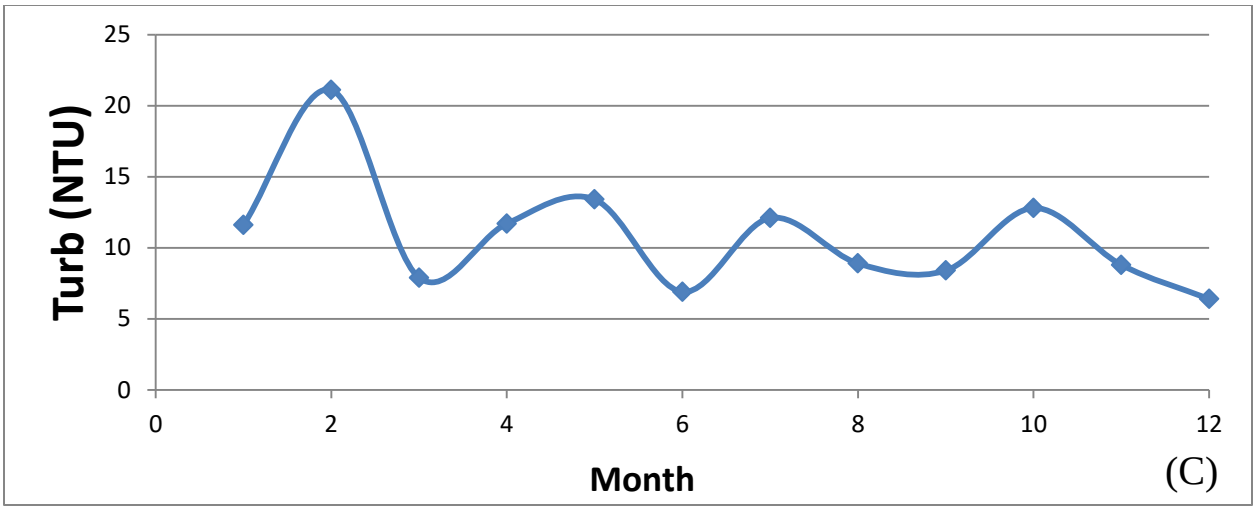

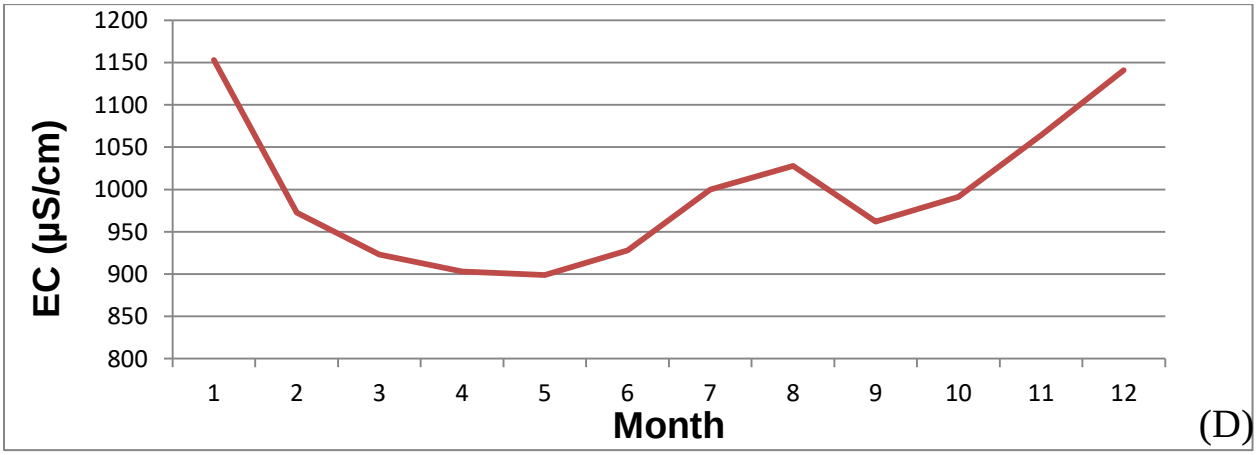

Figure (C.8): (A , B , C , D) water quality parameters variation in station (S3) for year 2017.

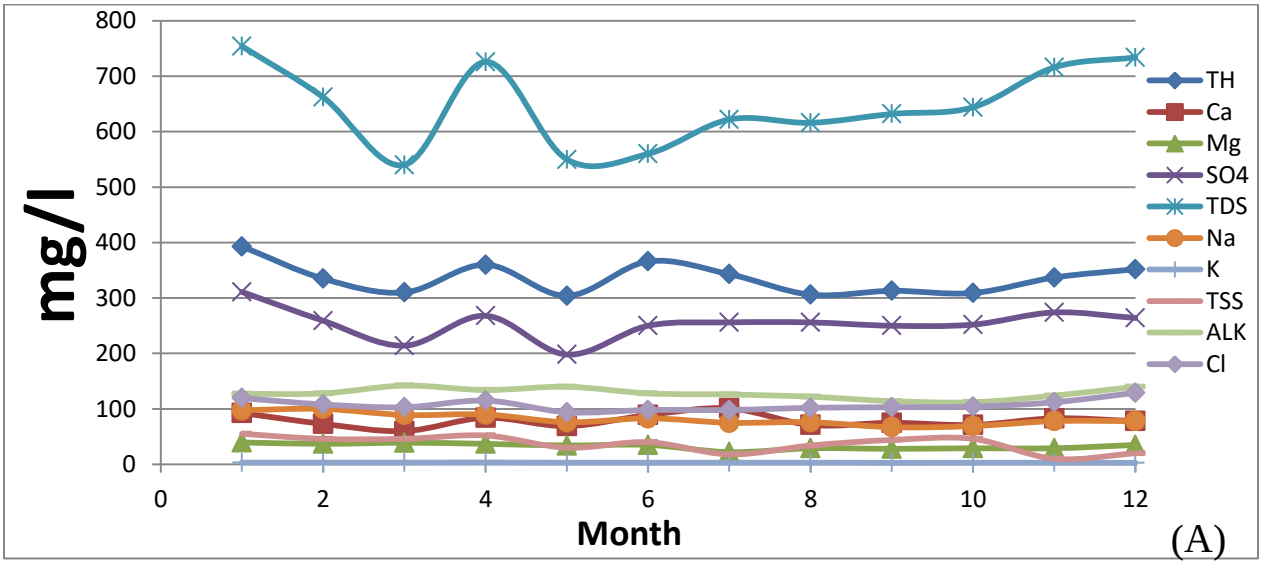

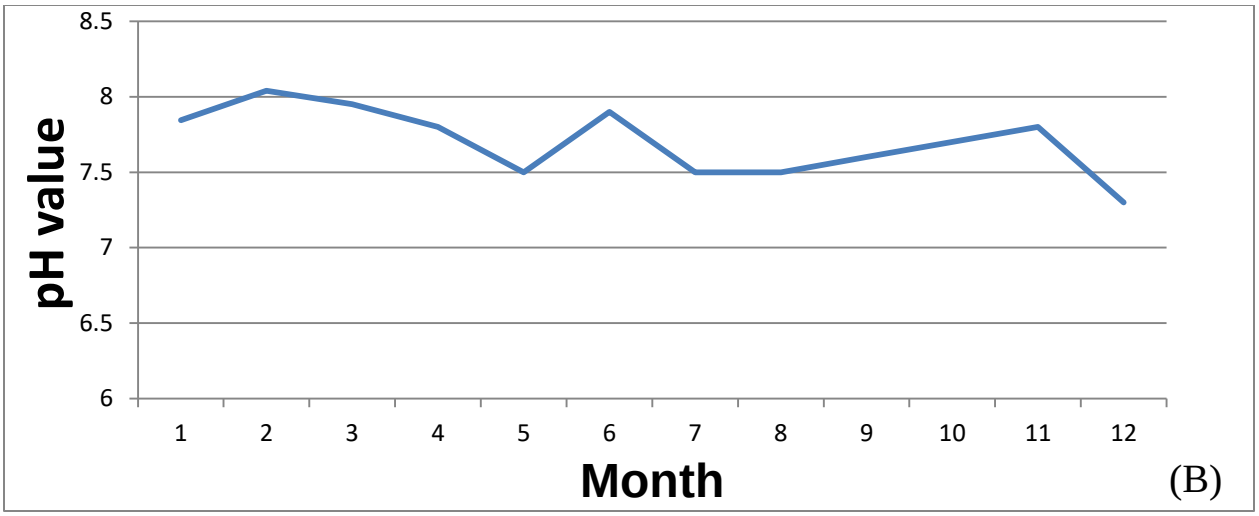

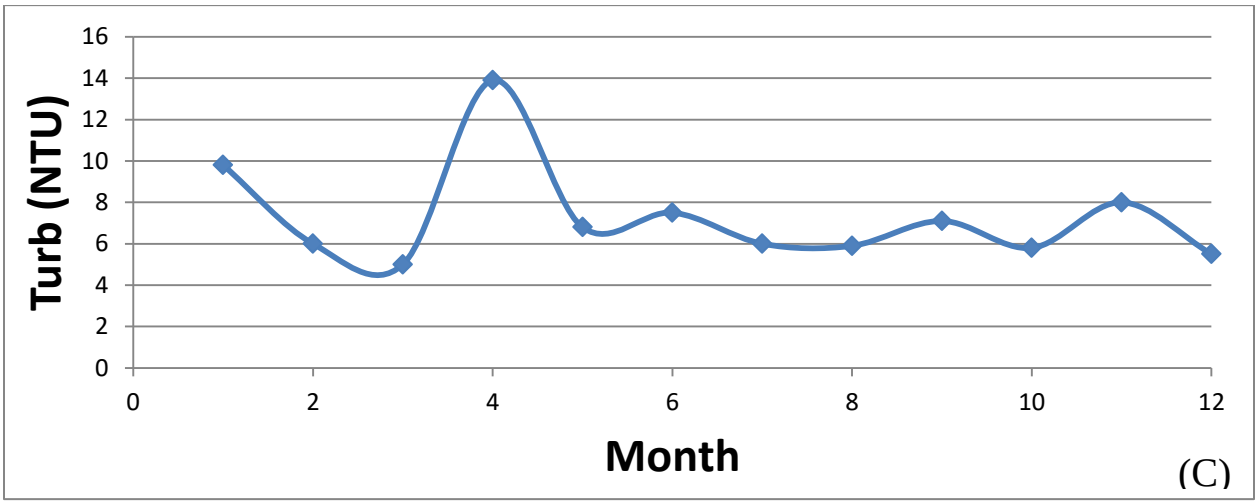

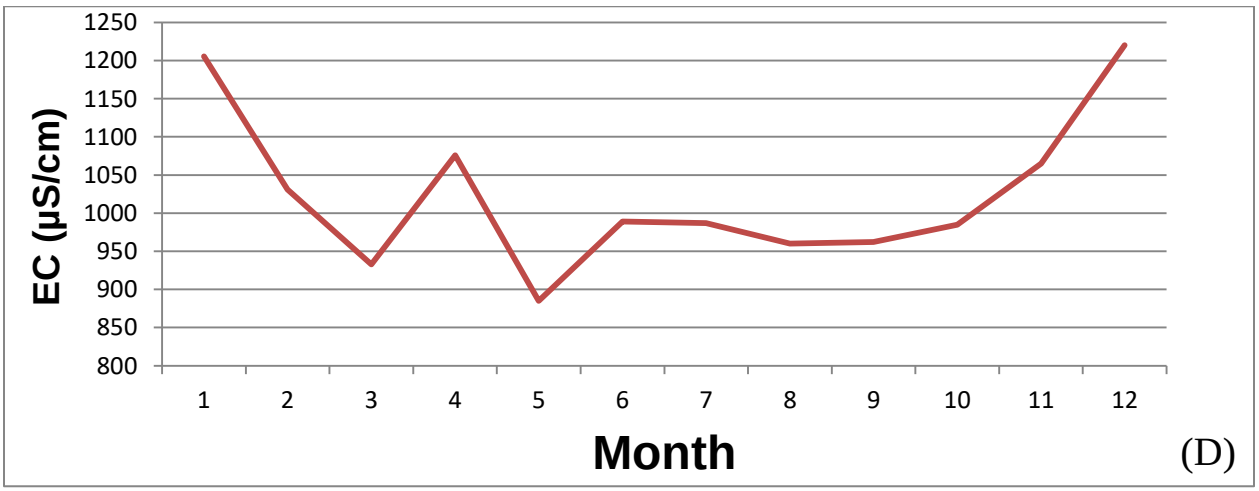

Figure (C.9): (A , B , C , D) water quality parameters variation in station (S4) for year 2017.

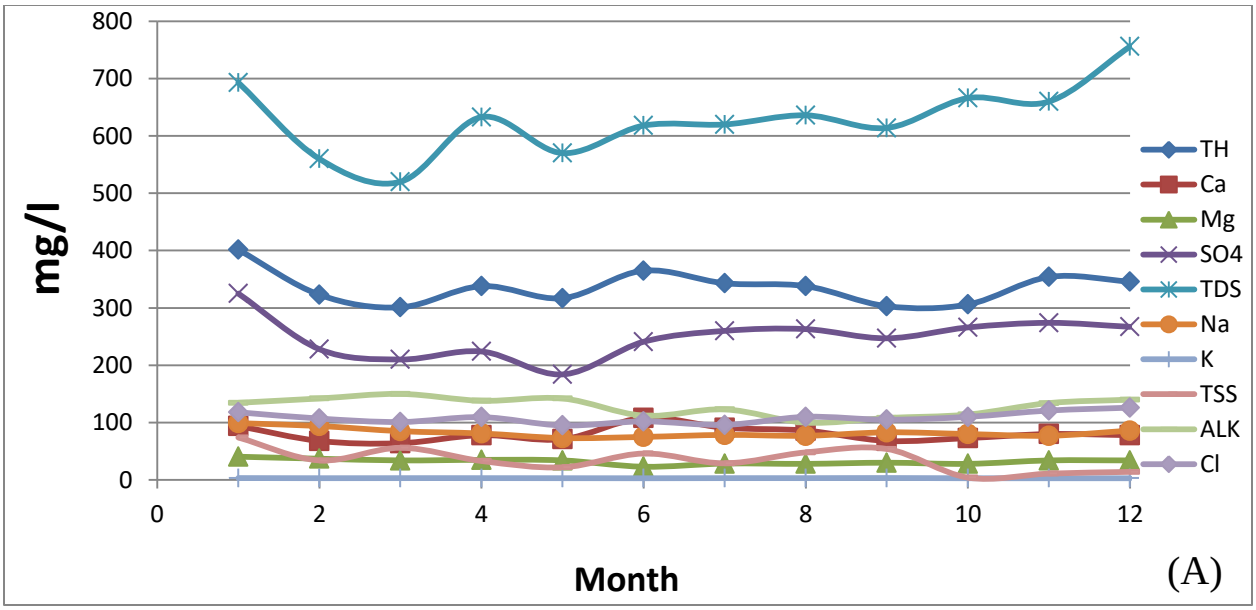
800
700
600
500
400
300
200
100
0
mg/l
0
2
4
6
8
10
12
Month
TH
Ca
Mg
SO4
TDS
Na
K
TSS
ALK
Cl
(A)

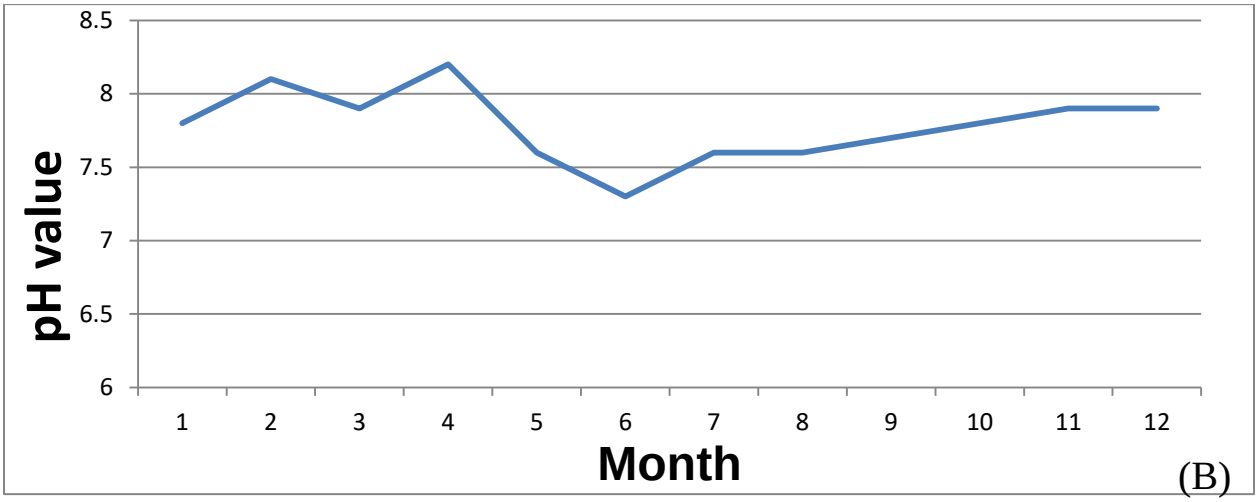
8.5
8
7.5
7
6.5
6
pH value
1
2
3
4
5
6
7
8
9
10
11
12
Month
(B)

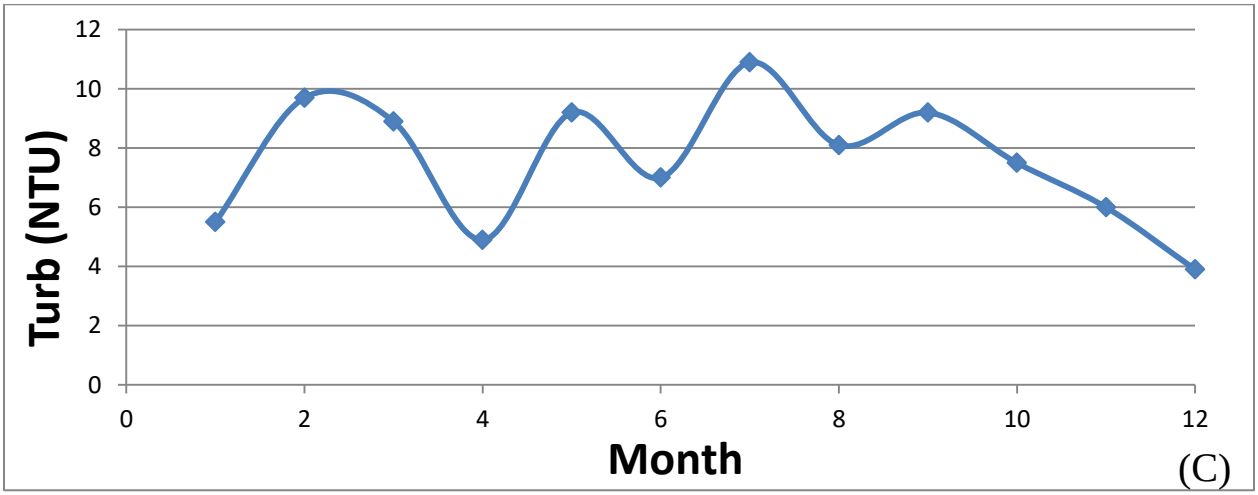
12
10
8
6
4
2
0
Turb (NTU)
0
2
4
6
8
10
12
Month
(C)

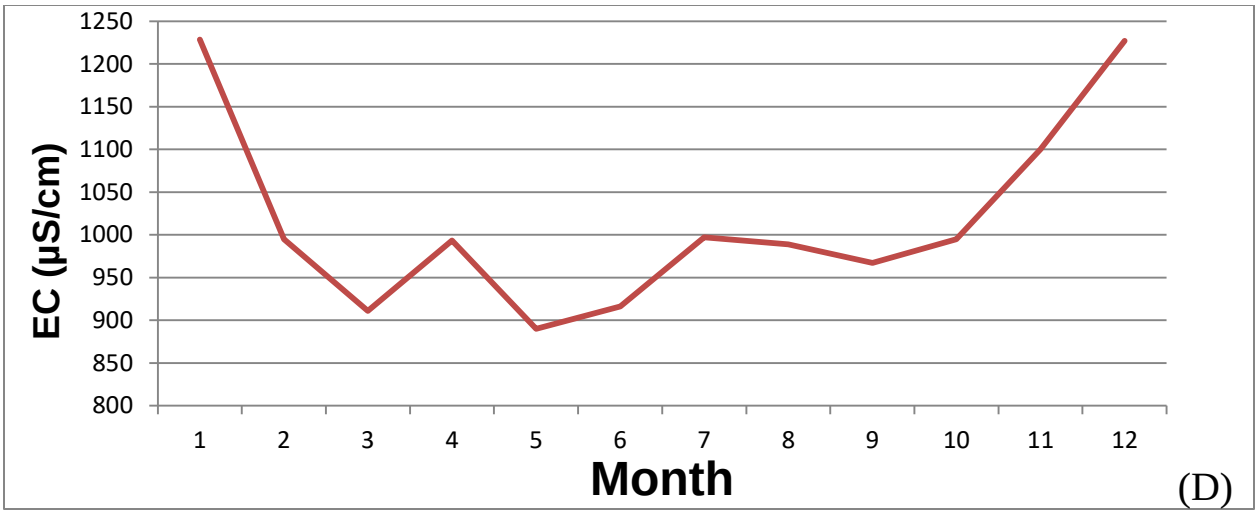

Figure (C.10): (A , B , C , D) water quality parameters variation in station (S5) for year 2017.

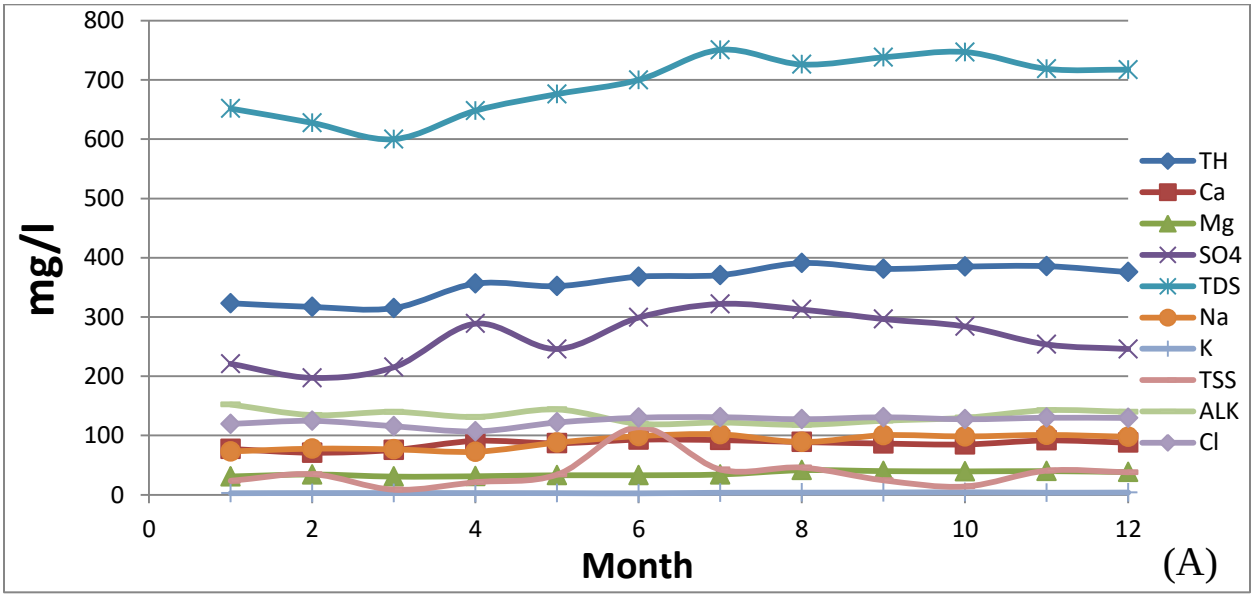

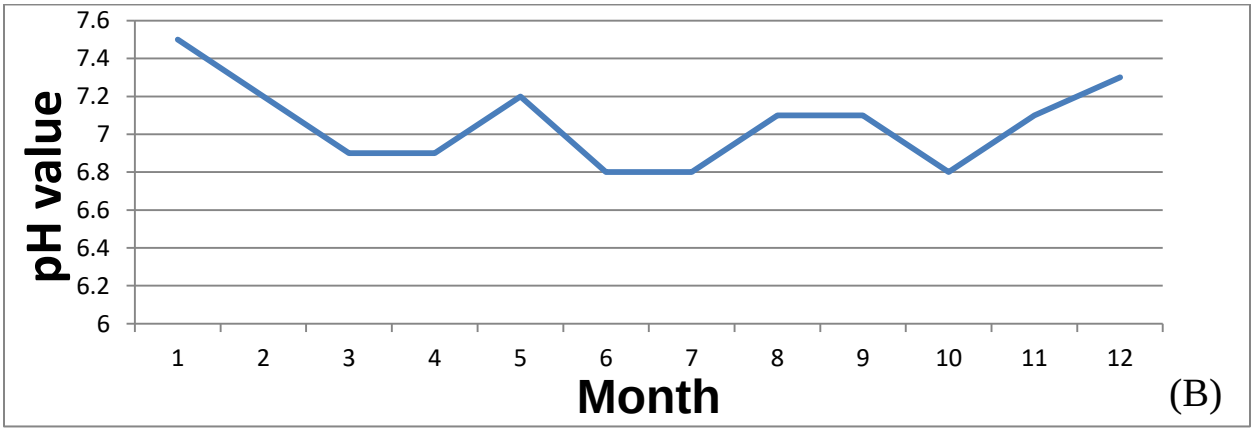

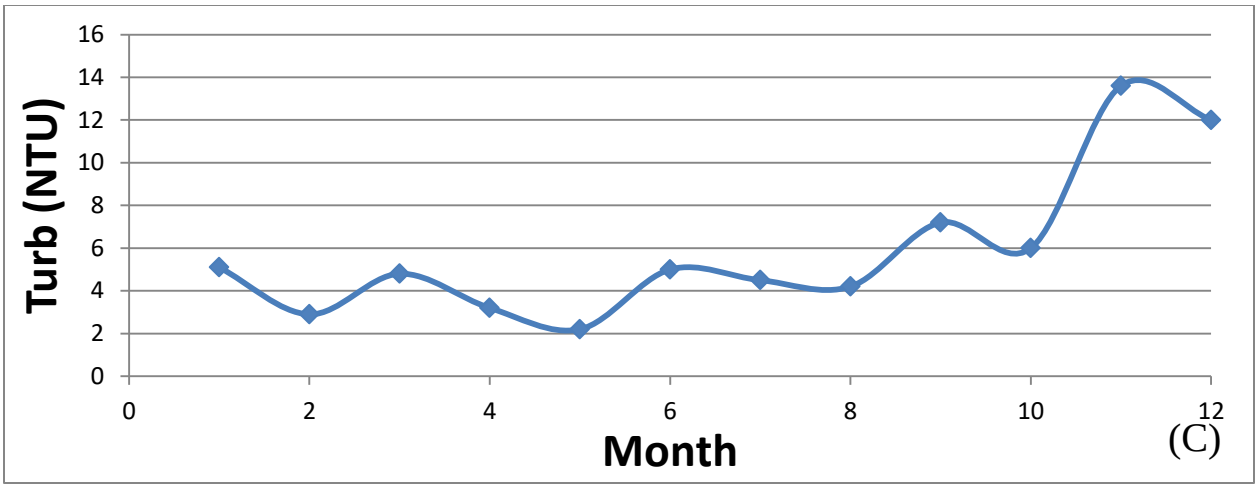

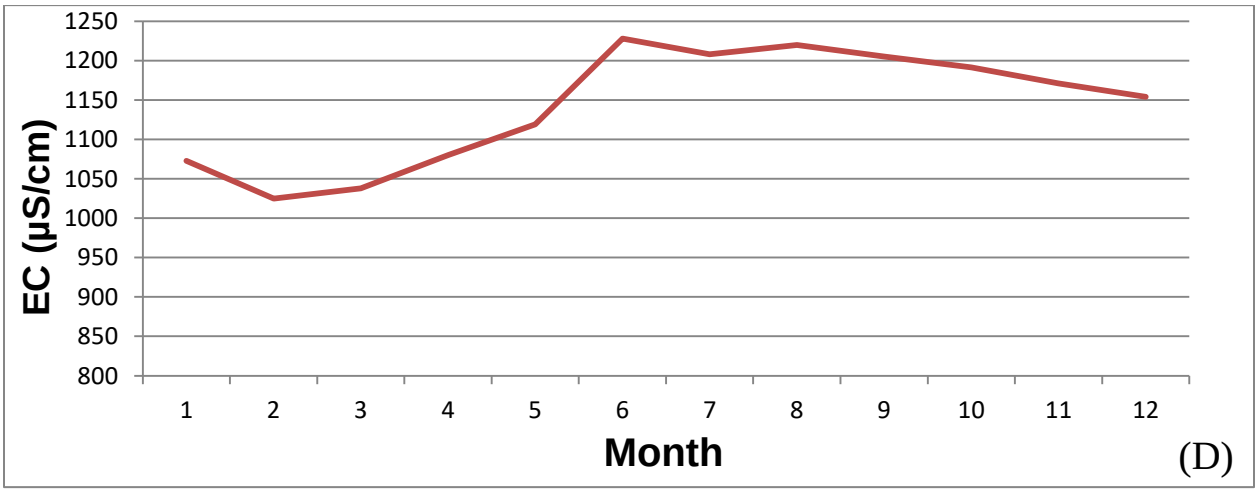

Figure (C.11): (A , B , C , D) water quality parameters variation in station (S1) for year 2018.

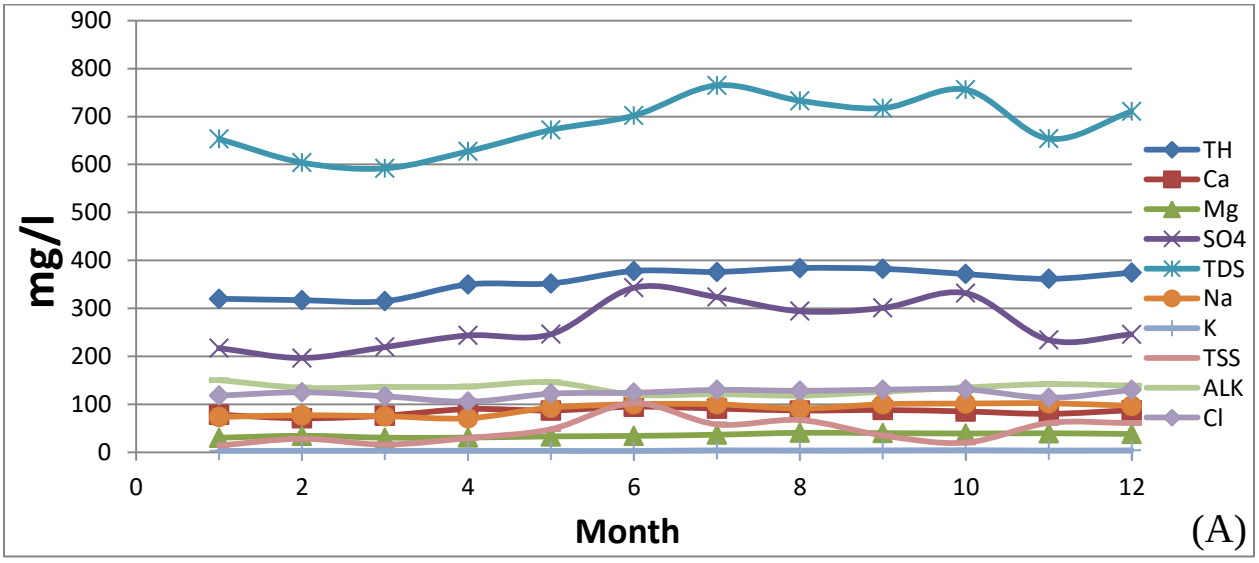

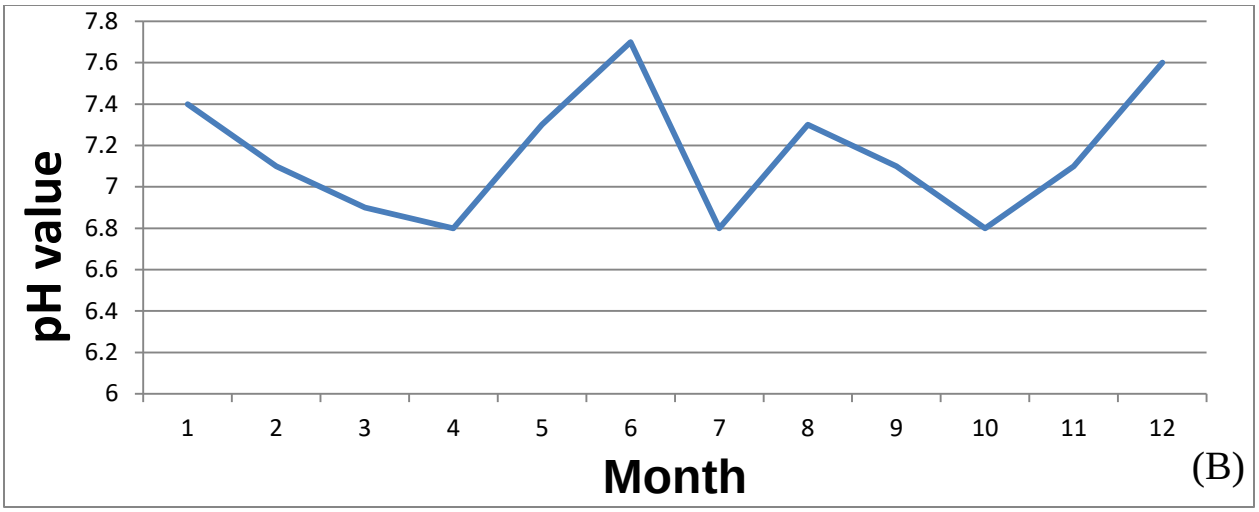

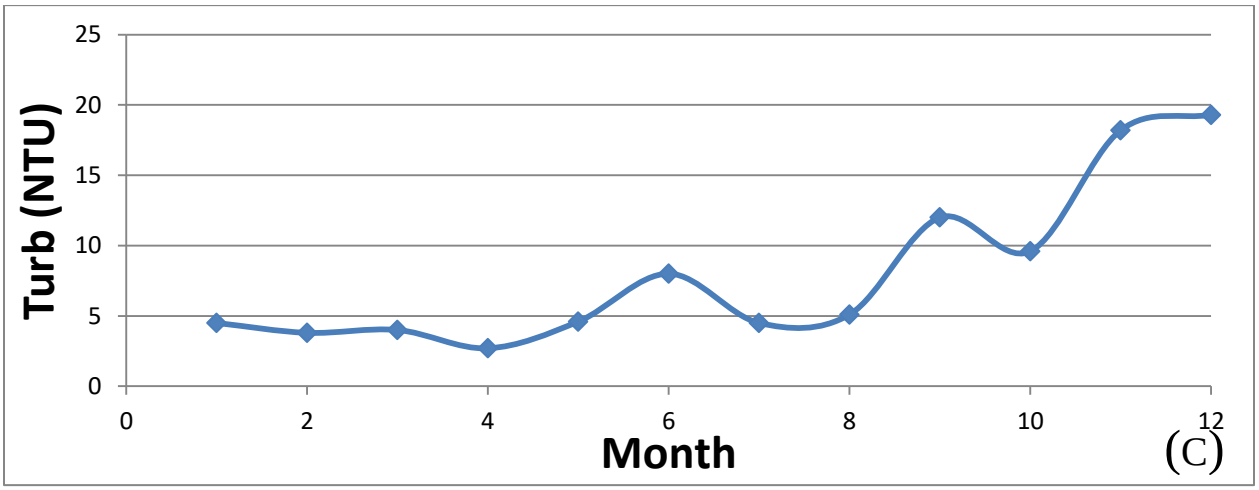

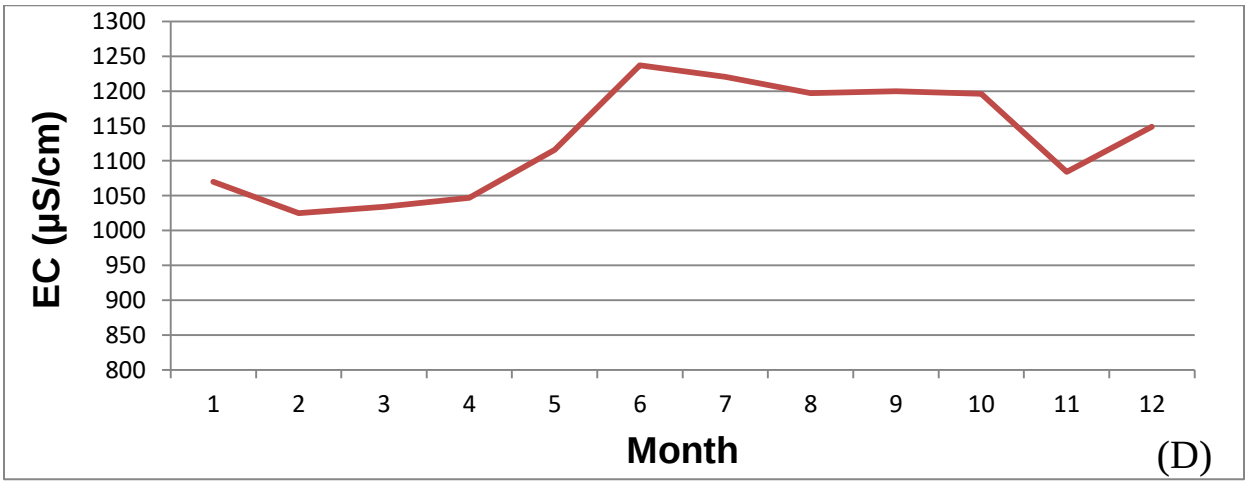

Figure (C.12): (A , B , C , D) water quality parameters variation in station (S2) for year 2018.

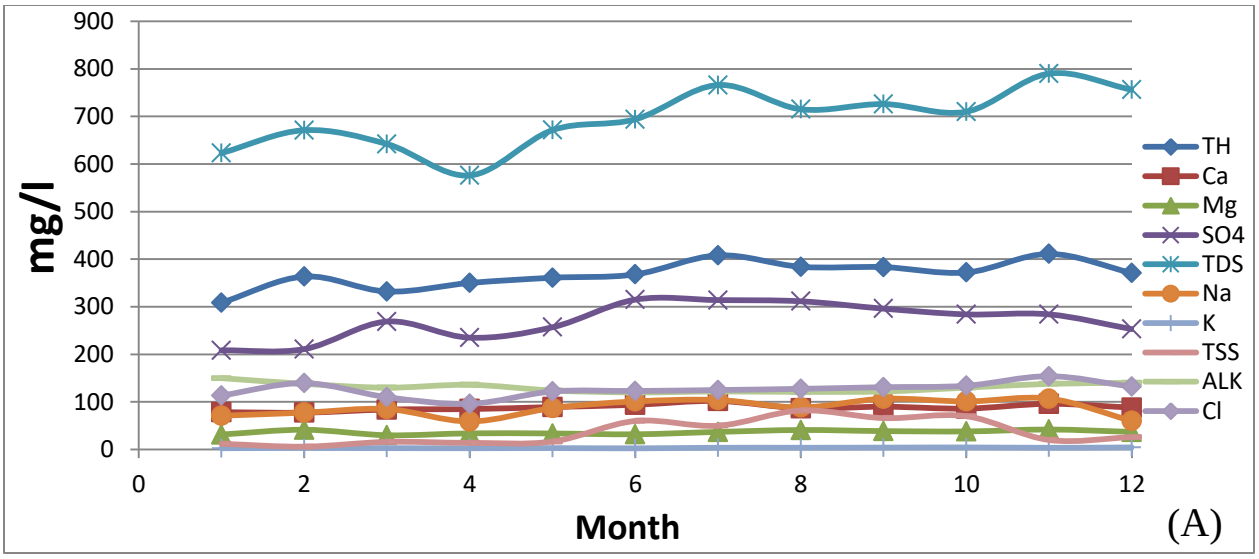
900
800
700
600
500
400
300
200
100
0
mg/l
0
2
4
6
8
10
12
Month
TH
Ca
Mg
SO4
TDS
Na
K
TSS
ALK
Cl
(A)

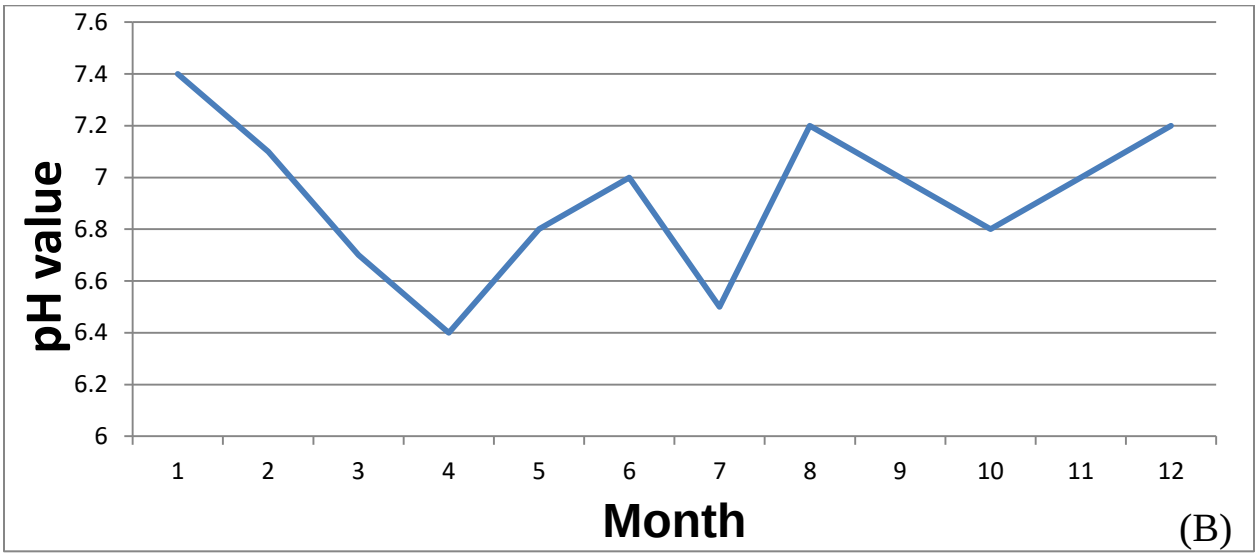
7.6
7.4
7.2
7
6.8
6.6
6.4
6.2
6
pH value
1
2
3
4
5
6
7
8
9
10
11
12
Month
(B)

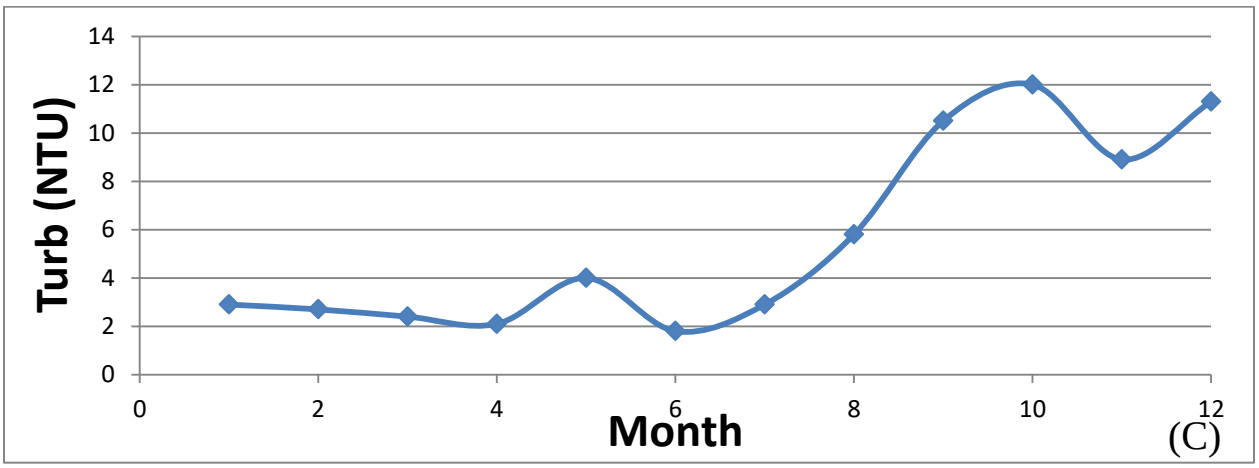
14
12
10
8
6
4
2
0
Turb (NTU)
0
2
4
6
8
10
12
Month
(C)

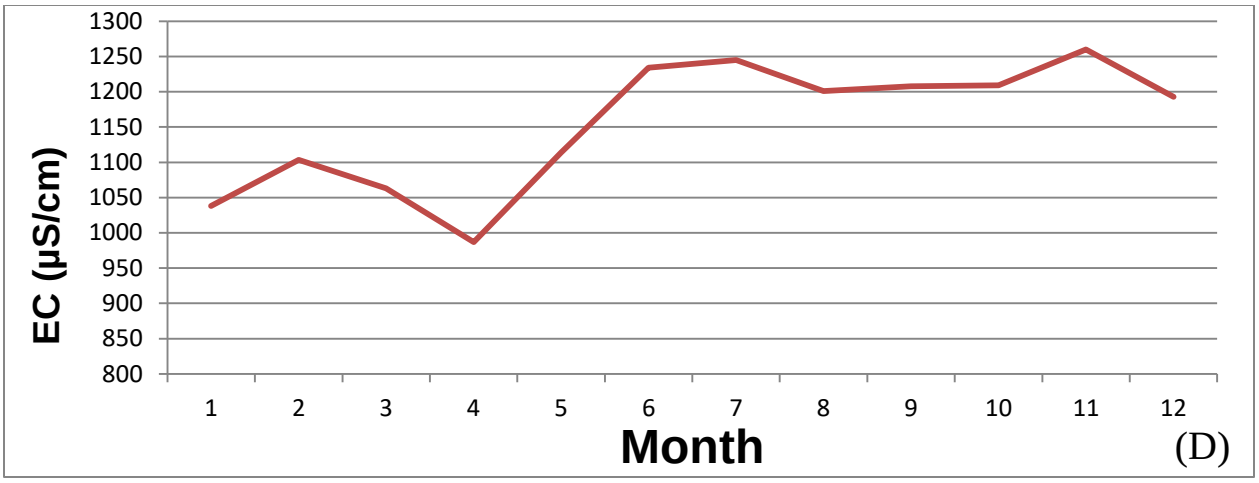

Figure (C.13): (A , B , C , D) water quality parameters variation in station (S3) for year 2018.

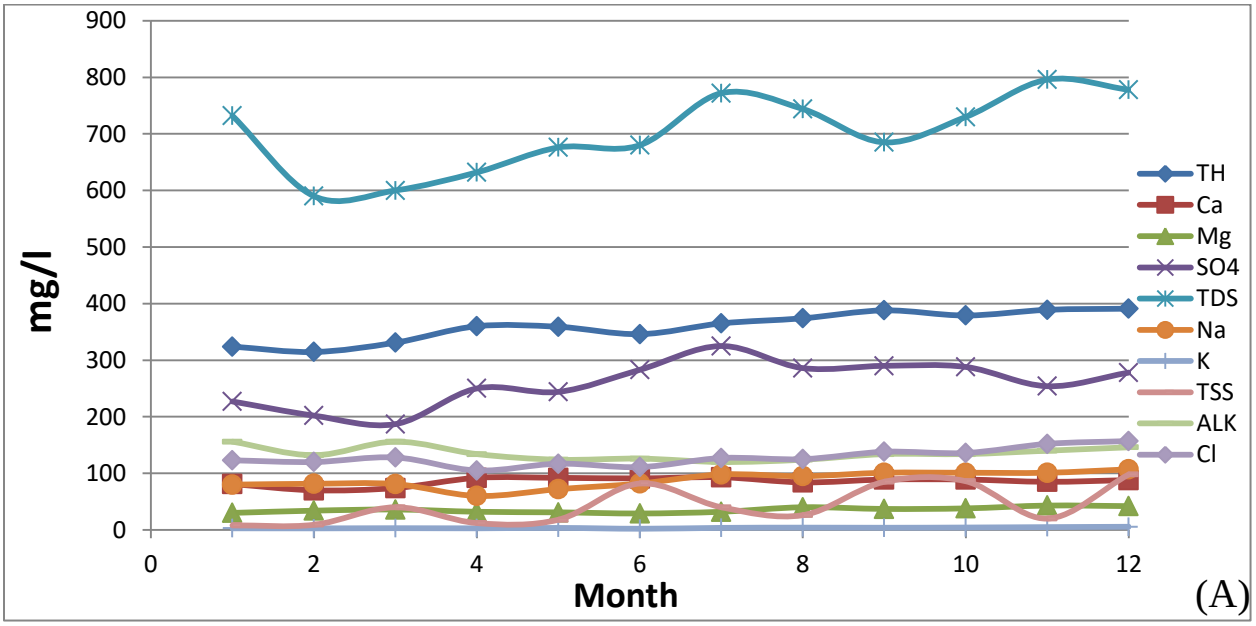

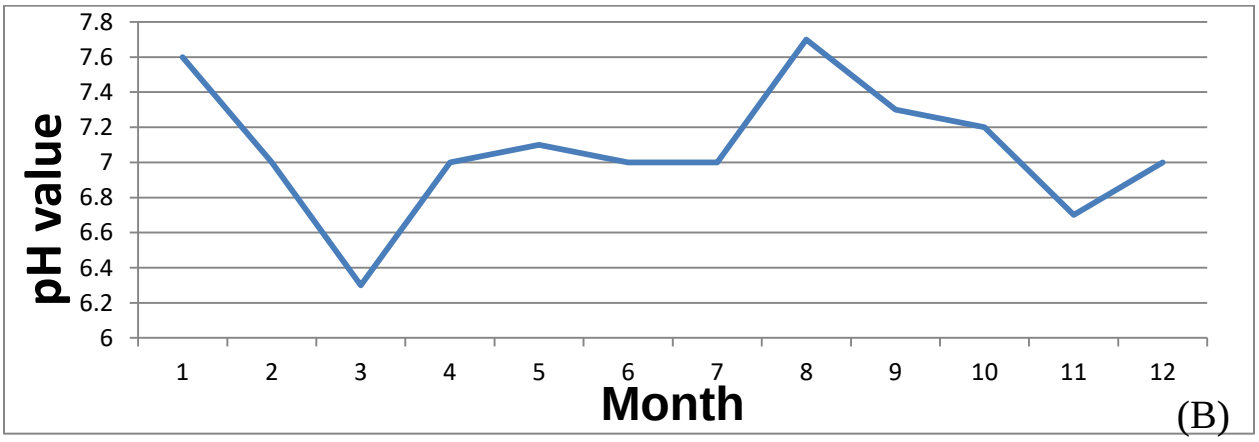

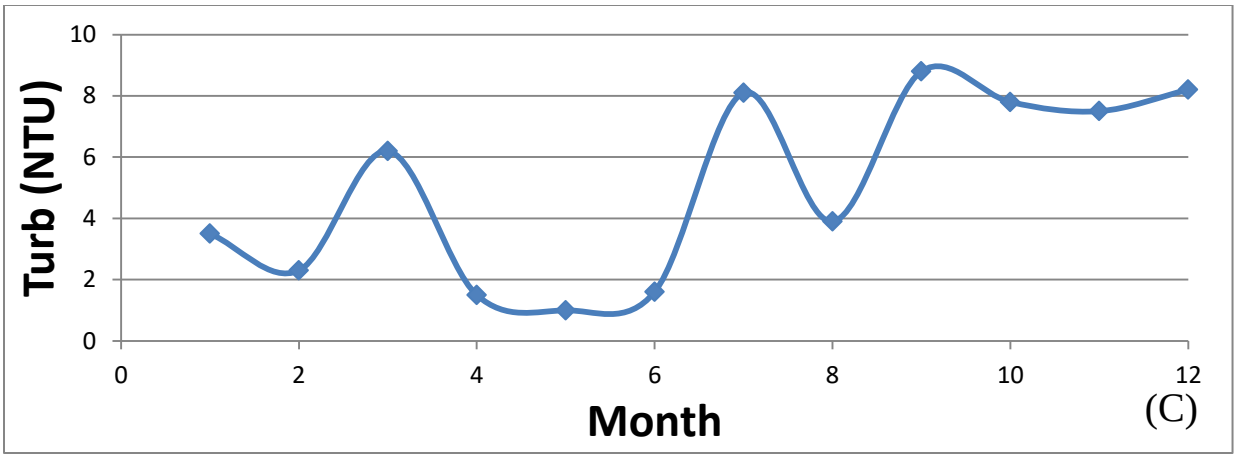

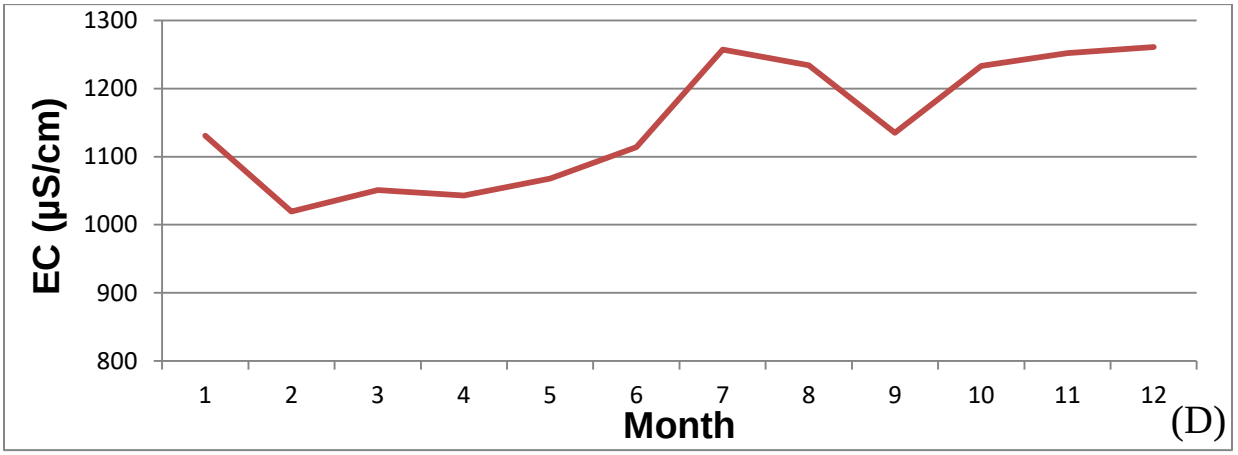

Figure (C.14): (A , B , C , D) water quality parameters variation in station (S4) for year 2018.

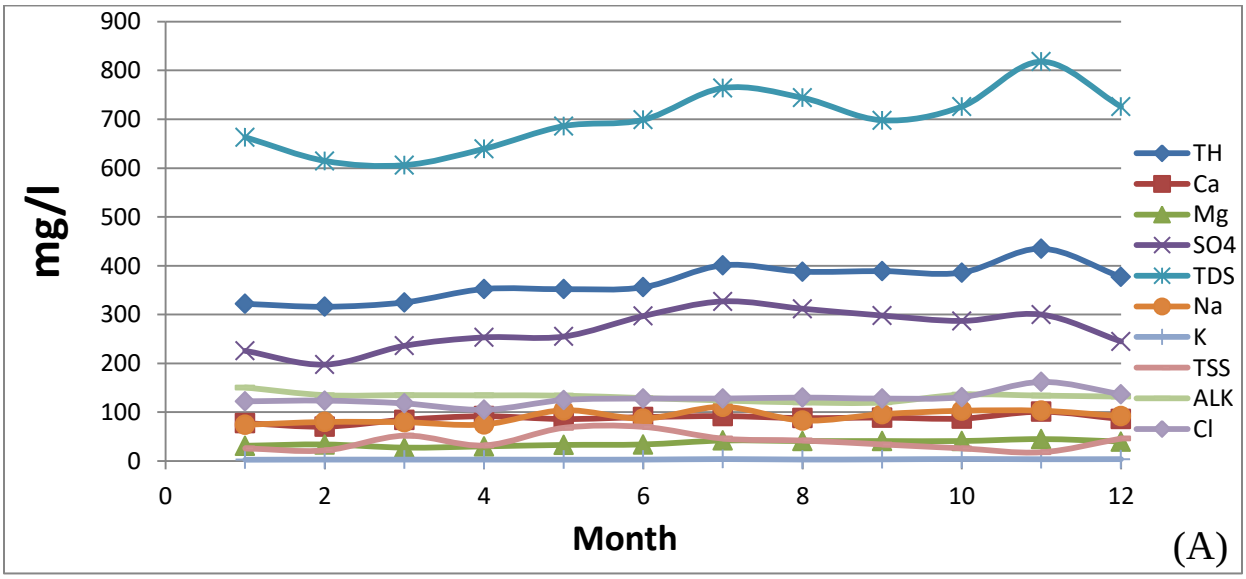

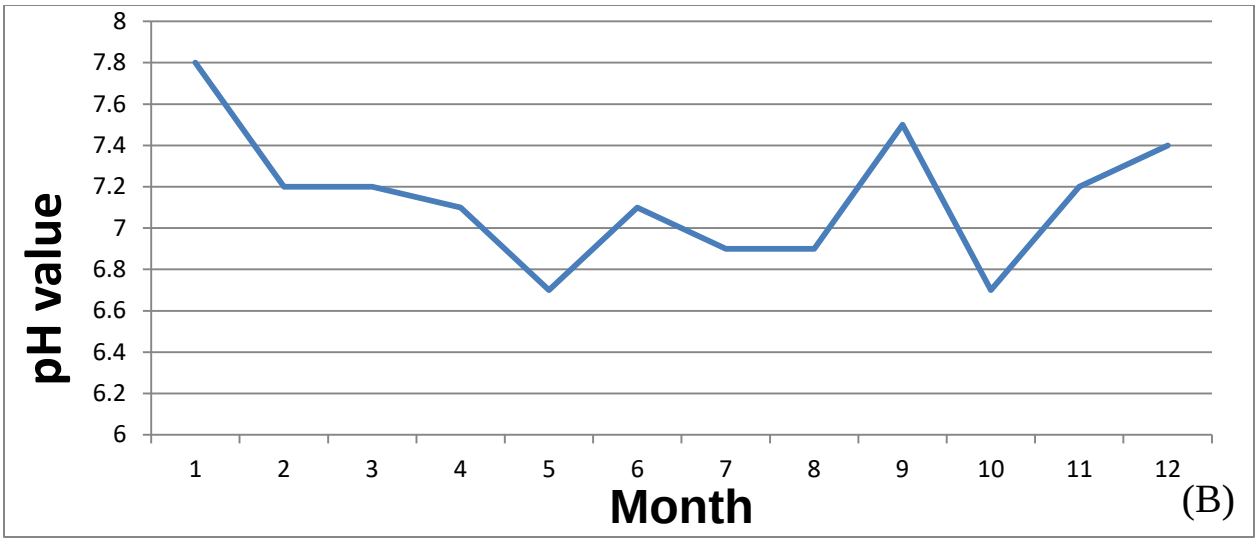

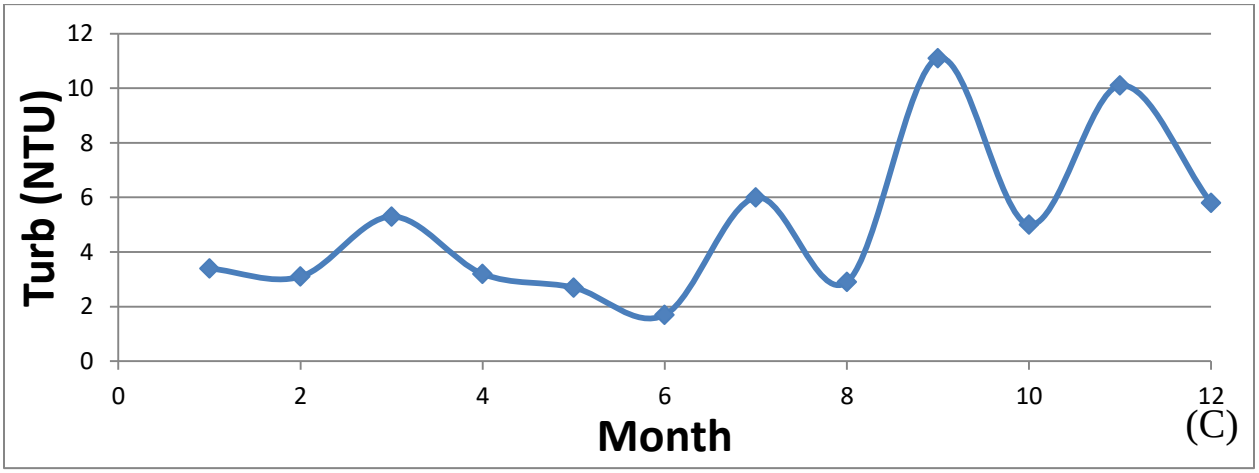

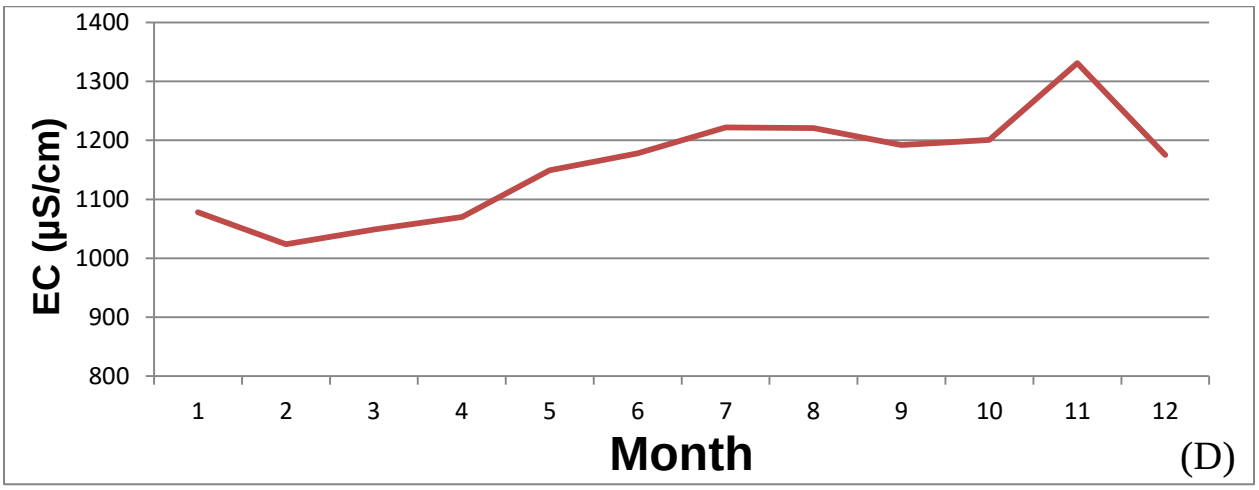

Figure (C.15): (A , B , C , D) water quality parameters variation in station (S5) for year 2018.

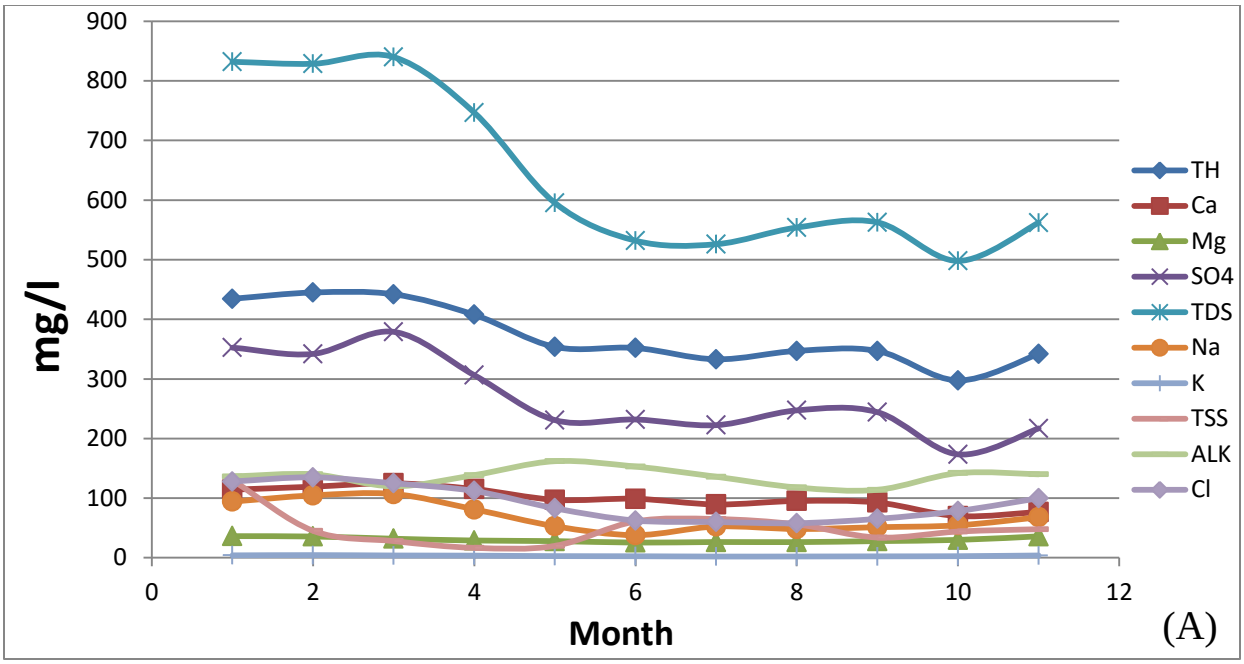
900
800
700
600
500
400
300
200
100
0
mg/l
0
2
4
6
8
10
12
Month
TH
Ca
Mg
SO4
TDS
Na
K
TSS
ALK
Cl
(A)

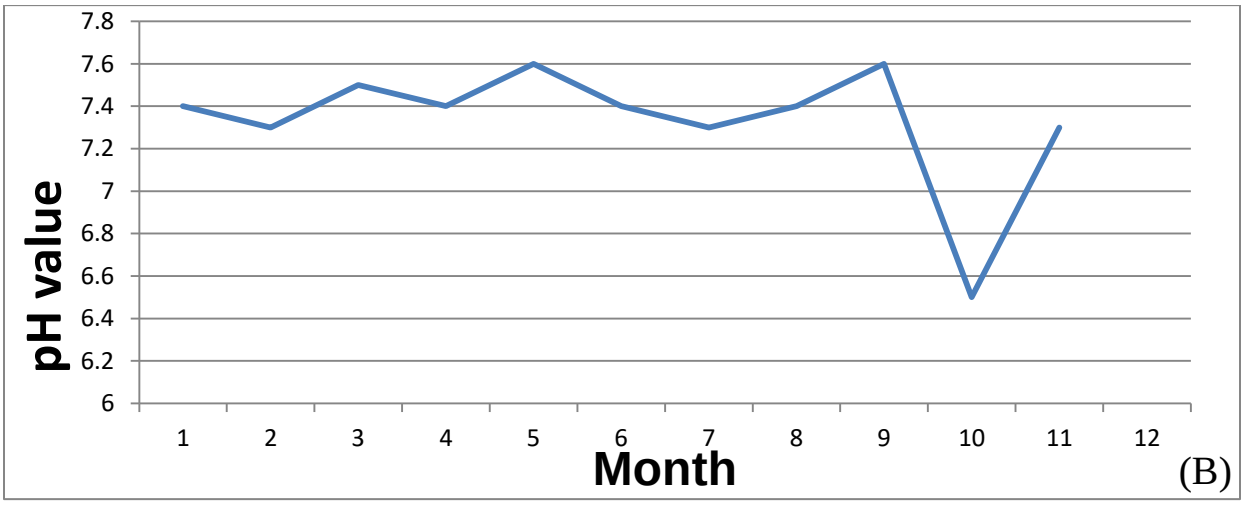
7.8
7.6
7.4
7.2
7
6.8
6.6
6.4
6.2
6
pH value
1
2
3
4
5
6
7
8
9
10
11
12
Month
(B)

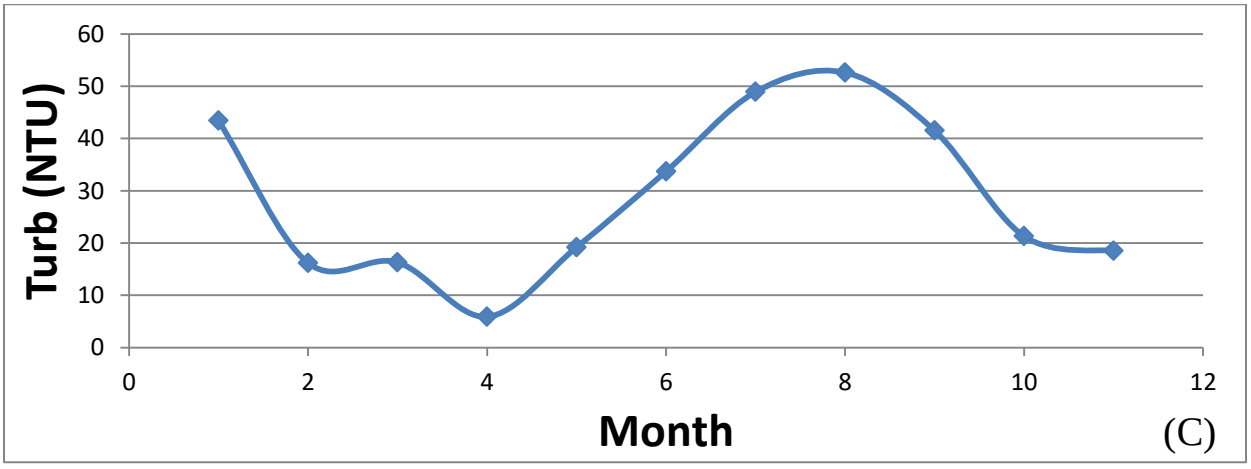
60
50
40
30
20
10
0
Turb (NTU)
0
2
4
6
8
10
12
Month
(C)

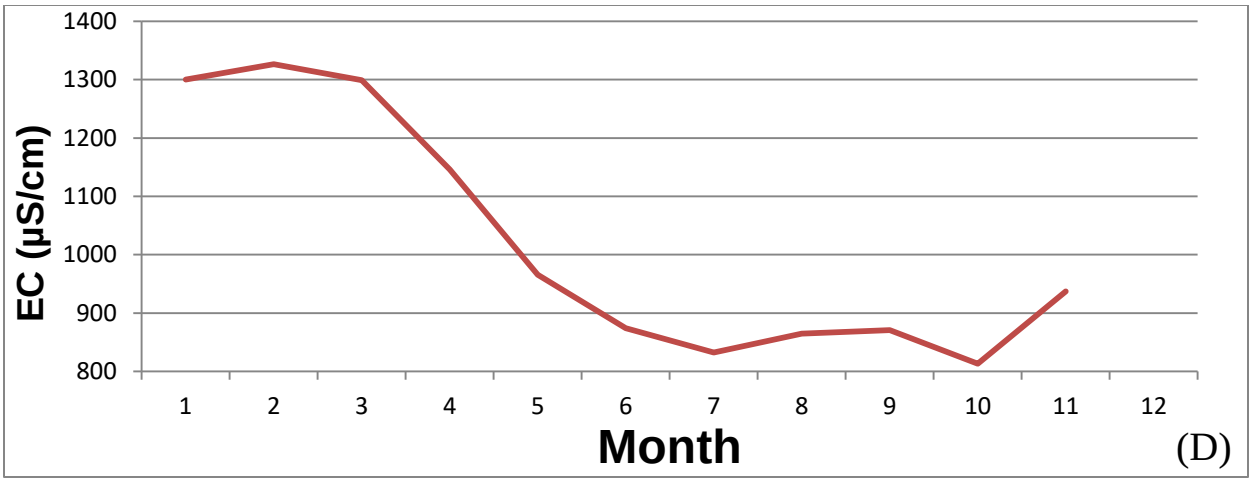

Figure (C.16): (A , B , C , D) water quality parameters variation in station (S1) for year 2019.

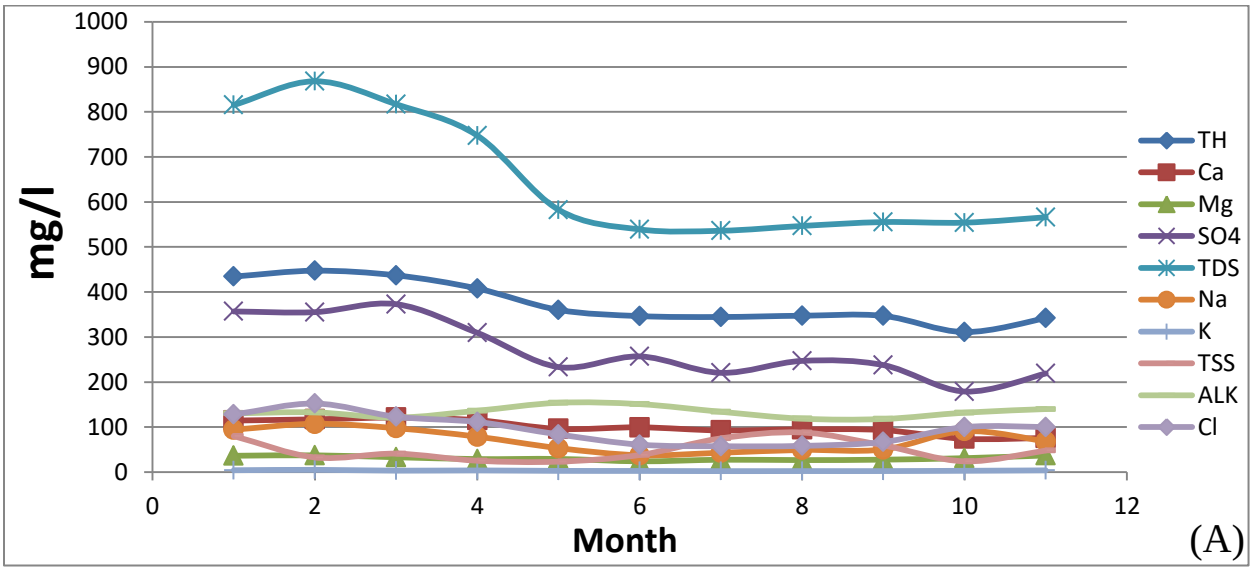

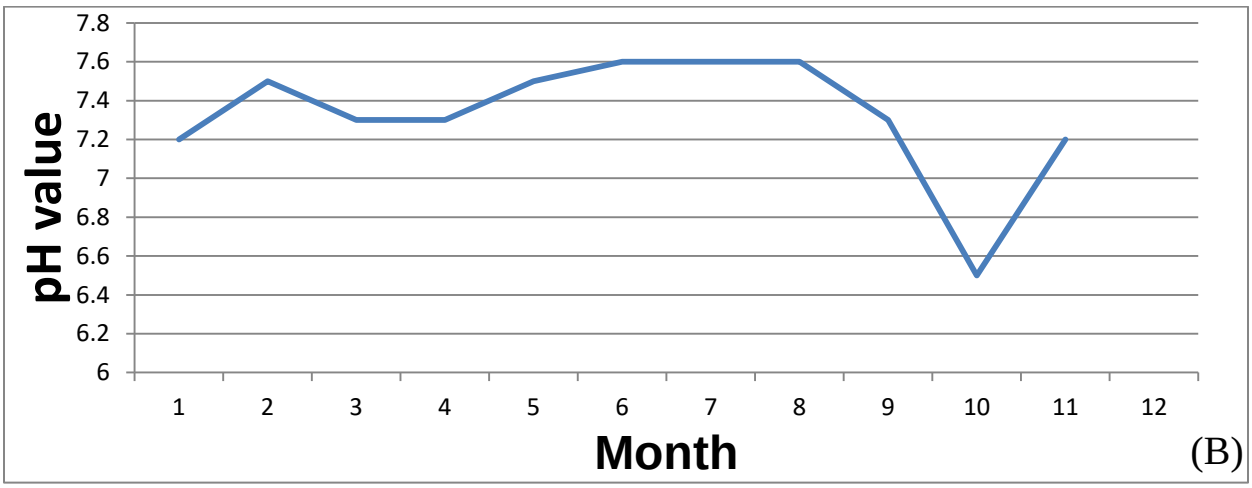

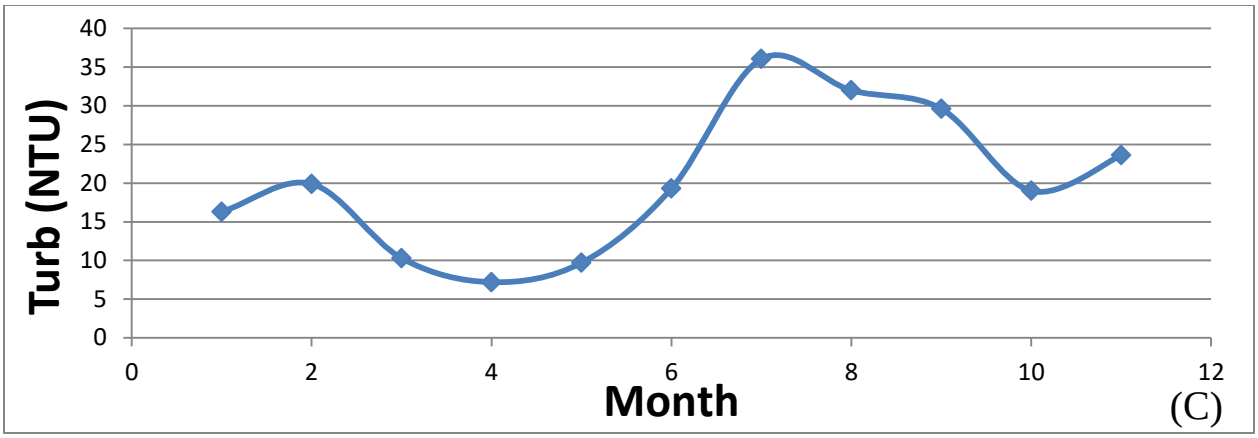

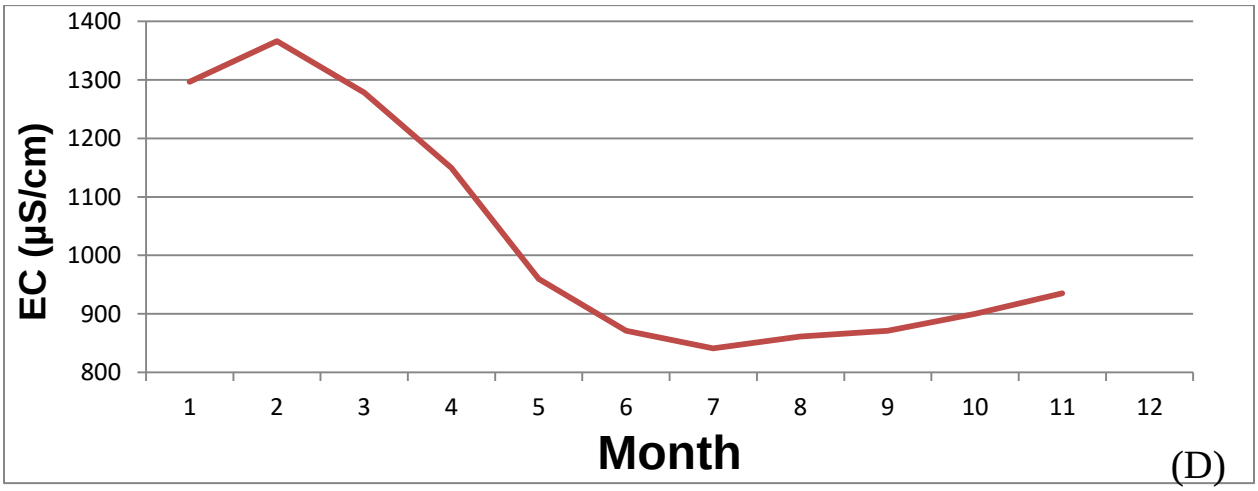

Figure (C.17): (A , B , C , D) water quality parameters variation in station (S2) for year 2019.

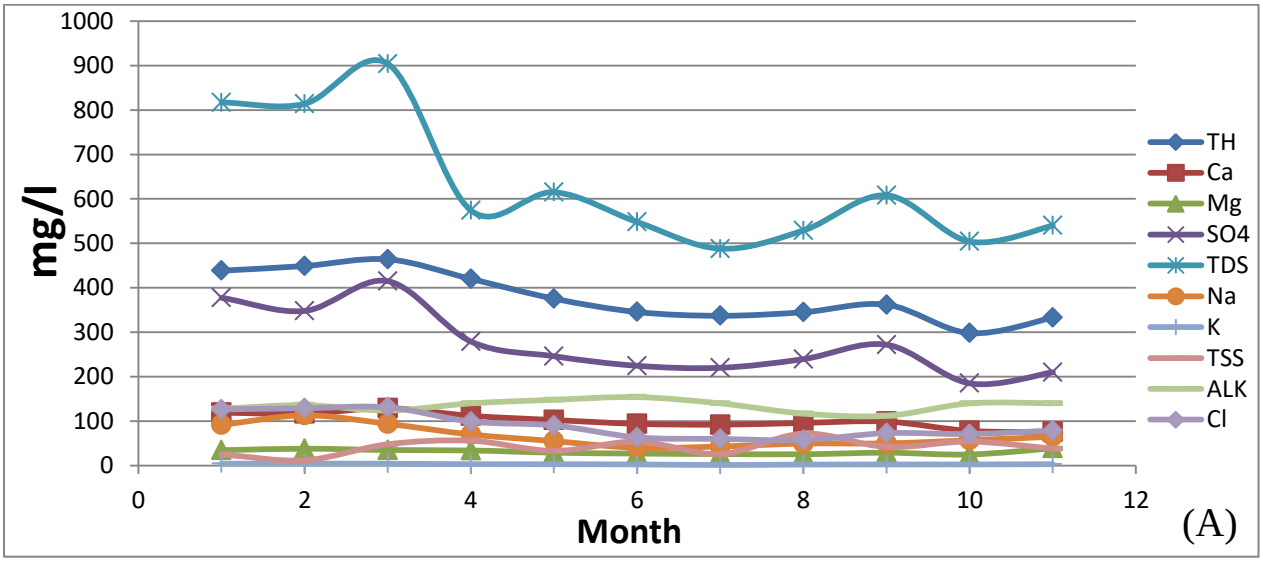

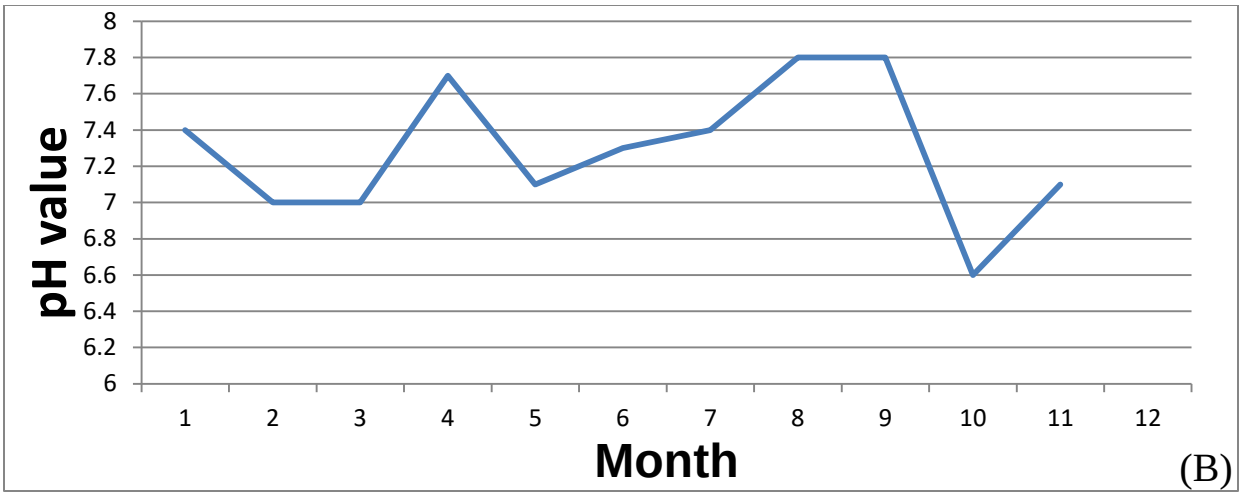

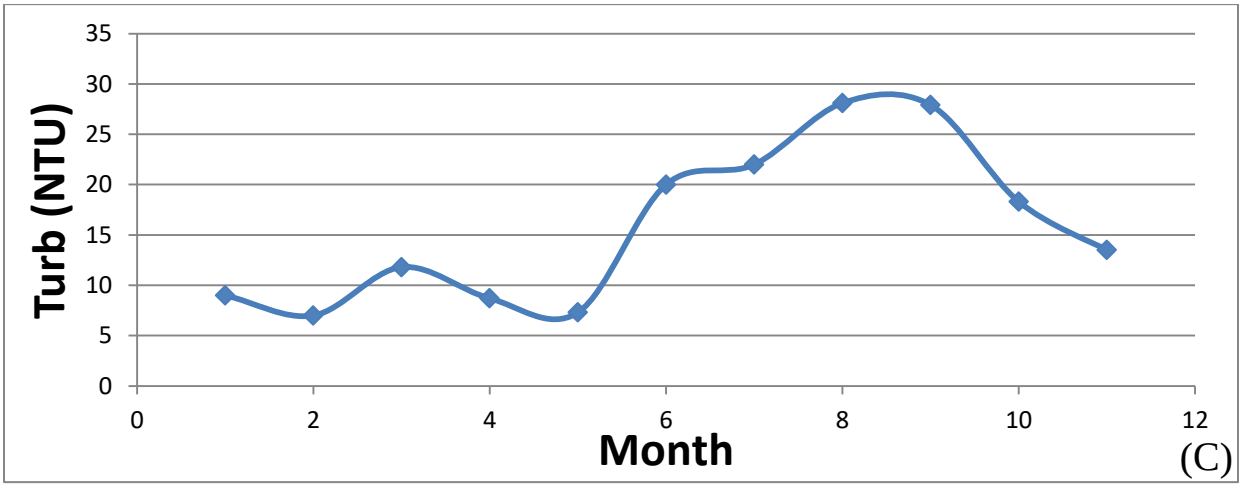

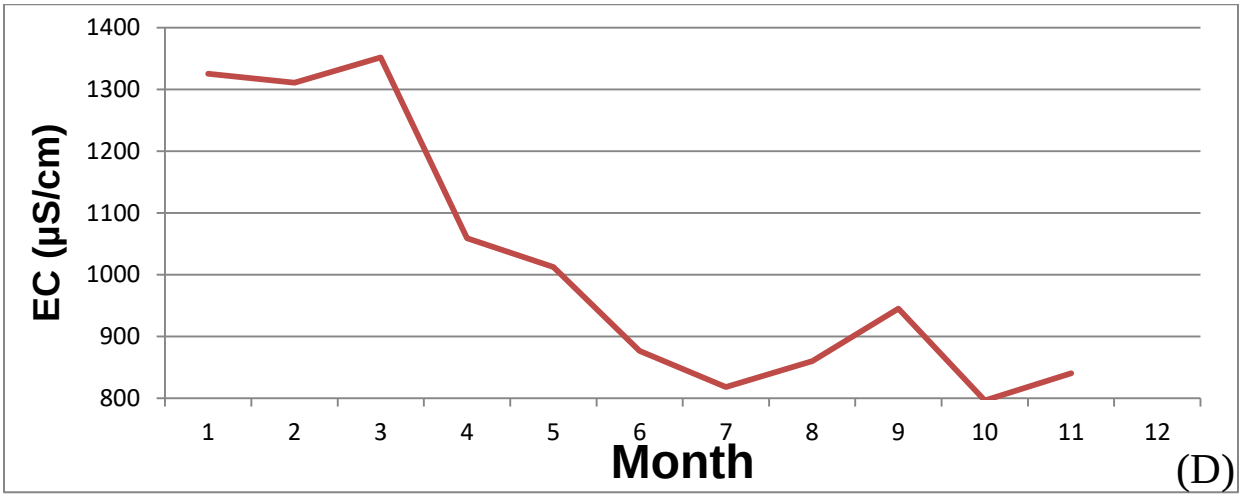

Figure (C.18): (A , B , C , D) water quality parameters variation in station (S3) for year 2019.

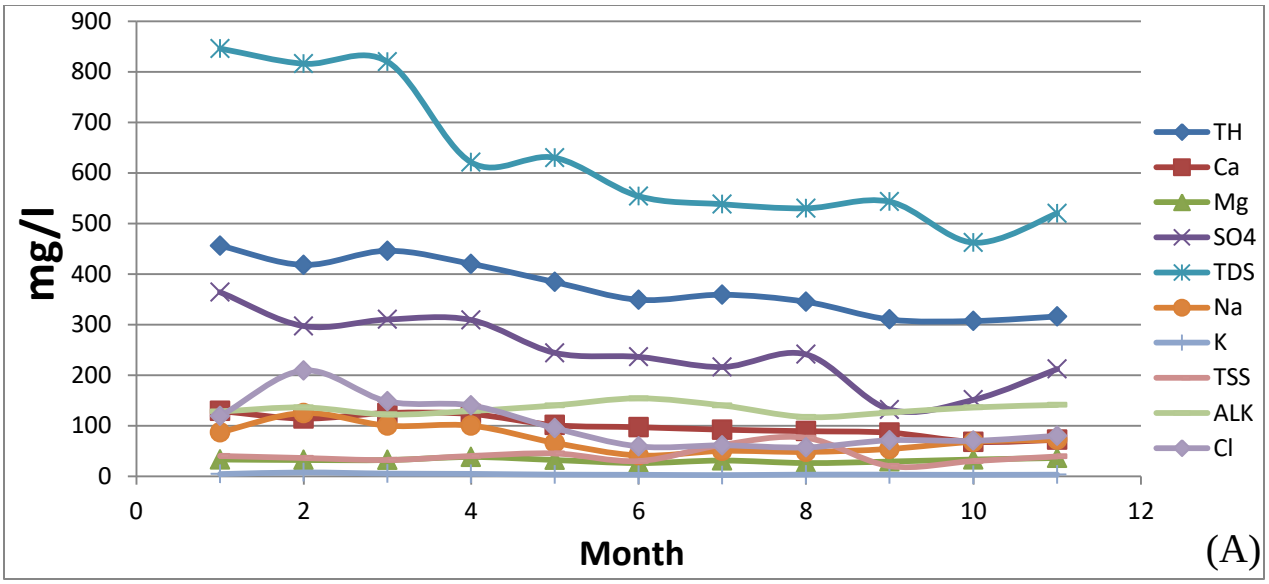
900
800
700
600
500
400
300
200
100
0
mg/l
0
2
4
6
8
10
12
Month
TH
Ca
Mg
SO4
TDS
Na
K
TSS
ALK
Cl
(A)

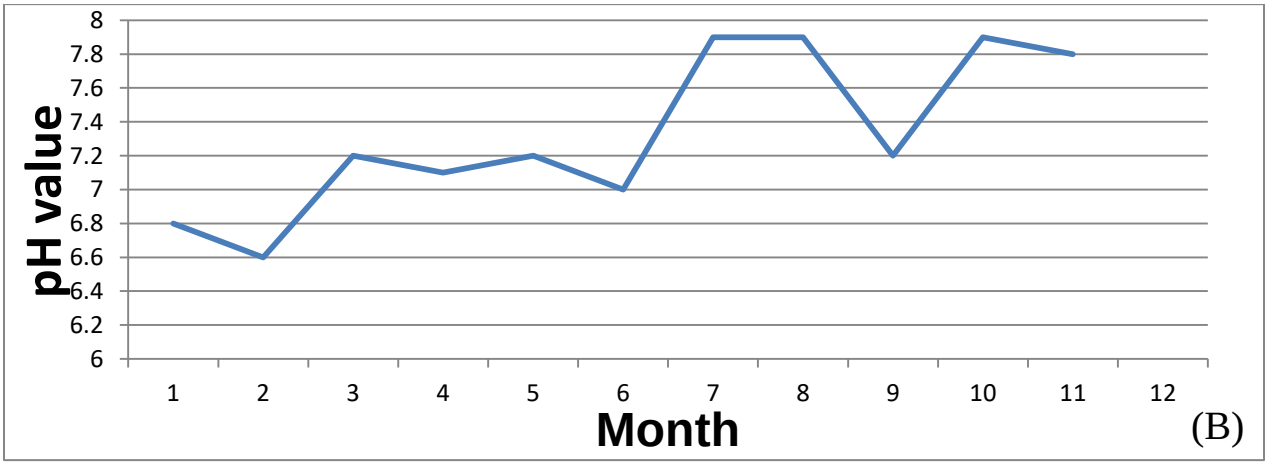
8
7.8
7.6
7.4
7.2
7
6.8
6.6
6.4
6.2
6
pH value
1
2
3
4
5
6
7
8
9
10
11
12
Month
(B)

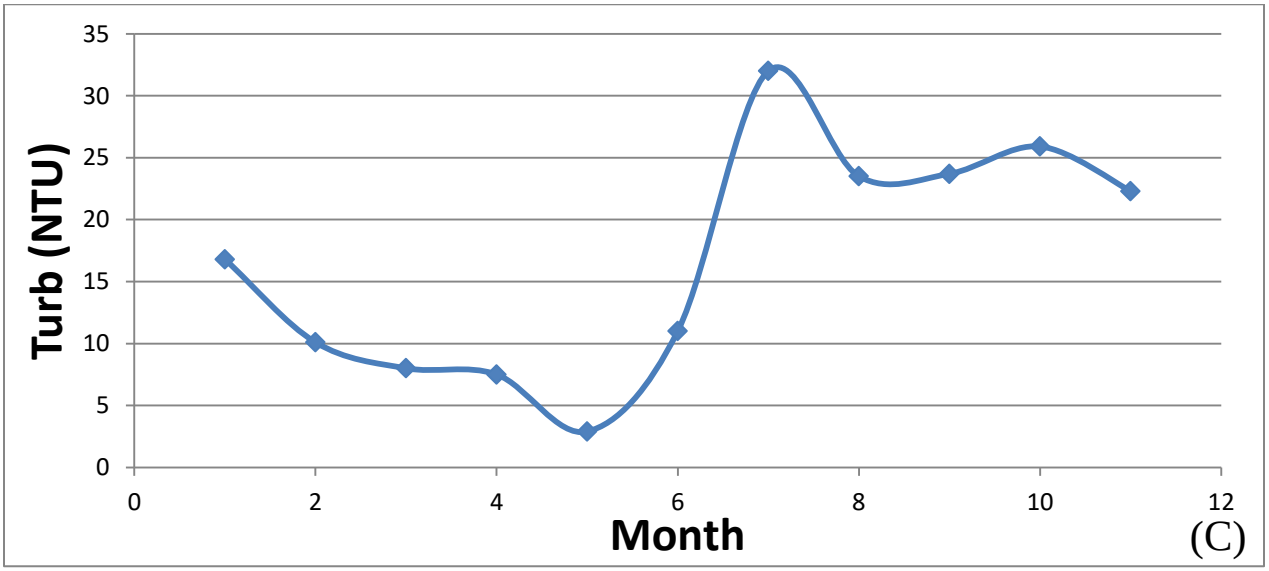
35
30
25
20
15
10
5
0
Turb (NTU)
0
2
4
6
8
10
12
Month
(C)

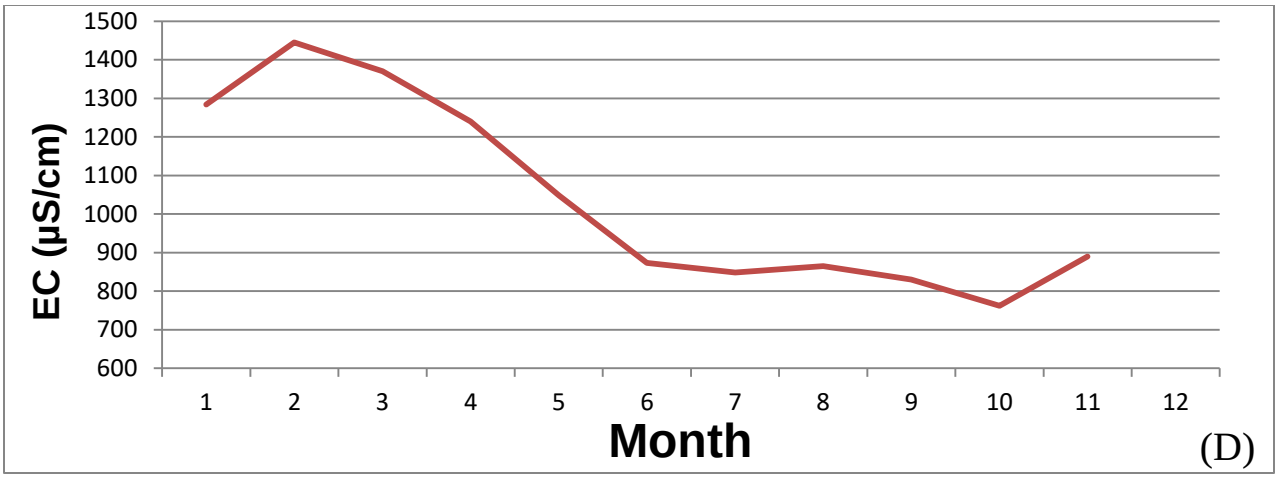

Figure (C.19): (A , B , C , D) water quality parameters variation in station (S4) for year 2019.

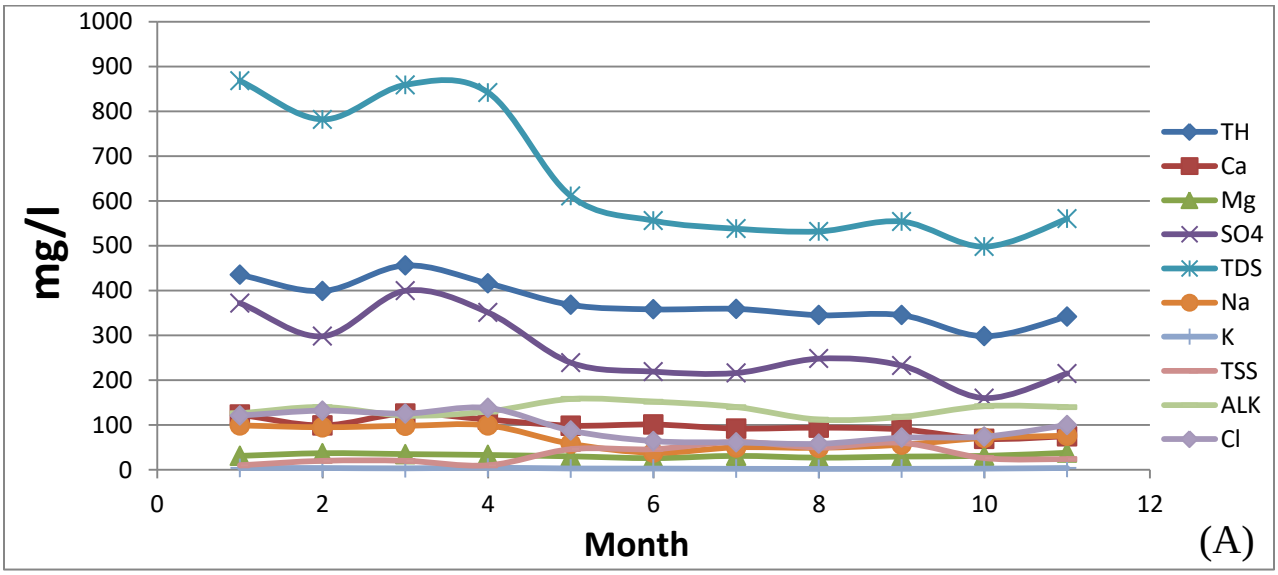

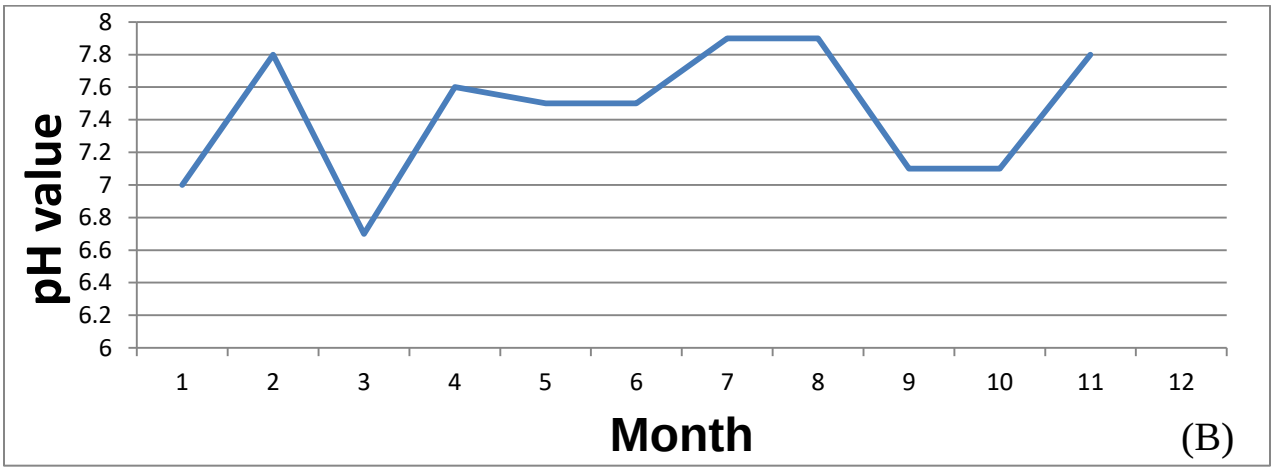

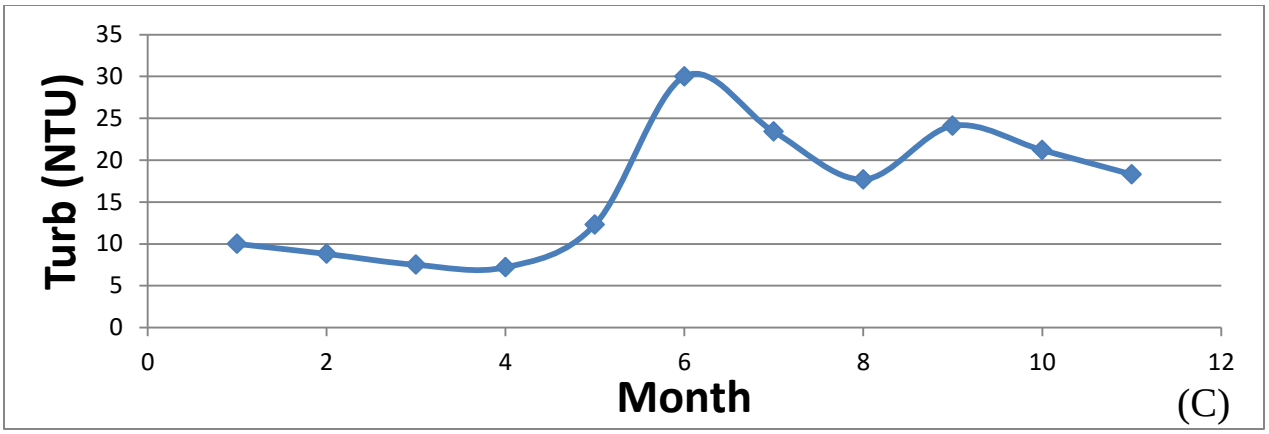

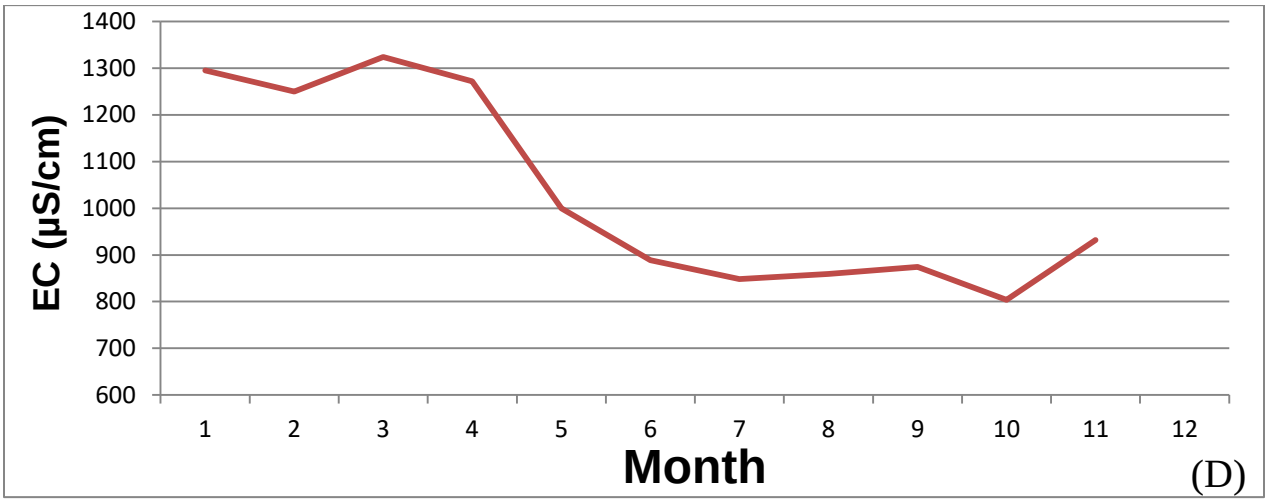

Figure (C.20): (A , B , C , D) water quality parameters variation in station (S5) for year 2019.

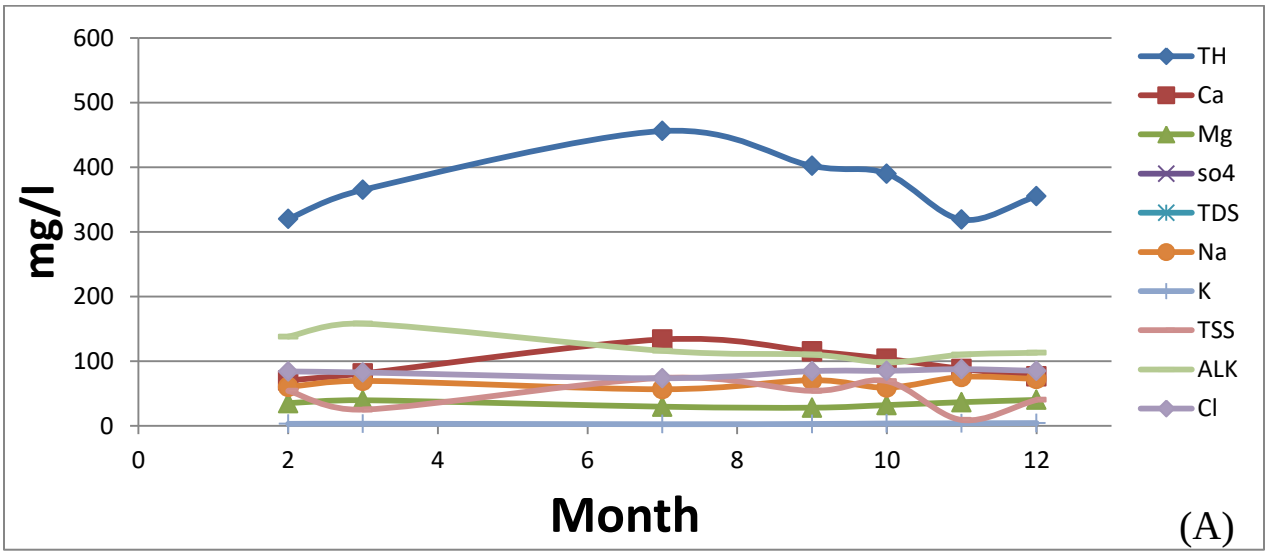

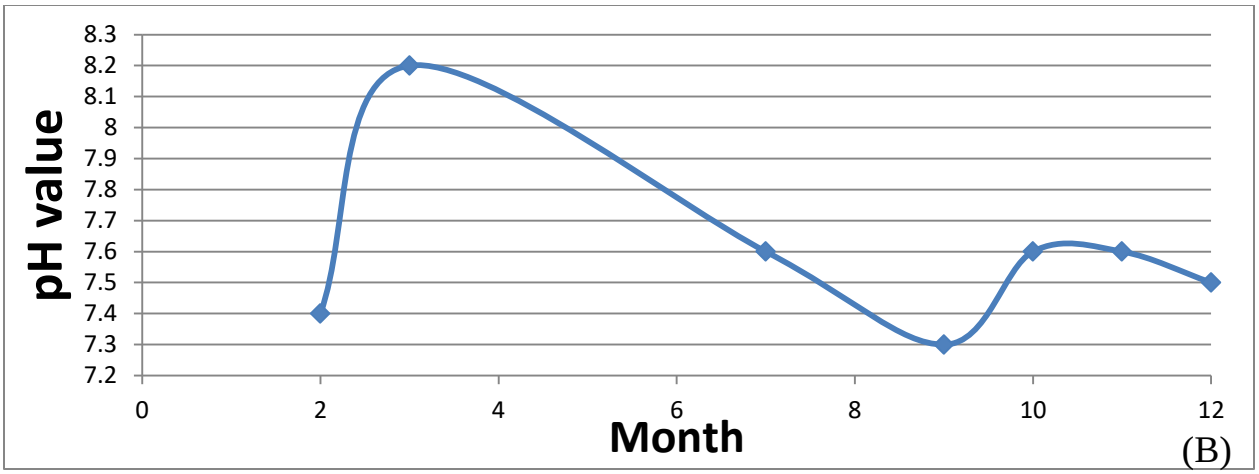

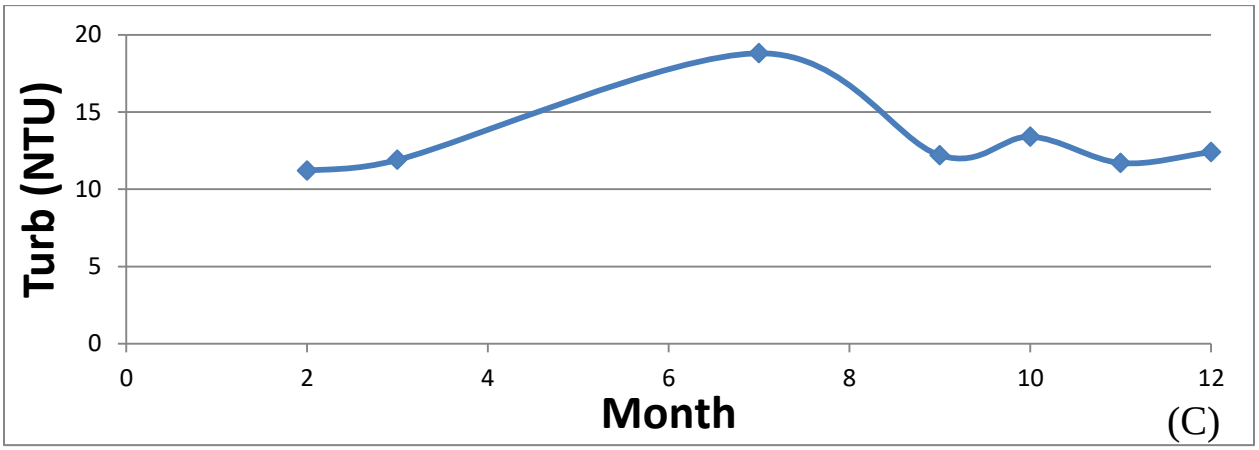

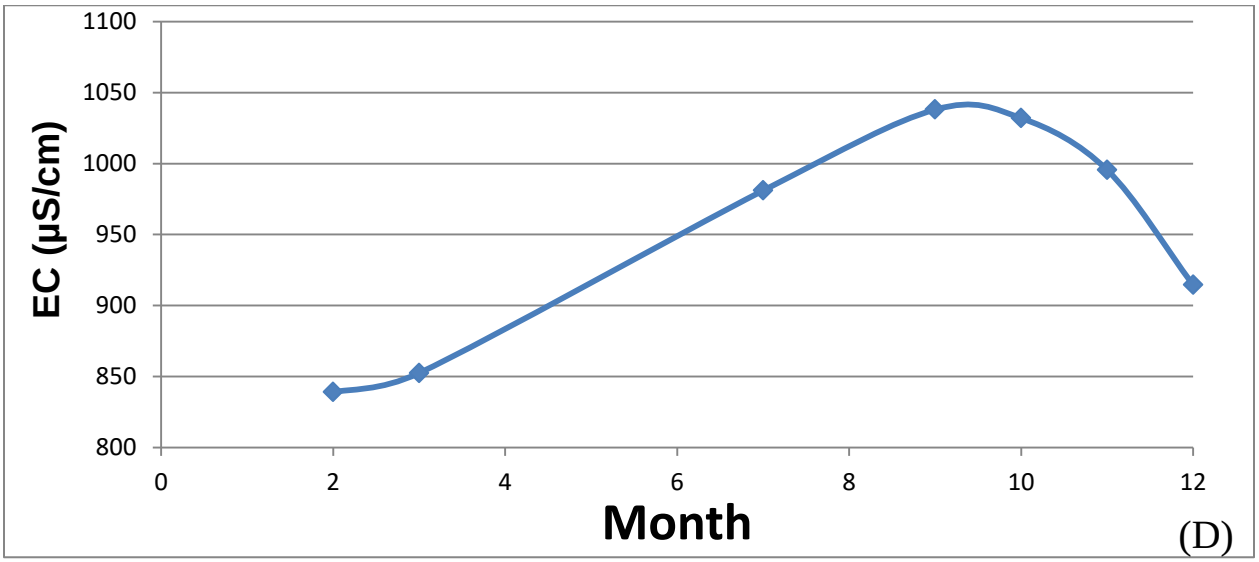

Figure (C.21): (A , B , C , D) water quality parameters variation in station (S1) for year 2020.

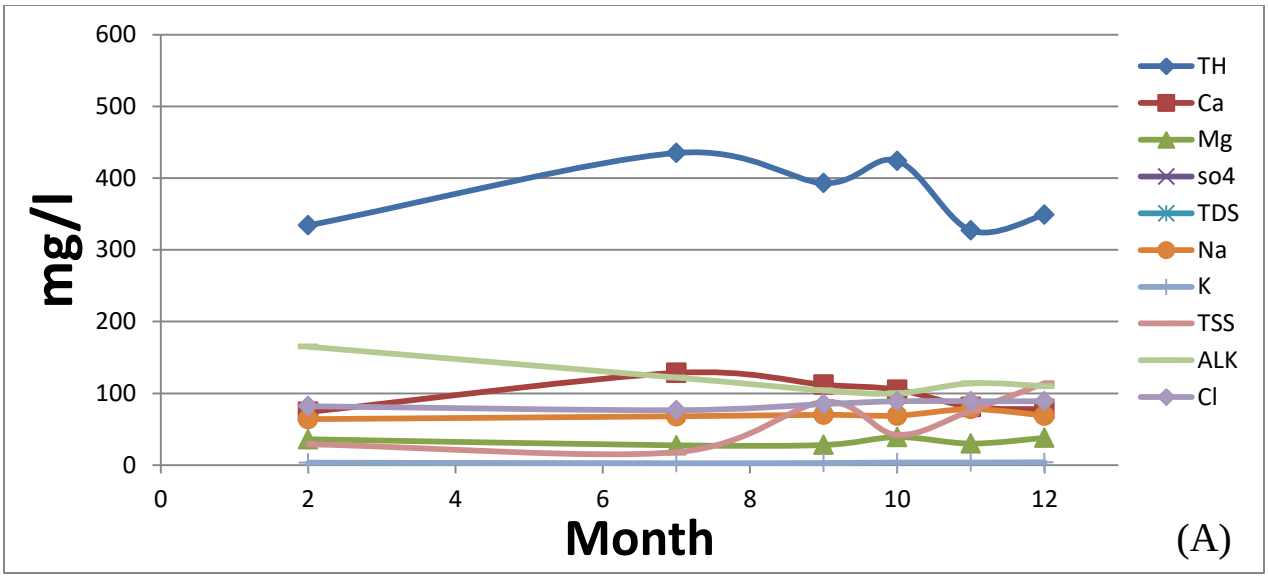
600
500
400
300
200
100
0
mg/l
0
2
4
6
8
10
12
Month
TH
Ca
Mg
so4
TDS
Na
K
TSS
ALK
Cl
(A)

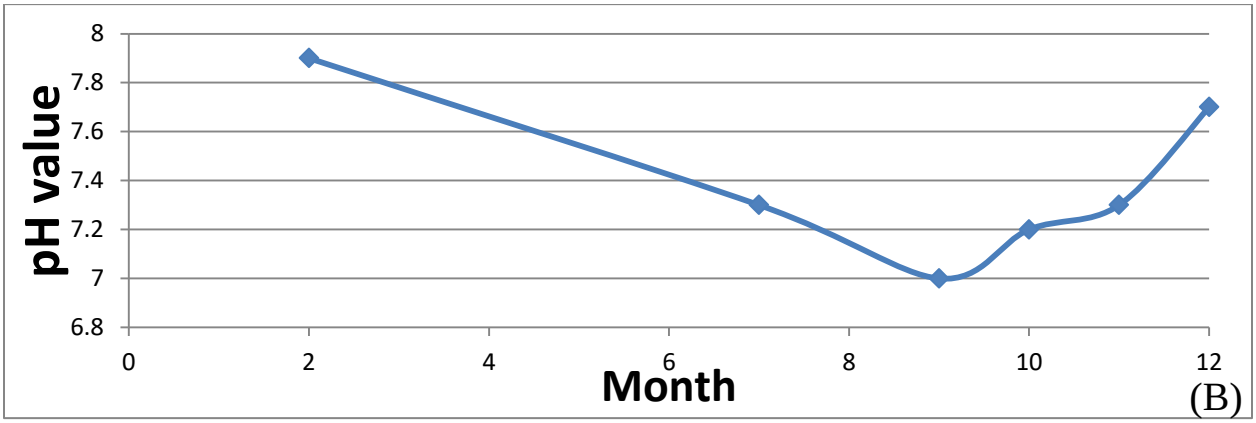
8
7.8
7.6
7.4
7.2
7
6.8
pH value
0
2
4
6
8
10
12
Month
(B)

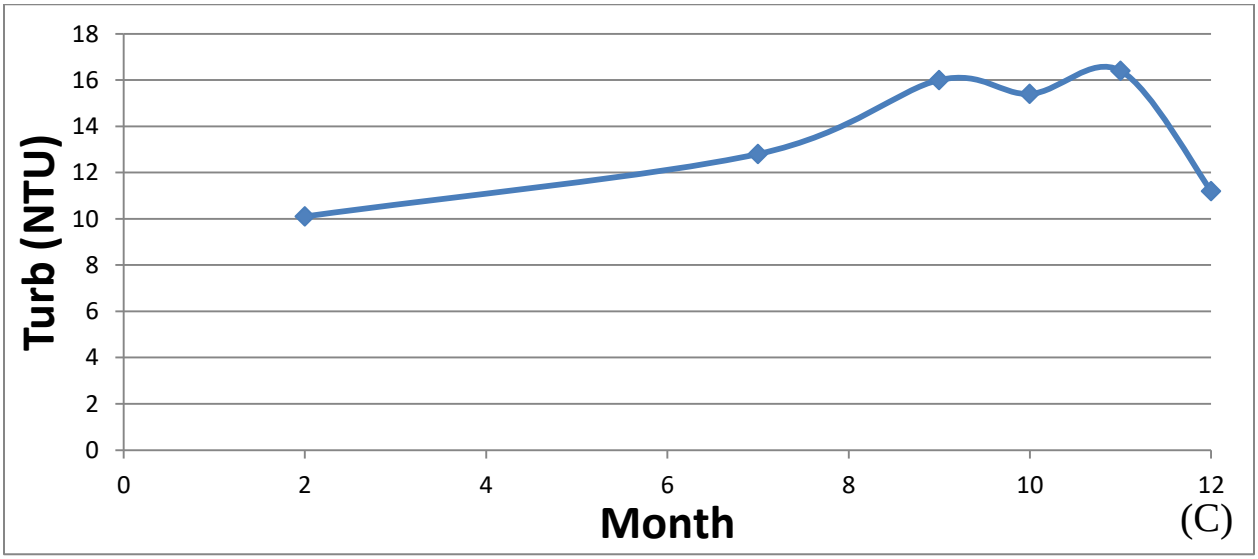
18
16
14
12
10
8
6
4
2
0
Turb (NTU)
0
2
4
6
8
10
12
Month
(C)

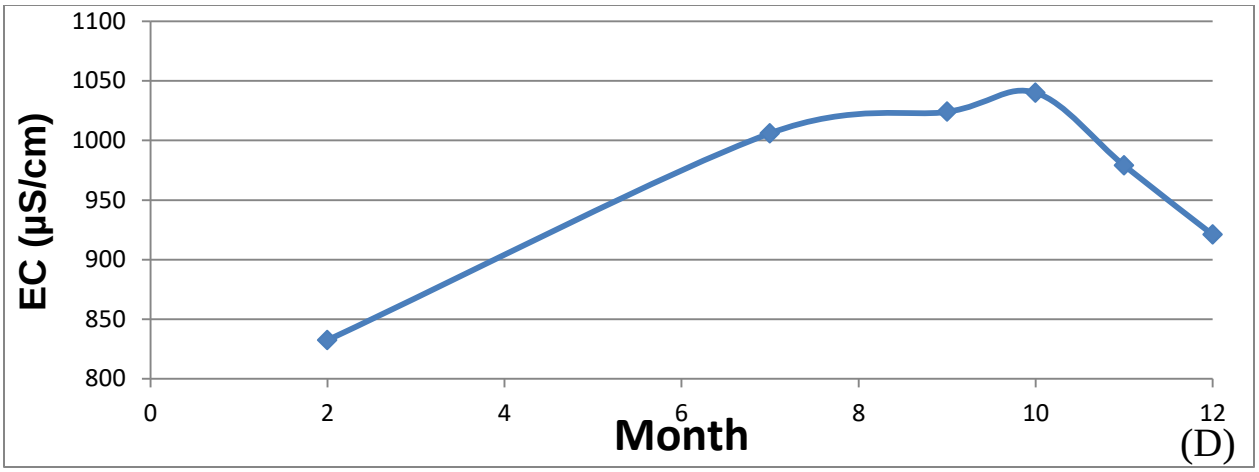

Figure (C.22): (A , B , C , D) water quality parameters variation in station (S2) for year 2020.

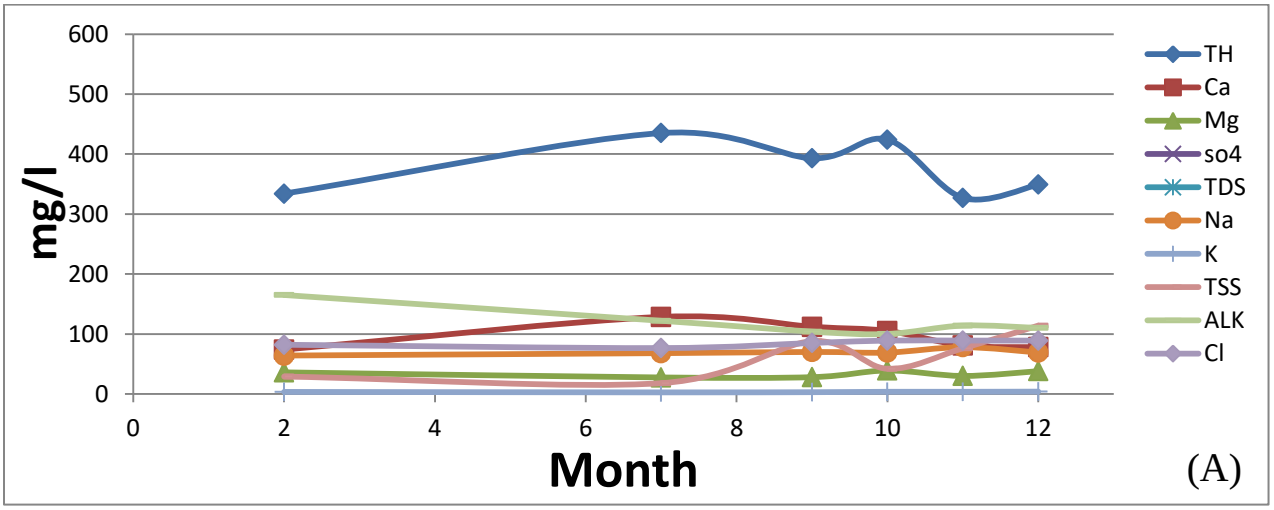

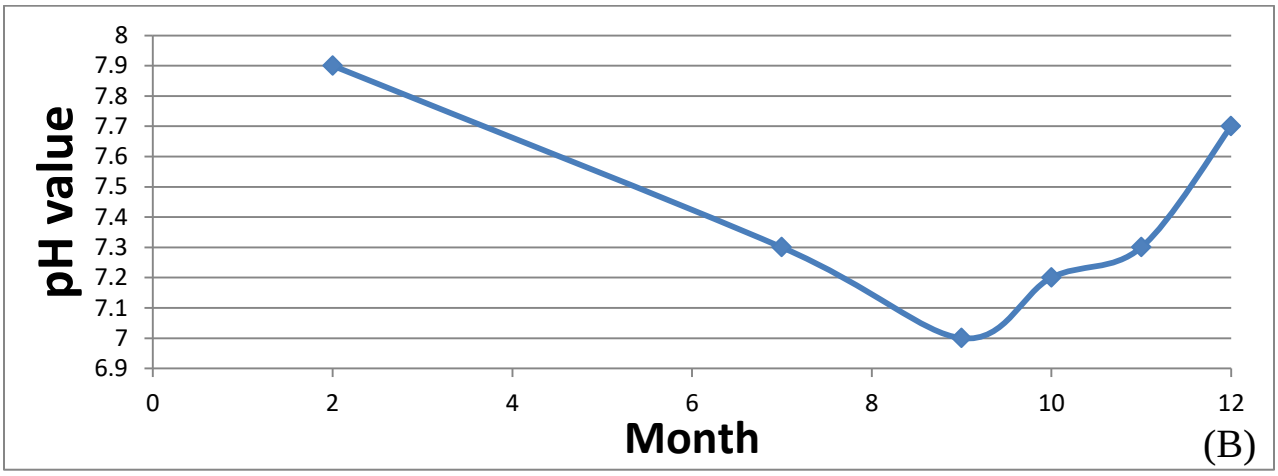

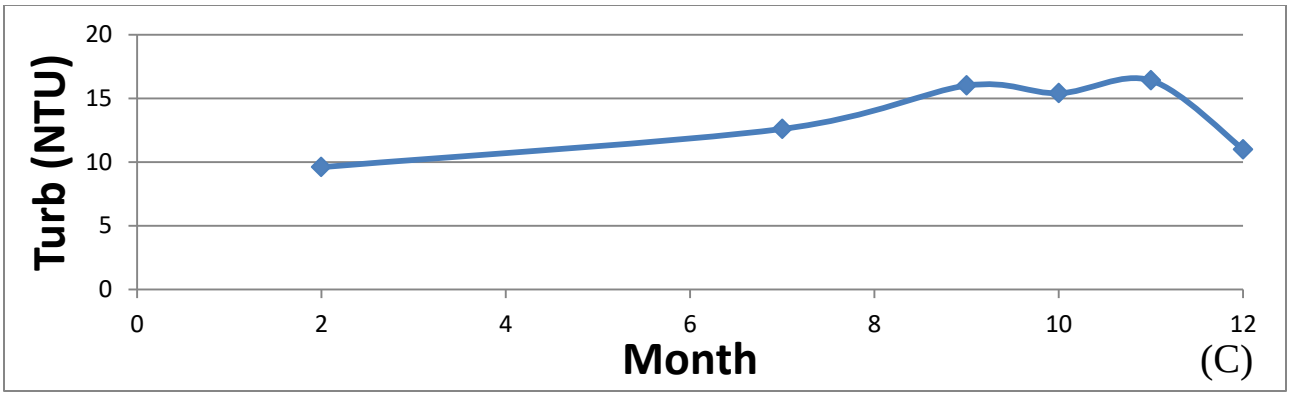

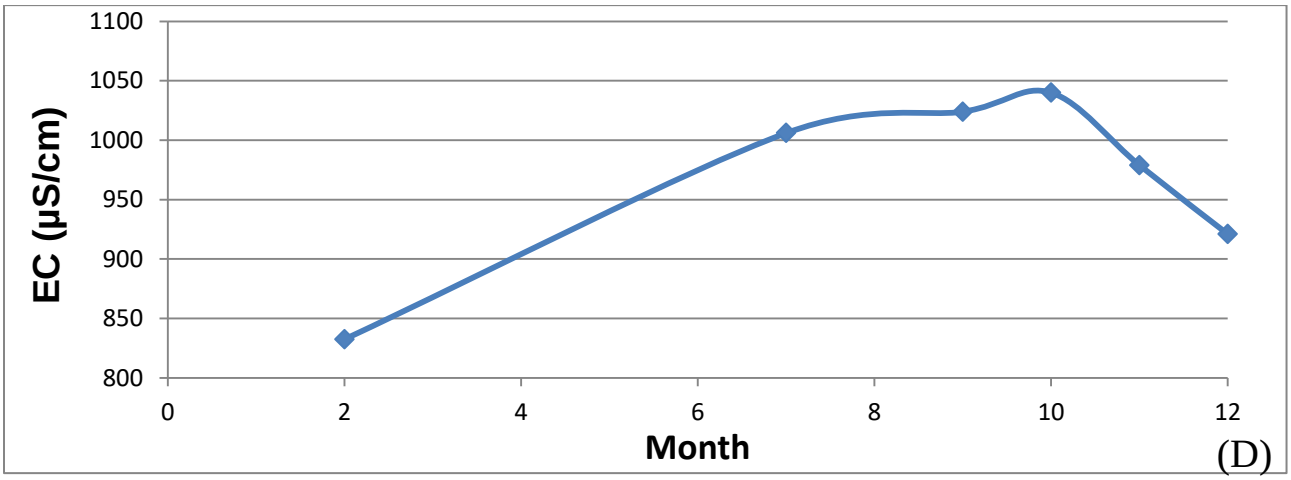

Figure (C.23): (A , B , C , D) water quality parameters variation in station (S3) for year 2020.

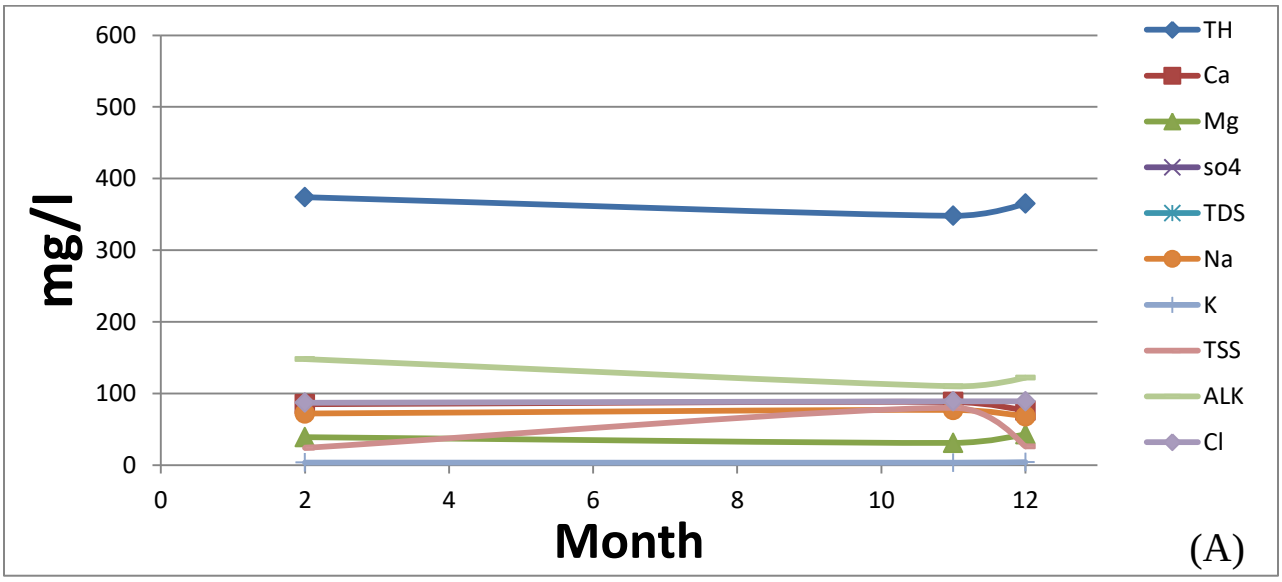

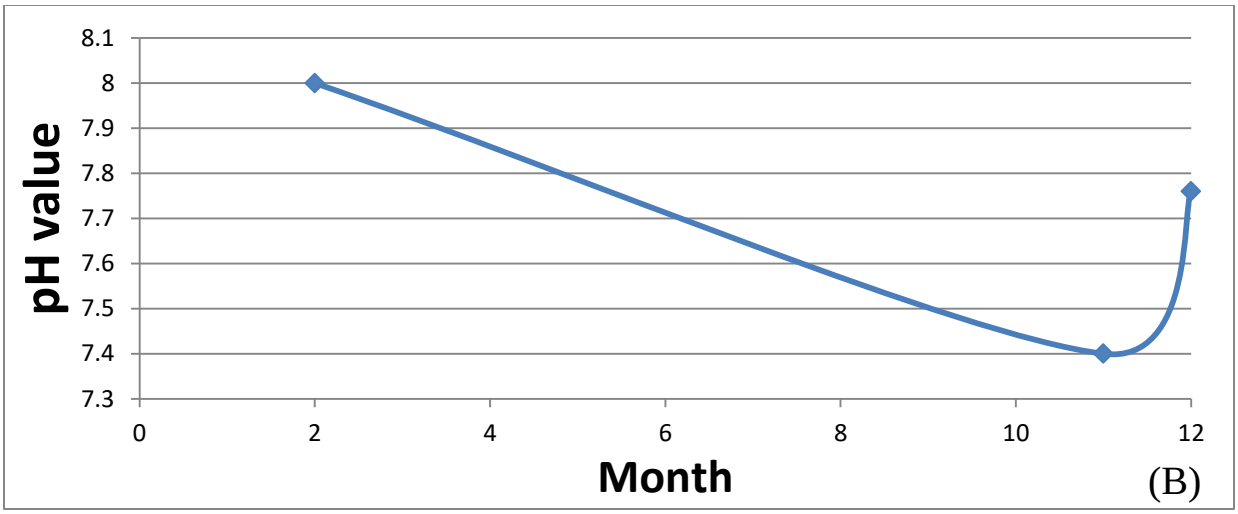

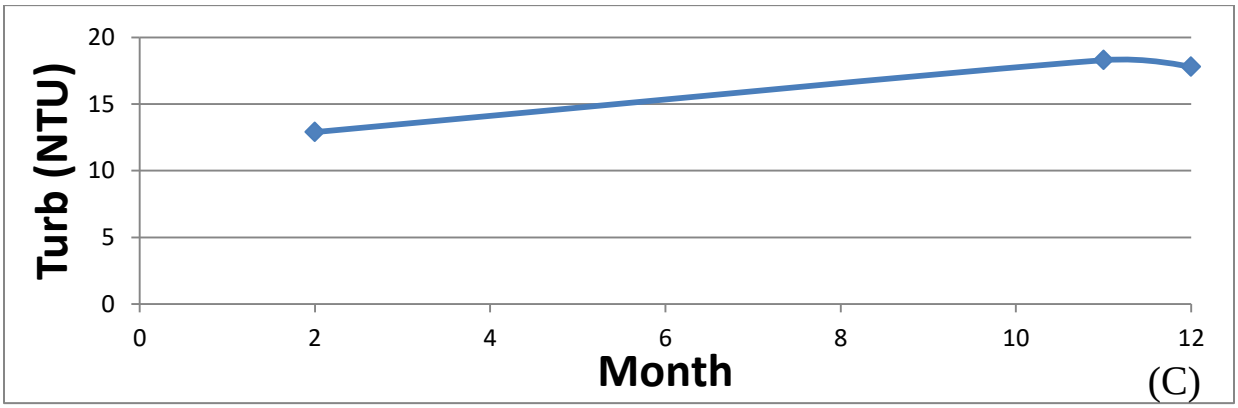

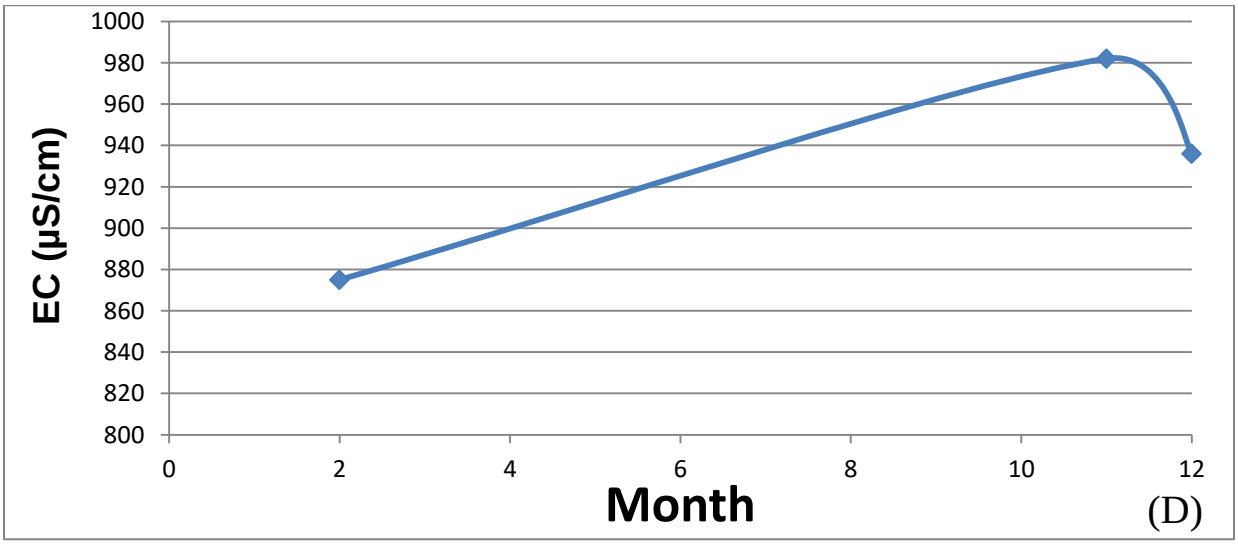

Figure (C.24): (A , B , C , D) water quality parameters variation in station (S4) for year 2020.

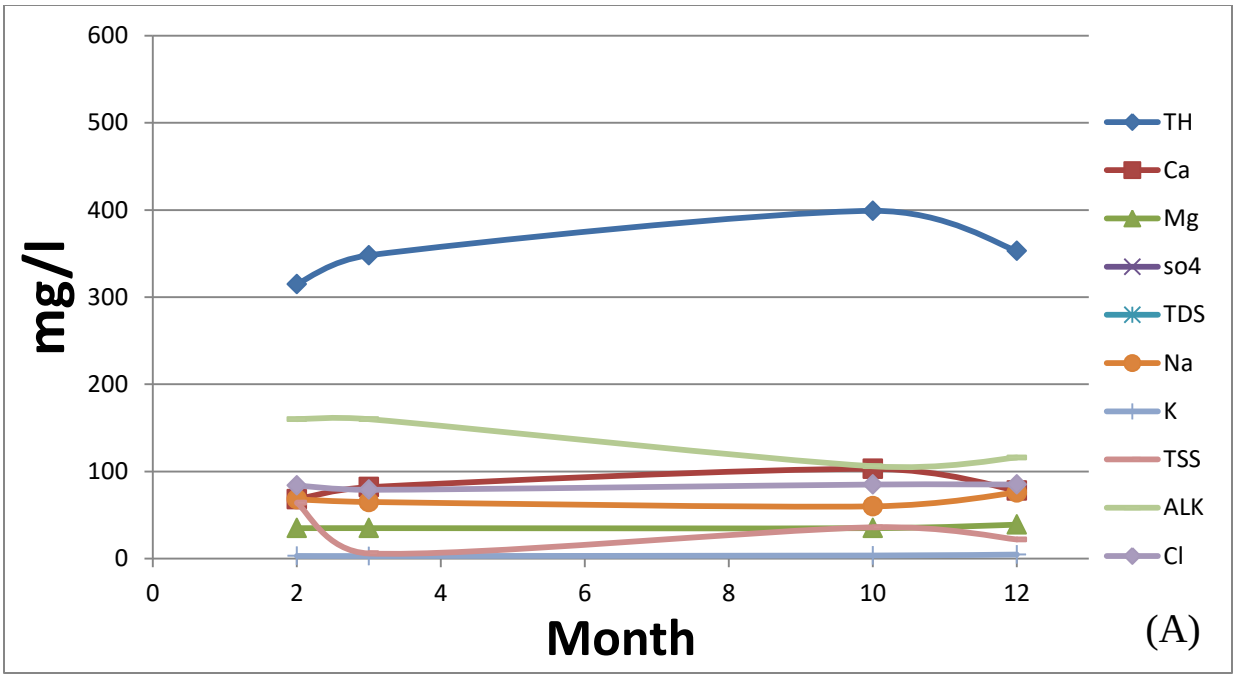
600
500
400
300
200
100
0
mg/l
0
2
4
6
8
10
12
Month
TH
Ca
Mg
so4
TDS
Na
K
TSS
ALK
Cl
(A)

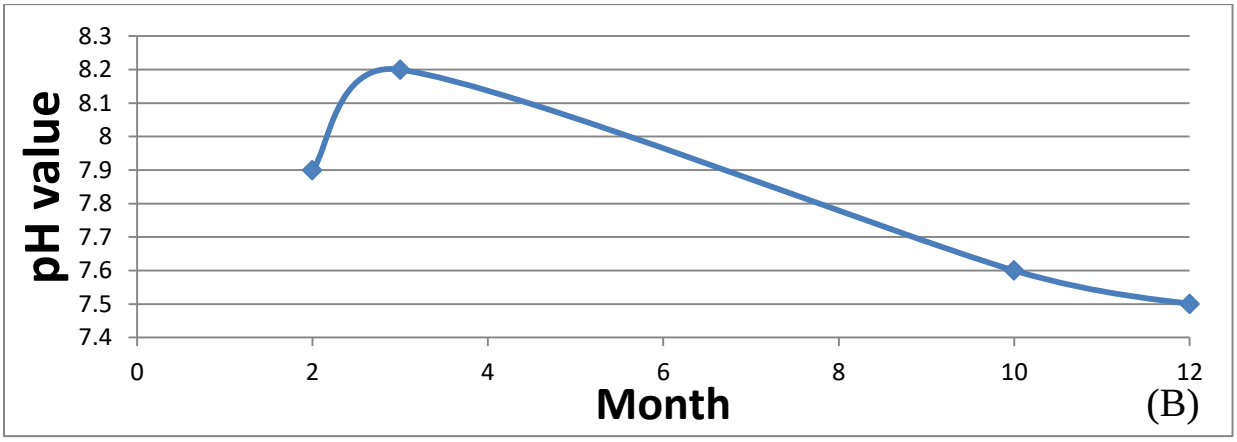
8.3
8.2
8.1
8
7.9
7.8
7.7
7.6
7.5
7.4
pH value
0
2
4
6
8
10
12
Month
(B)

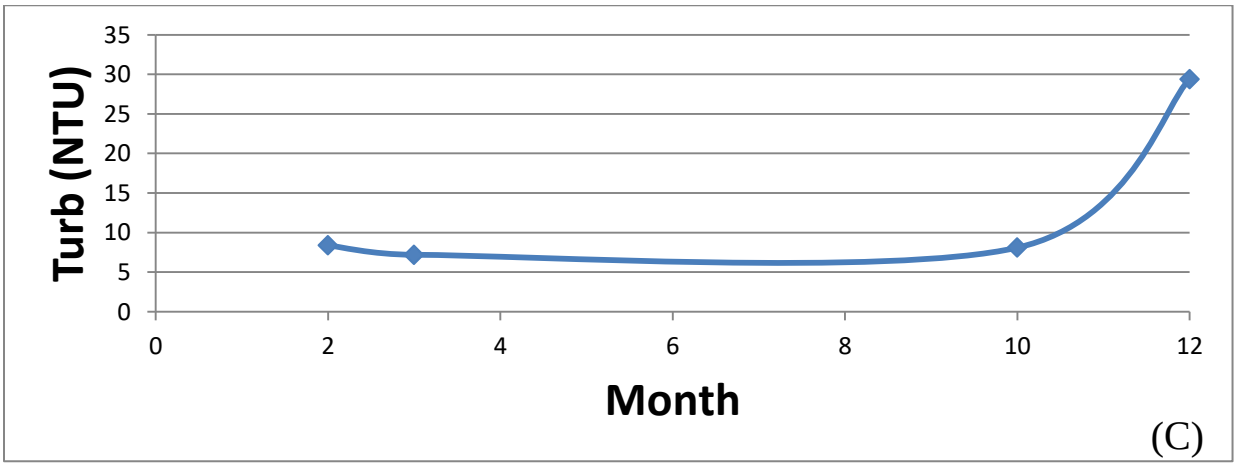
35
30
25
20
15
10
5
0
Turb (NTU)
0
2
4
6
8
10
12
Month
(C)

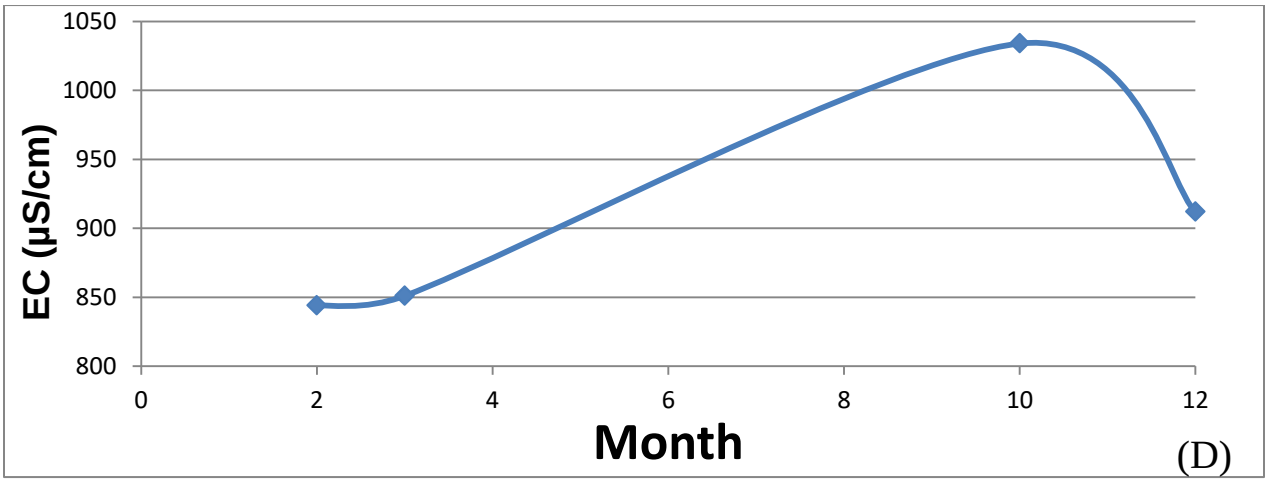

Figure (C.25): (A , B , C , D) water quality parameters variation in station (S5) for year 2020.

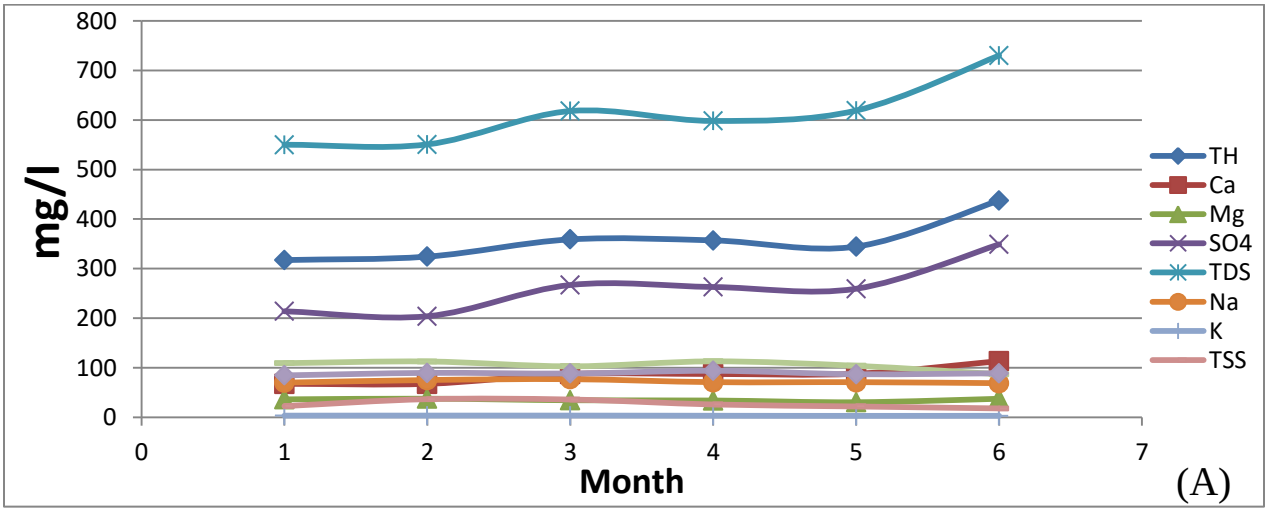

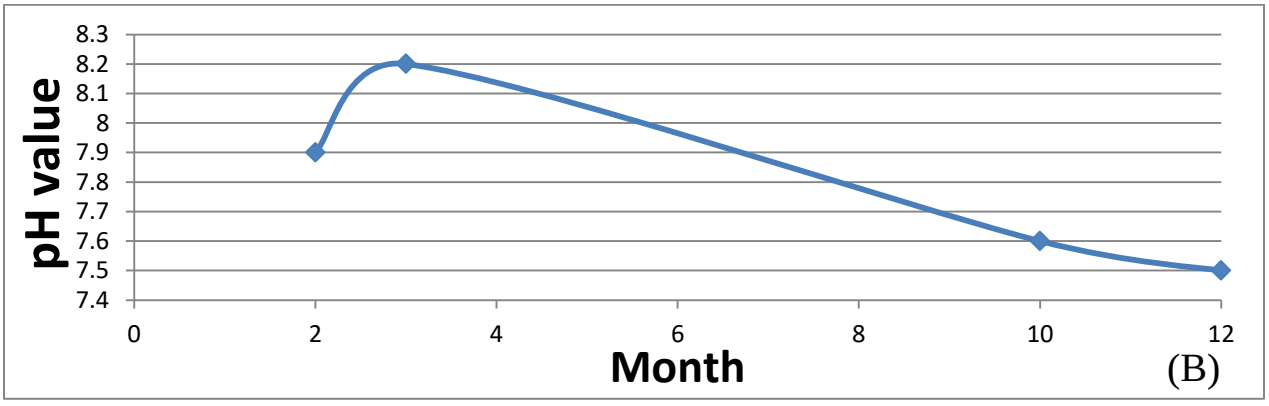

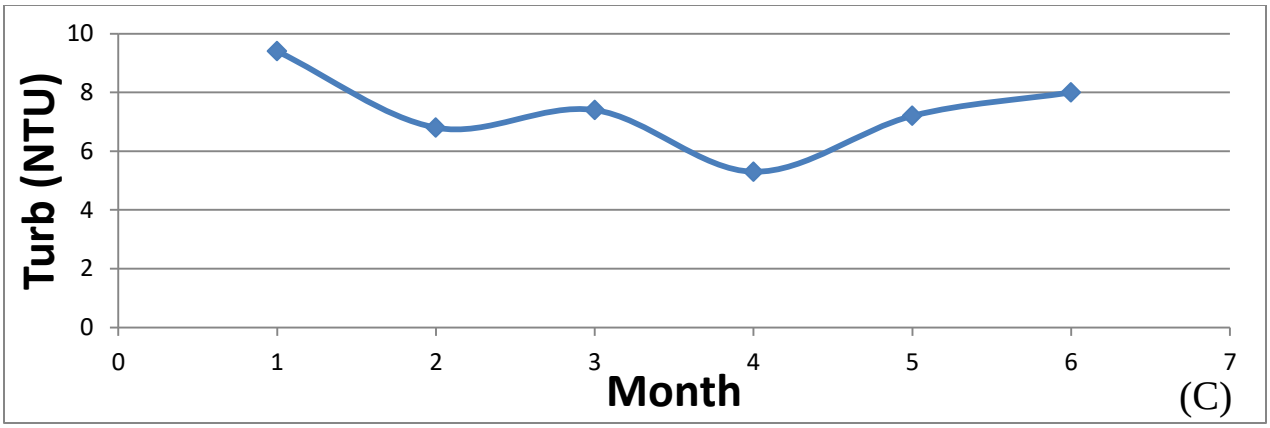

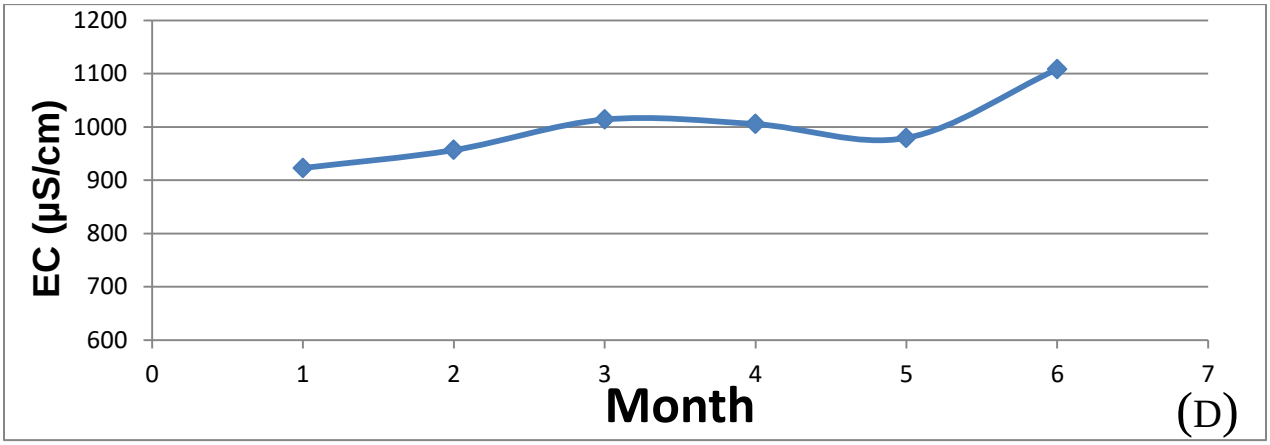

Figure (C.26): (A , B , C , D) water quality parameters variation in station (S1) for year 2021.

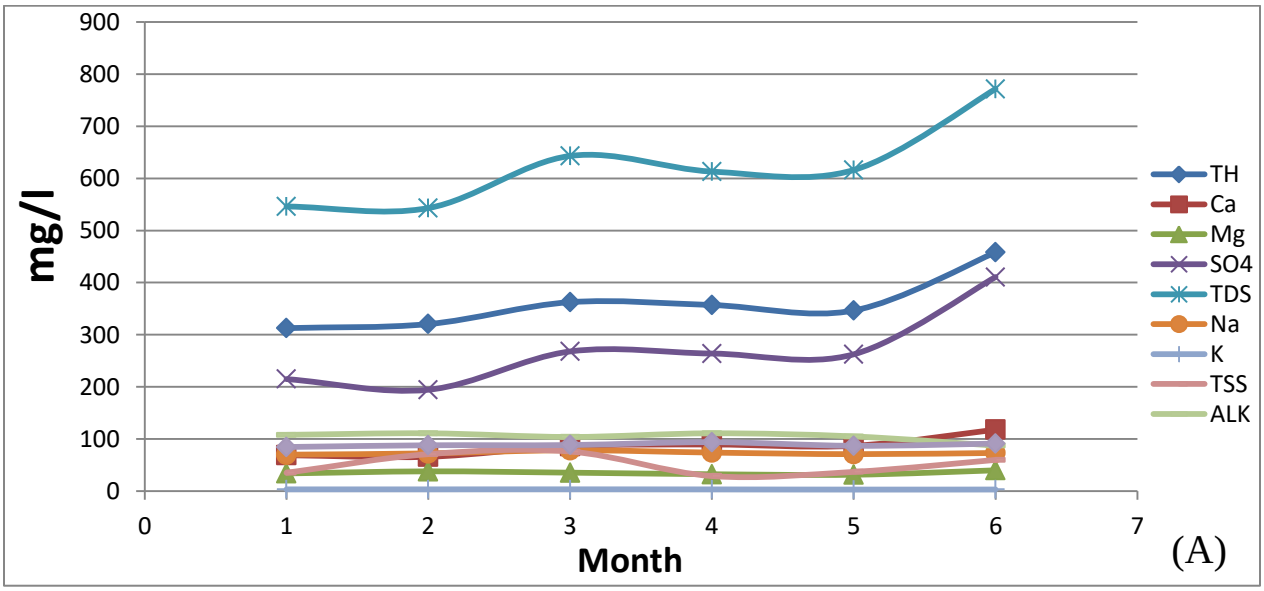

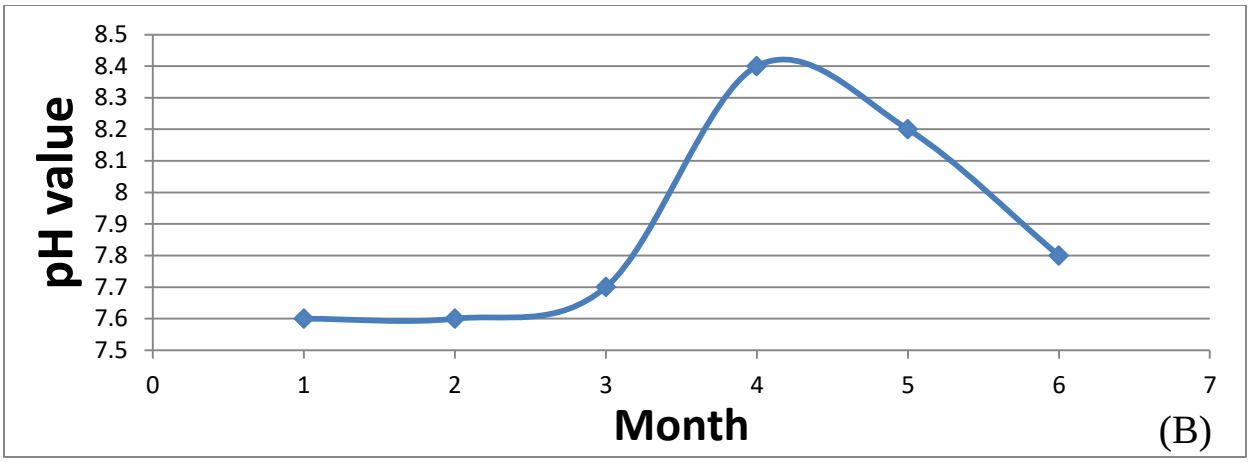

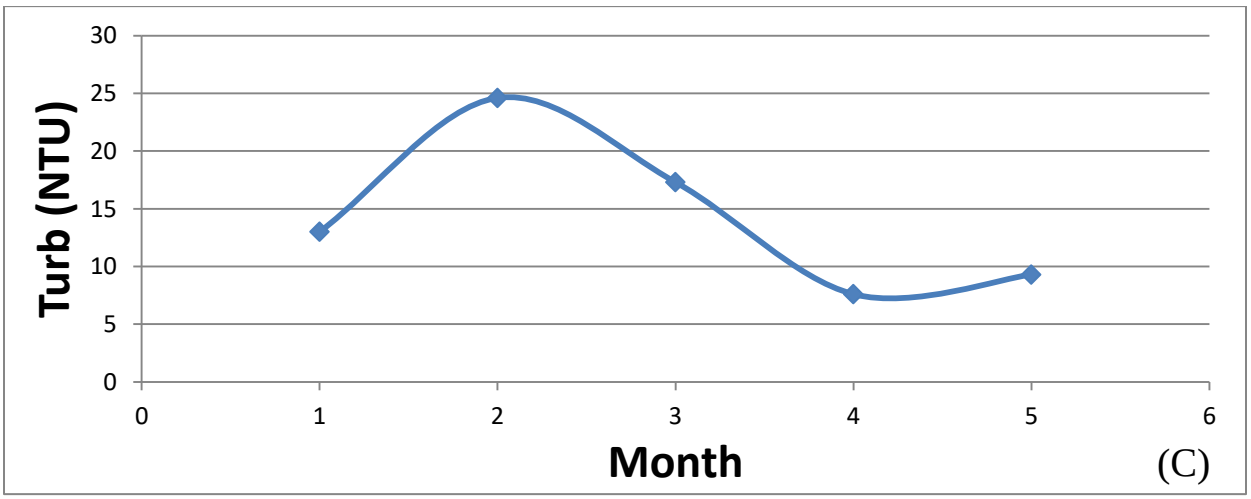

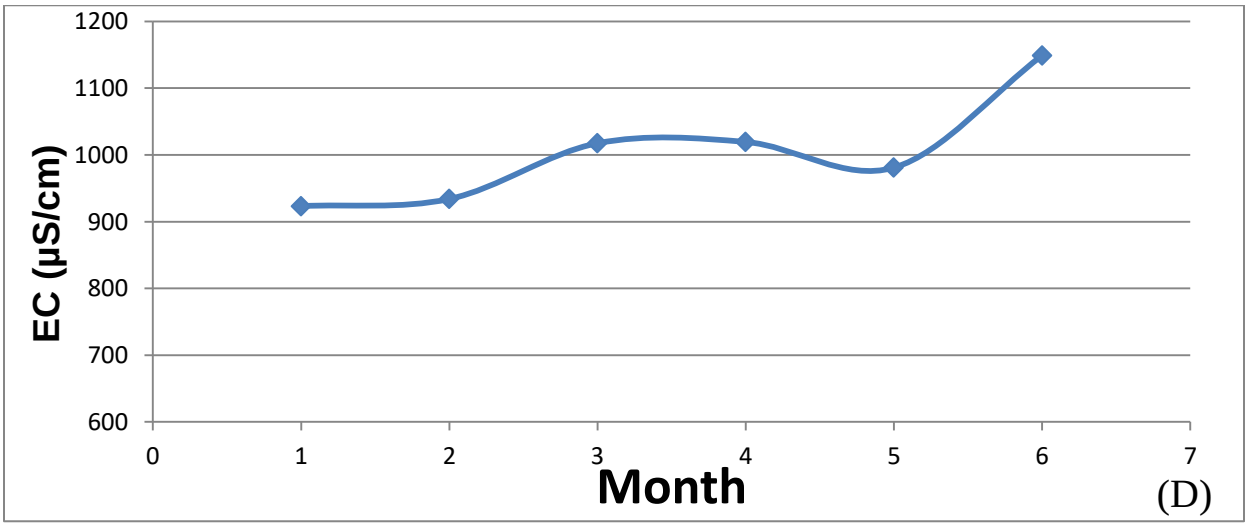

Figure (C.27): (A , B , C , D) water quality parameters variation in station (S2) for year 2021.

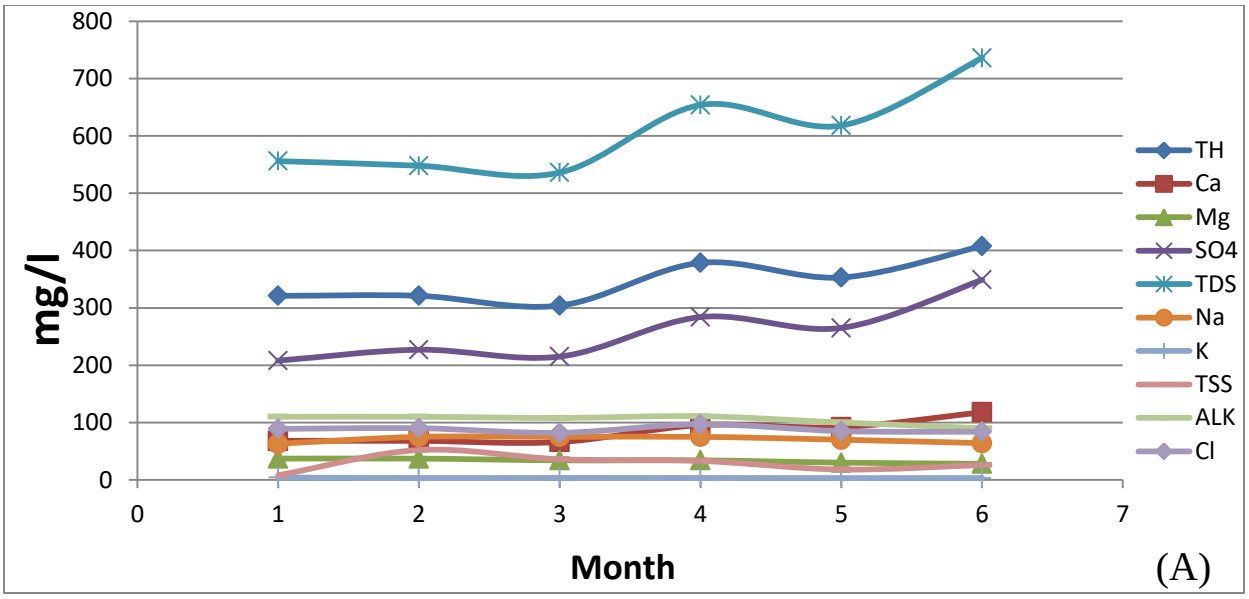
800
700
600
500
400
300
200
100
0
mg/l
0
1
2
3
4
5
6
7
Month
TH
Ca
Mg
SO4
TDS
Na
K
TSS
ALK
Cl
(A)

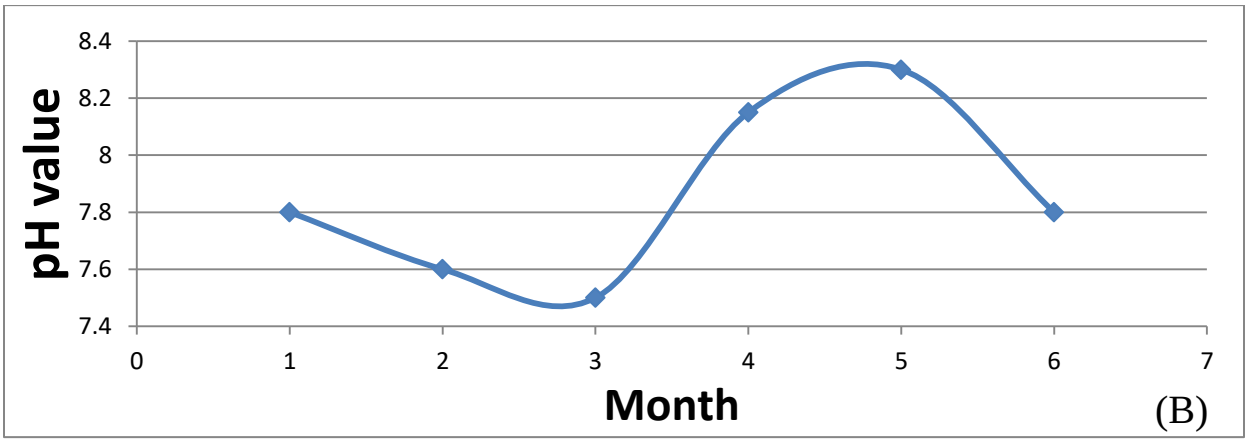
8.4
8.2
8
7.8
7.6
7.4
pH value
0
1
2
3
4
5
6
7
Month
(B)

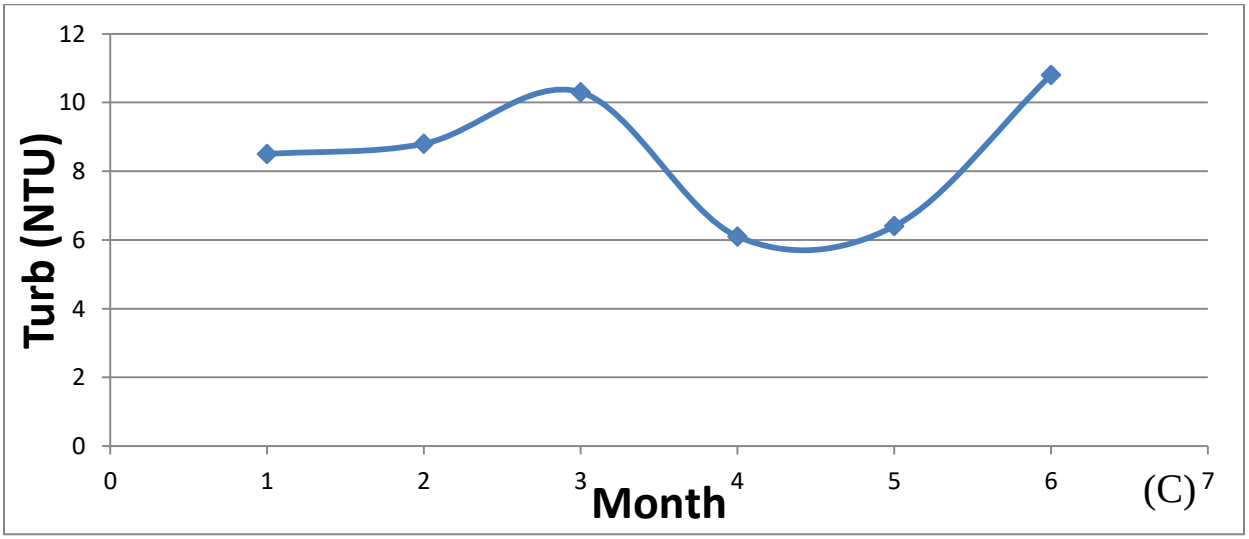
12
10
8
6
4
2
0
Turb (NTU)
0
1
2
3
4
5
6
7
Month
(C)

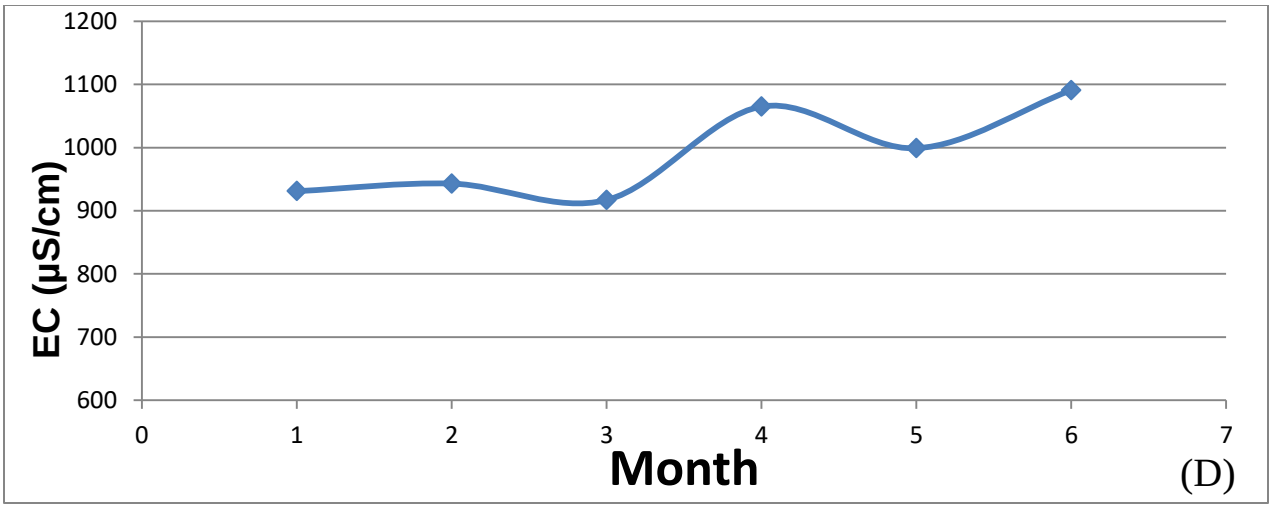

Figure (C.28): (A , B , C , D) water quality parameters variation in station (S3) for year 2021.

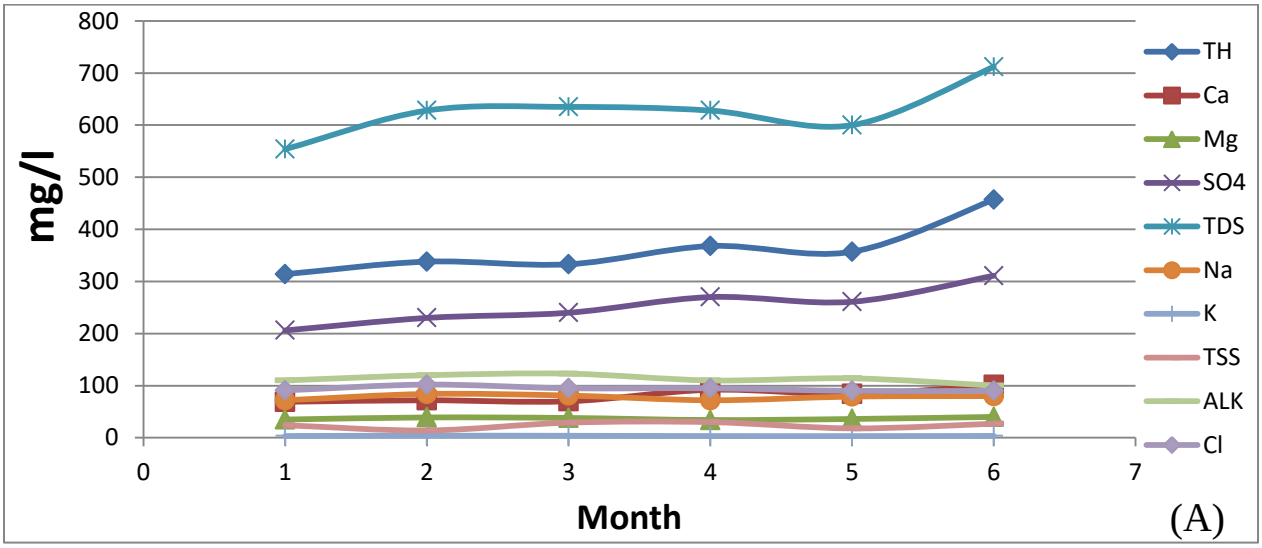

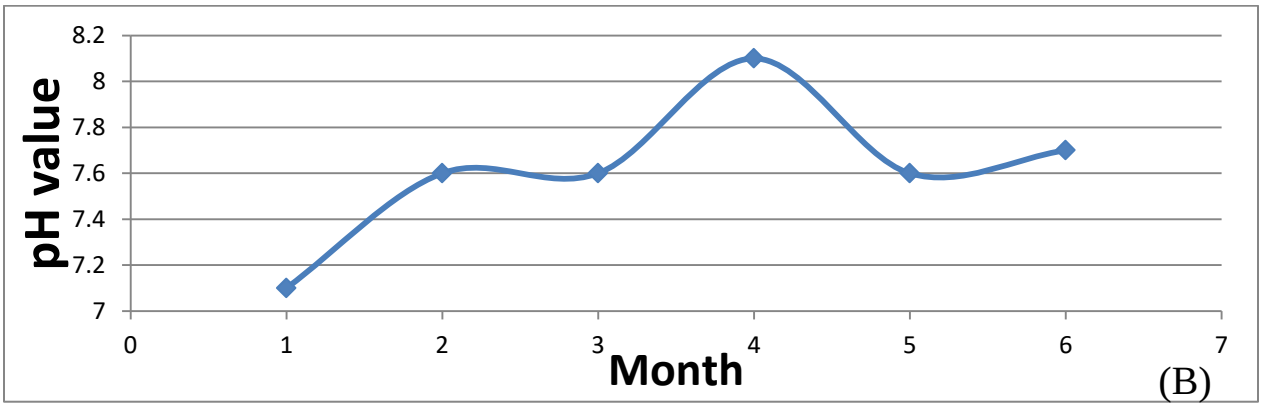

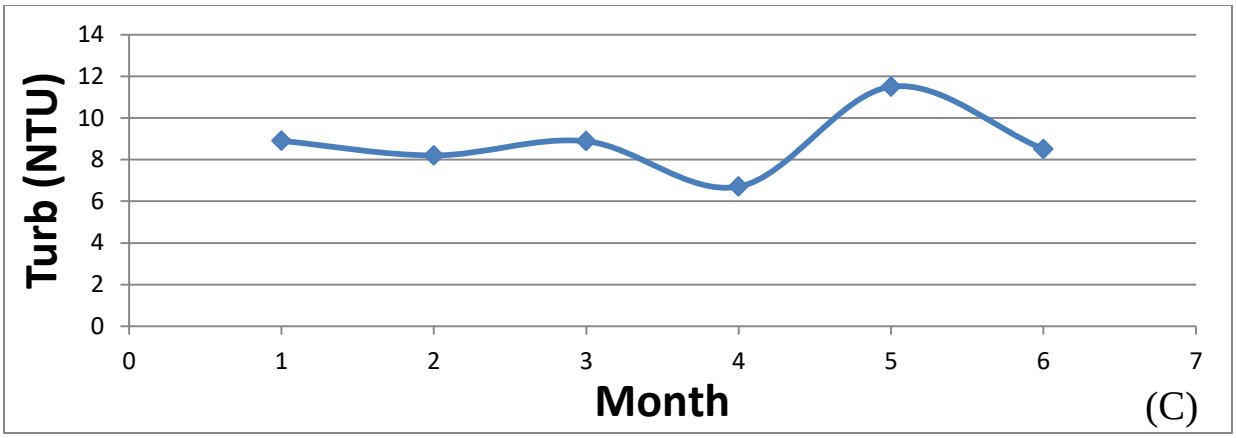

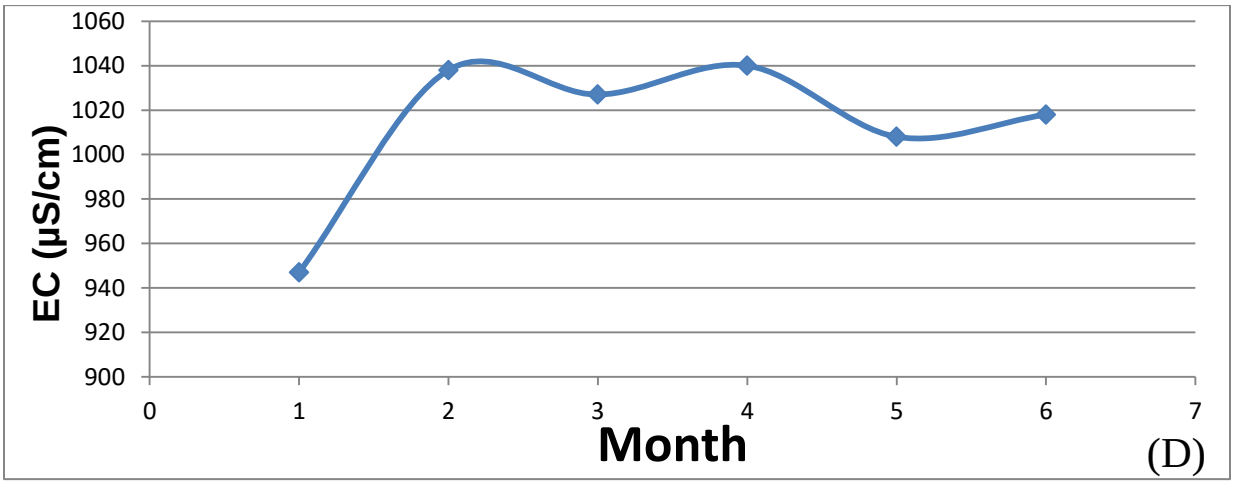

Figure (C.29): (A , B , C , D) water quality parameters variation in station (S4) for year 2021.

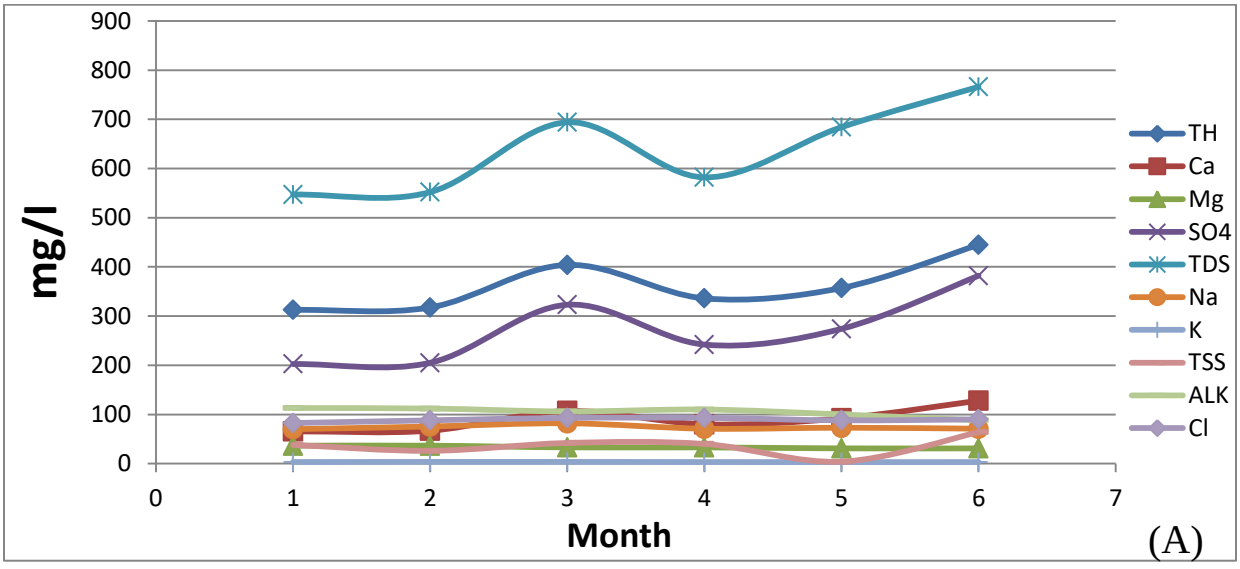

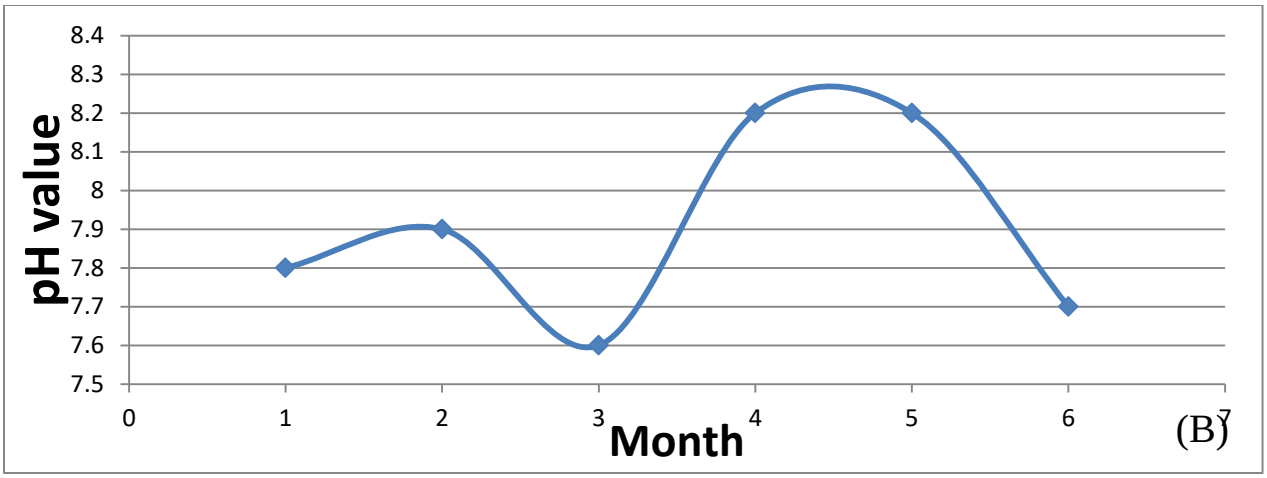

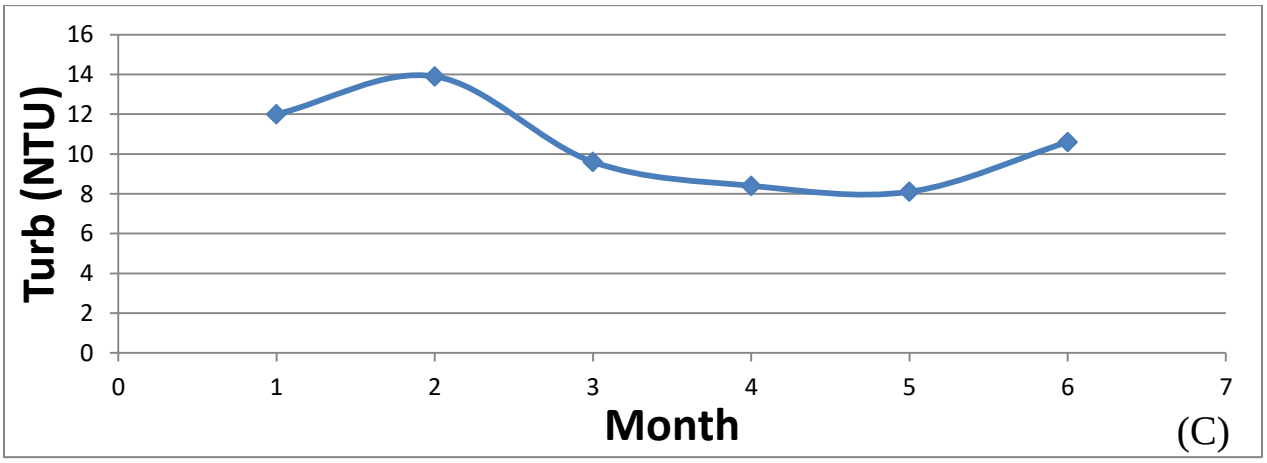

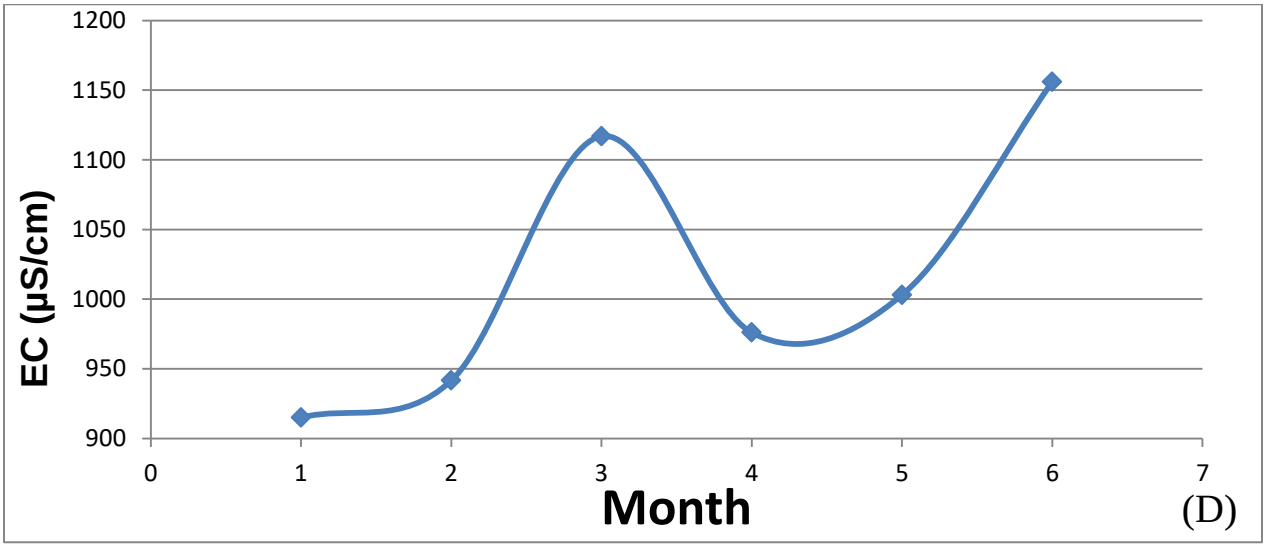

Figure (C.30): (A , B , C , D) water quality parameters variation in station (S5) for year 2021.

الخلاصة

منذ أن تم تطوير الأنشطة الصناعية والبشرية بطرق مختلفة في العراق ، فإن جودة المياه آخذت في التدهور على طول نهر الحلة ، المورد الوحيد للمياه في مدينة الحلة لمياه الشرب. في هذا البحث ، تمت محاكاة مؤشر جودة المياه الحسابي (WQI) على طول النهر بناءً على تقنية GIS وطريقة IDW . عناصر جودة المياه بما في ذلك العكارة (Turb) ، التوصيلية الكهربائية (EC) ، أيونات الهيدروجين (pH) ، إجمالي المواد الصلبة المعلقة (TSS) ، أيونات الكلوريد (Cl) ، أيونات الكبريتات (SO4) ، القلوية (ALK)) ،العسرة الكلية (TH) ، أيونات الكالسيوم (Ca) ، أيونات البوتاسيوم (k) ، أيونات الصوديوم (Na) ، أيونات المغنيسيوم (Mg) ، وإجمالي المواد الصلبة الذائبة (TDS) لتحديد WQI من يناير 2016 إلى يونيو 2021 اعتمادًا على مجموعات البيانات من خمس محطات لأخذ العينات تقع على طول النهر لمدينة الحلة.

أظهرت نتائج هذه الدراسة أن نهر الحلة ملوث بشكل خطير لأن قيم WQI عالية ، وقد تم تطوير نماذج الانحدار الخطي إحصائياً لإيجاد علاقة رياضية بين WQI ومعايير جودة المياه. لوحظ أن WQI في نهر الحلة له علاقة معنوية مع التعكر فقط (نسبة موجبة) ، وهذه العلاقة بين WQI والعكارة في النهر محدودة بقيمة WQI وهي (220) ، وبالتالي ، تم تطوير نموذجين للانحدار الخطي والتحقق من صدقهما: أحدهما لقيم WQI أكبر من 220 والآخر للقيم الأقل من 220.

يوفر استخدام تقنية الاستشعار عن بعد بيانات لتقييم ومراقبة جودة المياه في المسطحات المائية. وهكذا ، في هذه الدراسة ، تم اختبار صور القمر الصناعي لاندسات 8 (2016 إلى 2021) إحصائيًا لتطوير نماذج خطية قادرة على تقدير معلمات جودة المياه في النهر بناءً على البيانات الميدانية ، أظهرت النتائج أن سبع معاملات لها علاقة معنوية مع نسبة النطاقات الطيفية (قيمة p أقل من 0.05). يرتبط بعضها (TDS و SO4 و ALK) ارتباطًا إيجابيًا بنسبة النطاقات (Band10 / Band3 و Band10 / Band3 و Band10 / Band4 و Band3 / Band7) ، على التوالي. ترتبط العناصر الأخرى (Mg و Ca و TH و pH) عكسيًا بـ (Band4 / Band7 و Band1 / Band4 و Band1 / Band4 و Band1 / Band2) ، على التوالي. و EC و Turb ليس لديهم ارتباط معنوي بأي نسبة نطاقات.

بالإضافة إلى ذلك ، أظهرت مصفوفة الارتباط بين WQI والنطاقات الطيفية أن WQI لها ارتباط بيرسون بأكثر من 50٪ وقيمة p أقل من 0.05 مع band 10, band 3. العلاقة المعنوية بين WQI والنطاقات

الطيفية في النهر محدودة بقيم WQI ، والتي هي (WQI أقل من 50 ، WQI بين 50 و 250 ، و WQI أكثر من 250). أظهرت قيمة WQI الأقل من 50 علاقة مهمة مع النطاق في Band 3 ، أظهرت قيمة WQI بين 50 و 250 علاقة كذلك مع Band 3، وأظهرت قيمة WQI التي تزيد عن 250 علاقة كبيرة مع Band 10. ونتيجة لذلك ، تم تطوير ثلاثة نماذج انحدار خطي والتحقق من صحتها اعتمادًا على على قيم حد WQI.

علاوة على ذلك ، كانت خرائط GIS تستخدم للتنبؤ بخريطة WQI والتعكر كخريطة توزيع لتغطية منطقة الدراسة بأكملها. أظهرت خرائط GIS لحوض نهر الحلة على طول مدينة الحلة أن أسوأ قيمة WQI كانت في عام 2019 بسبب ارتفاع درجة العكارة. من ناحية أخرى ، كانت أفضل قيمة WQI والتعكر في عام 2018. ومع ذلك ، في عامي 2020 و 2021 ، كان هناك بعض التحسن في WQI والتعكر مقارنة بعام 2019.

جمهورية العراق
وزارة التعليم العالي والبحث العلمي
جامعة بابل
كلية الهندسة
قسم الهندسة البيئية

موديل بيئي لجودة المياه السطحية باستخدام تقنيات نظم المعلومات الجغرافية والاستشعار عن بعد: دراسة حالة لنهر الحلة ، العراق

رسالة

مقدمة الى كلية الهندسة في جامعة بابل كجزء من متطلبات نيل درجة

ماجستير في علوم الهندسة البيئية

إعداد:

فاطمة ذيبان هادي

أشراف:

أ.م.د. حسين علي مهدي

أ.د. نسرين جاسم المنصوري

1444 هـ 2023 م